CAPITAL UNIVERSITY OF SCIENCE AND TECHNOLOGY, ISLAMABAD


# Precipitation Variability in Connection with Various Potential Determinants

by

Erum Aamir

A thesis submitted in partial fulfillment for the degree of Doctor of Philosophy

in the

Faculty of Engineering
Department of Civil Engineering

2022

# Precipitation Variability in Connection with Various Potential Determinants

By

Erum Aamir

(DCE153002)

**Dr. Sajjad Ahmed, Professor**

**University of Nevada, Las vegas, USA**

**(Foreign Evaluator 1)**

**Dr. Berrin Tansel, Professor**

**Florida international University, USA**

**(Foreign Evaluator 2)**

**Dr. Majid Ali**

**(Thesis Supervisor)**

**Dr. Syed Shujaa Safdar Gardezi**

**(Thesis Co-supervisor)**

**Dr. Ishtiaq Hassan**

**(Head, Department of Civil Engineering)**

**Dr. Imtiaz Ahmad Taj**

**(Dean, Faculty of Engineering)**

**DEPARTMENT OF CIVIL ENGINEERING**

**CAPITAL UNIVERSITY OF SCIENCE AND TECHNOLOGY**

**ISLAMABAD**

**2022**

*Dedicated to my family*

# CAPITAL UNIVERSITY OF SCIENCE & TECHNOLOGY
# ISLAMABAD

Expressway, Kahuta Road, Zone-V, Islamabad
Phone:+92-51-111-555-666 Fax: +92-51-4486705
Email: info@cust.edu.pk Website: https://www.cust.edu.pk


## CERTIFICATE OF APPROVAL

This is to certify that the research work presented in the thesis, entitled "**Precipitation Variability in Connection with Various Potential Determinants**" was conducted under the supervision of **Dr. Majid Ali**. No part of this thesis has been submitted anywhere else for any other degree. This thesis is submitted to the **Department of Civil Engineering, Capital University of Science and Technology** in partial fulfillment of the requirements for the degree of Doctor in Philosophy in the field of **Civil Engineering.** The open defence of the thesis was conducted on **January 06, 2022**.

**Student Name :** Erum Aamir (DCE-153002)

---

The Examination Committee unanimously agrees to award PhD degree in the mentioned field.

**Examination Committee :**

(a) External Examiner 1: Dr. Khan Zaib Jadoon
Professor
IIU, Islamabad

(b) External Examiner 2: Dr. Naeem Ejaz
Professor
UET Taxila

(c) Internal Examiner : Dr. Mohammad Javed Hyder
Professor
CUST, Islamabad

**Supervisor Name :** Dr. Majid Ali
Professor
CUST, Islamabad

**Name of HoD :** Dr. Ishtiaq Hassan
Professor
CUST, Islamabad

**Name of Dean :** Dr. Imtiaz Ahmed Taj
Professor
CUST, Islamabad

# AUTHOR'S DECLARATION

I, **Erum Aamir (Registration No. DCE-153002)**, hereby state that my PhD thesis titled, '**Precipitation Variability in Connection with Various Potential Determinants**' is my own work and has not been submitted previously by me for taking any degree from Capital University of Science and Technology, Islamabad or anywhere else in the country/ world.

At any time, if my statement is found to be incorrect even after my graduation, the University has the right to withdraw my PhD Degree.

Erum Aamir

**(Erum Aamir)**

Dated: January, 2022 Registration No : DCE153002

# PLAGIARISM UNDERTAKING

I solemnly declare that research work presented in the thesis titled "**Precipitation Variability in Connection with Various Potential Determinants**" is solely my research work with no significant contribution from any other person. Small contribution/ help wherever taken has been duly acknowledged and that complete thesis has been written by me.

I understand the zero tolerance policy of the HEC and Capital University of Science and Technology towards plagiarism. Therefore, I as an author of the above titled thesis declare that no portion of my thesis has been plagiarized and any material used as reference is properly referred/ cited.

I undertake that if I am found guilty of any formal plagiarism in the above titled thesis even after award of PhD Degree, the University reserves the right to withdraw/ revoke my PhD degree and that HEC and the University have the right to publish my name on the HEC/ University Website on which names of students are placed who submitted plagiarized thesis.

Erum Aamir

**(Erum Aamir)**

Dated: January, 2022

Registration No : DCE153002

# *List of Publications*

It is certified that following publication(s) has been made out of the research work that has been carried out for this thesis:-

**(a) Journal paper**

1. Aamir, Erum, and Hassan, Ishitaq (2020). "The impact of climate indices on precipitation variability in Baluchistan, Pakistan." In: Tellus A: Dynamic Meteorology and Oceanography.

**(b) Conference Paper**

1. Aamir, Erum, and Ishitaq Hassan. "Trend analysis in precipitation at individual and regional levels in Baluchistan, Pakistan." In IOP Conference Series: Materials Science and Engineering; IOP Publishing: Bristol, UK,2018 p. 012042.

**(Erum Aamir)**
Registration No: DCE153002

# *Acknowledgements*


- In the name of Allah, the Most Gracious and Merciful, I am thankful to Almighty Allah, who blessed me with the intellect, courage, strength, and patience to complete **my research**.

- I would like to pay my sincere gratitude to my supervisor **Engr. Dr. Prof. Majid Ali** and co-supervisor **Engr. Dr. S. Shujaa Safdar** the for their extremely proactive cooperation and academic guidance for my research work.

- I am also thankful to **Engr. Dr. Ishtiaq Hassan** for his supervisory role during synopsis and research of precipitation variability. In addition I am thankful to CE faculty and Dean FoE for their valuable suggestions during my research work.

- I am thankful to **Engr. Dr. Prof. Sher Jamal, Dr. Zia Hashmi, Dr. Muhammad Latif and Engr. M. AbuBakar Tariq** for extended guidance through out the climate study, statistical analysis and modeling performed in this research.

- My deepest gratitude goes to my beloved parents, for their endless love, prayers, sacrifices and encouragement throughout my life and especially during my PhD. My PhD would have never been completed without their blessings and support. I am greatly indebted to and appreciate my husband Aamir Ghori, for his support. I am also thankful to my sweetest daughter Maria Aamir, my sons, Ismail Siddiqui Ghori and Usman Siddiqui Ghori for their love and support.

**(Erum Aamir)**

Registration No: DCE153002

# *Abstract*

Climate change due to global warming has given rise to many challenges, especially the variation in precipitation trends which are resulting in the extended possibility of more droughts and floods. Global Climate Risk Index (GCRI) has reported Pakistan as the 5th most affected and vulnerable country in the world which is an alarming situation. Baluchistan, the most affected province of Pakistan, is selected, as the study area for this doctoral research. Baluchistan is under drought warning by Pakistan Meteorological Department (PMD) and faced many severe droughts in the past few decades. According to the reports, 62 % of the people of Baluchistan are deprived of safe drinking water and more than 58 % of its land is uncultivated due to water scarcity. As a result, the water crisis in Baluchistan should be tackled on a war footing.

Mann-Kendall (MK) statistical test is used to identify the monthly significant precipitation trends in thirteen meteorological stations located in four regions of Baluchistan. Theil and Sens slope method (TS) is used to compute the magnitude of the trends. Partial Mann-Kendall (PMK) test is performed to study the trend variations in precipitation in the presence of climatic indices as covariates. Variability patterns of precipitation are identified through Principal Component Analysis (PCA) and their corresponding time series (PCs) are also made. Empirical Orthogonal Analysis (EOF) is performed on Sea Surface Temperature (SST), Sea Level Pressure (SLP), and Zonal Wind Surface (ZW-S) to determine the dominated teleconnections. Correlation analysis is also performed between time series of precipitation and climate indices, SST anomalies, atmospheric circulations such as SLP, Geopotential Heights (500 hpa), and Zonal winds (surface) to observe their relationship and influence on precipitation. Modeling, and validation are done using both Multilinear Regression (MLR) and Principal Component Regression (PCR) and prediction has been done for the next five years.

Baluchistan receives its greater portion of rainfall in the winter and spring months. Variation in trends, i.e. increase/decrease in precipitation are observed in months of January/June when the time series data is analyzed through Mann-Kendall test.

The change in precipitation, trends under the influence of climatic indices are determined through PMK for January and June in Region-1. EQWIN, ENSO-MEI, and EMI-MODOKI show moderate to strong influence on precipitation. Model using MLR technique identified the North Atlantic Oscillation (NAO), Arctic Oscillation (AO), EQWIN, and EMI-MODKOI as the potential determinants causing variability in the precipitation of Baluchistan. The second model using the PCR technique is also developed to address the multicollinearity among variables. Apart from other variables that are identified as potential determinants, PCR also shows that EQWIN is a significant potential determinant having a strong positive impact on precipitation variability in Baluchistan. Hence, endorsing the novelty of this doctoral research. PCR model produces more authentic, accurate, and statistically reliable results as compared to the MLR model. Other studies using both PCR and MLR techniques also confirm that PCR is better than MLR. Therefore, based on the current findings along with previous studies, it can be concluded that the PCR technique is better than MLR. And PCR is recommended for further study as well as for detailed analysis.

**Keywords**: Precipitation Variability, Trends Analysis, Potential Determinants, Climatic Indices, Mann-Kendall, Partial Mann-Kendall, Empirical Orthogonal Function, Multilinear Regression, Principal Component Analysis.

# Contents

# List of Figures

# List of Tables

# Abbreviations

| | |
|---|---|
| **ADB** | Asian Development Bank |
| **AGCM** | Atmospheric General Circulation Model |
| **AMO** | Atlantic Multi-decadal Oscillation |
| **AO** | Arctic Oscillation |
| **CEIO** | Central Equatorial Indian Ocean |
| **CPEC** | China Pakistan Economic Corridor |
| **CPIC** | China Pakistan Investment Corporation |
| **DMI** | Dipole Mode Index |
| **EEIO** | Eastern Equatorial Indian Ocean |
| **EMI** | ENSO Modoki Index |
| **ENSO** | El Nino Southern Oscillation |
| **EOF** | Empirical Orthogonal Functions |
| **EQUINOO** | Equatorial Indian Ocean Oscillation |
| **EQWIN** | Equatorial Indian Ocean Zonal Wind Index |
| **ESRL** | Earth System Research Laboratories |
| **GCRI** | Global Climate Risk Index |
| **GPH** | Geo-potential Heights |
| **ICTP** | Information Collection Transfer Processing |
| **IOD** | Indian Ocean Dipole |
| **IPCC** | Intergovernmental Panel on Climate Change |
| **ISMR** | Indian Summer Monsoon Rainfall |
| **JAMSTEC** | Japan Agency for Marine-Earth Science and Technology |
| **MEI** | Multivariate ENSO Index |
| **MK** | Mann-Kendall |

| | |
|---|---|
| **MLR** | Multiple Linear Regression |
| **NAO** | North Atlantic Oscillation |
| **NCAR** | National Center for Atmospheric Research |
| **NCEP** | National Centers for Environmental Prediction |
| **NOAA** | National Oceanic Atmospheric Administration |
| **OBOR** | One Belt One Road |
| **OLR** | Outgoing Longwave Radiation |
| **PC** | Principal Component |
| **PCA** | Principal Component Analysis |
| **PCR** | Principal Component Regression |
| **PDO** | Pacific Decadal Oscillation |
| **PMD** | Pakistan Meteorological Department |
| **PMK** | Partial Mann-Kendall |
| **QBO** | Quasi-biennial Oscillation |
| **R1JANP** | Region 1 January Precipitation |
| **R1JUNP** | Region 1 June Precipitation |
| **SDG** | Sustainable Development Goals |
| **SLP** | Sea Level Pressure |
| **SSE** | Sens Slope Estimator |
| **SST** | Sea Surface Temperature |
| **SPEEDY** | Simplified Parameterizations, PrivitivE-Equation Dynamics |
| **TS** | Theil and Sens slope |
| **UNDP** | United Nations Development Programme |
| **WEIO** | Western Equatorial Indian Ocean |

# Chapter 1

# Introduction

## 1.1 Prologue

Planet Earth is warming up, according to a report of the Internal Governmental Panel on Climate Change (IPCC) there is an average rise in temperature of 0.85°C globally from 1880-2012 [1-3]. The IPCC has predicted the temperature increase of 2.5 to 10 °F over the succeeding century [4]. This rise in the global temperature of the planet is causing deep, devastating and catastrophic effects on the planet, mankind, environment, ecosystem, and biodiversity [5-6]. Climate change has raised multiple challenges for mankind, such as droughts, floods, lightnings, windstorms, thunderstorms, hailstorms, tornados, cyclones, hurricanes, heat waves and cold waves [7-8]. Climate change is expected to affect people globally in terms of altering their physical activities [9-10]. Studies have already reported variation in intensity and frequency of precipitation pattern, extremes in temperature, increase in the intensity of hurricanes, melting of glaciers, rise in sea level endangering the low altitude islands, unprecedented thunderstorms, droughts, more recurrence of dangerous hot and cold waves, seasonal variation, increase in flooding and landslide, increased air pollution in different parts of the world [11-12]. Climate change risks threat that cannot be irreversible and may lead mankind to extinction [13-14]. Evidence of climate change adversities are obvious all around the globe [15-26].

South Asia, due to its population, demography, economy and importance, is a hot spot for climate change impact [27-28]. Global climate change is adversely impacting the Asian region, as this region is experiencing a rise in frequency and magnitude of extreme precipitation events [29-33]. But, on the other hand, climatologists have also predicted significant rise in drought risk [34-37]. Pakistan, having a very significant, decisive location in South Asia, is also sternly effected by floods and droughts due to climate change [38]. Studies have reported heavy floods from 2000 to 2015 due to extreme precipitation events in Pakistan, India and China [39-43]. Understanding variation in occurrence and magnitude of extreme precipitation events is of utmost significance in comprehending the relevant developing issues, linked with it such as, flash floods, thunderstorms, cyclones, landslides, mudslides, downpours, glacial lake outburst floods, dryness and droughts. And to issue warnings and alerts, preparing plans and layout their mitigation techniques [44-46]. Furthermore, inconsistency in rainfall grossly impact agriculture, food production and security, hydro-power generation, availability of water, unpredictability inland navigation, ecosystem, biodiversity and disaster management sector, ultimately resulting in increasing the risk of high mortality [47-52].

Global Climate Risk Index (GCRI) is a global indexing organization that publishes annual reports and enlists the most vulnerable countries due to climate change catastrophes. The analysis in the report is based on the impacts of extreme weather incidents, level of exposure, vulnerability, associated socio-economic data and death tolls. The annual risk index in the report shows the level of exposure to extreme events, which countries must take as warnings in order to be ready for more recurring and/or more severe events. Pakistan was ranked as the eighth most vulnerable nation by the Global Climate Risk Index report from 1998 to 2017 [53]. Additionally, the GCRI report's latest version in 2018 has updated Pakistan from 8th position to 5th position as the most affected and the most vulnerable country. According to the same GCRI report, Pakistan has lost 9,989 lives, suffered economic losses worth $3.8 billion and experienced 152 major weather events [54]. The report further emphasized that Pakistan is not only in the list of most effected and most vulnerable countries, but Pakistan's vulnerability is increasing

with each passing day. There are several other international reports and reporting agencies, like the United Nations Development Programme (UNDP) and Asian Development Bank (ADB) which are endorsing the susceptibility of Pakistan to climate change adversities [55-56]. GCRI in their report, encourages the world, and concerned authorities, for taking measures to cope with the danger, risk and challenges that climate change poses to mankind. The vulnerable region, such as Baluchistan should be on high priority. Baluchistan, the new vibrating economic front of Pakistan, has faced many recurring severe droughts in the past few decades due to continuous decreasing precipitation patterns [57-62]. This PhD research has taken up Baluchistan province as a study area because of its rich natural resources, vibrating economy, and international Gwadar port. Undoubtedly numerous climate studies have pointed out the decreasing precipitation pattern of Baluchistan but no focused research, statistical analysis, and prediction modeling has been done on Baluchistan.

## 1.2 Research Motivation and Problem Statement

Precipitation is the key factor in controlling the agricultural sector of any country. All agricultural countries monitor their precipitation pattern closely because it plays a vital role in agriculture, infrastructure development for water resources and their better management for optimum utility. Pakistan is also an agricultural country and one of the major components of it's economy depends on it. The agricultural sector contributed nearly 22.04% of GDP in 2019 according to government statistics [63-64]. Accordingly, the agriculture sector is the largest employer, fascinating 44% of the country's total labor force. Anthropogenic activates have changed the weather patterns of the entire world including the precipitation trend of the study area i.e. Baluchistan province [65-70]. Variation in precipitation has an adverse impact on agriculture consequently effecting the infrastructure, GDP and economy of any country [71-72]. Concurring to the United Nations Development Program (UNDP) [73] reports, Pakistan will become a water scarce country from a water stressed country by 2025, if serious measures are not taken now.

The situation is already worse in Baluchistan. Water is already scarce in the said region and precipitation, which is the main source of fresh water is also decreasing. All around the world groundwater plays a major supporting role in the agriculture sector. Similarly, crop production in Baluchistan predominantly relies on ground water. Groundwater table has depleted sharply due to recurring droughts, extensive pumping and decrease in precipitation. The Ground water table is decreasing at an alarming rate of 5 meters annually in some valleys like Quetta, Pishin and Mustang [74-76]. According to a report in daily Dawn, 62% of Baluchistan people are deprived of safe drinking water and nearly 58% of Baluchistan's area is nonproductive due to water scarcity [77]. Baluchistan also suffers from devastating sporadically catastrophic flash floods due to torrential rainfall. Almost every year, it is manifested on electronic and print media that during monsoon due to torrential rainfall, devastating flooding occurs causing loss of precious human life, property, and livestock. These facts are duly admitted through the published print media.

According to a WHO report, heavy rainfall on 20 $^{th}$ February 2019 affected 3 districts of Baluchistan . In Turbat alone, 150,000 people were affected, and 15 health facilities were damaged due to rainfall [78]. Therefore, Baluchistan's precipitation trend should be thoroughly investigated and monitored closely. Furthermore, it is also worth noticing that a substantial portion of CPEC and Gwadar port is also located in this province, such overlook may put CPEC, Gwadar port along with a foreign investment of $62 billion at risk [79]. This research work will help to achieve Sustainable Development Goals (SDGs) 2030 which are universal call made by the United Nations in the form of seventeen (17) SDGs.They aim to transform our world. This study addresses three SDGs namely, **SDG # 6: Clean water** because precipitation address 60% need of fresh water in the study area, and also recharge the depleting ground water. **SDG # 11: Sustainable sites and communities** to reduce the negative impact of natural disasters, such as flooding/drought, heat/cold waves and **SDG # 13: Climate action** as precipitation patterns, strongly control the frequency of droughts and floods [80, 81]. It will increase awareness, of people against climate change.

Thus, the problem statement is as follows: *"There is a perpetual decrease in precipitation trend of Baluchistan. Precipitation is the only source of fresh water in Baluchistan. The decrease in precipitation trend has caused catastrophic droughts and famine like situations in past few decades [82-85]. Global warming and consequent climate change appear to be responsible for the variation in the precipitation trend [86-87]. Variability in precipitation trend due to climate change is one of the major challenge faced by Pakistan and the province of Baluchistan where the situation is already worse. This scenario has led to recurring droughts of different span and intensity since last few decades and has caused famine in some areas [57]. The situation after 2013 has become even more distressing due to 74% decrease in precipitation resulting in adverse impacts on agriculture, livestock, water administration, food security and livelihoods etc. Pakistan Meteorological Department (PMD) has issued several drought alert warning for the province of Baluchistan,and the most recent one was in 03 june 2021 due to 60% decrease in Baluchistan Precipitation [88].This study will help people of Baluchistan to plan their crop cultivation, livelihood and livestock. It will also increase awareness of people about flash flood due to unprecedented torrential rain. Study will also reduce the danger and impact of flood and drought by the early warnings."*

### 1.2.1 Research Questions

The research questions related to this doctoral study are listed below :

- What could be the dominating precipitation trend of the study area?
- Which climatic indices, or large scale oceanic-atmospheric circulations are causing a significant influence on the precipitation trend of the study area?
- Is there any correlation between the factors effecting precipitation? How significant is that correlation?
- How different modeling techniques can be used to validate and predict the potential determinants causing precipitation variability?

### 1.2.2 Research Hypotheses

This doctoral research is conducted on basis of the following research hypothesis, which is tied up with the first and second research questions.

*Hnull1 = There is no trend in the precipitation pattern of the study area.*
*Halt1 = There is a trend in the precipitation pattern of the study area.*

*Hnull2 = The climatic indices, and large scale oceanic-atmospheric circulations are independent variables.*
*Halt2 = The climatic indices, and large scale oceanic /atmospheric circulations are dependent variables.*

*Hnull3 = The factors effecting precipitation have a significant correlation.*
*Halt3 = The factors effecting precipitation have no significant correlation.*
Furthermore, Pearson correlation is performed to test research question number 3 and statistical modeling is performed to test research question number 4.

## 1.3 Overall Goal of the Research Program and Specific Objectives of this PhD Study

The overall goal of the research program is to find potential determinants that cause variability in the precipitation trend.

The specific objectives of this doctoral study are:

- *To carry out trend analysis of precipitation, study the variation in trend, and identify significant determinants influencing precipitation.*
- *To conduct impact analysis of large scale oceanic, atmospheric circulations and significant potential determinants influencing precipitation trends.*

- *To develop two different models for identifying the potential determinants defining precipitation variability.*
- *Comparing the output of the models and recommend the best among them.*

## 1.4 Scope of Work and Study Limitations

The study is performed using monthly precipitation data from 13 PMD stations located all over Baluchistan. Climate indices North Atlantic Oscillation (NAO), Arctic Oscillation (AO), Atlantic Multi-decadal Oscillation (AMO), Multivariate ENSO Index (MEI), ENSO Modoki Index (EMI), Dipole mode index (DMI), and Pacific Decadal Oscillation (PDO) relevant to the study area are selected. The novel indices Equatorial Indian Ocean Zonal Wind Index (EQWIN), which was never considered in the study area was selected to establish the innovation of this study. Large atmospheric and oceanic circulation (SLP, SST, GPH, and ZW) at 850 hpa, 500 hpa, 300hpa, 200hpa are considered. Statistical techniques Mann-Kendall (MK), Partial-Mann Kendall (PMK), Empirical Orthogonal Function (EOF) analyses, Multi Linear Regression (MLR) and Principal Component Regression (PCR) are use to identify the potential determinants.

The study period is confined to 39 years (1977-2015) due to the non-availability of continuous data prior to 1977. A span of 39 years is not enough to study multi-decadal climate indices like PDO and AMO because their cycles may vary 20-30 and 20-40 years respectively [89-90]. High resolution gridded data is not available for most of the indices except SST, which would otherwise be beneficial in obtaining the refined EOF patterns and improving the significance of the results. PMD stations are irregularly and sparsely located in Baluchistan which results in difficulty to interpolate and extrapolate the data. Climate and weather prediction involves complex processes and huge reanalysis data sets, having multicollinearity. In addition, precipitation data is not normally distributed hence not suitable for parametric analysis. Therefore, nonparametric analyses are performed which are less powerful than parametric analysis.

### 1.4.1 Rationale behind the Selection of Variables

Baluchistan's weather is mainly governed by Westerly Disturbances in winter and spring months and by Monsoon in summer months. Climate indices that influenced the Westerly Disturbance are NAO and AO. Whereas Monsoon is influenced by DMI, EQWIN, ENSO-MEI and EMI-MODOKI indices. Furthermore, the decadal and multi-decadal indices of PDO in the Pacific Ocean and AMO in the Atlantic Ocean enhances or suppresses the effects of NAO, AO, DMI, EQWIN and ENSO. Therefore, the precipitation in Baluchistan may be influence by the above-mentioned climate indices. ENSO-MEI, EMI-MODOKI, PDO are sea surface temperature (SST) based indices in the Pacific Ocean, whereas AMO is SST based index in the Atlantic Ocean and DMI is SST based indices in the Indian Ocean. NAO and AO are sea level pressure related index in the Atlantic Ocean and Arctic region. EQWIN is the atmospheric counterpart of DMI in the Indian ocean based on zonal winds. Hence, SST, SLP, GPH and ZW are considered as large ocean and atmospheric circulations for studying the correlation with the Baluchistan precipitation.

## 1.5 Novelty of Doctoral Study, Research Significance and Practical Implementation

The novelty of the current study is to assess the impact of climatic indices namely Dipole Mode Index (DMI), Equatorial Indian Ocean Zonal Wind Index (EQWIN), Multivariate ENSO Index (MEI) and ENSO Modoki Index (EMI) that have never been evaluated on the study area i.e. Baluchistan province in addition to previously assessed North Atlantic Oscillation (NAO), Arctic Oscillation (AO), Atlantic Multi-decadal Oscillation (AMO) and Pacific Decadal Oscillation (PDO) on precipitation trend in said region. In previous studies, the relationship between the climatic indices and precipitation on Pakistan was carried out using Correlation Coefficient whereas, in the current work, Partial Mann-Kendall (PMK) is used to

study the influence of climatic indices on precipitation. Statistical analysis and modeling in climate are very important but it has drawbacks like huge data set, complex process, and correlated predictors. To overcome these drawbacks, two different modeling techniques namely, Multi Linear Regression (MLR) and Principal Component Regression (PCR) are adopted. MLR technique is simple and easy to follow, however, it cannot address the multicollinearity among predictors. To combat multicollinearity, another technique known as; Principal Component Regression (PCR) is selected. PCR not only addresses multicollinearity among predictors but also reduces data sets and variables. PCR helps in finding the most relevant predictors that are responsible for causing maximum variability in the precipitation. The study is further enhanced by post estimation residual analysis to check the validity of all estimated equations. Independent and identically distributed residuals guarantee the validity of the results of estimated models. For this purpose, concurrent auto-correlation and heteroscedasticity tests are employed. After validation and estimation, both the techniques were compared to propose the best between them for climate study.

This study will help the people of Baluchistan, by early an warning to adopt mitigation measures against droughts and flash floods due to unprecedented precipitation variation. It will also assist CPEC authority and Gwadar port authority to deal with precipitations odds in the long term. In addition, this study would be useful for National Disaster Management Authority (NDMA) and policy makers to comprehend the situation given in view of the climate change to make policies, strategies and preventive measures. The analysis done in this current study will be baseline research to compare the effect of anthropogenic activity on precipitation trends. Furthermore, this study would be helpful for the meteorologist to better tune their models for accurate weather prediction.

## 1.6 Brief Methodology

The brief methodology to obtain the objectives of this study is as follows:

**Literature Review:** A comprehensive literature review is conducted to identify the research problem and to set the objectives of the study.

**Data Acquisition, Analyses and determination of trends:** Initially, the data for the dependent variable (precipitation) and potential determinants (climatic indices and variables responsible for the changes in large-scale circulations) is acquired. Then, the precipitation data is analyzed for normality, skewness and kurtosis using different statistical tools. The trend in precipitation data is then determined by using non-parametric techniques.

**Influence of variables on precipitation:** The influence of potential determinants (climatic indices and large-scale circulations) on precipitation is identified by using trend analysis, pattern analysis with Empirical Orthogonal Functions and association of potential determinants with principal components of precipitation.

**Multi Linear Regression (MLR) Modeling and Validation:** The regression model is prepared for the estimation of potential determinants defining precipitation variability with the help of MLR by using Climate Indices and Large-scale Circulations. The outcome of the analysis is validated through different statistical tools and techniques. The model obtained is then put to test for post estimation analysis to verify the validity and accuracy. **Principal Component Regression (PCR) Modeling and Validation:** Principal Component Regression (PCR) is a technique for transforming data to make un-correlated regressors known as Principal Components (PCs) and to use them instead of original data. The use of PC's helps reduce the redundant variables and addresses multicollinearity. The model output is subjected to post estimation analysis for validity and accuracy check. Future prediction was performed. The models obtained from both MLR and PCR techniques are then compared for their best suitability.

**Conclusion and Recommendation:** Based on the analyses and modelings that are being carried out, conclusions are made, and future recommendations are proposed accordingly.

## 1.7 Thesis Layout

The brief layout of this thesis is as follow, which is also depicted through the flow chart in Figure 1.1.

**Chapter 1** provides a broader overview of the research work being carried out in this study. It defines the problems at hand that need to be addressed due to climate change and global warming . The novelty of the study is also discussed in this chapter. Furthermore, research questions and research hypotheses that needs to be addressed for achieving the overall goal of this doctoral study are also identified herewith. Thus, the chapter offers a broader perspective to conduct the research.

**Chapter 2** includes a comprehensive literature review of the subject at hand. This chapter not only highlights the drought condition and water scarcity prevailing in Baluchistan, but also explains the significance of precipitation for the survival of the people of Baluchistan, in terms of it's infra structure, economy, trade, finance, demography, environment, culture, and socio- economic conditions. This chapter also explains the other important reasons, like the presence of Gwadar port, China Pakistan Economic Corridor CPEC, one of the biggest Exclusive Economic Zone (EEZ) and foreign investment of $62 billion, to perform this study.

**Chapter 3** outlines the research methodology that is adopted to carry out the precipitation trend analysis. The methods and techniques are discussed in depth that is utilized to do this analysis. Furthermore, collection of precipitation data for the study span (1977-2015) i.e. 39 years from 13 stations of the study area, processing of data as per accepted standards in the literature review, quality tests on the data to validate its appropriateness for research work and trend analysis that are being carried out on the data are explicitly described. Chapter 3 also deals with the impact and influence of large scale oceanic and atmospheric circulation on the study area. It describes the variation and its significance in the precipitation trend caused by climatic indices due to naturally occurring large-scale oceanic,

atmospheric circulation and climate variables, like; sea surface temperature, sea level pressure, zonal wind and geopotential height at significant atmospheric levels.

**Chapter 4** comprises of developing model by using Multilinear Regression Analysis (MLR) technique for estimation of the potential determinants that are responsible for causing the variability in the precipitation trend of the study area. It includes performance indices of the model and post estimation residual analysis to check the validity of all estimated equations.

**Chapter 5** contains modeling and validation by applying Principal Component Regression Analysis (PCR) to find the potential determinant causing the variability in the precipitation trend of the study area. PCR is the most suitable technique for climate modeling as climate prediction is a very complex process, that involves a huge data set and a large number of independent variables. PCR helps to find significant variables that explain most of the variance in the data set. One of the serious drawbacks of climate modeling is that the independent variables might be highly correlated. PCR modeling technique is the best way to address multicollinearity. PCR uses uncorrelated Principal Components (PC) as regressors in place of original variables. This chapter also includes the comparison of both the modeling techniques (i.e., PCR and MLR) based on their performance indices and post estimation residual analysis and that ends up with the recommendation of best the modeling technique for climate study.

**Chapter 6** shows the conclusions drawn from the trend analysis, statistical analysis and modeling that is being carried out in the study. Some future recommendations are also made in this chapter.

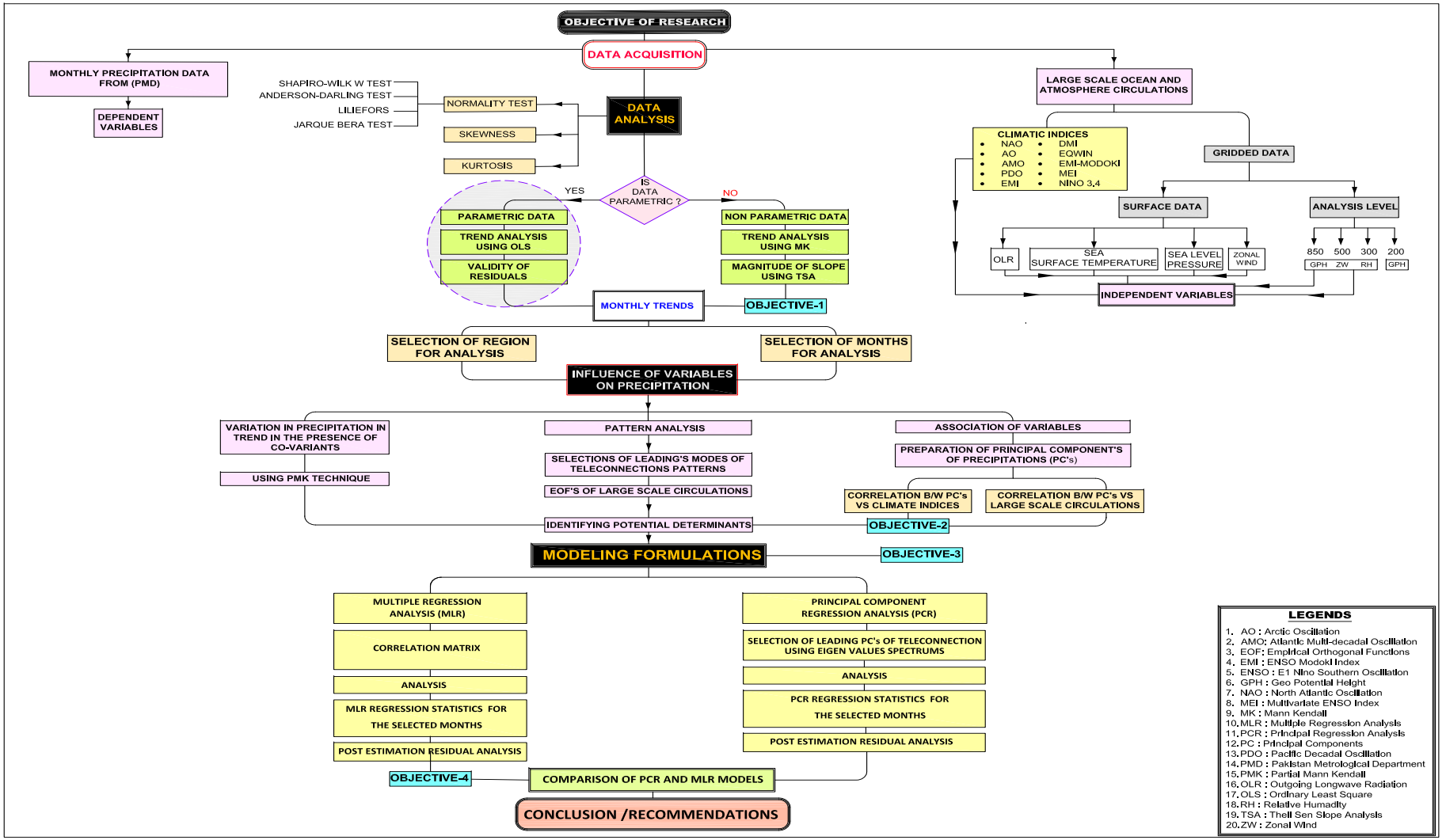


FIGURE 1.1: Flow Chart Showing Thesis Layout

# Chapter 2

# Literature Review

## 2.1 Background

Climate change and global warming had influenced the precipitation pattern of the entire planet [91-93]. The precipitation trend had gained worldwide attention as its variation can led to numerous severe dynamic and long-term catastrophic incidents [94-95]. It had caused significant disasters like cloud bursts, flooding, and severe droughts [96-99]. Monitoring and assessing the Spatio-temporal dynamics of precipitation patterns and their variability in the context of climate change has become mandatory in climatology, particularly in a country like Pakistan, where the economy is dependent mainly on rain-fed agriculture. Agriculture is one of the most climate-sensitive sectors of the economy [100].

Numerous research studies carried out in the past were successful in establishing the fact that large scale atmospheric and oceanic circulation (also known as teleconnections) were linked with many different phenomena around the world like global warming, variability in the stratosphere ozone, unprecedented ocean warming, wildfire, droughts floods, bird migration, bird population dynamics, fish population, marine and terrestrial ecosystem, Siberian snow cover, river hydrology, etc. [101-103]. The most dominant effect of teleconnections was on the

weather and climate of our planet and variations in the precipitation trend [104-107]. Thus, teleconnections patterns were described as recurring and persistent, large-scale patterns of temperature, pressure and circulation anomalies extending over large geographical areas [108-111]. Some of these teleconnections were of planetary-scale in size and span over entire ocean basins and continents [112-117]. Teleconnections referred to the climate variability in sea surface temperature, sea surface pressure, zonal wind, humidity, etc., in the troposphere and between non-contiguous geographic regions [118]. Teleconnections are the fundamental component of the climate system globally, with the frequency of climate variations on weekly, monthly, interannual and decadal time scales [119-121]. This variation may have a very strong to weak or insignificant influence on precipitation trends causing drought, down pours and torrential rains. A comprehensive understanding of these teleconnections is helpful in planning water resources, agriculture and livelihood. For example, there were several different teleconnections patterns around the globe and the two most prominent and well-known were El Nino Southern Oscillation (ENSO) and North Atlantic oscillation (NAO) [122]. ENSO impacts were sensed in remote regions of the globe through its atmospheric teleconnections. Climatologists claimed that the ENSO was responsible for the seasonal hurricane in the Northwest Atlantic region. ENSO can also be related to extreme weather events worldwide, such as severe droughts and powerful windstorms [123-128]. ENSO was affecting the commodity market worldwide by creating a wet and dry spell, as shown in Figure 2.1.

The North Atlantic Oscillation (NAO) was considered as one of the main source of climate variability in Eurasia, Greenland, North America, and North Africa [129]. NAO played a significant role in controlling weather and climate over the Atlantic region, including the United Kingdom, as shown in Figure 2.2 [130].

Besides ENSO and NAO, the teleconnection patterns, namely, AO in the Arctic Ocean, IOD and EQWIN in the Indian Ocean and multidecadal teleconnection patterns of AMO and PDO also have significant influence on the global climate [131-136]. The current study focuses on determining the precipitation trends and influence of teleconnections (variables) on precipitation in Baluchistan, Pakistan.

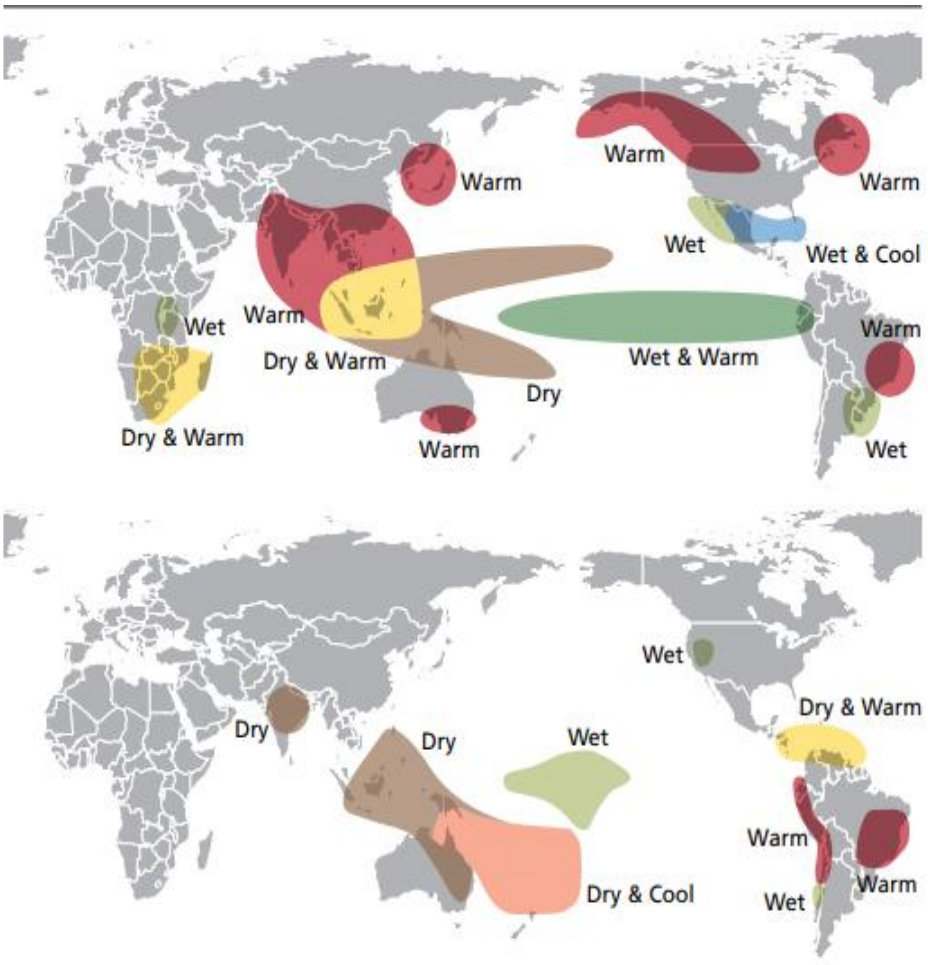


FIGURE 2.1: The remote effects of El Nino Southern Oscillation (ENSO)[137].

These influencing variables may be the potential determinants causing precipitation variability in this region.

## 2.2 Precipitation Pattern in Baluchistan

About 58% of Baluchistan's total rainfall occurs in winter due to Western Depression, arising from the Mediterranean Sea and 31% of the total rainfall occurs during the monsoon season, originating from the Bay of Bengal. Its precipitation is less affected by the monsoon; however, the influences of tropical storms in coastal areas in autumn were prominent [138]. The province of Baluchistan had faced many severe droughts and was already under drought warning by Pakistan

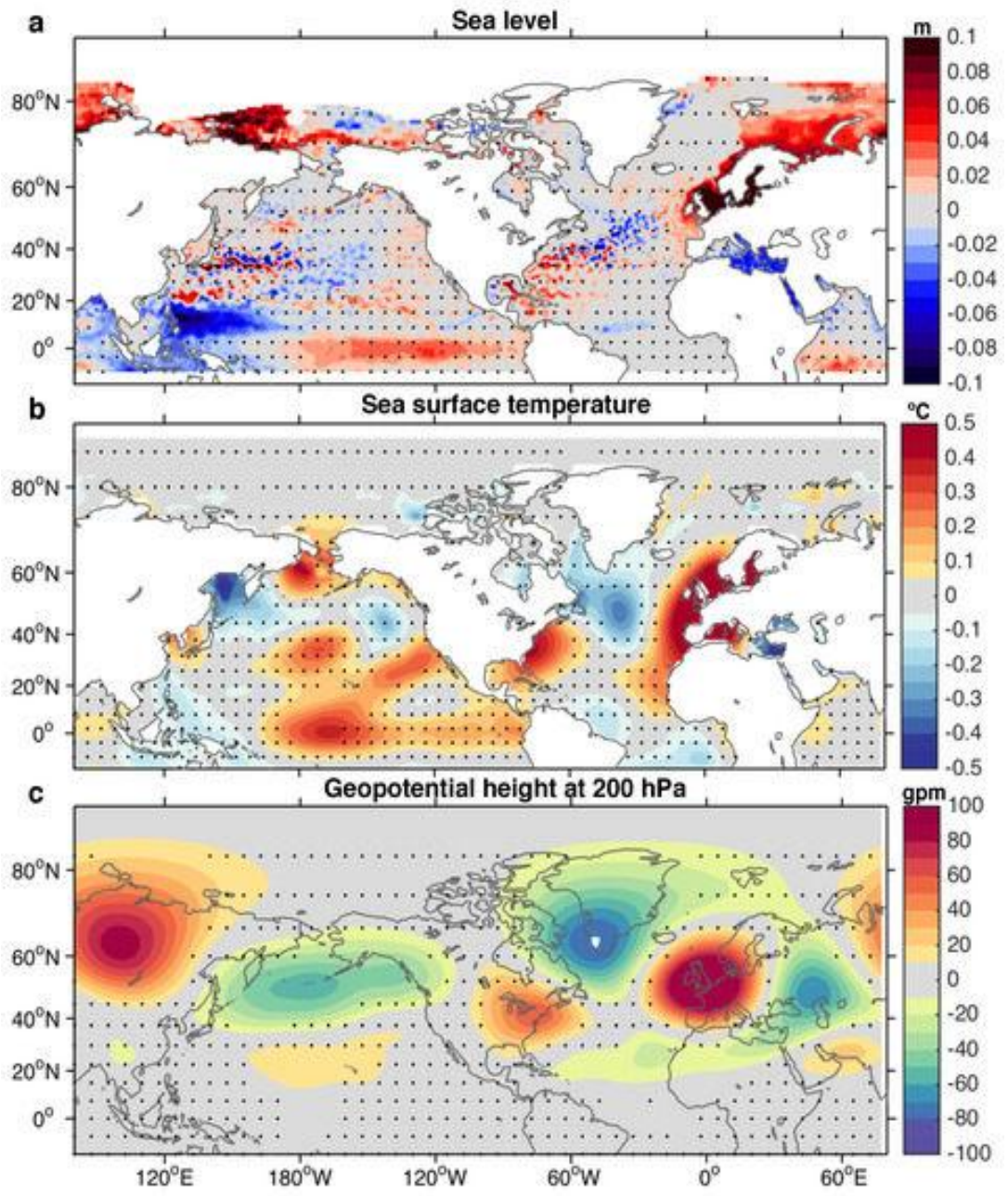


FIGURE 2.2: Impact of North Atlantic Teleconnection Patterns on Northern European Sea Level Pressure, Sea Surface Temperature and Geo-Potential Height at 200 hpa [139].

meteorological department [140-142]. Droughts were mainly due to long-term precipitation variability and most of the studies connected them to climate dynamics [143]. Droughts had been observed to occur every four out of ten years in Pakistan, with Baluchistan province being the most drought-prone region [144-147]. Droughts had adverse impacts on the agriculture sector and their severity may

lead to food scarcity and famine [148-150]. Droughts can be more acute in semi-arid and arid regions. Pakistan's two-thirds of the land area lying in semi-arid and arid climate zones, which means that they were prone to droughts [151-154]. Several studies had reported a significant increase in heat waves frequency over Baluchistan province, which was a clear warning of more frequent and more intense droughts in the future. Pakistan Meteorological Department (PMD) off and on issue drought warnings for Baluchistan province, and the most recent one was on 03 June 2021. Recently few drought studies had also been done on Baluchistan province; however, no dedicated research had been carried out on the precipitation variability, and its link to large scale dynamics, statistical analysis and climate modeling.

Baluchistan province also suffered from devastating, sporadically and catastrophic flash floods due to erratic, unprecedented torrential rainfalls on its rugged mountains, hills, valleys and challenging topography. The erratic precipitation pattern of Baluchistan not only vary from year to year but it also vary within the year. Almost every year, it is manifested on electronic and print media that during monsoon, due to torrential rain, devastating flooding is caused along the drainage rivers causing loss of property,infrastructure, livestock and human life [155-156]. Although there is no accurate inventory of damages or the record of catastrophe, but the facts are duly admitted through the published print media and worldwide organization like World Health Organization (WHO) [157].

Last year damages due to torrential rains and flash floods as reported by World Health Organization (WHO), are presented in Table 2.1.

Table 2.1: Destruction due to Torrential Rains and Flash Flood in Baluchistan [157].

| **S.No** | **Stations** | **Affected** | **Displaced** | **Damaged** |
|---|---|---|---|---|
| 1 | Lasbella | 40,000 | 1,500 | - |
| 2 | Killa Abdullha | 55,000 | - | - |
| 3 | Turbat | 150,000 | 250-300 | 15 Health Facilities |
| 4 | Pashin | 120,000 | 8,000 | |
| 5 | Khuzdar | 60,000 | | |

## 2.3 Impact of Climate Indices on Precipitation Variability

Climatic indices were known to be the quantitative diagnostic representation of large-scale oceanic, atmospheric circulations and teleconnection patterns. These were the spatial patterns occurring in the stratosphere in the form of atmospheric and oceanic circulation. They were responsible for various remote anomalies, climate/weather, droughts/flood, extreme events, over large distances around the world [158-162]. They are of planetary scale, global scale, synoptic scale and regional scale as explained earlier. Climate indices are known to influence the precipitation pattern and trend of the study area through teleconnection. The global impact and influence of the most common climatic indices such as NAO, AO, AMO, IOD-DMI, IOD-EQWIN, PDO, ENSO-MEI, ENSO MODOKI (ENSO-EMI) are discussed below to understand their magnitude, scale, power, influence, control, supremacy, importance, intensity and strength in weather and climatology.

### 2.3.1 Global Scale Influence of Oceanic-Atmospheric Climatic Indices

Through numerous research it was well established that oceanic-atmospheric climatic indices had significant impacts on climate globally [163-171]. Few of the studies are discussed here in this context. A study conducted recently on the hydro-climatological attributes like temperature, precipitation, and potential evapotranspiration (PET), over century-spread data (1901- 2002) to understand the influence of different El Nino Southern Oscillation (ENSO) phases on the varying precipitation patterns across **North India** during the monsoon season. Trends and shifts were assessed using non-parametric statistical tests showed that the El Nino years had a strong influence in causing the hydro-climatological events compared to La Nina and neutral years. The study also helped climate researchers and policymakers to understand the importance, impact and variability resulting from

the various ENSO phases in the monsoon season as monsoon mainly dominates the precipitation pattern over South Asia [172].

A study conducted over 56 years (1961-2016) using Continuous Wavelet Transform (CWT) to evaluate the correlation between two major oceanic-atmospheric indices of the Pacific Ocean, i.e., El Nino Southern Oscillation (ENSO) and the Pacific Decadal Oscillation (PDO), with the western U.S. Snow Water Equivalent (SWE). The analysis discovered that ENSO, as compared to PDO, had a much stronger influence on Snow Water Equivalent (SWE). In Addition, regions closer to the ocean and at lower elevations showed a higher correlation as compared to the inland areas with higher elevation. The study contributed to facilitate climate forecasters and regional water managers [173]. Oceanic-atmospheric oscillations, consisting of Pacific Decadal Oscillation (PDO), North Atlantic Oscillation (NAO), Atlantic Multidecadal Oscillation (AMO), and El Nino Southern Oscillation (ENSO) throughout 1900-2008, were selected to predict annual precipitation using Support Vector Machine (SVM), Artificial Neural Network and Multivariate Linear Regression with a 1-year lead time. Precipitation predictions conducted for the upper Colorado River Basin was found to be best with the combination of PDO, NAO, and AMO indices, whereas the combination of AMO and ENSO was best for precipitation predictions in the lower Colorado River basin. When the results were compared, it was noticed that the SVM model provides better precipitation estimates as compared to that by Artificial Neural Network and Multivariate Linear Regression models [174]. Similar studies, based on the SVM model, were also carried out on spring-summer streamflow for 6-9 months in advance by incorporating the same oceanic-atmospheric oscillation indices in the model. [175, 176]. The study confirmed that the SVM model came out to be better as compared to Artificial Neural Network (ANN), and Multiple Linear Regression (MLR) model.

A data-driven model, based on Least-square Support Vector Machine (LSSVM), was developed that used interannual and decadal-scale oceanic-atmospheric oscillations, i.e., Pacific Decadal Oscillation (PDO), North Atlantic Oscillation (NAO), Atlantic Multidecadal Oscillation (AMO), and El Nino Southern Oscillation (ENSO),

to generate streamflow volumes for the peak seasons (April-October) for a period from 1955-2006. Both individual oscillation and combined oscillations analysis were done, which revealed that AMO index at the individual level and PDO, NAO, and ENSO indices in combination showed a pronounced effect. Overall, the SVM model was come out with a very good streamflow prediction for **Kaidu river, Xinjiang, China**. Also SMV was found to be a better modeling approach than Artificial Neural Network (ANN) and Multiple Linear Regression (MLR). The study was found to be useful for water managers in improving the planning and management of water resources [177]. Another study attempted to investigate the association between the regional streamflow patterns and three large-scale climate signals, i.e., El Nino Southern Oscillation (ENSO), Pacific Decadal Oscillation (PDO), and Atlantic Multi-decadal Oscillation (AMO). Non-parametric test, coupled discrete wavelet transform analyzing 237 streamflow stations for 62 years (1951-2012) was adopted. The results indicated significant positive (negative) trends and shifts in the northeastern and northwestern regions. Among the climate signals, ENSO showed the highest association ,AMO showed strong associations and PDO showed the least influence among the three. The results explained the teleconnections between the climate indices and the US streamflow variations. Results also helped to improve regional flow regulations [178].

Another research was conducted to evaluate the relationship between the Pacific Ocean climate variability and western US streamflow by using the singular-valued decomposition (SVD) technique. The data included sea-surface temperatures (SST), geopotential height index of 500 mbar (Z500), and 90 unimpaired western US stream flows from 1960-2010. The SVD model developed a Spatio-temporal relationship for each major hydrologic region with Pacific Oceanic variability. Apart from conventional El Nino Southern Oscillation (ENSO) and Pacific Decadal Oscillation PDO regions, new regions in Pacific were identified that was strongly related to the basin in the western USA. The model SVD resulted in improved correlation values of smaller spatial regions over larger regions [179]. Singular Value Decomposition (SVD) and wavelet analyses were applied to the regional streamflow of the conterminous United States and climate variabilities

like surface temperature (SST), 500-mbar geopotential height (Z500), 500-mbar specific humidity (SH500), and 500-mbar east-west wind (U500) of the Pacific and the Atlantic Ocean. The analyses helped to understand the interconnections between streamflow and climate variabilities. Both the SVD and wavelet analyses established the conclusion that the streamflow variability of the regions were strongly associated with the ENSO. The Wavelet Coherency (WTC) analyses of ENSO/PDO/AMO and the regional streamflow patterns revealed that the warm phase of SST in the ENSO-like region was positively correlated with Southwest regions and negatively correlated with Northwest streamflow. Pacific and Atlantic Ocean SST, Z500, and SH500 had a weak influence on the streamflow variability of the Northeast and the Southeast regions. The Northwest streamflow was highly correlated with both ENSO and PDO while AMO showed the highest correlation with the Southeast streamflow. The study was helpful to understand the teleconnection of climate variables with regional streamflow and stream flow prediction [180].

Another study utilized singular-value decomposition (SVD) for the period from 1961 to 2016 for determining the correlation between Snow Water Equivalent (SWE) and climate indices of Pacific and Atlantic oceans. The changing characteristics of (SWE) in the western United States and their teleconnections with the Pacific and Atlantic Oceans climatic attributes (i.e.(SST), 500-mbar geopotential height (Z500), 500-mbar east-west wind (U500)) were noticed in this study as well. The study findings helped to understand oceanic dynamics, seasonal forecast and water resources management [181]. Pacific Decadal Oscillation (PDO), Southern Oscillation Index (SOI), and Pacific Ocean (SST) were used to influence the precipitation and streamflow volumes of southwestern United States, especially California. The Sacramento River Basin (SRB) and the San Joaquin River Basin (JRB) in California had a record of recurring droughts and frequency of the historic low flow events. This research was conducted to enhance the traditional tree-ring chronology (TRC)-based streamflow reconstruction by incorporating the predictors of SST, PDO, and SOI along with TRC, in a stepwise linear regression (SLR) model. The method was successfully applied to selected gauges located in

the Sacramento River Basin (SRB) and the San Joaquin River Basin using five SLR models (SLR 15), and reconstructions were developed from 1801 to 1980 with an overlap period of 1933-1980. The research came up with an improved reconstruction skill by using the SST in combination with TRC. Overall, this study helped in a better understanding of the past regional hydrological-climatic variabilities. Additionally, the approach could be easily transferred to other watersheds [182].

Sacramento San Joaquin River Basin, California was selected as a study area for analysis using Singular Valued Decomposition (SVD) to observe the teleconnections of the streamflow corresponding to 500 mbar geopotential height, Sea Surface Temperature, 500 mbar specific humidity (SHUM500), and 500 mbar U-wind (U500). Non-parametrical technique was used to screen SVD teleconnections which were then used as the streamflow predictors in the non-linear regression models (K-nearest neighbor regression and data-driven support vector machine). New Spatial results were found by the SVD results that had not been included in existing predefined indices. The non-parametric model indicated the teleconnections of SHUM500 and U500 being better streamflow predictors compared to other climate variables. The regression models were suitable for drought-affected regions. The research performed was straightforward, and robust in providing qualitative streamflow forecasts that helped water managers in making policy and managing watersheds [183]. The trend analysis of the Coupled Model Intercomparison Project 5 (CMIP5)'s temperature and precipitation models for the entire Colorado River Basin were conducted. The study period selected was of 104 years (1900-2004). To find trends, four different versions of the MK test were used. Nonparametirc Theil- Sen Approach (TSA), was performed in the study. The results showed that the trends in temperature models were relatively consistent as compared to precipitation. The results clarified uncertainties and natural variabilities of temperature and precipitation. [184, 185].

Monthly precipitation, temperature and streamflow over a study period of 105 years (1906-2010) of Colorado River Basin (CRB) were analyzed using Mann-Kendall test and Pettitt test. The results indicated that the streamflow was increased during the winter-spring months and decreased during the summer-autumn

period. The shifts coincided with coupled phases of El Nino Southern Oscillation and Pacific Decadal Oscillation. The same non-parametric techniques were used and more or less the same results were reported [22]. The study helped for the water managers to understand the changing patterns of monthly precipitation and temperature on regional scales [186, 187].

Another research was carried out to explore the relationship between Western US streamflow and two of the most critical oceanic-atmospheric with having substantial effects in this area, namely, El Nino Southern Oscillation (ENSO) and Pacific Decadal Oscillation (PDO). Continuous, cross and wavelet coherence were used to analyze the relation between streamflow and climate indices. Both the ENSO and PDO showed a strong correlation with streamflow from 1980-2005. ENSO and PDO showed a strong correlation with streamflow in 10-12 years and 8-10 years band, respectively. The study helped to understand the connection between the climate indices and streamflow [188]. Oceanic, atmospheric indices have significant influence on precipitation. For strengthening this concept, the study was conducted by using 04 climatic indices. The adopted data-driven model K-star was used for long-term precipitation forecast. The model efficiency was evaluated by using loss error, namely MAE, RMSE, PBIAS, NSE, LEPS and SK. The model based on the K-star technique was found to have good predicting power. The model was helpful for long-term water resources planning and management [189]. Another very similar study was conducted to find the trend and shift using Wavelet Transform, Mann-Kendall and Pettit's test. The study was focused on analyzing variability in seasonal temperature, precipitation, and streamflow across the Midwestern United States. Two oceanic indices, namely El Nino Southern Oscillation (ENSO) and Pacific Decadal Oscillation (PDO), were also selected to find the correlation with climate variables. The results helped water managers to improved the efficiency of streamflow in the Midwestern United States [190].

Singular value statistical approach was adopted in the study, which showed a strong association between streamflow and selected climate indices.The oceanic atmosphere and indices selected were NAO, PDO, AMO and interdecadal (warm -cold phases). All indices had significant influence on the seasonal stream flow of

continental USA. The study helped improved the stream flow prediction. It also improved the streamflow management and planning [191]. Another study was conducted to investigate the change in stream flow for all four seasons for a period of 60 years (1951-2010). The study adopted non-parametric Mann-Kendall technique to find out the trend. The findings helped water management, policymaker in improving their planning of water resources under various climatic conditions [192]. Four climatic indices, namely ENSO, PDO, AMO and NAO were used to forecast streamflow in Western United States. Streamflow forecasts were done using a multiclass kernel-based data-driven support vector machine (SVM) model. Reconstructed data was used from 1658-1952 and the instrumental record was used from 1953 to 2007. The SVM model prepared was able to provide excellent predictions. The combined oscillation indices aided in better predictability as compared to the individual oscillations. Also, the SVM modeling results were better when compared with that of the multiple linear regression model. The SMV results were robust and were supposed to be very useful for long-term water resources planning and management [193]. A very similar study was conducted on Gunnison River Basin and San Juan River Basin in the Upper Colorado River Basin. With the same climatic indices, namely PDO, NAO, AMO and ENSO, the study reported the same results that the SVM model was better than artificial neural network and multiple linear regression. The outcome of the study provided helpful information for the planning and management of water resources within these basins [194].

A study over the Colorado River Basin was conducted using Mann-Kendall and Spearman's rho (to evaluate trend changes), rank-sum test (to identify the step-change in seasonal precipitation) and k-nearest neighbor (KNN) (to estimate seasonal precipitation). The results indicated a decrease in the upper basin and an increase in the lower winter precipitation resulted from an abrupt step change. The analysis of seasonal changes and estimates of precipitation helped Colorado River Basin water managers to improve management and to enhance the water resources [195].

Rainfall and other precipitation levels are important factors affecting crop selection and ecological changes in a region. Accurate prediction of precipitation trends had

an essential role in a country's future economic development [196-199]. Climate variability, particularly precipitation and temperature, had received a great deal of attention worldwide. The magnitude, intensity and frequency of precipitation varies according to the locations. Hence, examining the spatiotemporal dynamics of meteorological variables in the context of changing climate, particularly in countries where rain-fed agriculture is very important. Such types of studies were vital to assess climate-induced changes, and helped in suggesting feasible adaptation strategies also [200-203].

Trend analysis of precipitation can be performed using both parametric and non-parametric statistical techniques [204-207].The parametric analysis includes linear regression, which needs independent normally distributed data. Nevertheless, the required data scarcely exists for hydrometeorological variables [208]. On the other hand, non-parametric analysis was usually employed due to its simplicity as compared to parametric technique. Generally, Mann-Kendall (MK) and Sens Slope Estimator (SSE) were used for non-parametric analysis [209, 210]. Most of the studies that had been carried out for trend analysis in Pakistan had used non-parametric technique [211-213]. Non-parametric technique was also recommended by World Metrological Department (WMD) for such analysis [214].

### 2.3.2 Trend Analysis Using Mann-Kendall (MK)

Mann-Kendall (MK) test is widely used in various research for trend identification. It is a well established statistical technique to investigate the precipitation trends on different time scales like daily, monthly, seasonally and annually in climatology. Ahmed et al. [215] used MK trend test, bias, root mean square error to evaluate the performance of gridded precipitation products over Baluchistan province Pakistan. Iqbal and Athar [216] also adopted non-parametric Mann-Kendall statistical technique for trend analysis of precipitation and teleconnections over six administrative regions of Pakistan.The study included 38 years (1976-2013) of precipitation data from 42 stations. The result explained the precipitation variability linkages with large-scale circulations. Recently Naz et al. [57] adopted the

MK test to study Baluchistan's drought trends. Baluchistan was selected because of its worse condition due to recurring, prolonged droughts, erratic precipitation patterns, and dependence on agriculture, livestock and precipitation.

The Mann-Kendall test had been strongly recommended by World Meteorological Organization to detect the trends in hydro- meteorological datasets [214]. The MK test is very important because it does not require any hypothesis for the statistical distribution of the data and can be implemented to the datasets with inconsistent and uneven sampling intervals. The frequency of extreme precipitation occurrence was studied by gathering data of fourty one stations and analyzed through non-parametric Kolmogorov-Smirnov test. The study noted a rise in extreme precipitation events in the country. Investigation of precipitation trends through Dunnett T3 test and Variance Analysis of 30 years showed a decrease in precipitation trends. Hussain and Lee [217] examined data of 15 stations for seasonal variability of extreme precipitation events. MK test and simple linear regression were used. Increasing and decreasing of seasonal trends in extreme precipitation was identified in southwestern and northeastern part of Pakistan.
Mann-Kendall test was also adopted to explored changes in extreme precipitation events in Punjab by using data of five stations. However, no considerable trend was identified in the study [218]. Similarly, Ijaz Ahmad et al. [219] studied precipitation trends in the Swat River basin. MK and Spearman's Rho test was applied on data from 13 stations and mixture of increasing and decreasing trends were found.

### 2.3.3 Variation in Trend in Presence of Covariate Using Partial Mann-Kendall (PMK)

The influence of large-scale climate indices on the precipitation time series is examined using the Partial Mann-Kendall (PMK) test. PMK is one of the best one-step procedures that do adjustment for covariates (influencing variables) and trend testing simultaneously [220, 221]. The strength of linear association between

two variables is measure by using the Pearson correlation method. PMK is a different method to investigate the variation in precipitation's trend in the existence of climate indices which are the covariates. Precipitations trends (response variable) can be evaluated in the presence of the related covariates using PMK when the effect of the explanatory variable is removed [222, 223].

### 2.3.4 Influence of Large-scale Circulations and Climate Indices on Precipitation Variability

Climate variation is mainly due to large-scale ocean circulations, atmospheric circulations, moisture transportation and heat fluxes. Large-scale ocean circulations were examined under the influence of teleconnections which revealed the oceanic and atmospheric pattern of our climate [224-227]. Analyses of teleconnections patterns, their development and influence gave a better understanding of climate change [228-230].
The recurring pattern of global precipitation variability had been linked to climatic indices and ware discussed in numerous research [231]. Some of the climate indices like NAO, ENSO, PDO were known for their extended and remote impacts on far flung part of the world [203, 208, 211]. ENSO had dominating recurring impact on Asia Summer Precipitation [128].

The important large scale oceanic-atmospheric oscillations that were known to affect Pakistan's climate are North Atlantic Oscillation (NAO), Arctic Oscillation (AO), Atlantic Multi-decadal Oscillation (AMO), Indian Ocean Dipole-Dipole mode index / Indian Ocean Dipole-Equatorial Indian Ocean Zonal Wind index (IOD-DMI/IOD-EQWIN), Pacific Decadal Oscillation (PDO) and El Nino Southern Oscillation (ENSO) including Multivariate ENSO Index/ ENSO Modoki Index (ENSO-MEI/EMI) [110, 123, 216, 235].
**These large scale oceanic and atmospheric oscillations are discussed in detail in section 3.2.5.** Their **impacts in terms of (positive and negative) phases** on monthly precipitation pattern are discussed as follow:

**North Atlantic Oscillation (NAO)** is the standardized **Sea Level Pressure (SLP)** between the subtropical high at the Azores and low in Iceland. The positive/negative) phase of NAO indicates a stronger/weaker) than usual subtropical high-pressure center [110, 232-234]. Syed et.al [248] reported after regional modeling with RegCM3 NAO had a significant influence on the climate specifically precipitation and temperature. The focused areas for modeling mainly consists of Pakistan, Afghanistan and Tajikistan. A detailed analysis including simulated storm characteristics showed that the NAO and ENSO precipitation signals over the region were mainly associated with intensification of western disturbances originating in the eastern Mediterranean, middle east regions and moving eastward across the study area. The intensification occured during the (positive/negative) NAO phases resulted in increased/decreased of precipitation. The intensification was correlated with the effect of an increased/decreased Sea Level (SLP) and 500 hPa trough which, developed over the region during these NAO (positive/negative) phases. The study also concluded that precipitation increased during the positive phase of NAO and decreased during the negative phase NAO.

**Arctic Oscillation (AO)** The Arctic Oscillation (AO), also known as Northern Hemisphere annular mode is a climate variability of large-scale. The AO is a climate pattern described by the counterclockwise circulating winds around the arctic at 55°N latitude. AO index is related to the degree in which Arctic air enters middle latitudes. AO is characterized by surface atmospheric pressure patterns. When the AO is in its positive phase, a ring of strong winds circulating the north pole acts to restrain colder air across polar regions. In the positive phase of the AO index, the surface pressure is low in the polar region. This encourages the middle latitude jet stream to blow strongly and steadily from west to east, hence keeping cold Arctic air confined in the polar region. And in the negative phase, the circulating band of wind around the north pole becomes weaker, allowing an easier southward diffusion of colder arctic air mass which, increases storminess into the mid-latitudes. In this phase, there are more chances of high pressure in the polar region, the strength of zonal winds is mostly weak, and more penetration of freezing polar is predicted [122, 123, 232].

**Atlantic Multi-decadal Oscillation (AMO)** The AMO is defined as the detrended low-pass-filtered annual mean **Sea Surface Temperature (SST)** anomalies averaged over the north Atlantic basin [236]. Understanding the relationship between the AMO and Asian monsoon would be of great help for climate prediction and agricultural planning in Asian countries. The warm phase of AMO leads to positive Sea Surface Temperature (SST) anomalies in the eastern Indian ocean and maritime continent through coupled feedbacks. AMO warm phase also induces more local precipitations [237].

**Indian Ocean Dipole mode index (IOD)** is normally characterized by anomalous cooling of **Sea Surface Temperature (SST)** in the southeastern equatorial Indian Ocean and the anomalous warming of SST in the western equatorial Indian Ocean. IOD influence was noted in the precipitation of coastal areas, western areas, and Baluchistan regions. The same behavior was also found during the monsoon season and relatively more precipitation was observed during the positive phase of IOD. The southeasterly wind brought unusual moisture from the high-pressure areas over the Arabian sea, which caused an anticyclone. It brought more moisture from the Arabian sea to the coastal and southwestern parts of Pakistan and Baluchistan region during the positive IOD phases [216]. Therefore, positive phase of IOD may possibly be used for precipitation prediction during the monsoon season [232, 238].

**Pacific Decadal Oscillation (PDO)** is a **prolonged El Nino-like pattern of climate variability in the Pacific Ocean** and has been observed during the twentieth century. During the warm (positive) phase, the western Pacific Ocean cools and part of the eastern ocean warms on the contrary during cool (negative) phase, the western Pacific warms and part of eastern Pacific Ocean remains cool [239]. The impact of the ENSO on the northwestern Pacific is not fixed, and it depends on the phase of Pacific Decadal Oscillation.

The substantial impact of Pacific Decadal Oscillation phase change should be considered while analyzing the interannual variability in the low latitude western north Pacific Ocean.

**El Nino Southern Oscillation (ENSO)** is composed of an oceanic component El Nino (La Nina), which is characterized by **warming (cooling) of surface water in the tropical eastern Pacific Ocean**, and an atmospheric component by the southern oscillation, which is characterized by changes in **Sea Level Pressure (SLP)** in the tropical western Pacific. The El Nino and La Nina are important quasiperiodic temperature fluctuations in the surface water of tropical eastern Pacific Ocean [240]. Regional climate modeling, focused on the modeling of temperature and precipitation with emphasis on El-Nino Southern Oscillation (ENSO) and North Atlantic Oscillation (NAO), was carried out by Syed et al. [248]. The study area was Pakistan, Afghanistan and Tajikistan. The study depicted that precipitation increased during the warm phase of ENSO and decreased during the cold phase of ENSO. When the warm (cold) oceanic phase was in effect, the Sea Level Pressure (SLP) in the western Pacific was also high (low) [232, 239-24].

### 2.3.5 Empirical Orthogonal Functions (EOFs) and Principal Components

Empirical Orthogonal Functions (EOFs) and Principal Component Analysis (PCA) was applied in many studies to analyze the relationship of precipitation's trend and climate indices [242-244]. Haroon and Rasul [245] used PCA for identification of main types of oscillation in Outgoing Longwave Radiation (OLR) during the summer season and summer's precipitation (on an inter-annual basis) over Pakistan. The strong negative correlation of OLR with leading PC of summer precipitation (i.e., the indication of clouds presence) was also suggested in the study. Different research and studies also adopted Empirical Orthogonal Functions (EOFs) and Principal Component Analysis (PCA) technique to investigate the relation of atmospheric circulations with precipitation pattern index. The studies selected variables like global sea surface temperature, sea level pressure to find out potential predictors that are responsible for causing variability. It was concluded in their studies that the winter-spring precipitation in Pakistan is

strengthened/weakened by the positive (negative) of NAO. And the potential predictors for winter- spring precipitation in Pakistan could be ENSO, NAO and AO. Another research was carried out over the Arabian sea on vertically integrated moisture movement adopting EOF. The study showed clear increasing/decreasing of monsoon precipitation pattern over South Asia and predominantly over Pakistan. Study was further enhanced when the dipole pattern was found obvious on the region by using regression analysis [246].

### 2.3.6 Correlation of Climatic Indices

It is well established through research studies that ENSO and NAO have influenced the weather of Pakistan regionally and locally [129,130]. Increased impact of ENSO over NAO was suggested by [122]. Hadley and Walker's circulations are firmly influenced by ENSO. The strengthening and weakening of Hadley cell had significant influence over the monsoon precipitation pattern of South Asia [247]. ENSO teleconnection also had links with different PDO cycles in past 145 years. Iqbal and Athar [216] inspected the influence (IOD, NAO, AO, ENSO, PDO, AMO, and QBO) over Pakistan adopting Pearson's Correlation at different levels like 5%, 10% and 15%. It was reported that on a monthly basis, IOD had a very strong to strong correlation with precipitation, AO had a strong, and PDO had moderate correlation in Baluchistan. On an annual basis, AMO showed a moderate correlation, and ENSO showed a very strong correlation but on seasonal basis.

ICTP-AGCM (SPEEDY) was used recently to carry out the study on ENSO Modoki. A substantial influence of ENSO Modoki was observed not only over South Asia but also on Pacific, Atlantic, North and South America and African. Hadley cell (encourages/discourages) was found to be associated with, the positive/negative phase of ENSO (EL-Nino/La Nina), which consequently has substantial influence on South Asia [230]. Multiple regression model was used by Adnan et al. [210] to make correlated PCs to investigate the variability and predictability of monsoon precipitation over, on an interannual and intra-annual basis.

The model output was robust and accurate. The model was used proficiently in predicting inter-annual monsoon precipitation also. Based on several studies and research correlation of each oscillation with the precipitation pattern of Pakistan can be summarized as follows:

**North Atlantic Oscillation (NAO)** showed a positive correlation in Azad Jammu and Kashmir (AJK) and Khyber Pakhtun Khawa (KPK) regions with very strong correlation. The negative phase of the NAO exhibited correlation in KPK, AJK, and Punjab regions [216]. NAO was negatively correlated with the Winter precipitation of Baluchistan but are insignicant (their significance is in between 20% to 35%) and thus can be ignored [235, 248].

**Arctic Oscillation (AO)** The positive (negative) phase of the AO showed correlation with Baluchistan, Punjab, Sindh, and Azad Jammu and Kashmir region(s) with strong significance [216, 235]. The positive phase of AO increases the pressure gradient between extratropical and polar north Atlantic, forcing to develop low pressure over east of the Caspian sea and its secondaries, which affect Northern Pakistan. The positive and negative pressure anomaly over west Europe and north Africa, respectively, intensifies the Asian westerly jet stream over north Africa and Middle East extending up to NW India. The jet intensifies the western disturbances (WDs) and produces more precipitation over Northern Pakistan [122].

**Atlantic Multi-decadal Oscillation (AMO)** has a positive correlation with monsoon rainfall. The correlation of AMO was observed on Punjab region with very strong significance [236]. AMO is positively correlated with winter precipitation up to 8% signicance. AMO is in its warmer phase since 1997 and it was observed from the time series that the strength of NAO and AO are weakened during the warm AMO phase. The decreasing trend may be due to the weakening of NAO strength during the past few decades, which was negatively affecting the winter precipitation in Baluchistan region. AMO was found to be influencing the summer precipitation pattern of Baluchiatan. The influence was determined through correlation analysis, but it's strengths was weak therefore stands insignificant [235].

**Indian Ocean Dipole mode index (IOD)** the significant influence of Indian Ocean Dipole mode index was observed over entire Pakistan, which was responsible for extreme precipitation as well as drought [232, 235, 238]. Iqbal and Athar [216] reported a positive correlation between Indian Ocean Dipole mode index and precipitation in Sindh region, particularly in the coastal areas with very strong significance.The study also reported a similar correlation between Indian Ocean Dipole mode index and precipitation in the Baluchistan region as well. The positive phase of Indian Ocean Dipole mode index showed correlation with the Sindh, Punjab, Baluchistan, and Azad Jammu and Kashmir regions with very strong to strong significance.

**Pacific Decadal Oscillation (PDO)** showed a positive correlation in Gilgit Baltistan (GB) region, AJK, and Baluchistan regions with a very strong, strong, and moderate significance, respectively [216]. The substantial impact of Pacific Decadal Oscillation phase change should be considered while analyzing the interannual variability in the low latitude western north Pacific. Because the phase of the Pacific Decadal Oscillation has impact on the north western Pacific region through El Nino Southern Oscillation. Also, the interannual relationship between ENSO and the winter monsoon is weak and insignificant in the warm phase of the Pacific Decadal Oscillation [239].

**El Nino Southern Oscillation (ENSO)**, as already explained in section 2.3.3, it is composed of an oceanic component El Nino (La Nina), which is characterized by warming (cooling) of surface water in the tropical eastern Pacific Ocean, and an atmospheric component by the southern oscillation, which is characterized by changes in Sea Level Pressure (SLP) in the tropical western Pacific. The El Nino and La Nina are important quasiperiodic temperature variations in the surface water of tropical eastern Pacific Ocean [240]. The El Nino Southern Oscillation exhibited correlation in Northern areas of Pakistan (i.e., Khyber Pakhtunkhwa and AJK). Studies have shown that there is significant influence of El Nino Southern Oscillationon the spatiotemporal change patterns of three hydro-climatological variables like temperature, precipitation, and potential evapotranspiration (PET) during the monsoon season [235, 249].

## 2.4 Regression Analysis

Numerous predicting models have been developed from the mid of last century till to date using the regression technique. Regression is a widely used statistical technique in business, social, behavioral sciences, biological sciences, climate prediction, and many other areas [250-255]. Regression is a statistical, empirical technique and is widely used in business, social and behavioral sciences, biological sciences, climate prediction and many other areas [256-258]. Multiple Linear Regression is remarkably useful when it is required to predict a dependent variable (i.e., predictand) from a (very) large set of independent variables (i.e., predictors). MLR has proven to be a powerful method of analysis due to sample size and residual distributions. It is not only applied for theory confirmation, but it can also be used to recommend post estimation checks. Different orders of linear and non-linear multiple regression models are widely used for predicting time series based data set [259-261]. Multiple Linear Regression (MLR) models can contemplate more than one predictor for precipitation prediction. There are some constraints of the multiple regression technique for example multicollinearly, interrelation, extreme observation and non-linear relationship between dependent and independent variables.

### 2.4.1 Simple Regression Analysis

An analysis of normalized rainfall of nearly 167 observatory stations all over South Asia was conducted by Ramchandran. Researchers had used regression analysis and Artificial Neural Network to developed their model for the prediction of essential oil content. [262]. An interesting study in 2018 was conducted to investigate the atmospheric concentration of four important trace gases over Pakistan, namely Carbon monoxide (CO), tropospheric columns of formaldehyde (HCHO), nitrogen dioxide ($NO_2$) and ozone ($O_3$). A statistical model was developed in the research to find the long-term association of trace gases over the region using the MLR technique. The multiple linear regression technique was selected because of its

simplicity and ease to understand the linkage between the predictors and the predictand, as compared to other methods [263]. A study over Assam of similar nature was conducted to predict Indian summer monsoon rainfall variation using regression analysis [250].

### 2.4.2 Multiple Linear Regression Analysis (MLR)

Multiple Linear Regression (MLR) analysis is not only used in climate and weather prediction but also in many other field-like social sciences, business, etc. Numerous climate prediction models have been developed by using MLR. A study on climate was done using linear multiple regression technique in which researchers investigated the relationship between climate parameters and sugarcane harvest [264]. Multivariable polynomial regression was used to study time series of plant motion and nutrient recovery for future growth [265]. Research on children growth was conducted using multiple polynomial regression to find out their growth potential. The study was very successful and effectively used in real life [266].

A robust rainfall forecasting model with only 4% error was made on summer rainfall. The regression analysis model was based on El-Nino, Arabian SST, Europe pressure gradient, wind pattern of 50 hpa, Northwest Europe temperature, and ocean temperature of South Indian [267]. Another study on climate adopted Multiple-Linear Regression (MLR) and local polynomial non-parametric technique to forecast Summer Monsoon Rainfall (SMR) on Thailand. The forecasting rainfall model showed a variance of 0.6 when compared to observe rainfall data. Indian Dipole Oscillation (IOD), Wind Speed, Sea Level Pressure (SLP), Sea Surface Temperature (SST) and El- Nino Southern Oscillation (ENSO) were taken into consideration for this study [268].

A study on the frequency of heavy rainfall was carried out in South Korea in 2005. The decision tree in the study included analysis based on Artificial Neural Network (ANN) and Multiple-Linear Regression (MLR). The research had 45 potential predictors for the model [269]. A rainfall prediction model of Myanmar was made using Multiple Polynomial Regression (MPR) analysis and Multiple-Linear

Regression (MLR) in 2008. A comparison of MPR and MLR was conducted in the study and analysis showed more accuracy of MPR over MLR [270].
A trafiic study using traditional 4-step MLR was done to forecast traffic volumes, and direct demand forecasting. Good and consistent results were achieved by using MLR [271]. Support Vector Machines (SVM) was used to present a weather prediction model. Maximum daily temperature data was given as an input after processing through linear regression to SVM for prediction [272].

### 2.4.3 Post Estimation Analysis

Post-estimation residual analysis is very important and widely used technique to validate all estimated equations in the model. Rainfall prediction study using Multilinear Regression (MLR) was carried out in Assam. The model selected maximum temperature, minimum temperature, wind speed, mean sea level as predictors. The model successful reported 63% variation in the precipitation using MLR technique. This study also reported post estimation tests to validate the model including, F test and t-test [250]. A study exploring temporal trends and seasonal behavior of tropospheric trace gases over Pakistan by exploiting satellite data in 2018 performed post estimation residual analysis test namely Durbin Watson (DW) for autocorrelation in residuals, ARCH test for checking the Heteroskedasticity in residuals, AR test, Normality test and overall F -test [263].

## 2.5 Principal Component (PC) Regression Analysis

Researchers are interested in make future predictions regarding weather due to climate change, as it impacts us all in one way or the other [158, 212, 256]. In the current context of climate change and predictions of the future number of data is needed regarding weather and climate. Data is essential for the generation

of models. Numerous new techniques have been tested to generate more reliable predictions models. With the innovation in new modeling techniques, more data sources have also become available to researchers. But having a lot of data also made the research confused in their selection. And it is difficult to find the variables that are really important for the research when there are so many variables to consider. In this scenario, Principal Components Analysis (PCA) technique is very helpful. PCA is used as a tool in exploratory data analysis; it also helps to find the most important variables that explain most of the variance in the data, known as principal components (PCs) [273]. Principal Components Regression (PCR) make Principal Components (PC) which are small sets of un-correlated, most important predictors. The leading PCs account for the largest fraction of the temporal variance in a field of predictors. The PCs are non-correlated in time, eliminates the problem of multicolinearity. Aline and Claudio [274] proposed a method of for improving regional dynamic downscaling of rainfall over the Amazon River and Northern Brazil by MLR model using PCA.

Another study was designed to forecast crop yields under future climate scenarios county-specific PCR models were estimated in 14 U. S. states. Crop yields were forecasted in response to three GCMs: CSIRO 3. 5 (the coldest), CGCM 3. 1, and MIROC 3. 2 (the warmest). Their results indicated: 1) future climate scenarios generally had modest effects on crop yields in the northern states was compare to the southern states; 2) warmer climate scenarios generate lower crop yields; 3) the north-south differences in climate change effects were larger for warmer scenarios, and 4) soil type explained why some southern states have modest yield responses across climate scenarios [275].

Chaleeraktrakoon, and Khwanket [276] studied the annual maximum daily rainfalls. Statistical downscaling of model was carried out in the study to describe the linkage between large-scale climate variables and annual maximum daily rains (AMDR) at a local site in Chi and Mul River Basins, Thailand. The study also proposed down-scaling model based on principal component analysis (PCA) of global climate variables using Singular Value Decomposition (SVD). The SVD technique used was good and efficient for calculating the standardized principal

components (SPC) of the climate variables. The model was tested with two popular general circulation models, GCMs, (HadCM3 and CGCM3) and available 41-year (1961 - 2001) AMDR data at six sites in the Chi and Mul River Basins Thailand. Kim and Oh [277] studied the problem of predicting seasonal precipitation over East Asia from actual observations and multimodal ensembles. In their article a method based on data-adaptive PCA (DPCA) was proposed, that was adopted for non-Gaussian distributed data. In addition to investigate the utility of DPCA for climate study, a data adaptive principal component regression for seasonal precipitation prediction, having DPCA and a regularized regression technique was also porposed. The proposed method was also applied to nine general circulation models for prediction of precipitations on the summer seasons (June, July, and August). The prediction ability of the proposed method was evaluated in comparison with observations and model outputs (prediction) .

Adnan et al. [210] predicted the inter and intra-annual variability of the monsoonal rainfall over Pakistan and its possible drivers using a linear statistical forecast model. The model was based on principal component (PC) regression analysis. For prediction purpose, highly correlated PCs of sea level pressure, horizontal and meridional winds were selected. Also the observed rainfall during the study period 2001 to 2013 were ingested in a stepwise multiple regression model. The prediction model was also validated for 2014 to 2015. The results reprted the correlation coefficient, mean absolute error, mean bias, and root mean square error of 0.75, 42.23, 14.92 and 60.65, respectively. The model exhibits strong and powerful skills in predicting the inter and intra-annual monsoonal rainfall variability over Pakistan.

### 2.5.1 Principal Components (PCs)

A huge amount of data, particularly if it is secondary data, creates confusion during analysis. Researchers find it difficult to select relevant variable from a vast data set. It is imperative during analysis to use pertinent and most important variables. To solve this problem, principal components analysis (PCA) is used.

PCA also assists in making relevant, constructive, predictive model [273]. In addition, due to the presence of multicollinearity among the variables, principal component regression is performed. The original set of variables are transformed into new set of un-correlated variables through PCA. Most likely the first few components representing maximum variation in the data set are selected by using eigenvalue spectrum analysis. The regression analysis is thus performed on the selected variables. It is a mathematical technique, which does not require the user to specify the statistical model or assumption about the distribution of original variants. PCs are artificial variables and often, it is not possible to assign physical meaning to them. Furthermore, PCA transforms the original set of variables into a new set of un-correlated variables. However, it should be noted that if original variables are not correlated, then there is no use in performing PCA [278].

### 2.5.2 Rules for Retaining Principal Components

Principal Component Analysis (PCA) creates as many Principal Component (known as PCs) as the number of grids/stations are there in the study. After initial Principal Components (PCs) are made, only the significant PCs are selected. Selection of PCs are made on their significance and meaningfully representation in the original correlation matrix [279]. The most important advantage of PCA is in reducing data. PCR helps in analysis, where a number of variables is more than the number of observations as in discriminant analysis and regression analysis. In such cases, PCA is helpful by reducing the dimensionality of data.

### 2.5.3 Development of Principal Component Regression

Principal Component Regression (PCR) is a type of regression analysis, which considers PC as independent variables instead of adopting original variables. The PCs are the linear combination of the original variables which can be obtained by PCA. The PCA transforms the original set of intercorrelated independent variables to a new set of uncorrelated variables (i.e PCs). The use of these PCs as

independent variables is quite useful in the multiple regression models to avoid the multicollinearity problem and to identify the variables which are the most significant in making the prediction. The PCR models have been developed by using PCs as inputs to predict and to compare the same with multiple linear regression models. It has been found that the incorporation of PCs as independent variables in the regression models improved the model prediction as well as reduced the model complexity by eliminating multicollinearity. Principal components regression (PCR) is a method for combating multicollinearity and results in estimation and prediction better than ordinary least squares when it is used successfully. With this method, the original climatic variables are transformed into a new set of orthogonal or non-correlated variables called PC of the correlation matrix. This transformation ranks the new orthogonal variables in order of their importance. It eliminating some of the PC to affect a reduction invariance [280].

### 2.5.4 Post Residual Component Analysis

Post estimation analysis is widely used to validate the model being calculated using regression analysis. Ul-Saufie et al. [281] worked to enhance the prediction capability of Multiple Linear Regression analysis by using Principal Component Analysis. The study was focused on calculating the concentration of Particulate Matter (PM10), which was an air pollutant in Malaysia. Model validation was established by reporting indicators such as Prediction Accuracy (PA), Coefficient of Determination ($R^2$), Index of Agreement (IA), Normalized Absolute Error (NAE) and Root-Mean-Square Error (RMSE). Improved results of prediction models were achieved using principal component supplementing Multiple Linear Regression analysis. Forecasting water demand and supply is necessary to create any water-related infrastructure and water resources management. Better the accuracy, better would be forecasting and subsequent water supply and sanitation. Multiple regression analysis is widely used in literature to find out water demand and supply also. Nevertheless, due to highly correlated variables, multiple regression analysis may generate inaccurate results. Principal component regression

analysis is used to combat multicollinearity issues. Haque et al. [282] developed a model to forecast water demand and supply for New South Wales, Australia and used principal component regression analysis. The results of principal component regression analysis were more authentic as compared to that of multiple linear regression analysis. It showed improvement in terms of relative error, bias, Nash-Sutcliffe Efficiency (NSE), and accuracy factor values by 3.4, 2.92, 0.44, and 1.04 %, respectively.

Another study was performed to forecast wheat crop yield. Weather variables on weekly basis were used, such as, minimum, and maximum temperature, relative humidity, solar energy and wind speed. Four models were prepared using principal component analysis with time as a predictor and wheat crop yield as a predictand variable. Based on post estimation analysis indicators like $R^2$ Adjusted R, percent deviation of forecast, Root Mean Square Error (RMSR) models were compared, and it was found that models 1 and 3 produced better results [283].

## 2.6 Summary

Mann-Kendall (MK) test is selected to study the precipitation trend of the study area. Partial Mann-Kendall (PMK) is adopted to study the impact of climate indices on precipitation trend. Empirical Orthogonal Functions (EOFs) analysis is used to make the pattern for studying the influence of climate indices, atmospheric and oceanic circulations. Multilinear Regression Analysis (MLR) is selected to develop the model for estimation of potential determinants defining precipitation variability in Baluchistan province, using parameters such as Climate Indices, Geopotential Height (GPH), Zonal Wind (ZW), Relative Humidity (RH), Sea Level Pressure (SLP) and Sea Surface Temperature (SST) at various level. Principal Component Regression (PCR) analysis is use to develop the model for estimating the potential determinants defining precipitation variability in Baluchistan province and addressing the multicollinearity among selected variables.

## 2.7 Research gap

A comprehensive critical review along with limitation assessment of previous studies for precipitation trend analysis was carried out in this chapter which helped in highlighting certain voids that needed attention and feasible solution. Some of the identified gaps pertinent to precipitation trend, climate indices influence, identification of potential determinants, contemporary modeling techniques for climate study can be summarized as:

The study area lacks focused research on the potential determinant effecting the precipitation trend. Precipitation trend is perpetually decreasing and has finally led to serious drought and famine, for example, the drought in 1999-2002. Most of the previous research works were based on the climate indices, namely North Atlantic Oscillation (NAO), Arctic Oscillation (AO), Atlantic Multi-decadal Oscillation (AMO), Indian Ocean Dipole (IOD), Pacific Decadal Oscillation (PDO) and El Nino Southern Oscillation (ENSO) including Multivariate ENSO Index/ ENSO Modoki Index (ENSO-MEI/EMI). To the best of the author's knowledge no study is carried out on the ENSO Modoki Index (EMI), Equatorial Indian Ocean Zonal Wind Index (EQWIN), which does have significant impact on the precipitation trend of the study area. There is a dire need to use contemporary modeling techniques to carry out statistical modeling, compare the results and recommend the best for the future.

# Chapter 3

# Precipitation Variability due to the Impact of Climate Indices

**Publications related to this chapter are listed below**

**RELATED ISI IF JOURNAL PAPER**

**Published**

Aamir, E., and Hassan, I., 2020. **"The impact of climate indices on precipitation variability in Baluchistan, Pakistan."** In: Tellus A: Dynamic Meteorology and Oceanography. (IF 1.932).
DOI: 10.1080/16000870.2020.1833584

**CONFERENCE PAPER**

**Published**

Aamir, E., and Hassan, I., 2018. **"Trend analysis in precipitation at individual and regional levels in Baluchistan, Pakistan."** In IOP Conference Series: Materials Science and Engineering; IOP Publishing: Bristol, UK, p. 012042.
DOI:10.1088/1757-899X/414/1/012042

## 3.1 Background

Baluchistan precipitation trend appears to be affected from the climate variability since last few decades. Only half a century ago, this mineral-rich province had flowing streams, Karez and underground wells, which were deemed adequate. Today, due to continuous decrease in precipitation, over exploitation and extensive pumping, the streams and Karez, are dried up and the ground water table has alarmingly depleted, ultimately creating famine-like situation in some of its districts [284]. This chapter aims to determine possible linkages of precipitation trend variation with ten climatic indices, namely North Atlantic Oscillation (NAO), Arctic Oscillation (AO), Atlantic Multi-decadal Oscillation (AMO), Indian Ocean Dipole-Dipole mode index / Indian Ocean Dipole-Equatorial Indian Ocean Zonal wind index (IOD-DMI/IOD-EQWIN), Pacific Decadal Oscillation (PDO), El Nino Southern Oscillation (ENSO) including Multivariate ENSO Index/ ENSO Modoki Index (ENSO-MEI/EMI) and the statistical significant of the trend is also to be determined in this chapter.

## 3.2 Methodology

### 3.2.1 Study Area

The biggest province of Pakistan in terms of area, covering 347,200 square kilometers (134, 051 square miles) is Baluchistan, which is nearly 45% of Pakistan's total land area. It is located in the southwestern part of the country [138, 142]. Baluchistan enjoys an 800 km long coastline along NE of the Arabian Sea, which is very famous for its upwelling phenomenon. Its Exclusive Economic Zone (EEZ) comprises an area of 196,600 square kilometers. Here, the climate is a hot desert type with extreme heat and cold. It is divided into four climatic regions as shown in Figure 3.1. The weather of Baluchistan is mainly affected by Western Disturbances in spring and winter months, and it is less influence by monsoon.

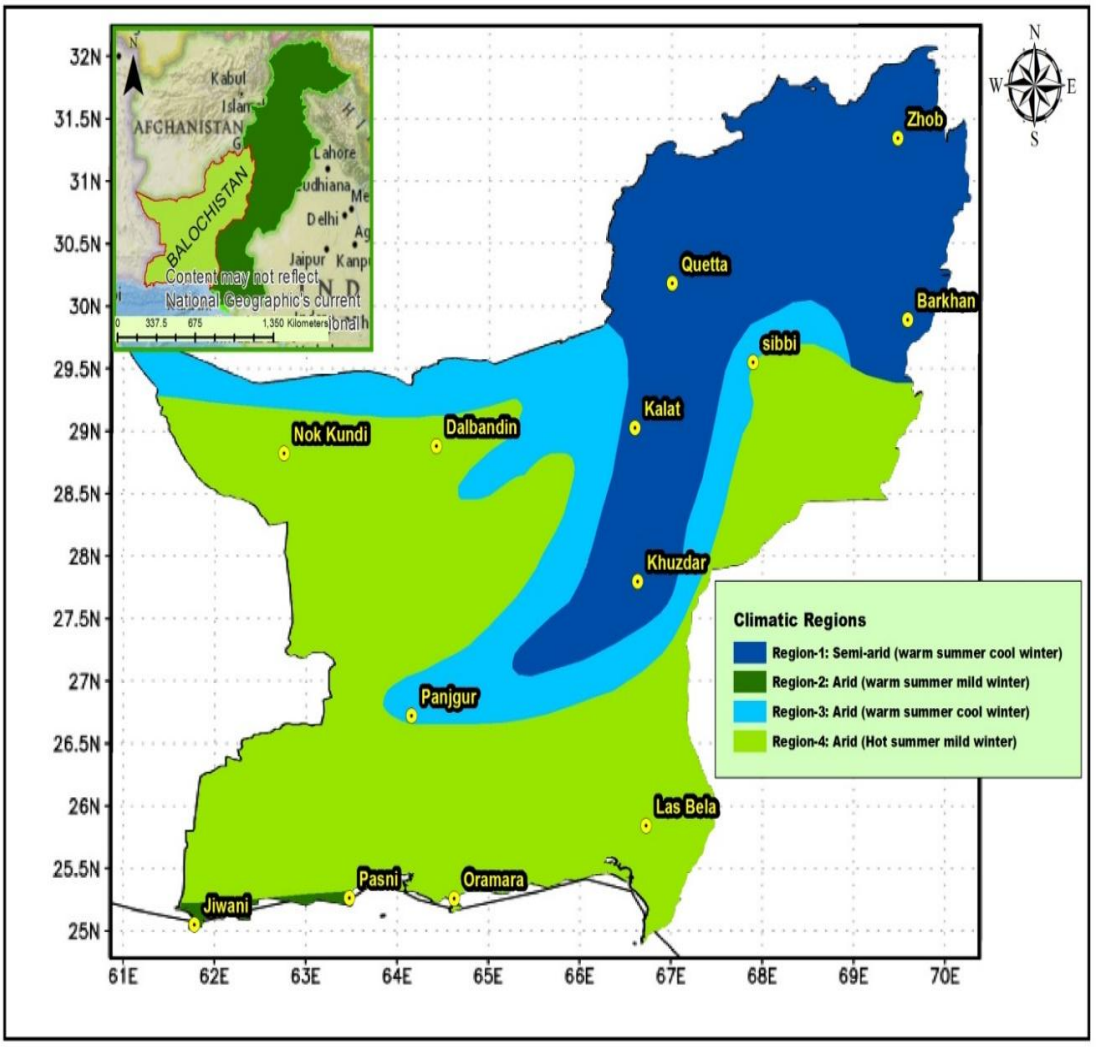


FIGURE 3.1: Study Area and Location of Selected Pakistan Meteorological Department (PMD) Stations in Baluchistan with Regional Distribution (Courtesy of PMD Pakistan).

### 3.2.2 Reasons for Selecting the Study Area

Baluchistan is selected as the study area for this research because of the multiple reasons; Firstly, the Maximum routes of the China Pakistan Economic Corridor (CPEC) pass through Baluchistan. China Pakistan Economic Corridor (CPEC) has a direct impact on the Gross Domestic Product (GDP),foreign investment, and international trade, of the country. However, the infrastructure of Baluchistan relies on water resources and management, which is strongly influenced by precipitation. Secondly, it is the largest province area-wise, yet it is still the most

undeveloped province due to drought as pointed out by the Economic Survey of Pakistan which proves that precipitation, being the main source of freshwater plays a vital role in economic development. Thirdly, this research will provide a baseline study for future comparative effects of OBOR, CPEC, and other anthropogenic activity on the climate of Baluchistan. Fourth, Baluchistan's topography, mountains, rugged terrain, coastline, extreme weather, relative continental position, atmospheric current, orographic barriers, surface condition, anthropogenic activity and atmospheric particulate address most of the factors that can be the potential determinant to effect precipitation trend. Fifth, Baluchistan is a prosperous land in terms of natural resources like Natural Gas, Coal, Precious Gas, Marble, Zinc, Copper, Lead, etc. Sixth, Baluchistan, despite of many odds, still has attracted foreign investment of $62 billion in phases and will attract much more in the future. Seventh, Baluchistan is currently the province with the most vibrating economy and future opportunities.

### 3.2.3 Data Sources

Monthly Precipitation data in millimeters is acquired from Pakistan Meteorological Department (PMD). Thirteen stations, namely Barakhan, Dalbandin, Jiwani, Kalat, Khuzdar, Lasbella, Nokkundi, Ormara, Pasni, Punjgur, Quetta, Sibbi and Zhob throughout Baluchistan are chosen based on authentic source (i.e., PMD), completeness and availability of data. The distribution of stations in different climatic regions within Baluchistan are shown in Figure 3.1. The study period constitutes thirty nine (39) years from 1977 to 2015 and validation period from (2016-2020) for the selected stations in Baluchistan. Data collected from PMD is on monthly basis in (mm/month) for each of the weather stations and is converted into monthly means. The average monthly and annual precipitation within the study period is tabulated in Table 3.1.

Pakistan Meteorological Department (PMD) has divided Baluchistan province into four climatic regions. According to PMD, region 1 includes Barakhan, Kalat, Khuzdar, Quetta, and Zhob. Region 2 includes Panjgur, and Sibbi. Region 3

TABLE 3.1: Average Precipitation Data of Baluchistan of 39 years (1977-2015).

| Table-1. Average Precipitation (mm) from 1977-2017 | | | | | | | | | | | | | | |
|---|---|---|---|---|---|---|---|---|---|---|---|---|---|---|
| Stations | | Winter | | | Spring / Pre-Monsoon | | | Monsoon | | | | Post-Monsoon | | Annual precipitation |
| | | Dec | Jan | Feb | Mar | Apr | May | Jun | Jul | Aug | Sep | Oct | Nov | |
| Barakhan | Eastern | 6.5 | 13.1 | 21.1 | 31.3 | 34.6 | 24.7 | 48.2 | 108.4 | 84.6 | 35 | 9.1 | 4.9 | 421.5 |
| Kalat | Eastern | 30.3 | 34.7 | 37.8 | 31 | 11 | 3.9 | 6.7 | 16.3 | 13.4 | 4.6 | 5 | 5.8 | 200.5 |
| Khuzdar | Eastern | 14.7 | 16.5 | 30.9 | 29.3 | 16.3 | 14.1 | 16.5 | 51.2 | 56.6 | 9.1 | 6.5 | 4.3 | 266.0 |
| Lasbella | Eastern | 7.3 | 4.8 | 11.4 | 10.4 | 7.4 | 19.7 | 11.2 | 53.2 | 39.3 | 8.6 | 5 | 1.9 | 180.2 |
| Quetta | Eastern | 30.8 | 53.8 | 51.7 | 55.5 | 26 | 7.5 | 4 | 12.5 | 11.1 | 3.1 | 5.7 | 8.8 | 270.5 |
| Sibbi | Eastern | 5.6 | 10.1 | 17.9 | 22.3 | 9.8 | 6 | 15.7 | 38.6 | 39.1 | 12.4 | 3.1 | 1.6 | 182.2 |
| Zhob | Eastern | 9.2 | 17.1 | 26.9 | 43.5 | 29.1 | 14.8 | 17.7 | 56.2 | 44.8 | 11.1 | 5.8 | 5.6 | 281.8 |
| Dalbandin | Western | 9.4 | 16.8 | 16 | 20.5 | 4.8 | 1.3 | 3 | 3.7 | 0.7 | 0.1 | 2.2 | 3.1 | 81.6 |
| Jiwani | Western | 20.2 | 22.9 | 22.5 | 14.3 | 3.7 | 0.1 | 7.6 | 3 | 2.3 | 0 | 1.1 | 3.6 | 101.3 |
| Nokkundi | Western | 2 | 7.8 | 9.6 | 8.7 | 2.2 | 0.2 | 2 | 0.7 | 0.3 | 0 | 0.5 | 0.6 | 34.6 |
| Ormara | Western | 11.8 | 10.7 | 10 | 9.9 | 1.6 | 0.2 | 9.7 | 11.3 | 3.8 | 0.3 | 2 | 0.5 | 71.8 |
| Punjgur | Western | 10 | 12.8 | 15 | 15.1 | 8.3 | 3.5 | 5 | 12.1 | 7.7 | 1.7 | 2.1 | 1.6 | 94.9 |
| Pasni | Western | 19.8 | 22 | 14.9 | 16.4 | 2.3 | 0.5 | 6.7 | 5.2 | 7.7 | 0.5 | 2.3 | 1.7 | 100.0 |
| **Monthly Avg.** | | 13.7 | 18.7 | 22.0 | 23.7 | 12.1 | 7.4 | 11.8 | 28.6 | 24.0 | 6.7 | 3.9 | 3.4 | |
| **Seasonal Sum** | | 54.3 | | | 43.2 | | | 71.1 | | | | 7.3 | | |

*Note: Red color shows the histogram of monthly precipitation among stations; Brown color shows the histogram of monthly precipitations among region; Green color shows seasonal; whereas Blue color shows annual precipitation.*

is arid with warm summer and cold winter includes Dalbandin, Nokkundi, and Lasbella. The last region 4 of Baluchistan province is arid with hot summer and mild winter. This region includes Jiwani, Ormara, and Pasni. All these stations receive scattered precipitation in the post- monsoon season when continental air prevails near to coastal line like Gwadar, Pasni, Ormara and Jiwani.

### 3.2.4 Precipitation Data Analysis

The precipitation time series data being used in this doctoral study is first assessed for its characteristics (Kurtosis and skewness), distribution type, changes, cycles, outliers, missing values, and homogeneity. The characteristics of annual time series data of 13 stations over the study period is calculated and the results are shown in Table 3.2.

Skewness is a measure of the symmetry in distribution. A normally distributed dataset (i.e., symmetrical) data set has a skewness equal to 0. Kurtosis measures the amount of probability in the combined sizes of the two tails bell-shaped curve. The kurtosis of normally distributed data is equal to 3. If the kurtosis of a data set is greater than 3, then the dataset has heavier tails than a normal distribution.

TABLE 3.2: Linear Regression on Annual Time Series

| **S.No** | **Stations** | **Mean** | **Standard deviation** | **Kurtosis** | **Skewness** |
|---|---|---|---|---|---|
| 1 | Barakhan | 421.500 | 140.047 | 0.769 | 0.455 |
| 2 | Dalbandin | 81.601 | 48.085 | -0.214 | 0.585 |
| 3 | Jiwani | 101.300 | 88.784 | 2.266 | 1.519 |
| 4 | Kalat | 200.500 | 170.917 | 10.050 | 2.612 |
| 5 | Khuzdar | 266.000 | 118.215 | 1.147 | 0.994 |
| 6 | Lasbella | 180.200 | 115.972 | 1.134 | 1.137 |
| 7 | Nokkundi | 34.600 | 37.975 | 5.998 | 2.202 |
| 8 | Ormara | 71.800 | 92.889 | 11.605 | 3.031 |
| 9 | Panjgur | 94.900 | 56.881 | 3.950 | 1.641 |
| IO | Pasni | 100.001 | 81.228 | 0.902 | 1.034 |
| 11 | Quetta | 270.502 | 152.860 | 9.365 | 2.542 |
| 12 | Sibbi | 182.203 | 89.558 | -0.724 | 0.310 |
| 13 | Zhob | 281.859 | 92.734 | -0.101 | 0.193 |

And if the kurtosis is less than 3, then the dataset has lighter tails than a normal distribution. Skewness and kurtosis can be used to characterize the data set for its distribution (normal or not). But both skewness and kurtosis are heavily dependent on the sample size. Even several hundred data points may not give a very good estimate of the true kurtosis and skewness. As such, normality check of a dataset cannot be relied upon for a small dataset such as the current study data set of 39 years. Therefore, check for normality is done by applying tests, namely Shapiro-Wilk W test, Anderson-Darling, Lilliefors and Jarque-Bera test [285]. The normality check tests are performed on the time series and the results are presented in Table 3.3. Normality test runs on annual precipitation time series data shows that the time series data of only four stations, namely Dalbandin, Sibbi, Zhob, and Barakhan, are normally distributed and mostly, the data is not normally distributed.

Since the time-series data of Dalbandin, Sibbi, Zhob, and Barakhan is normally distributed therefore parametric tests of Simple Linear Regression (SLR) with least-square fit can be performed to calculate the trend in the time series data. SLR is utilized to calculate the trend slope, its significance and validity to detect the trend in the time series precipitation data. Provided that the validity of the

TABLE 3.3: Normality Tests on Annual Time Series

| **S.No** | **Stations** | **Shapiro-Wilk** | **Anderson-Darling** | **Lilliefors** | **Jarque-Bera** |
|---|---|---|---|---|---|
| 1 | Dalbandin | passed | passed | passed | passed |
| 2 | Jiwani | failed | failed | failed | failed |
| 3 | Kalat | failed | failed | failed | failed |
| 4 | Lasbella | failed | failed | failed | failed |
| 5 | Nokkundi | failed | failed | failed | failed |
| 6 | Ormara | failed | failed | failed | failed |
| 7 | Panjgur | failed | failed | failed | failed |
| 8 | Pasni | failed | failed | failed | failed |
| 9 | Quetta | failed | failed | failed | failed |
| IO | Sibbi | passed | passed | passed | passed |
| 11 | Zhob | passed | passed | passed | passed |
| 12 | Khuzdar | failed | failed | failed | failed |
| 13 | Barakhan | passed | passed | passed | passed |

test is determined by checking the normal distribution of residuals obtained from Simple Linear Regression. Simple Linear Regression (SLR) analysis with least square fit test is run on the annual time series data of precipitation for detecting the trends and the results are presented in Table 3.4.

TABLE 3.4: Linear Regression on Annual Time Series

| **S.No** | **Stations** | **$R^2$** | **Regression Slope** | **p-value** | **Result** | **Residual normality** |
|---|---|---|---|---|---|---|
| 1 | Dalbandin | 0.0499 | -0.9179 | 0.166 | No trend | passed |
| 2 | Jiwani | 0.07532 | -2 0969 | 0.087 | No trend | failed |
| 3 | Kalat | 0.0015 | 0.5609 | 0.811 | No trend | failed |
| 4 | Lasbella | 0.0541 | -2.3279 | 0.149 | No trend | failed |
| 5 | Nokkundi | 0.015 | 0.403 | 0.451 | No trend | failed |
| 6 | Ormara | 0.003 | 0.4423 | 0.736 | No trend | failed |
| 7 | Panjgur | 0.062 | -1.2097 | 0.121 | No trend | failed |
| 8 | Pasni | 0.0357 | -1.3075 | 0.243 | No trend | failed |
| 9 | Quetta | 0.1264 | -4.707 | 0.024 | Decreasing | failed |
| IO | Sibbi | 0.038 | 1.509 | 0.228 | No trend | passed |
| 11 | Zhob | 0.0534 | -1.8367 | 0.151 | No trend | passed |
| 12 | Khuzdar | 0.0302 | - 1.7735 | 0.283 | No trend | failed |
| 13 | Barakhan | 0.017 | -1.590 | 0.419 | No trend | passed |

The results in Table 3.4 show no significant trend in any station except Quetta, but Quetta failed in validity as its residuals are not normally distributed. The conclusion which is drawn from it is that the parametric tests are not suited for conducting the trend analysis on the annual precipitation because mostly the data is not normally distributed and does not have the same standard distribution. If the data is normally distributed, then their residuals are failed to pass the validity test. Hence, non-parametric test like Mann-Kendall (MK) and Spearman's Rho (SR) test should be adopted to evaluate the significant trends in the precipitation time series data. Theil Sen's Slope Analysis (TSA) should be used for calculating the magnitude of the slope.

### 3.2.5 Teleconnections and Climatic Indices

Present in the stratosphere the large-scale teleconnections are spatial patterns, displaying the atmospheric and oceanic circulation. They are responsible for remote relations between climate anomalies, including extreme events, drought, floods and precipitation variability over large distances around the globe [286-296]. Teleconnections are Sea Surface Temperature, Sea Level Pressure anomalies, persistent and can last for short as well as long duration like for 1 to 2 weeks or 20 to 40 years. Climatic indices are the diagnostic quantitative representation of these teleconnections/large-scale oceanic and atmospheric circulation patterns. These climatic indices are developed against the teleconnections patterns by climatologists to use for statistical analysis, modeling and predictions purposes. Climatologists have established this fact through numerous research and studies that climate indices have a strong impact on the climate /weather around the globe and also that climate indices, namely NAO, AO, AMO, IOD-DMI, IOD-EQWIN, PDO, ENSO-MEI, ENSO MODOKI (ENSO-EMI) have significant influence on the precipitation trend over the study area through teleconnections [117, 118, 232, 284]. However, their influence is neither quantified nor mentioned in most of the studies. The influence is merely an approximation like strong, moderate, weak and very weak, etc. [216]. Data of climate indices for this study is downloaded

from NOAA-ESRL Physical Sciences Division except IOD, which is downloaded from JAMSTEC and listed in Table 3.5. A brief description of the climate indices is provided below, whereas the domain used to define the teleconnections pattern is provided in Table 3.5.

Table 3.5: Description of Climate Indices

| **Climate Indices** | **Source** | **Domain to Define Index** |
|---|---|---|
| NAO | www.esrl.noaa.gov | Icelandic Low: 50N-320, 55N-320; 75N-360, 70N-360; approx.<br>Azores High: 25N-315,30N-315, 45N-355, 50N-355; approx. |
| AO | www.esrl.noaa.gov | Artic Poles; North of 20N |
| AMO | www.esrl.noaa.gov | 0-60N; 280-360 approx. |
| DMI | www.jamstec.go.jp/aplinfo | |
| | /sintexf/e/index.html | EEIO; 0-10S; 90-110<br>WEIO; 10N-10S; 50-70 |
| EQWIN | www.esrl.noaa.gov | CEIO: 5N-5S; 60-90 |
| ENSO-MEI | www.esrl.noaa.gov | 30N-30S; 100-290 |
| ENSO-MODOKI | www.esrl.noaa.gov | MODOKI-A (Right): 10N-10S; 165-240<br>MODOKI-B (Center): 5N-15S; 250-290<br>MODOKI-C (left): 20N-10S; 125-145 |
| PDO | www.esrl.noaa.gov | Pacific Ocean; North of 20N |

**3.2.5.1 The North Atlantic Oscillation (NAO)** Index is based on the sea-level surface pressure anomaly between the Subtropical (Azores) High and Subpolar (Iceland) Low [102-103]. In the positive (stronger) phase, above-normal pressure over the Azores and below normal pressure over Iceland prevails. In the negative phase, weak high pressure over the Azores and weak low pressure over Iceland prevail, as shown in Figure 3.2. The positive phase leads towards increased

westerlies which follows the northern track which, is used to result in cool summers and mild, wet winters in central Europe [101, 129-130]. The negative phase of NAO leads towards suppressed westerlies and as a result, the northern European area suffers cold, dry winters. The storms track southwards toward the Mediterranean Sea and much into northern Asia [136].

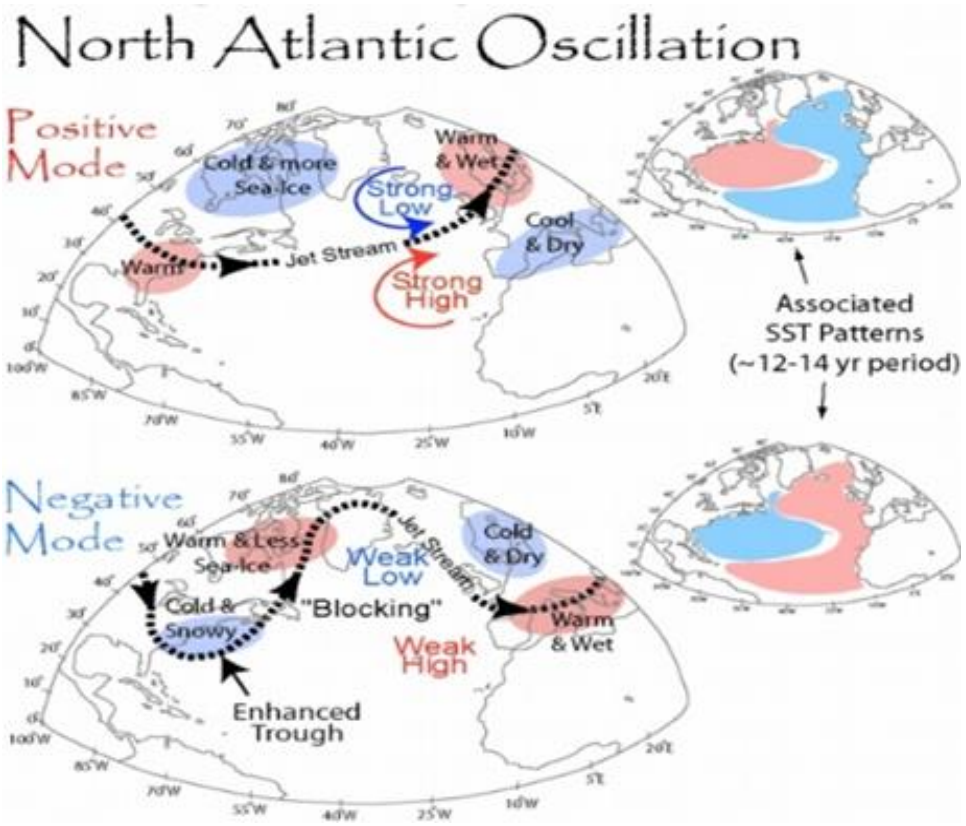


FIGURE 3.2: The positive and negative phases of North Atlantic Oscillation (NAO) [297].

**3.2.5.2 The Arctic Oscillation (AO)** is a form of atmospheric circulation over the Northern Hemisphere, particularly from mid to high. In the positive phase, low air pressure on the Arctic and high air pressure over the Atlantic Oceans and Northern Pacific are observed, as shown in Figure 3.3. The regions in the mid-latitudes experience less Cold Air Outbreaks (CAOs). The positive phase is associated with a strong polar vortex which constrains the cold Arctic air to the North. Jet stream remains zonal and storm tracks in Northeast direction.

During the negative phase, higher air pressure on the Arctic and lower air pressure over the Atlantic Oceans and Northern Pacific is observed as, shown in Figure 3.3. The negative phase is associated with a weaker polar vortex allows the cold air to invade the USA and Europe. The regions in the mid-latitudes can undergo waves of chilly air. Jet stream takes a more meridional path with the trough over USA/Europe and crests over North Atlantic. Storms that follow a more direct and Eastward direction is often called Nor'easters [122].

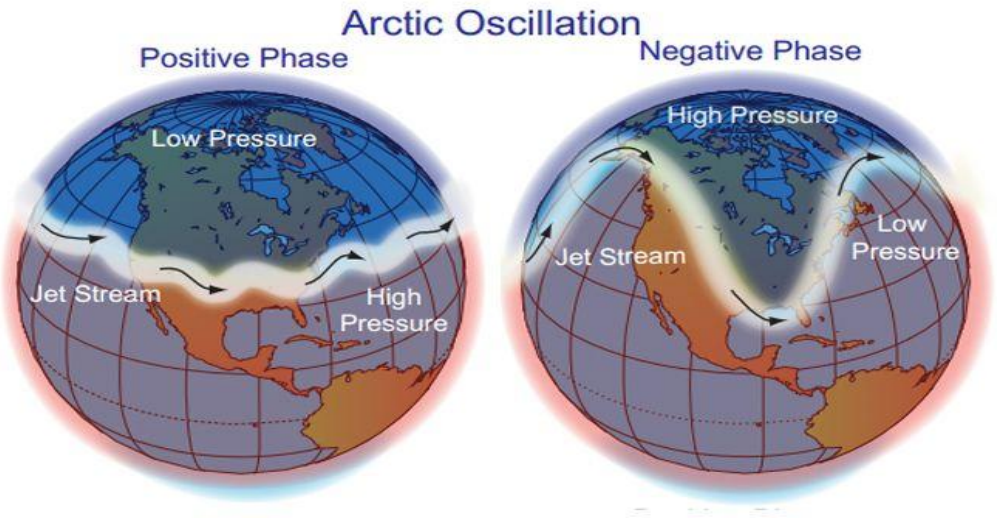


FIGURE 3.3: The positive and negative phases of Arctic Oscillation (AO) [298].

**3.2.5.3 The Atlantic Multi-Decal Oscillation (AMO)** is characterized by an SST anomaly in the North Atlantic and consists of the warm phase and cool phases with periods of 20-40 years approximately as shown in Figure 3.4. From the early 1960s to the mid 1990s, the Atlantic Multi-Decal Oscillation (AMO) index had shown a relatively cool phase and from 1997 till 2021, the Atlantic Multi-Decal Oscillation (AMO) has been in a warm phase. Atlantic Multi-Decal Oscillation (AMO) has a positive correlation with monsoon rainfall. The Atlantic Multi-Decal Oscillation (AMO) may influence the monsoon through the summer North Atlantic Oscillation (NAO) and further through the equatorial zonal winds that increase the moisture flow over the sub-continent region by enhancing the southwesterly flow.

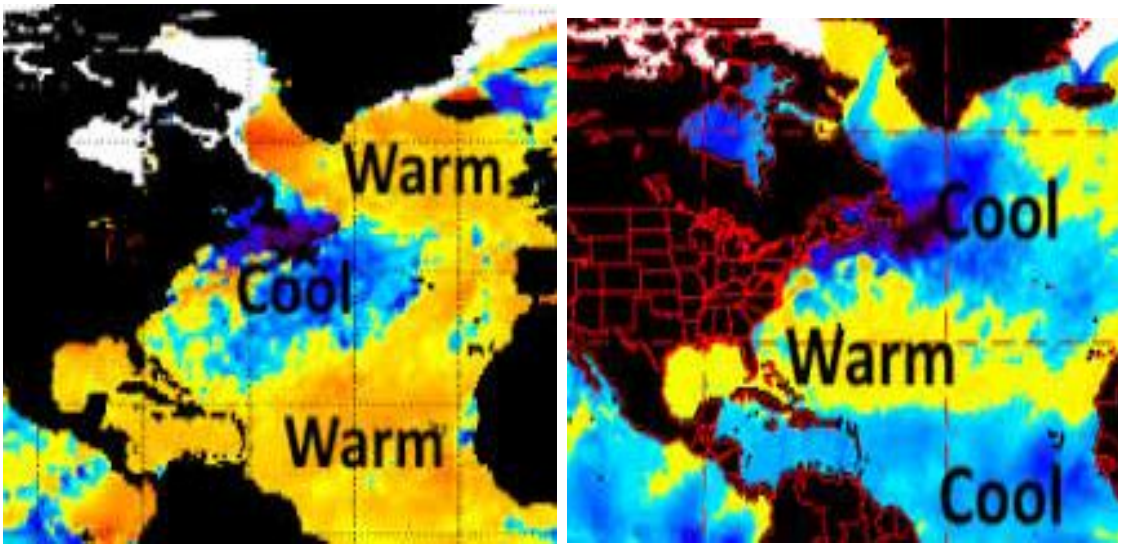


FIGURE 3.4: The positive and negative phases of Atlantic Multi-decal Oscillation (AMO) [299].

**3.2.5.4 The Dipole Mode Index (DMI)** is the ocean segment of the Indian Ocean Dipole (IOD) and depends solely on Sea Surface Temperature (SST) inconsistencies. DMI estimates the contrast between SST peculiarities in two locations of the Indian Ocean: West Equatorial Indian Ocean (WEIO), 50E-70E and 10S-10N and East Equatorial Indian Ocean (EEIO); 90E-110E and 10S-0. During the positive phase, water in the eastern region is cooler and it is warmer in the western Indian Ocean as compared to the usual temperature, as shown in Figure 3.5. This positive phase benefits the sub-continent region by directing monsoon towards it. During the negative phase, water in the eastern region is warmer and it is cooler in the western Indian Ocean as compared to the normal the temperature as shown in Figure 3.5. The negative phase IOD has been found over the study area, creating several dry years and positive IOD has produced more precipitation [116, 119].

**3.2.5.5 Equatorial Indian Ocean Oscillation (EQUINOO)** is the atmospheric segment of IOD. It is the fluctuation of atmospheric cloudiness between the Eastern Equatorial Indian Ocean (EEIO) and Western Equatorial Indian Ocean (WEIO). The index that describes EQUINOO is EQWIN, which is the negative of the standardized zonal wind anomaly over the Central Equatorial Indian Ocean

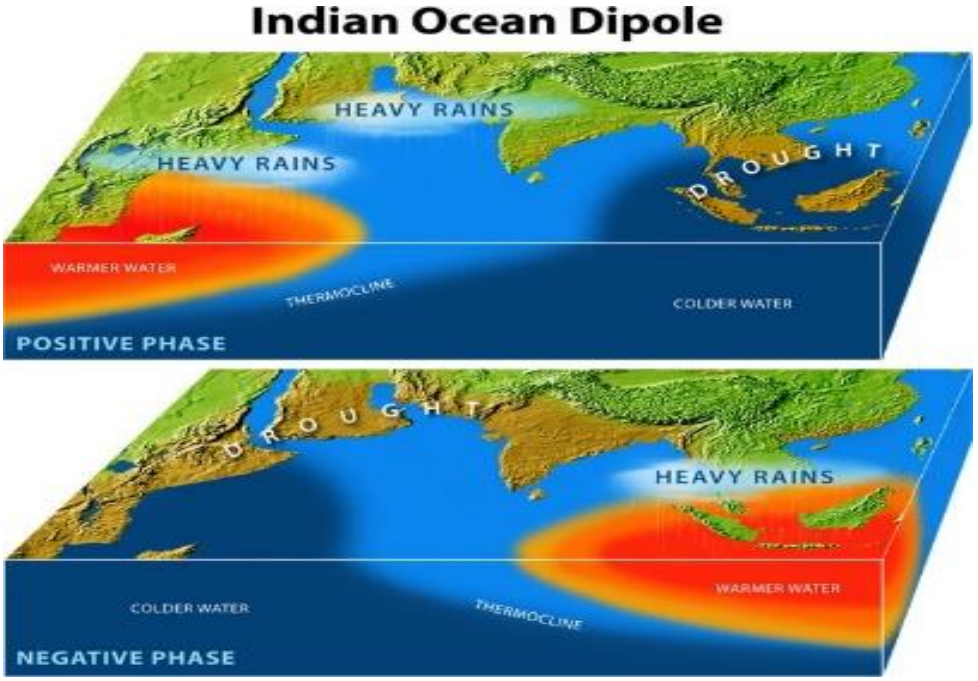


FIGURE 3.5: The positive and negative phases of Dipole Mode Index (DMI) [300].

(CEIO) region [86]. The EQWIN index is highly correlated with the difference between the OLR of WEIO and EEIO. In the positive phase of EQUINOO, enhanced cloudiness is observed over the WEIO as compared to the EEIO and vice versa in the negative phase, as shown in Figure 3.6. The positive phase of EQUINOO is favorable to the monsoon and is believed to have impact on the influence of the El-Nino through teleconnection.

**3.2.5.6 El Nino Southern Oscillation (ENSO)** is the periodic variability of every two to seven years in sea surface temperature (El Nino) and the air pressure of the superimposing atmospheres Southern Oscillation across the equatorial Pacific Ocean as shown in Figure 3.7. El Nino and its contrary La Nina both have a disturbing effect on monsoon climatic conditions in many different parts of the world. Tropical Pacific's six important parameters, namely Sea: Surface Temperature (SST); Sea Level Pressure (SLP); Surface Air Temperature (AT); Zonal (U) and Meridional (V) components of the Surface Wind and lastly, the

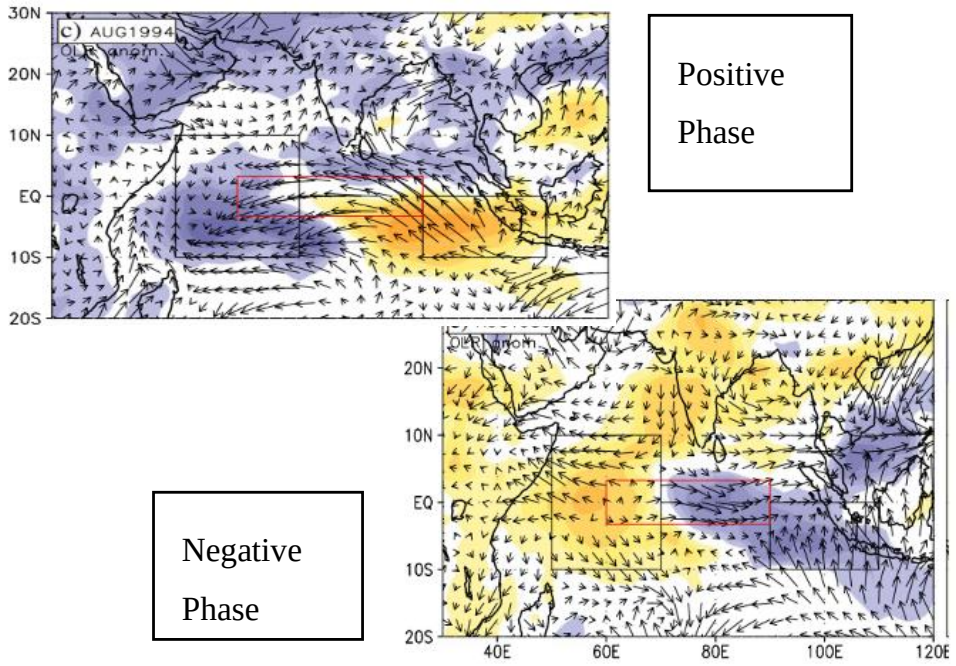


FIGURE 3.6: The positive and negative phases of Equatorial Indian Ocean Oscillation (EQUINOO) [301].

total Cloudiness fraction of the sky (C) combine to form the Multivariate ENSO Index MEI, which incorporates most information than any other indices [90, 106, 116, 122, 124].

**3.2.5.7 ENSO Modoki Index (EMI-MODOKI)** This index describes the distinctive SST anomalies in the tropical Pacific Ocean. It has two phases La Nina Modoki: colder central Pacific flanked by warm eastern and western Pacific, El Nino Modoki: warm anomaly of the central Pacific when bordered by cold anomalies on both east and west sides of the ocean as shown in Figure 3.8. The latest research reveals that ENSO Modoki has distinct teleconnections that have far-flung reaching influences. It even affects the precipitation over the sub-continent and South Africa [230].

**3.2.5.8 The Pacific Decadal Oscillation (PDO)** is the common climate disparity in the Sea Surface Temperature (SST), Sea Level Pressure (SLP) of the Pacific basin adjacent to North America. It has two phases, warm or cold,

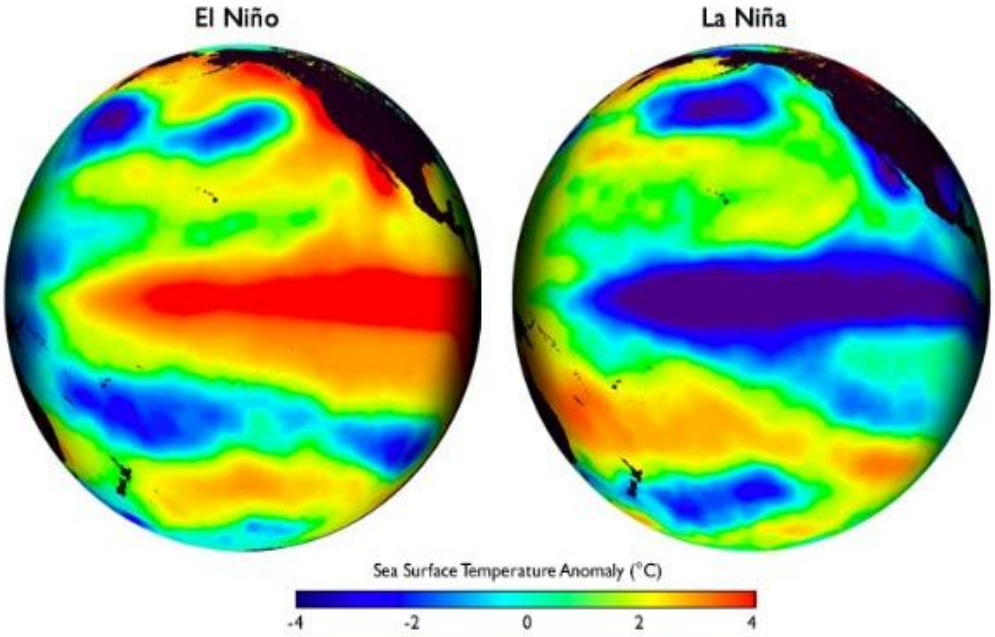


FIGURE 3.7: The positive and negative phases of El Nino Southern Oscillation (ENSO) [302].

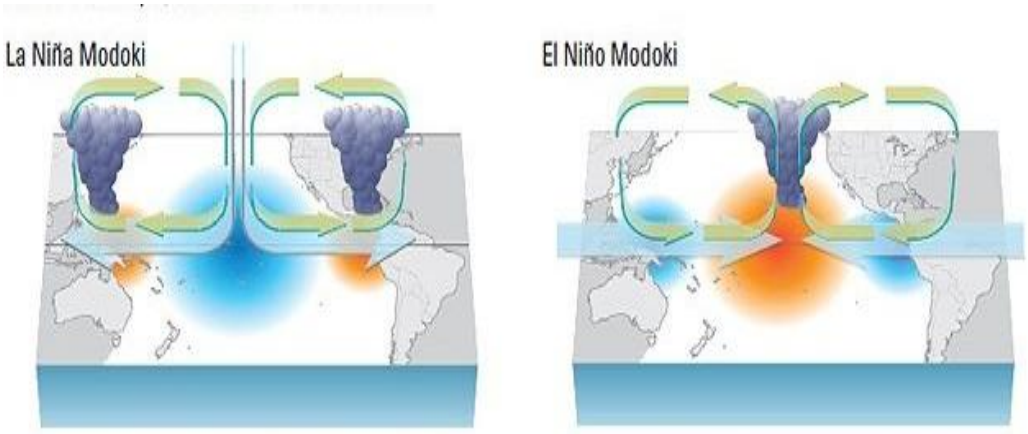


FIGURE 3.8: The positive and negative phases of ENSO Modoki Index (EMI-MODOKI) [303].

that may last for 20 to 30 years. During the positive phase, Sea Level Pressure is below average over the North Pacific, or Sea Surface Temperature (SST) are inconsistent cool in the interior North Pacific and warm along the Pacific Coast of North America [89, 131]. During the negative phase, Sea Level Pressure (SLP) over the North Pacific is above average or warm Sea Surface Temperature (SST)

anomalies in the interior and cool Sea Surface Temperature (SST) anomalies along the North American coast prevail, as shown in Figure 3.9.

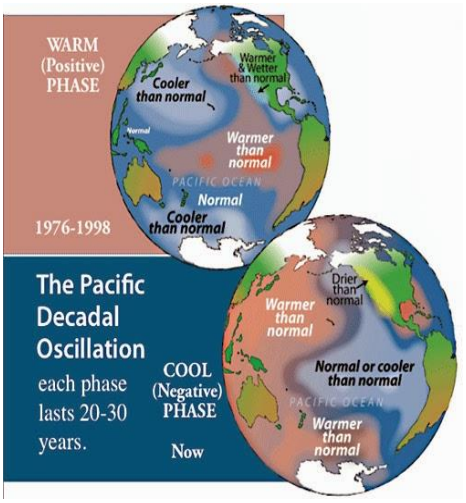


FIGURE 3.9: The Pacific Decadal Oscillation (PDO) [304].

### 3.2.6 Climate Variables

Atmospheric and oceanic climate variables such as Sea Surface Temperature (SST), Sea Level Pressure (SLP), Zonal Winds at the surface (ZW-Surface) and Geopotential Heights at 500 hpa level (GPH500) are considered to determine Empirical Orthogonal Maps (EOF) and their relationship with the precipitation variability [86, 117]. HADISST v1.1 1x1 degrees gridded data is downloaded from Met Office Hadley Center (https: //climatedataguide.ucar.edu/climate-data/sst-data-hadisst-v11.) whereas NCEP/NCAR Reanalysis 2.5 x 2.5 degree gridded data of SLP, GPH, Zonal Wind and OLR are downloaded from the NOAA-ESRL Physical Sciences Division website (https: //www.esrl.noaa.gov).

### 3.2.7 Statistical Techniques

Trends are examined using Mann-Kendall Tests in the monthly time series precipitation data for each of 13 stations [57, 220]. The slope of the trend is calculated using Theil Sens Slope, which is recommended for meteorological analysis [305].

The influence of climate indices on precipitation trends is assessed by the Partial Mann-Kendall test. The analysis is performed on individual stations for monthly time series data. Empirical Orthogonal Function (EOF) and principal component analysis (PCA) is used for calculating the precipitation variability in Baluchistan Region. The association between precipitation-climate indices and precipitation-climatic variables is determined by Pearson's correlation [306].

#### 3.2.7.1 Mann-Kendall for Trend Detection

Mann-Kendall (MK) test is largely used in identifying trends in climate variables [58, 128, 220, 221]. The MK test is a non-parametric test based on ranks and is not sensitive to sudden breaks in uneven data. The reasons for adopting the Mann-Kendall test is that it is strong and insensitive to the data with gaps and best for the data that is not normally distributed.

The MK test is one of the strong methods of identifying monotonic trends in precipitation data where the data is skewed and/or where data is either consistently increasing or decreasing in a time series and is not suitable when there are recurring trends. The Mann-Kendall statistic $S_x$ of the series x is given [40] as:

$$S_x = \sum_{i-l}^{n-1} \sum_{j=i+1}^{n} sgn\left(X_j - X_i\right) \tag{3.1}$$

where

$$sgn\left(X_j - X_i\right) = \begin{cases} +1 & \text{if}\left(X_j - X_i\right) > 0 \\ 0 & \text{if}\left(X_j - X_i\right) = 0 \\ -1 & \text{if}\left(X_j - X_i\right) < 0 \end{cases} \tag{3.2}$$

Where, $i$ and $j$ are the rank of observation of the $X_i$ and $X_j$ of the time series. The variance associated with $S_x$ is given as

$$\text{Var} = \frac{n\left(n-1\right)\left(2n+5\right) - \sum_{i=1}^{g} t_i\left(t_i-1\right)\left(2t_i+5\right)}{18} \tag{3.3}$$

Where $g$ is the groups of tied rank and t is ties in the group. For a sample size of $n > 10$ or larger, the MK statistics $Z_{mk}$ is computed by

$$Z_{mk} = \begin{cases} \frac{S_x - 1}{\sigma} & \text{for } S_x > 0 \\ \frac{S_x + 1}{\sigma} & \text{for } S_x < 0 \\ 0 & \text{for } S_x = 0 \end{cases} \tag{3.4}$$

Positive $Z_{mk}$ values show increasing trends, while negative $Z_{mk}$ values reflect decreasing trends. If $|Z_{mk}|$ is greater than $(Z_1 - \alpha)/2$ for the chosen value of significance level ($\alpha$), then the trends are considered significant, or when the p-value is smaller than the significance level ($\alpha$), the null hypothesis ($H_0$) of no trend is rejected in favor of the alternative hypothesis ($H_a$) and the trend is considered as a significant trend in the time series. $(Z_1 - \alpha)/2$ and p-value are obtained from the standard normal distribution table.

#### 3.2.7.2 Theil Sen's Slope (TSA)

TS is used to compute the magnitude of the trend. It is more robust than linear regression since it limits the influence of outliers and performs better even for the case of normally distributed data [305]. According to the TS method, the overall slope S* is the median of N values of slope S and is given by:

$$S* = \begin{cases} \frac{S_{N+1}}{2} & \text{if } N \text{ is odd} \\ \frac{\frac{S_N}{2} + \frac{S_{N+2}}{2}}{2} & \text{if } N \text{ is even} \end{cases} \tag{3.5}$$

Where, $S$ is the slope between any two values of a time series $x$. For time series $x$ having $n$ observations, there are possible $N = n \times (n-1)/2$ values of $S$ that can be calculated by using:

$$S = \frac{x_k - x_j}{k - j} \quad \text{where} \quad k \neq j \tag{3.6}$$

#### 3.2.7.3 Partial Mann-Kendall for Examining the Influence of Climatic Indices on Precipitation Trends

The influence of large-scale climate indices on the precipitation time series is examined by the Partial Mann-Kendall (PMK) test [216, 219, 220, 221]. PMK is among the best one-step procedures that adjust covariates (influencing variables) and trend testing simultaneously. Pearson correlation measures the strength of linear association between two variables. PMK is another approach to study the changes in trends of precipitation in the presence of climate indices which are the covariates. Trends in precipitation (response variable) can be assessed in the presence of the relevant covariates through PMK when the effect of the explanatory variable is removed [307].

In PMK, the effect of explanatory variables is studied on the response variable and the influence is calculated using the conditional mean and the conditional variance of the response variable. The test statistic for response variable y, with its covariate x being the explanatory variable, is given by

$$PMK = \frac{S_y - \hat{\rho} S_x}{\sqrt{(1-\hat{\rho})n(n-1)(2n+5)/18}} \tag{3.7}$$

Where $S_y$ is the Mann-Kendall statistics of the response variable, Sx is the Mann-Kendall statistics of the explanatory variable $\hat{\rho}$ denotes the conditional correlation between the MK statistics Sx and Sy. The PMK statistic is normally distributed with mean 0 and standard deviation 1.

#### 3.2.7.4 Empirical Orthogonal Analysis or Principal Component Analysis

Empirical Orthogonal Analysis is also called the Principal Component Analysis that finds the independent orthogonal variables (EOFs) and describes the maximum variability of a two-dimensional data set. The first dimension is the spatial location in which the EOF is being found and the second dimension is the time,

which represents the dimension in which realizations of this structure are sampled. EOF analysis is performed on precipitation and climate variables to determine the influencing climate indices of large-scale teleconnections patterns [242]. Mathematical expression is given below.

The relationship between the original time series A(x,y,t) in terms of B(x,y) and Principal Component P(t) is given by

$$A(x, y, t) = \sum_{k=1}^{n} (P(t) + B(x, y)) \tag{3.8}$$

Where, A(x,y,t) is the original time series as a function of time (t) and space (x,y). B(x,y) shows the spatial structures (x,y) of the major factors that can account for the temporal variation of A. P(t) is the Principal Component that explains how the amplitude of each EOF varies with time.

## 3.3 Results and Analysis

### 3.3.1 Spatial and Temporal Trends of Precipitations

Monotonic trends in monthly precipitation from 1977 to 2017 at thirteen (13) stations of Baluchistan province are found through Mann-Kendall (MK) tests at individual stations. Out of fifteen (15) statistically significant trends, ten (10) are decreasing trends, whereas five (5) are increasing trends Table 3.6. This indicates that decreasing trend is dominating in most of the stations in Baluchistan province and also accounts for the declining precipitation anomaly prevailing in Baluchistan province for the last couple of decades.

The slope of the significant trend is calculated by the Theil Sen slope method (TS). Spatial and temporal trends of monthly precipitations for all thirteen (13) stations are also shown with the help of pie diagram in Figure 3.10.

Table 3.6: Monthly Significant Increasing (Decreasing) Trends in Precipitation Individual Stations

| **Stations** | **Parameters** | **Jan** | **Feb** | **Mar** | **Apr** | **May** | **Jun** | **Jul** | **Aug** | **Sep** | **Oct** | **Nov** | **Dec** |
|---|---|---|---|---|---|---|---|---|---|---|---|---|---|
| Barakhan | S | -177 | -70 | -144 | -57 | -1 | 175 | -76 | 44 | -79 | 7 | -211 | -74 |
| - | p | **4.62%** | 43.14% | 10.57% | 52.20% | 99.10% | **4.93%** | 39.33% | 62.12% | 37.49% | 93.32% | **1.07%** | 38.76% |
| - | TS | -0.205* | -0.206 | -0.478 | -0.187 | 0.000 | 0.832* | -0.767 | 0.354 | -0.291 | 0.000 | 0.000 | 0.000 |
| Dalbandin | S | -132 | -43 | -79 | -53 | -98 | -21 | -42 | -67 | 13 | -24 | -91 | -208 |
| - | p | 13.74% | 62.70% | 37.29% | 54.73% | 22.36% | 76.83% | 49.35% | 27.46% | 74.52% | 71.94% | 23.49% | **1.64%** |
| - | TS | -0.240 | -0.027 | -0.113 | 0.000 | 0.000 | 0.000 | 0.000 | 0.000 | 0.000 | 0.000 | 0.000 | -0.051 |
| Jiwani | S | -13 | -158 | -72 | -93 | -30 | -59 | -34 | -58 | 0 | -32 | -72 | -245 |
| - | p | 88.23% | 6.31% | 39.71% | 19.20% | 20.49% | 30.99% | 57.93% | 41.59% | 0.00% | 48.30% | 24.04% | **0.37%** |
| - | TS | 0.000 | -0.002 | 0.000 | 0.000 | 0.000 | 0.000 | 0.000 | 0.000 | 0.000 | 0.000 | 0.000 | -0.074 |
| Kalat | S | -43 | 47 | 28 | -35 | 23 | 68 | -167 | -68 | 9 | -68 | 66 | -114 |
| - | p | 62.89% | 59.72% | 75.22% | 69.12% | 78.48% | 39.87% | 5.41% | 43.02% | 89.95% | 28.97% | 42.94% | 18.86% |
| - | TS | -0.079 | 0.130 | 0.004 | 0.000 | 0.000 | 0.000 | -0.117 | 0.000 | 0.000 | 0.000 | 0.000 | -0.049 |
| Khuzdar | S | -97 | -67 | 28 | -47 | 28 | 31 | -20 | -59 | 30 | -93 | -151 | -178 |
| - | p | 27.45% | 45.12% | 75.27% | 59.65% | 75.21% | 72.56% | 82.22% | 50.75% | 73.06% | 21.50% | 6.45% | **4.01%** |

| | | | | | | | | | | | | | |
|---|---|---|---|---|---|---|---|---|---|---|---|---|---|
| - | TS | -0.117 | -0.242 | 0.092 | -0.011 | 0.000 | 0.000 | -0.067 | -0.380 | 0.000 | 0.000 | 0.000 | -0.094 |
| Lasbella | S | 9 | -120 | 58 | 41 | 133 | 78 | -92 | -60 | 105 | -84 | -90 | -57 |
| - | p | 91.68% | 16.84% | 50.54% | 63.79% | 13.09% | 37.58% | 29.86% | 49.69% | 16.15% | 23.88% | 19.32% | 39.36% |
| - | TS | 0.000 | -0.046 | 0.000 | 0.000 | 0.292 | 0.004 | -0.225 | -0.150 | 0.000 | 0.000 | 0.000 | 0.000 |
| Nokkundi | S | 62 | 8 | -2 | 12 | 20 | 59 | -48 | -63 | 0 | 39 | -26 | -72 |
| - | p | 47.94% | 92.72% | 98.19% | 87.98% | 77.89% | 24.13% | 34.06% | 11.52% | 0.00% | 52.48% | 68.56% | 37.15% |
| - | TS | 0.000 | 0.000 | 0.000 | 0.000 | 0.000 | 0.000 | 0.000 | 0.000 | 0.000 | 0.000 | 0.000 | 0.000 |
| Ormara | S | -19 | -28 | -73 | -67 | -205 | 108 | 82 | 66 | 5 | -407 | -20 | -19 |
| - | p | 82.81% | 74.38% | 37.14% | 31.60% | **0.63%** | 7.82% | 30.15% | 35.46% | 92.09% | **0.01%** | 69.13% | 82.32% |
| - | TS | 0.000 | 0.000 | 0.000 | 0.000 | **0.000** | 0.000 | 0.000 | 0.000 | 0.000 | -0.005 | 0.000 | 0.000 |
| Panjgur | S | -28 | -93 | -56 | -32 | 135 | 18 | -195 | -78 | -5 | -76 | -90 | -176 |
| - | p | 75.17% | 29.40% | 52.60% | 70.43% | 8.89% | 80.07% | **2.28%** | 31.75% | 93.79% | 13.13% | 17.80% | **3.51%** |
| - | TS | 0.000 | -0.131 | -0.019 | 0.000 | 0.000 | 0.000 | -0.083 | 0.000 | 0.000 | 0.000 | 0.000 | 0.000 |
| Pasni | S | -52 | -64 | -60 | 0 | -35 | 15 | 10 | -116 | 6 | -50 | 49 | -91 |
| - | p | 55.68% | 46.03% | 48.35% | 100.00% | 38.15% | 81.53% | 89.61% | 12.19% | 89.54% | 27.30% | 42.43% | 28.44% |
| - | TS | -0.006 | 0.000 | 0.000 | 0.000 | 0.000 | 0.000 | 0.000 | 0.000 | 0.000 | 0.000 | 0.000 | 0.000 |

| | | | | | | | | | | | | | |
|---|---|---|---|---|---|---|---|---|---|---|---|---|---|
| Quetta | S | -224 | -44 | -157 | 130 | 165 | 206 | -33 | -12 | 153 | 8 | 76 | -169 |
| - | p | **1.19%** | 62.11% | 7.78% | 14.38% | 6.07% | **1.26%** | 70.15% | 88.99% | **3.14%** | 91.50% | 37.77% | 5.74% |
| - | TS | -1.223* | -0.265 | -0.966 | 0.200 | 0.019 | 0.000 | 0.000 | 0.000 | 0.001 | 0.000 | 0.000 | -0.543 |
| Sibbi | S | -69 | 23 | -91 | -42 | 154 | 186 | 22 | 21 | 153 | -57 | -61 | -63 |
| - | p | 43.55% | 79.55% | 30.66% | 62.80% | 6.78% | **2.59%** | 80.46% | 81.35% | 6.70% | 32.66% | 43.44% | 45.50% |
| - | TS | -0.031 | 0.000 | -0.185 | 0.000 | 0.000 | 0.000 | 0.042 | 0.069 | 0.000 | 0.000 | 0.000 | 0.000 |
| Zhob | S | -201 | -19 | -132 | -39 | 38 | 161 | 56 | -122 | 77 | -38 | -39 | -160 |
| - | P | **2.39%** | 83.08% | 13.81% | 66.12% | 66.85% | 7.04% | 52.93% | 17.06% | 38.20% | 61.98% | 64.03% | 6.63% |
| - | TS | -0.417* | -0.029 | -0.655 | -0.078 | 0.044 | 0.250 | 0.264 | -0.559 | 0.029 | 0.000 | 0.000 | -0.056 |

*Figures in bold represents significant correlations at 5% confidence level. * shows noteworthy Theil Sen Slope (TS). Where S is Mann Kendall statistic, p is significance probability (p-value) and TS is Theil Sen Slope.*

The TS of the significant noteworthy trends in Table 3.6. are shown with *. whereas others have significant trends, but their slopes are almost flat, hence they are ignored. Therefore, it can be inferred that generally, the decreasing trends of precipitation in January are dominant with a noticeable average slope of 0.615 mm/year. In contrast, increasing precipitation trends in June are prevailing with a pronounced average slope of 0.832 mm/year. The average precipitation of January and June is 18.7 mm and 11.8 mm, respectively. Thus, a significant decreasing trend having a of slope 0.615 mm/year in January is obvious, which may create dryness. In contrast, a significant increasing trend in June having slope 0.832 mm/year may create some heavy downpour conditions respectively. It may also be noted that the significant trend (increasing /decreasing) is found at stations located in Region 1. On the contrary, no trend is found at stations located in Regions 2, 3 and 4.

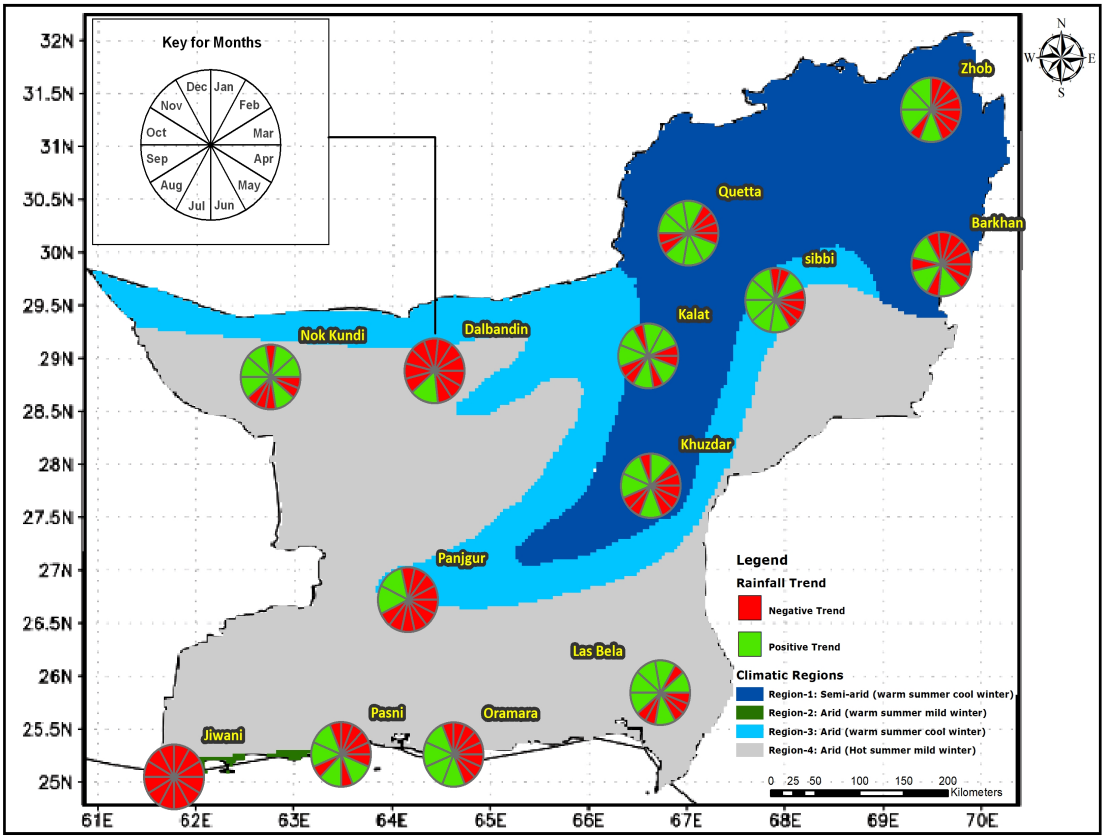


FIGURE 3.10: Spatial map showing positive and negative (Green and Red) trend in stations (Figure courtesy of PMD).

### 3.3.2 Influence of Climatic Indices on Precipitation Trends

The climatic indices pertinent to Baluchistan which would have influenced these decreasing (increasing) precipitation trends in January (June) are determined. The changes in precipitation trends in the presence of influencing variables North Atlantic Oscillation (NAO), Arctic Oscillation (AO), Atlantic Multi-decadal Oscillation (AMO), Equatorial Indian Ocean Zonal Wind Index (EQWIN), ENSO Modoki Index (EMI), Multivariate ENSO Index (MEI), Dipole mode index (DMI), and Pacific Decadal Oscillation (PDO) are determined through the PMK on monthly precipitation at the individual station.

The PMK determining influence is classified as weak, moderate and strong influence as described in Table-3.7. The variation in precipitation trends for the significant decreasing (increasing) trends of January and June are tabulated in Table-3.7. It can be seen from Table-3.7 that all the climatic variables mentioned above have a weak influence on precipitation trends except EQWIN and ENSO-MEI and EMI-MODOKI, which have moderate to strong impact on precipitation trends.

TABLE 3.7: Region1 Precipitation Modes (EOFs) and Corresponding PCs for the Month January and June

| **Months** | **Stations** | **NAO** | **AO** | **AMO** | **DMI** | **EQWIN** | **PDO** | **ENSO-MEI** | **EMI-MODOKI** |
|---|---|---|---|---|---|---|---|---|---|
| January | Barakhan | Weak (-) | Weak (-) | Weak (-) | Weak (-) | Strong (-) | Weak (-) | Weak (-) | Strong (-) |
| - | Quetta | Weak (-) | Weak (-) | Weak (-) | Weak (-) | Moderate (-) | Weak (-) | Weak (-) | Strong (-) |
| - | Zhob | Weak (-) | Weak (-) | Weak (-) | Weak (-) | Strong (-) | Weak (-) | Moderate (-) | Strong (-) |
| June | Barakhan | Weak (+) | Weak (+) | Weak (+) | Weak (+) | Strong (+) | Weak (+) | Weak (+) | Strong (+) |

(+ve) shows increasing trends whereas (-ve) shows decreasing trends.

### 3.3.3 Influence of Climate Indices on Precipitation Variability

It is found through Mann-Kendall (MK) and Theil Sen's Slope Analysis (TSA) that precipitation trends are significant in January and June. Most of the stations with significant precipitation trends are located in the Region 1 of Baluchistan province. As it can be seen in Table 3.1, Region 1 comparatively receives a larger portion of Baluchistan precipitation whereas, other regions receive less precipitation and remain dry. It can also be seen in Table 3.1 that the major share of precipitation is in monsoon (June, July, August and September) followed by winter (December, January and February). January (June) are focused month, in which the stations in Region 1 show decreasing (increasing) trends.The relationship of these months precipitation variability with the teleconnection patterns is determined through the following steps:

a. Variability patterns (modes) in the Region 1 precipitation are identified through principal component analysis and their corresponding time series (PCs) are constructed.

b. Correlation analysis is performed between time series of Region 1 precipitation (PCs.) and climate indices.

c. EOF analysis is performed on Sea Surface Temperature (SST), Sea Level Pressure (SLP), and Zonal Winds at surface (ZW-Surface) to find out the dominated teleconnection patterns prevailing January and June, which may have influenced the precipitation of Region 1 in Baluchistan province and explains the precipitation variability.

d. Correlation analysis is performed between time series of Region 1 precipitation and Sea Surface Temperature (SST) anomalies, atmospheric circulations such as; Sea Level Pressure (SLP), Geopotential Heights (500 hpa), Zonal Winds (surface), Outgoing Longwave Radiation (OLR) to observe their relationship and influence with Region 1 precipitation.

### 3.3.4 Linkages of January Precipitation Variability with Climate Indices

#### 3.3.4.1 Modes of Region 1 Precipitation for the Month of January

PCA is performed on the Region 1 Precipitation of January (R1JANP) form 1977 to 2017. The first three (3) EOFs explain 88.7% variation, capable enough to explain the precipitation variability in Region 1 Table 3.8. These three (3) PCs are then used to perform the correlation analysis with climate indices. The correlation between the time series of PCs and R1-JAN is shown in Table 3.8. The selected PC's and EOF's are shown with asterisk.

Table 3.8: Region 1 Precipitation Modes (EOFs) and Corresponding PCs for the Month January

| **EOFs** | **% Variability Explained** | **Cumulative(%)** | **PCs** | **Correlation Coeff.** | **p-value** |
|---|---|---|---|---|---|
| EOF1* | 53.80 | 53.80 | PC1 | 0.972 | **0.001** |
| EOF2* | 18.75 | 72.55 | PC2 | 0.177 | 0.267 |
| EOF3* | 16.15 | 88.70 | PC3 | 0.142 | 0.375 |
| EOF4 | 6.94 | 95.64 | PC4 | -0.024 | 0.882 |
| EOF5 | 4.36 | 100.00 | PC5 | -0.047 | 0.768 |

Bold figure represents significant correlations coefficients and probability at 5% and the "*" indicated the selected EOF's.

#### 3.3.4.2 Correlation of Region 1 Precipitation for the Month of January with Climate Indices

To find out the association of R1JANP with climate indices, correlation is performed between the time series of region precipitation PC (R1JANP-PCs) and

the climate indices for the respective month of January. The results are presented in Table 3.9. Large-scale teleconnection circulation patterns North Atlantic Oscillation (NAO) and Atlantic Oscillation (AO) show insignificant correlation with Region1 precipitation. Atlantic Multi Decadal Oscillation index (AMO) is positively correlated to PC3 at 7.91% confidence. Indian Ocean Dipole mode index (DMI) is positively correlated to PC2 at 12.39% confidence.

Equatorial Indian Ocean Zonal Wind Index (EQWIN), defined the Indian Ocean Circulation pattern as significant at 1.15% and is positively correlated to PC1. Large scale teleconnection pattern ENSO-MEI is negatively correlated to PC2 at 16.52% confidence. ENSO-MODOKI Index (EMI) is positively correlated to PC2 at 21.81% confidence, and it is also positively correlated to PC3 at 4.82% confidence level. Pacific Ocean Decadal Oscillation (PDO) is negatively correlated to PC1 at 20.51% confidence.

Table 3.9: Correlation between R1JANP-PCs and Climate Indices

| | **R1JANP-PC1** | | **R1JANP-PC2** | | **R1JANP-PC3** | |
|---|---|---|---|---|---|---|
| **Indices** | **Corrl. Coeff.** | **p-Value** | **Corrl. Coeff.** | **p-Value** | **Corrl. Coeff.** | **p-Value** |
| NAO | -0.1488 | 0.3532 | -0.1284 | 0.4236 | -0.1039 | 0.5178 |
| AO | 0.0517 | 0.7483 | -0.1479 | 0.3561 | 0.1278 | 0.4258 |
| AMO | -0.1020 | 0.5257 | 0.0269 | 0.8674 | 0.2774 | **0.0791** |
| DMI | 0.0546 | 0.7345 | 0.2442 | 0.1239* | -0.0698 | 0.6644 |
| EQWIN | 0.3758 | **0.0155** | -0.1089 | 0.4981 | 0.0352 | 0.8271 |
| ENSO-MEI | 0.0102 | 0.9497 | -0.2209 | 0.1652* | -0.1444 | 0.3678 |
| EMI-MODOKI | -0.0948 | 0.5554 | 0.1966 | 0.2181 | 0.3105 | **0.0482** |
| PDO | -0.2021 | 0.2051* | -0.0328 | 0.8386 | -0.0924 | 0.5654 |

Bold figures indicate significant correlation at 8% confidence, whereas'*' figures indicate correlation up to 20% significance.

#### 3.3.4.3 Leading Modes of Teleconnection Patterns for the Month of January

EOF analysis is performed on SST, SLP and ZW-Surface for January. The leading modes of EOFs are selected based on their distinguishability within their uncertainties. The non-degeneracy of Eigen spectrum is an important property and can be used for selecting leading modes of EOFs. The uncertainty estimates of January eigenvalues spectrum of the covariance matrix of SST and SLP are calculated by rule of thumb [242, 308]. Two eigenvalues of SST and three eigenvalues of SLP are well distinguishable from the rest of the spectrum as shown in Figure 3.11 (a and b). Therefore, three leading modes for each of the teleconnection patterns are considered for the analysis.

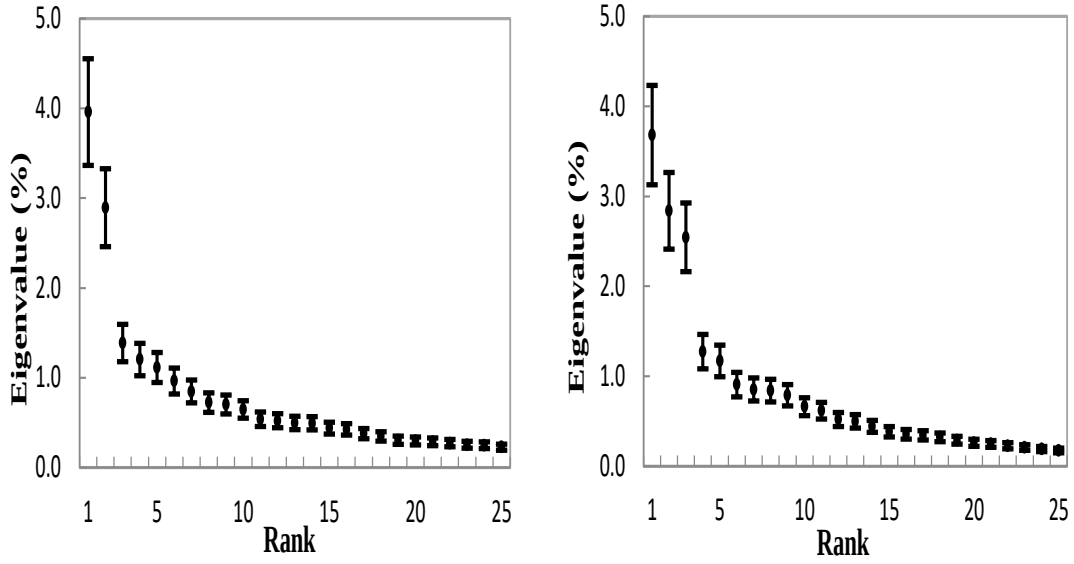


*a. Eigenvalue Spectrum (%) of the covariance matrix of January SST.*

*b. Eigenvalue Spectrum (%) of the covariance matrix of January SLP*

FIGURE 3.11: Eigenvalue Spectrums

Leading three modes EOF1(18%), EOF2(13%) and EOF3(6%) of Sea Surface Temperature (SST), , explain about 37% cumulative variability and show the patterns of PDO in North Pacific Ocean, EL-NINO, EMI-MODOKI (warm center

flanked by cold sides or vice-versa) in the Central Pacific Ocean, DMI pattern (though weak) in the Indian Ocean, whereas Atlantic Multi-decadal Oscillation (AMO), and North Atlantic Oscillation (NAO), (associated SST pattern) in North Atlantic Ocean. Leading modes of Sea Surface Temperature (SST) are shown in Figure 3.12 (a, b and c), respectively.

Figure 3.12 (x, y and z) show three leading modes of Sea Level Pressure (SLP). EOF1 (17%), EOF2 (13%), EOF3 (11%) of Sea Level Pressure (SLP), explain about 41% cumulative variability and show the patterns of ENSO, NAO and AO. EOF1 of Sea Level Pressure (SLP), shows anti-cyclonic circulation over Region 1 that is indicative of a negative association with influencing indices, whereas EOF2 and EOF3 show cyclonic circulation that is indicative of a positive association with influencing indices.

Leading modes of ZW-Surface are shown in Figure 3.13 (a, b and c) respectively. EOF1(10%), EOF2(7%) and EOF3(6%) of ZW-Surface explain about 23% cumulative variability. Since Equatorial Indian Ocean Zonal Wind Index (EQWIN), is highly correlated with the difference of Outgoing Longwave Radiation (OLR) in Eastern Equatorial Indian Ocean (EEIO) and Western Equatorial Indian Ocean (WEIO) regions, therefore the occurrence of Equatorial Indian Ocean Zonal Wind Index (EQWIN), can easily be detected by identifying the enhanced/suppressed convection (cloudiness) in WEIO/EEIO region. EOFs of OLR are shown in Figures 3.13 (x, y and z). EOF1 and EOF3 show weak whereas EOF2 shows a moderate pattern of Equatorial Indian Ocean Zonal Wind Index (EQWIN).

From the EOF analysis as mentioned above, it is clear that patterns of NAO (weak), AO (moderate to weak), AMO (moderate), DMI (moderate), Equatorial Indian Ocean Zonal Wind Index (EQWIN), (moderate), ENSO-MEI (moderate), EMI-MODOKI (strong) and PDO (moderate) are found in the three leading modes of January. Blue boxes show NAO Region in Atlantic Ocean. Black boxes show WEIO and EEIO region whereas green box show CEIO region in Indian Ocean. Red boxes show ENSO-MODOKI regions whereas magenta box show ENSO-MEI region in Pacific Ocean.

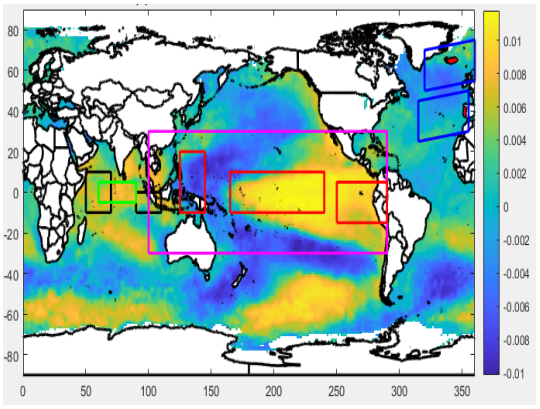

*(a) EOF1 of standardized SST for January shows the patterns of ENSO and PDO in Pacific Ocean*

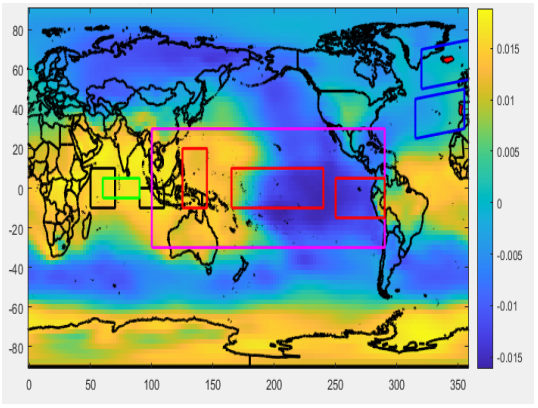

*(x) EOF1 of standardized SLP for January shows the patterns of ENSO-SOI and NAO pattern though not very distinguished*

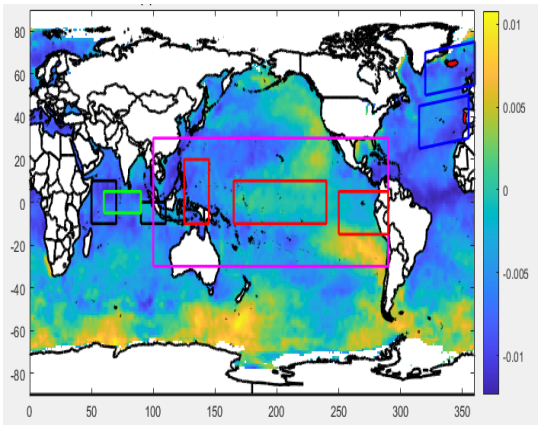

*(b) EOF2 of standardized SST for January showing the pattern of AMO in Atlantic Ocean and pattern of DMI in Indian Ocean*

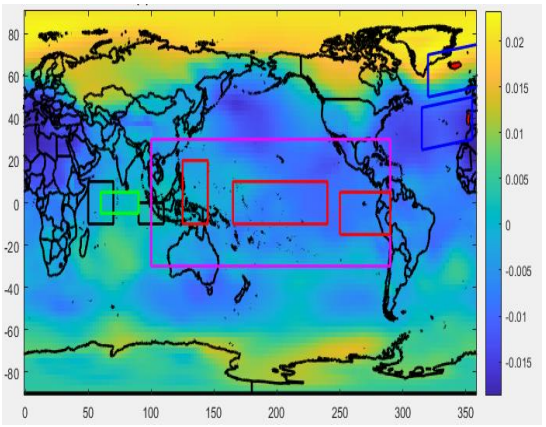

*(y) EOF2 of standardized SLP for January shows the pattern of AO*

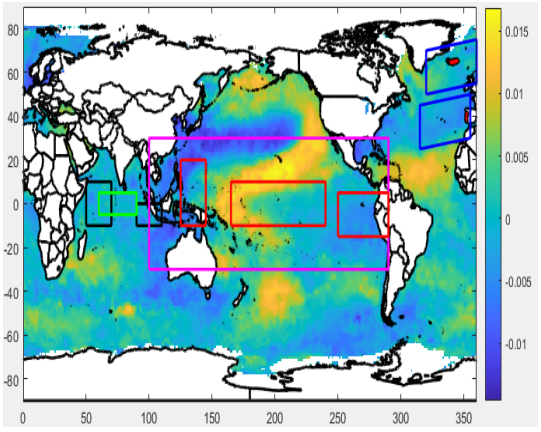

*(c) EOF3 of standardized SST for January shows patterns of PDO, EMI-MODOKI and NAO (SST associated patterns)*

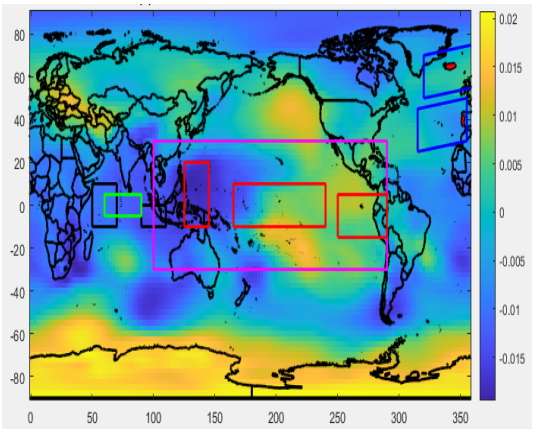

*(z) EOF3 of standardized SLP for January shows patterns of ENSO and NAO*

FIGURE 3.12: EOFs of standardized SST and SLP for January(1977-2017) [235].

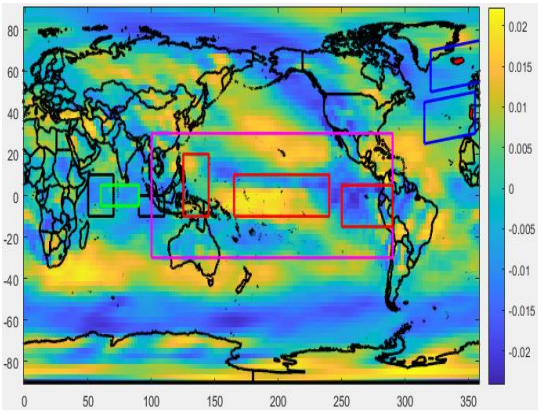

*(a) EOF1 of standardized SZW for January shows weak pattern of EQWIN*

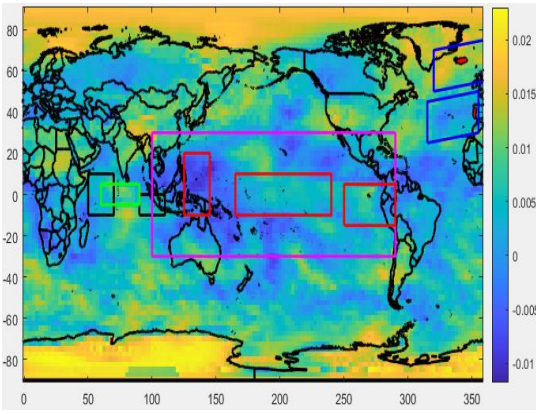

*(x) EOF1 of standardized OLR for January shows weak pattern of EQUINOO*

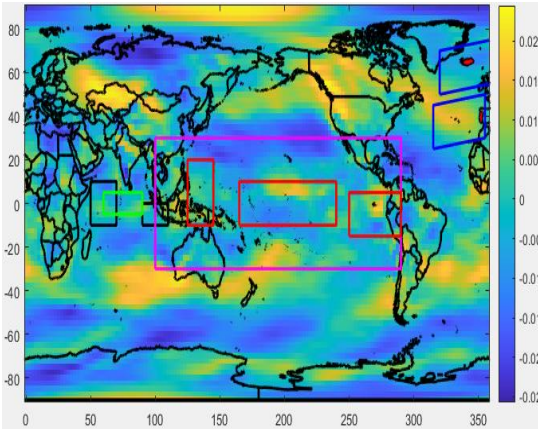

*(b) EOF2 of standardized SZW for January shows moderate pattern of EQWIN*

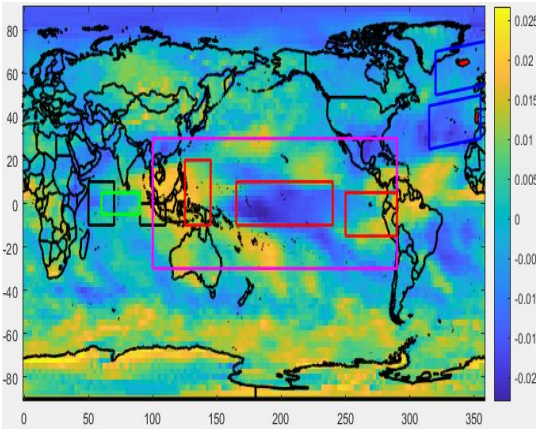

*(y) EOF2 of standardized OLR for January shows moderate pattern of EQUINOO*

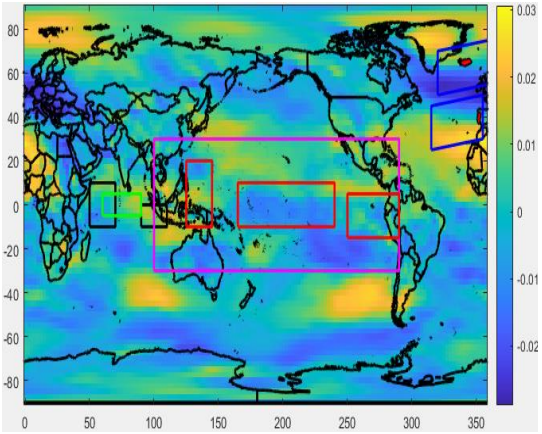

*(c) EOF3 of standardized SZW for January shows weak pattern of EQWIN*

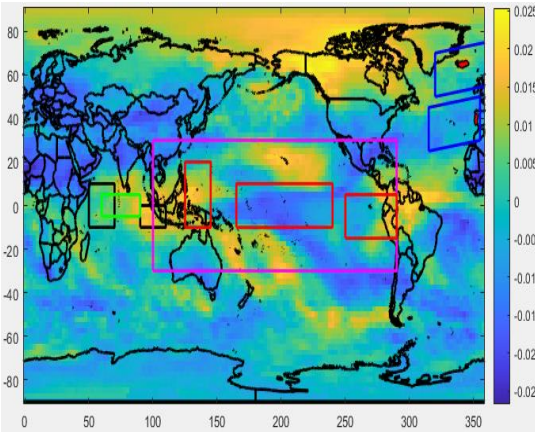

*(z) EOF3 of standardized OLR for January shows weak pattern of EQUINOO*

FIGURE 3.13: EOFs of Standardized SZW and OLR for January (1977-2017) [235].

#### 3.3.4.4 Relationship of Region1 Precipitation with SST Anomalies for January

The distribution of correlation coefficient between PCs (1, 2 and 3) and standardized Sea Surface Temperature (SST) for the month of January is shown in Figure 3.14. In tropical areas, PC-1 is positively correlated with Central-Eastern Pacific, whereas it is negatively correlated with Western Pacific, as shown in Figure 3.13(a). This Sea Surface Temperature (SST) anomaly is indicative of linkages of precipitation with ENSO-MEI. Still the correlation is mostly insignificant with some significant areas and may be considered as weak, which is in line with the findings in Table 3.12. Figure 3.14(b) and 3.14(c) show a negative correlation in the central area for EMI-MODOKI and a positive correlation in flank areas marked by red boxes, which is indicative of linkages of PC2 and PC3 with the EMI index. At mid and high latitudes, PC3 is negatively and positively correlated with Sea Surface Temperature (SST) analogous to Pacific Decadal Oscillation (PDO), index (Figure 3.14(c)).

In the tropical Indian ocean, PC1 is negatively correlated with Sea Surface Temperature (SST). PC2 and PC3 are positively correlated with Sea Surface Temperature (SST) in Western Equatorial Indian Ocean (WEIO) and negatively correlated with Sea Surface Temperature (SST) in Eastern Equatorial Indian Ocean (EEIO) regions which is indicative of linkages with Indian Ocean Dipole (IOD)-Dipole Mode Index (DMI). Still the correlation appears moderate to weak with some significant positive correlated areas.

In the Northern Atlantic Ocean, PC1 and PC2 (Figure 3.14(a) and 3.14(c)) correlations with Sea Surface Temperature (SST) anomalies are analogous to the North Atlantic Oscillation (NAO), associated Sea Surface Temperature (SST) pattern, thus indicative of an association with North Atlantic Oscillation (NAO). Figure 3.14(c) shows a positive correlation with Sea Surface Temperature (SST) in the Northern Atlantic, which is indicative of Atlantic Multi-decadal Oscillation (AMO) linkage with PC3.

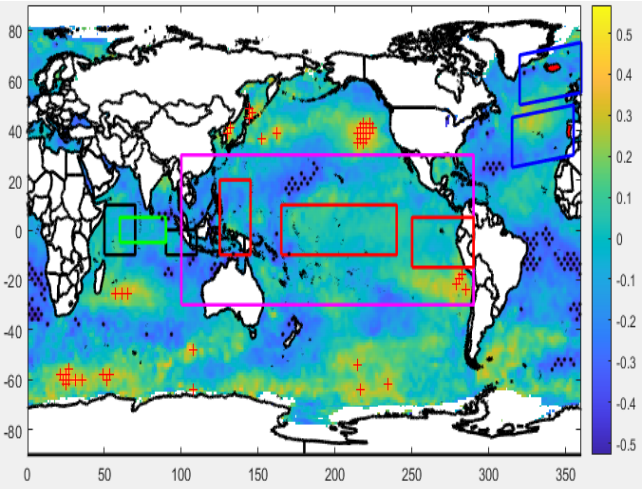


*(a) EOF1 of standardized SZW for January shows weak pattern of EQWIN*

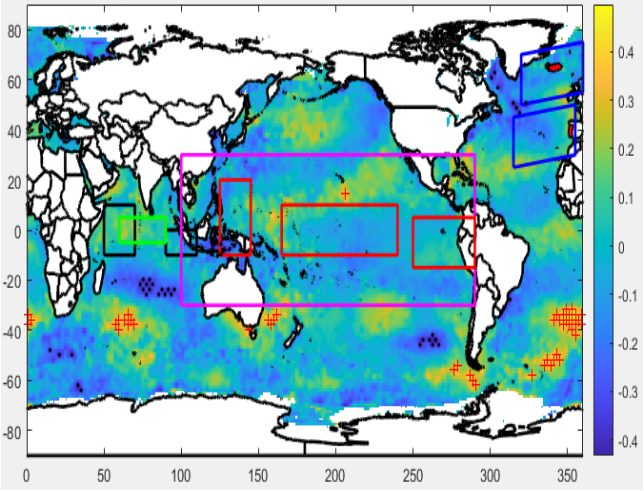


*(b) EOF2 of standardized SZW for January shows moderate pattern of EQWIN*

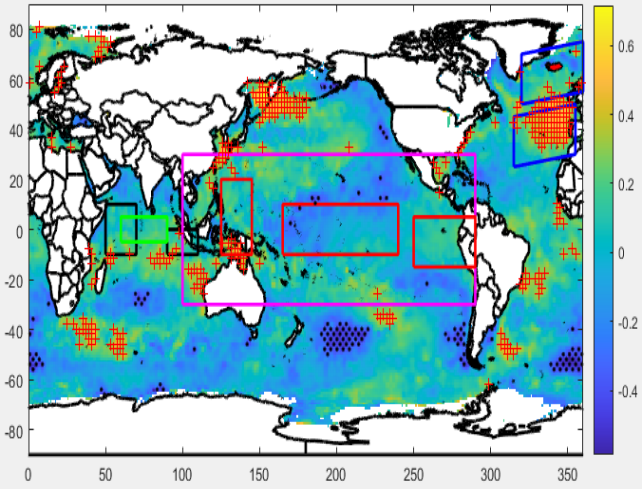


*(c) EOF3 of standardized SZW for January shows weak pattern of EQWIN*

FIGURE 3.14: Correlation between PCs of Region1 precipitation and standardized SST for January (1977-2017) [235].

#### 3.3.4.5 Relationship of Region1 Precipitation with Atmospheric Circulation Anomalies for January

The relationship of Region 1 precipitation with atmospheric circulations is studied by conducting the correlation analysis between PCs and atmospheric circulations SLP, GPH500. Figure 3.15 shows the distribution of correlation coefficient between PCs (1, 2, 3) and standardized SLP for January. In tropical regions, the pacific warm pool remains stabilized and does not show any significant correlation with Region 1 precipitation. Responding to PC1, the center tropical region shows negative correlation with SLP and positive correlation in flank areas marked by red boxes. This surface SLP anomaly is indicative of linkages with ENSO-MODOKI, but the correlation is mostly insignificant with some significant areas. PC3 shows a positive correlation over most of the tropical region with significant positive correlations in central tropics and a negative correlation in flank areas marked by red boxes, which is la-Nina EMI-MODOKI pattern.

In the Indian Ocean, responding to Sea Level Pressure (SLP), , PC1 shows significant positive correlation while PC-2 remains negatively correlated both without showing any distinguishable opposite anomalies similar to DMI. However, PC-3 exhibits minor positive and negative anomaly between the Western Equatorial Indian Ocean (WEIO) and the Eastern Equatorial Indian Ocean (EEIO) region similar to DMI pattern.

In the Northern Atlantic Ocean, a high-pressure anomaly is present over Iceland. In contrast a significant low-pressure anomaly is present over the Azores in response to the correlation of PC1 with SLP. This surface SLP anomaly is indicative of a strong (-) NAO pattern. This NAO anomaly is also accompanied by a low-pressure anomaly over Artic and high-pressure anomaly in northern Atlantic and the Pacific Ocean analogous to +AO pattern, but the correlation remains insignificant (weak). Responding to SLP, PC2 is positively correlated with the Azores region and is negatively correlated with the Iceland region, but the correlations remain insignificant (moderate to weak). This SLP anomaly is indicative of +NAO mode. PC2 correlation with SLP does not show any distinguishable anomaly

pattern similar to the +AO pattern in the Arctic. PC3 again shows a positive correlation with the Azores and a negative correlation with Iceland with insignificant correlations (moderate to weak). But responding to SLP, strong low-pressure anomaly exist with significant negative correlation and high-pressure anomalies with significant positive correlation in Northern Atlantic and insignificant positive correlation in North Pacific Ocean somewhat similar to +AO mode.

In order to understand the linkages of the observed signals of teleconnection including EMI-MODOKI, ENSO-MEI in the Pacific Ocean, DMI in the Indian Ocean, NAO, AO in the Atlantic Ocean with Region 1 precipitation through atmospheric circulations, the correlation of PCs (1, 2, 3) is performed with GPH500 as shown in Figure 3.14. The favorable precipitation counterpart of surface low pressure is high pressure at mid-troposphere (500 hpa), indicating cyclonic circulation. In contrast, the high pressure at the surface and low pressure at the mid-troposphere (500 hpa) is indicative of anti-cyclonic circulations. In response to correlations of PC1 with SLP and GPH500, Figure 3.15(a) shows low surface pressure at Region 1, whereas Figure3.15(a) depicts positive height anomaly (at GPH500) which is indicative of cyclonic conditions. Positive/negative SLP anomaly in Iceland / Azores with its counterpart negative/positive anomaly at 500 hpa extending all the way to the Mediterranean and the Middle East Region, which is indicative of linkages with NAO.

Furthermore, in the tropical Pacific region positive/negative/positive SLP anomaly with its counterpart negative/positive/negative in EMI-MODOKI regions are indicative of teleconnection with EMI-MODOKI Index. However, cyclonic condition exists in the Indian Ocean, represented by high SLP anomaly and low mid altitude anomaly at 500 hpa. For PC2 correlations with responding SLP and GPH500, Figures 3.15(b) and 3.15(y) show that the pressure conditions at the surface are not supportive of their counterpart pressure conditions at mid- altitude. Lastly, for PC3 correlations with SLP and GPH500, Figures 3.15(c) and 3.15(z) show anti-cyclonic conditions over Region 1 in response to anti-cyclonic condition at SLP and cyclonic condition at mid heights over tropical Indo-pacific region and North Atlantic region, which is indicative of reduced precipitation.

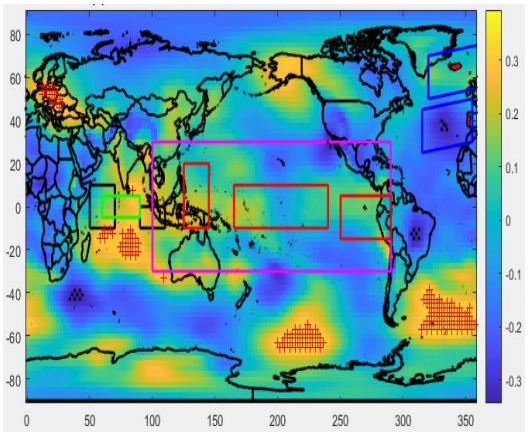

*(a) Correlation between PC1 of Region1 precipitation and standardized SLP for January.*

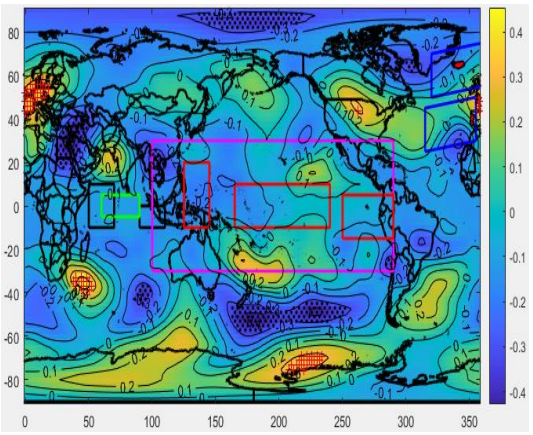

*(x) Correlation between PC1 of Region1 precipitation and standardized GPH500 for January*

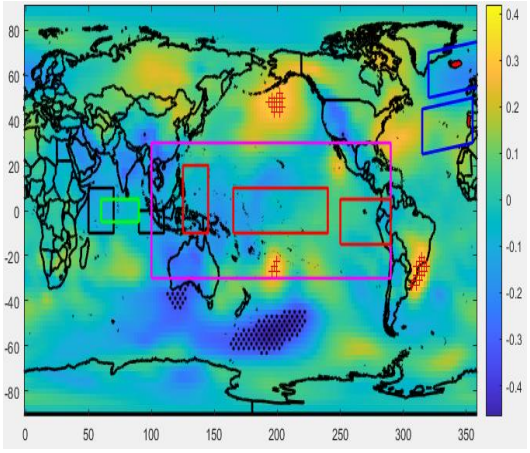

*(b) Correlation between PC2 of Region1 precipitation and standardized SLP for January*

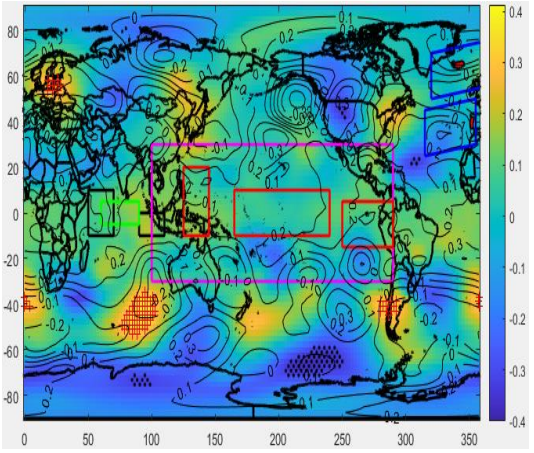

*(y) Correlation between PC2 of Region1 precipitation and standardized GPH500 for January*

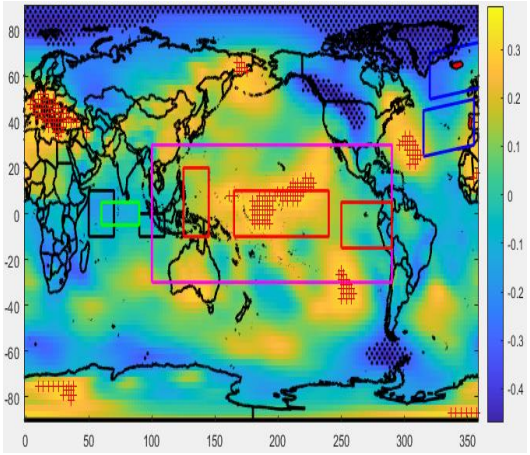

*(c) Correlation between PC3 of Region1 precipitation and standardized SLP for January*

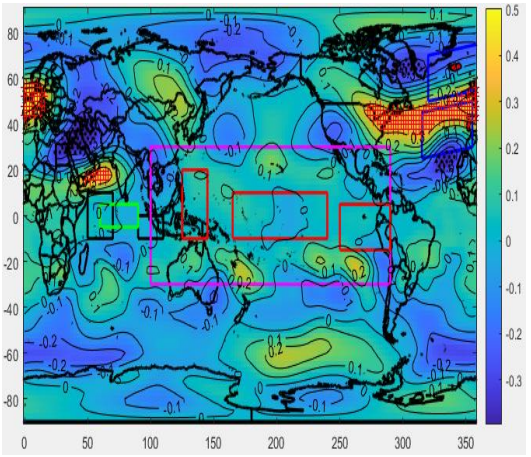

*(z) Correlation between PC3 of Region1 precipitation and standardized GPH500 for January*

FIGURE 3.15: Correlation between PCs of Region1 precipitation and standardized SLP and GPH500 for January (1977-2017) [235].

To ascertain the linkages of atmospheric circulations with Region1 precipitation, Empirical Orthogonal Function (EOF) modes of GPH500 are calculated. The target area is the 30S-90N and 0-360, where the teleconnection pattern under consideration are formed. The corresponding time series of the three leading modes (G1, G2, G3), which explain 50.31% combined variability, are extracted. The correlation matrix between G1, G2, G3 with PCs of Region 1 precipitation (PC1, PC2, PC3) is shown in Table 3.10. The matrix is formulated to determine the PCs of GPH500, which have a significant influence on the Region 1 precipitation through teleconnection via atmospheric circulations. Table 3.10 indicates that only G1 and G2 have a significant correlation with Region 1 precipitation PCs (PC1 or PC3) and are therefore considered for further analysis. The leading EOF modes (EOF1, EOF2) and the correlation of PCs of Region 1 precipitation (PC1, PC2) are shown in Figure 3.16.

TABLE 3.10: Correlation Matrix between PCs of GPH (G1, G2, G3) and PCs of Region1 Precipitation (PC1, PC2 and PC3)

| | **R1JANP-PC1** | | **R1JANP-PC2** | | **R1JANP-PC3** | |
|---|---|---|---|---|---|---|
| **GPH-Principal Components** | **Corrl. Coeff.** | **p-Value** | **Corrl. Coeff.** | **p-Value** | **Corrl. Coeff.** | **p-Value** |
| G1 | 0.3532 | **0.023** | 0.1062 | 0.508 | -0.2619 | **0.098** |
| G2 | -0.2594 | **0.101** | 0.1453 | 0.364 | -0.1598 | 0.318 |
| G3 | -0.0693 | 0.668 | -0.1881 | 0.239 | 0.2259 | 0.155 |

The correlation analysis is performed between the G1, G2 and climate indices to determine the influencing indices of Region 1 precipitation. The results are shown in Table 3.11, which indicates that Region 1 precipitation is linked to North Atlantic Oscillation, Atlantic Multi-decadal Oscillation, Dipole mode index, Equatorial Indian Ocean Zonal Wind Index, ENSO Modoki Index through atmospheric circulations.

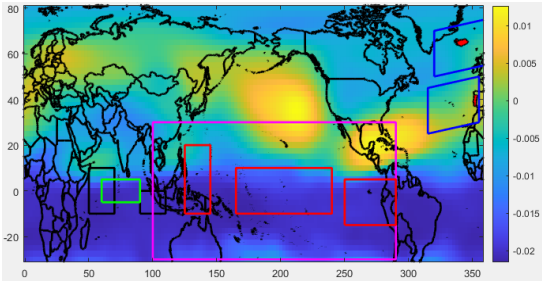

*(a) EOF1 of standardized GPH at 500 hpa in January.*

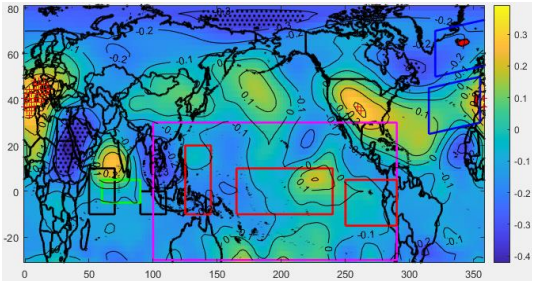

*(x) Correlation between PC1 of region1 precipitation and standardized GPH at 500 hpa*

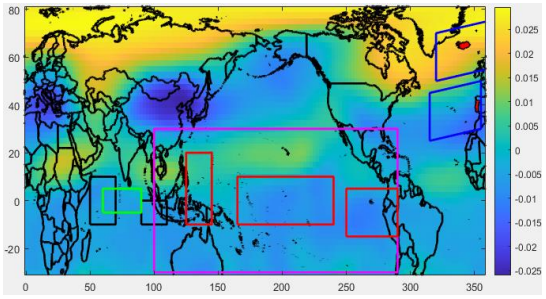

*(b) EOF2 of standardized GPH at 500 hpa in January.*

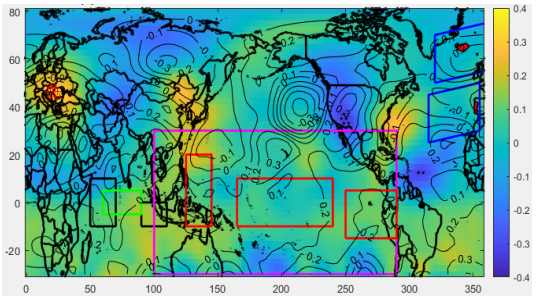

*(y) Correlation between PC2 of region1 precipitation and standardized GPH at 500 hpa.*

FIGURE 3.16: EOF modes of Standardized GPH (1977-2017) [235].

TABLE 3.11: Correlation between PCs of GPH (G1, G2, G3) and Climate Indices

| | **G1** | | **G2** | |
|---|---|---|---|---|
| **Indices** | **Corrl. Co-eff.** | **p-Value** | **Corrl. Co-eff.** | **p-Value** |
| NAO | -0.1475 | 0.3576 | 0.2284 | **0.1508** |
| AO | -0.0369 | 0.8188 | 0.1591 | 0.3203 |
| AMO | -0.4251 | **0.0056** | -0.0742 | 0.6449 |
| DMI | -0.1188 | 0.4595 | -0.2821 | **0.0739** |
| EQWIN | 0.3237 | **0.0390** | 0.0147 | 0.9272 |
| ENSO-MEI | 0.0650 | 0.6865 | 0.0366 | 0.8204 |
| EMI-MODOKI | -0.2029 | **0.2033** | 0.0631 | 0.6953 |
| PDO | -0.1510 | 0.3461 | -0.1802 | 0.2595 |

Bold figures indicate significant correlation at 20% confidence.

#### 3.3.4.6 Relationship of Region1 Precipitation with Surface Wind Anomalies for January

The distribution of correlation coefficient between PCs (1, 2 and 3) and standardized Zonal Winds at Surface (ZW-Surface) for the month of January is shown in Figure 3.17. As mentioned above, Equatorial Indian Ocean Zonal Wind Index (EQWIN) being highly correlated to Equatorial Indian Ocean Oscillation (EQUINOO), correlations of PCs with Outgoing longwave Radiation (OLR) is calculated to identify the influence of EQWIN index easily. In the tropical Indian Ocean at Western Equatorial Indian Ocean (WEIO) and Eastern Equatorial Indian Ocean (EEIO) regions, OLR anomalies are significantly correlated with the PC1, PC3 of Region 1 precipitation which is indicative of correlation with surface zonal winds, whereas the association with PC-2 remains insignificant. This surface zonal wind anomaly indicates the Equatorial Indian Ocean Zonal Wind Index (EQWIN) significant positive correlation with Region 1 January precipitation (R1JANP).

In other words, it can also be reported as Equatorial Indian Ocean Zonal Wind Index has a substantial positive correlation with the January precipitation of stations located in region 1 namely

Barakhan

Khuzdar

Kalat

Quetta

Zhob

The Equatorial Indian Ocean Zonal Wind Index (EQWIN) index is the atmopheric segemnt of Indain Ocean diapole. Equatorial Indian Ocean Zonal Wind Index (EQWIN) which is the negative anomaly of Outgoing longwave Radiation (OLR), hence is to be multiplied with -1.

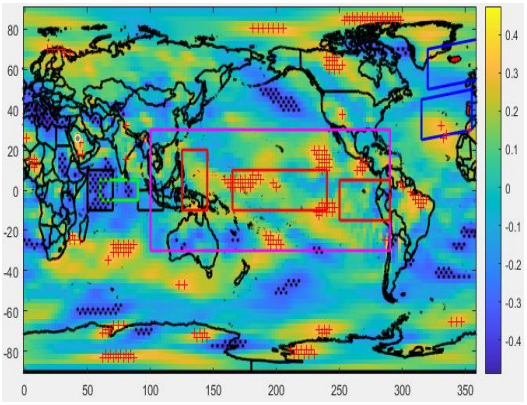

*(a) Correlation between PC1 of Region1 precipitation and Standardized ZW-Surface for January shows strong pattern of EQWIN.*

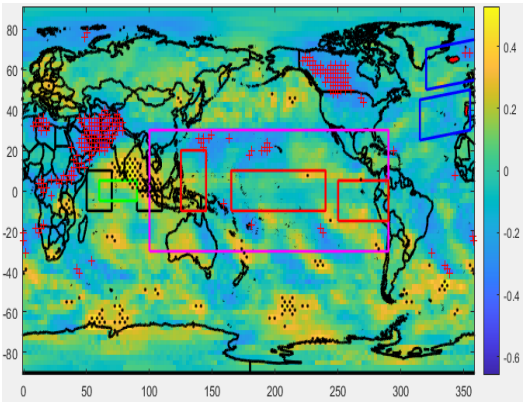

*(x) Correlation between PC1 of Region1 precipitation and Standardized OLR for January shows weak pattern of EQWIN*

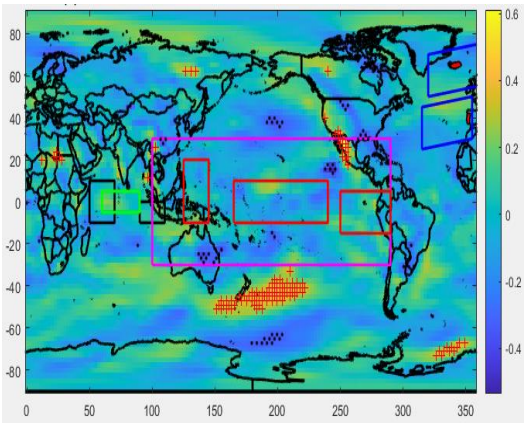

*(b) Correlation between PC2 of Region1 precipitation and Standardized ZW-Surface for January shows weak pattern of EQWIN*

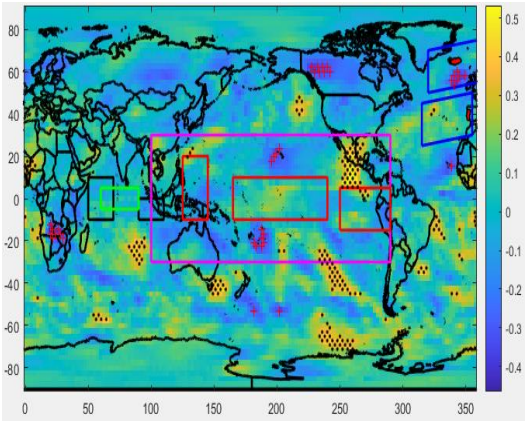

*(y) Correlation between PC2 of Region1 precipitation and Standardized OLR for January shows weak pattern of EQWIN*

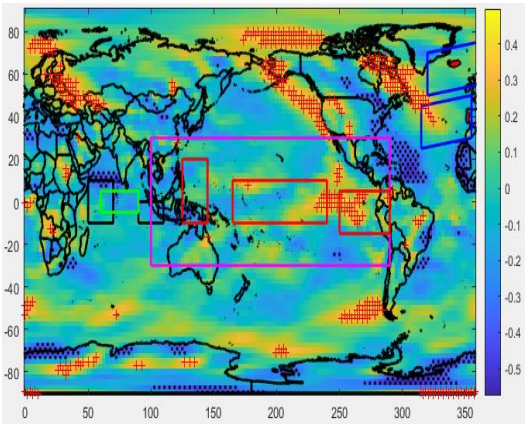

*(c) Correlation between PC3 of Region1 precipitation and Standardized ZW-Surface for January shows moderate pattern of EQWIN*

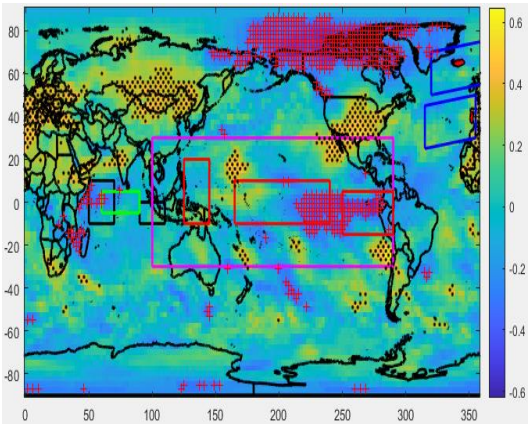

*(z) Correlation between PC3 of Region1 precipitation and Standardized OLR for January shows moderate pattern of EQWIN*

FIGURE 3.17: PCs of Standardized ZW-Surface and OLR for January (1977-2017) [235].

#### 3.3.4.7 Time Lag Relationship of PCs with Climate Indices for January

The time-lag relationship for the correlation coefficient of PCs with the climate indices is also examined in this study. As mentioned earlier, three PCs of Region 1 precipitation are considered. Time-lag relationships of only those PC-Climate Index relationship is considered, which is most significant. For example, out of the three relationships between PCs and NAO, only PC1-NAO is most significant which is shown in Table 3.9. The time-lag relationship indicates that except NOA, all the other climate indices (AO, AMO, DMI, EQWIN, ENSO-MEI, EMI-MODOKI and PDO) are at their maximum significance level with the respective principal mode (PC) preceding to the month of January. NAO attains its maximum negative significance in December of the year preceding the month of January. Time-lag relationship also shows that NAO, AO, ENSO-MEI and PDO are negatively correlated whereas AMO, DMI, EQWIN and ENSO-MODOKI are positively correlated with their respective principal modes of precipitation.

#### 3.3.4.8 Result Analysis for January

The results obtained from all the above analyses are summarized in Table 3.12, along with the comparison with the previously obtained results of correlation and Partial Mann-Kendall analysis. Thus, from the analysis, it can be concluded that the influence of NAO and AO on Region1 precipitation is insignificant (weak). Since none of the previous studies are focused on Baluchistan therefore, there is not much literature available to support the argument that NAO mode enhances (reduces) the precipitation in Baluchistan. However, Ahmed et al. [219] found out that the positive (negative) NAO mode strengthens (weakens) winter-spring precipitation in Pakistan; similarly, Athar et al. [232] found out that NAO shows a correlation with Baluchistan without mentioning whether the correlation is positive or negative. Therefore, it can be inferred that NAO and AO have a weak influence on the January precipitation in Baluchistan. The influence of AMO,

DMI, ENSO-MEI and PDO are significant up to 20% confidence (may be considered as moderate). Lastly the influence of EQWIN and EMI-MODOKI are significant up to 5% confidence (may be considered as strong).

Table 3.12: Summary of Analysis Results for Region 1 precipitation and Climate Indices for January

| | | | | **Correlation b/w PCs and anomalies of** | | |
|---|---|---|---|---|---|---|
| **Indices** | **Partial Mann-Kendall** | **Correlation b/w PCs and Climate Indices** | **EOF Analysis** | **SST** | **Atmospheric Circulation** | **Zonal Winds and OLR** |
| NAO | Weak | Insignificant | Weak | Weak | Moderate | – |
| AO | Weak | Insignificant | Moderate to Weak | – | Weak | – |
| AMO | Weak | Significant at 7.9 % | Moderate | Moderate | – | – |
| DMI | Weak | Significant at 12.4 % | Moderate | Moderate | – | – |
| EQWIN | Strong to Moderate | Significant at 1.5% | Strong | – | – | Strong |
| ENSO-MEI | Moderate to Weak | Significant at 16.5% | Moderate | Weak | – | – |
| EMI-MODOKI | Strong | Significant at 4.8% | Strong | Strong | – | – |
| PDO | Weak | Significant at 20.5% | Moderate | Moderate to Strong | – | – |

#### 3.3.4.9 Discussion of Results - January

**Weak insignificant effect of -NAO/-AO**

The negative phase of the North Atlantic Oscillation (NAO) has a weak influence

on the precipitation of Baluchistan. During the negative phase of North Atlantic Oscillation (NAO), the Atlantic Jetstream and storm tracks more southerly path, gathers moisture from the Mediterranean Sea crosses this region. The embedded western disturbances in the westerlies are responsible for the precipitation under favorable conditions. **Contrary to this,** Ahmed et al. [219] found that the positive (negative) phase of NAO strengthens (weakens) winter-spring precipitation in the Northern parts of Pakistan above 31.5-degree latitude as the Atlantic jet stream and storm track more northernly path and are responsible for the precipitation (whereas Baluchistan is mostly located below 31.5 degree latitude).

Athar et al. [232] found that North Atlantic Oscillation (NAO) is correlated with precipitation in Baluchistan without mentioning whether the correlation is positive or negative. Yadav et al. [122] suggest that the winter precipitation in the western Indian region is influence by positive NAO/AO. The positive/negative pressure anomaly intensifies the Asian westerly jet stream over North Africa and the Middle East extending up to Northwest India. The jet stream intensifies the western disturbances and is responsible for increased precipitation over Northern Pakistan and Northwest India. The effect of AO, either positive or negative, is insignificant over this region.

In **contrast** to this, Midhuna and Dimri [229] suggest that the positive AO has more influence on the winter monsoon precipitation over the Himalayas and western Indian region. Stronger westerlies from the Atlantic Ocean increase the strength of WDs over the region along with the strong pressure gradient resulting in moisture transport, thus responsible for excess precipitation during winter. In addition to that, during the positive AO phase, strong wave activity flux is seen at the Arabian Sea and adjacent areas, which indicates a strong mid-latitude Rossby wave response.

**Moderate effect of -ENSO-MEI/+DMI/+AMO/-PDO**

The negative phase of ENSO-MEI (La-Nina) has a moderate effect on the winter precipitation of this region. **This is in line with the findings of the previous studies on this region**. Azmat [309] suggests that during negative ENSO episodes, cooler than normal ocean temperatures in the equatorial Central Pacific

act to restrain the formation of rain-producing clouds in the region. Mid-latitude depressions are inclined to be weaker than normal. La Nina episodes include large-scale changes in the atmospheric winds across the tropical Pacific, including increased winds from the east across the eastern Pacific in the lower atmosphere and greater winds from west over the eastern tropical Pacific in the upper atmosphere. These conditions explain an increased strength of the equatorial Walker Circulation. Winter season rainfall activity over Pakistan is suppressed under similar La Nina conditions during fall. However, if La Nina event is declining and its intensity becomes weak during winter relative to the previous quarter (fall), i.e., increase in sea surface temperature, then rainfall activity over Pakistan tends to lie between normal to greater than normal. The positive phase of Dipole mode index (DMI), , an index of Indian Ocean dipole, has a moderate effect on the winter precipitation of this region.

In **contrast**, Adnan et al. [310] suggest that Dipole mode index (DMI), values show only a minimal negative correlations with the winter rainfall for northern Pakistan. But these negative correlation were weak and negligible. No studies were conducted to study the impact of DMI specifically on this region. Warm ENSO condition adversely affects the rainfall over this region, but the occurrence of strong positive Dipole mode index (DMI), diminishes the adverse effect of warm ENSO, which in turn otherwise helps in increasing precipitation over this region. Similarly, Chakrborty et al. [311] suggest that the interannual variation of moisture flux is strongly modified by positive IOD and positive ENSO events, which **confirms** the findings of this study. In the course of these events, the moisture transport from the Red Sea toward the mountainous region of Asir Province of Saudi Arabia increases. As a result, rain activity during November through April increases.The negative phase of PDO and positive phase of AMO have moderate effect on the winter precipitation of this region. AMO and PDO are indices showing the multi-decadal variations in SST in North Atlantic and North Pacific Ocean and are negative phase-locked.The negative phase of PDO enhances the effect of cold ENSO (La-Nina), whereas the positive phase of AMO weakens the effect of NAO/AO but modestly effect the warming of the Indian Ocean.

**Significant effect of +EQWIN AND +EMI-MODOKI**

EQWIN, which is the index for the EQUINOO in the Indian Ocean, has a significant positive correlation with the precipitation in Baluchistan, whereas the positive phase of EMI-MODOKI, an index of large-scale tripole anomalous condition in the equatorial Pacific Ocean, also has a significant positive correlation in this region. Ashok et al. [312] confirm the findings of the current study by suggesting that relatively higher rainfall was observed over the Indian subcontinent during El Nino MODOKI season as compared to the El Nino dry periods.

## 3.3.5 Linkages of June Precipitation Variability with Climatic Indices

### 3.3.5.1 Modes of Region 1 Precipitation for the Month of June

PCA is performed on the R1JUNP the first three EOFs explain 90.82% variation, capable enough to explain the precipitation variability in Region 1. These three PCs are then used to perform the correlation analysis with climate indices. The correlation between time series of PCs and R1JUNP is shown in Table 3.13.

Table 3.13: Region 1 Precipitation Modes (EOFs) and Corresponding PCs for the Month of June

| **EOFs** | **Variability Explained** | **Cumulative** | **PCs** | **Correlation Coeff.** | **p-value** |
|---|---|---|---|---|---|
| EOF1 | 58.61% | 58.61% | PC1* | 0.7793 | **0.0001** |
| EOF2 | 16.19% | 74.80% | PC2* | -0.5306 | **0.0003** |
| EOF3 | 16.02% | 90.82% | PC3* | 0.1521 | 0.3425 |
| EOF4 | 5.68% | 96.50% | PC4 | -0.1578 | 0.3246 |
| EOF5 | 3.50% | 100.00% | PC5 | -0.2188 | 0.1693 |

Bold figures represent significant correlations, coefficients and probability at 5%, whereas '*' indicates the selected modes.

#### 3.3.5.2 Correlation of Region 1 Precipitation with Climate Indices for June

In order to find out the association of R1JUNP with climate indices, correlation is performed between the time series of Region1 precipitation PC (R1JUNP-PCs) and the climate indices for the month of June. The results are presented in Table 3.14. Large-scale teleconnection circulation patterns North Atlantic Oscillation index (NAO) is negatively correlated to PC2 at 11.05% confidence. Artic Oscillation index (AO) is negatively correlated but is insignificant. Atlantic Multi Decadal Oscillation index (AMO) is negatively correlated to PC3 but is insignificant. Indian Ocean Dipole mode index DMI is positively correlated to PC1 but is insignificant. EQWIN defined the Indian Ocean circulation pattern positively correlated to PC1 at 0.4% confidence. Large scale teleconnection pattern ENSO-MEI is negatively correlated to PC3 but is insignificant. ENSO-MODOKI index (EMI-MODOKI) is positively correlated to PC3 but is insignificant. Pacific Ocean decadal oscillation (PDO) is negatively correlated to PC2 at 4.57% confidence level.

Table 3.14: Correlation between R1JUNP-PCs and Climate Indices

| | **R1JUNP-PC1** | | **R1JUNP-PC2** | | **R1JUNP-PC3** | |
|---|---|---|---|---|---|---|
| **Indices** | **Corrl. Coeff.** | **p-Value** | **Corrl. Coeff.** | **p-Value** | **Corrl. Coeff.** | **p-Value** |
| NAO | -0.2530 | **0.1105** | -0.0091 | 0.9549 | -0.0521 | 0.7463 |
| AO | -0.1120 | 0.4858 | 0.0179 | 0.9114 | -0.0406 | 0.8011 |
| AMO | -0.0625 | 0.6978 | -0.0371 | 0.8178 | 0.0629 | 0.6958 |
| DMI | 0.1503 | 0.3483 | 0.1437 | 0.3699 | -0.0520 | 0.7470 |
| EQWIN | 0.4397 | **0.0040*** | -0.0111 | 0.9449 | -0.2191 | 0.1687 |
| ENSO-MEI | 0.0257 | 0.8732 | 0.0970 | 0.5464 | -0.1468 | 0.3597 |
| EMI-MODOKI | 0.1170 | 0.4662 | -0.0295 | 0.8549 | 0.1264 | 0.4309 |
| PDO | 0.1338 | 0.4044 | -0.3139 | **0.0457*** | -0.1096 | 0.4951 |

Bold with asterisk figures indicate significant correlation at 8% confidence, whereas bold figures indicate correlation up to 20% significance.

#### 3.3.5.3 Leading Modes of Teleconnection Patterns for the Month of June

EOF analysis is performed on SST, SLP and ZW-surface for June also. The uncertainty estimates of June eigenvalues spectrum of the covariance matrix of SST and SLP are calculated and are used for selecting leading modes of EOFs. Two eigenvalues of SST and four eigenvalues of SLP are well distinguishable from the rest of the spectrum, as shown in Figure 3.18(a) and (b). Therefore, three leading modes for each of the teleconnection patterns are considered for the analysis.

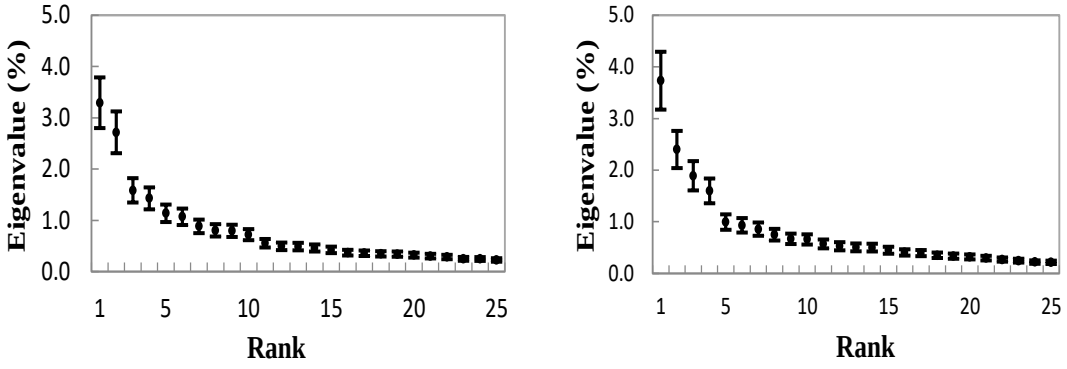


*a. Eigenvalue Spectrum (%) of the covariance matrix of June SST.*

*b. Eigenvalue Spectrum (%) of the covariance matrix of June SLP.*

FIGURE 3.18: Eigenvalue Spectrum (%) of the Covariance Matrix of June SST and SLP.

Three leading modes, EOF1(15%), EOF2(12%) and EOF3(7%) of Sea Surface Temperature (SST), , explained about 34% cumulative variability and showed the teleconnection patterns of ENSO, EMI-MODOKI (warm center flanked by cold sides: cold center flanked by warm sides) in Central Pacific Ocean, Atlantic Multi-decadal Oscillation (AMO), in North Atlantic Ocean, North Atlantic Oscillation, (associated SST pattern) in North Atlantic Ocean, DMI pattern (though weak) in the Indian Ocean. Leading modes of Sea Surface Temperature (SST), are shown in Figure 3.19(a), (b) and (c). Figure 3.19(x), (y) and (z) shows three leading modes of Sea Level Pressure (SLP). EOF1(17%), EOF2(11%) and EOF3(9%) of Sea Level Pressure (SLP), explain about 37% cumulative variability and show the patterns of ENSO, NAO and AO (though not very distinguishable).

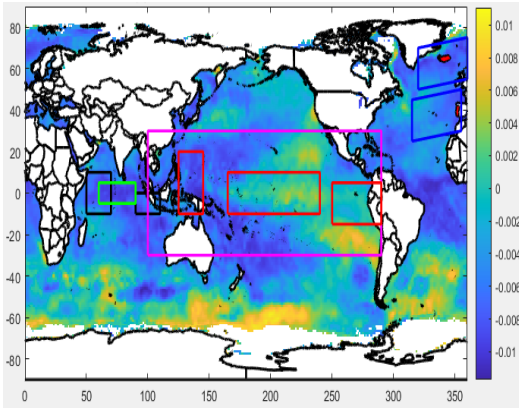

*(a) EOF1 of standardized SST for June shows the patterns of EMI-MODOKI and AMO.*

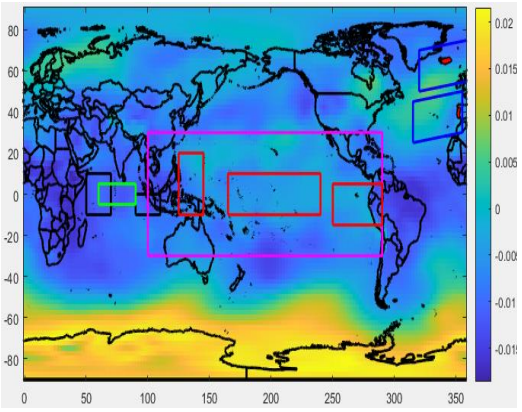

*(x) EOF1 of standardized SLP for June shows the pattern of NAO though not very distinguished*

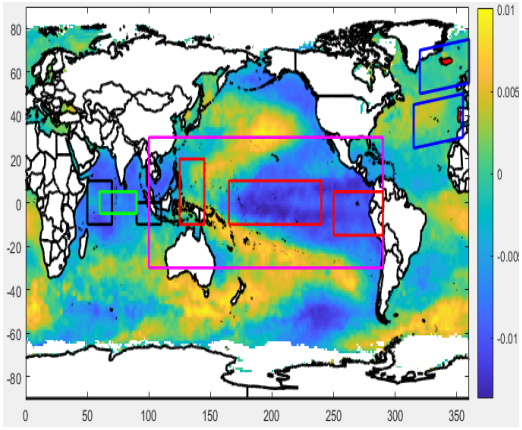

*(b) EOF2 of standardized SST for June shows the patterns of NAO, ENSO-MEI and PDO.*

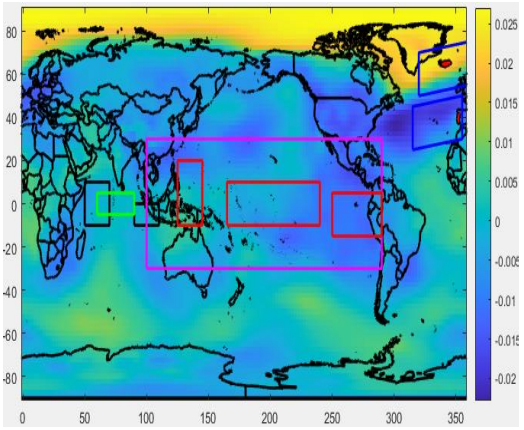

*(y) EOF2 of standardized SLP for June shows the pattern of NAO*

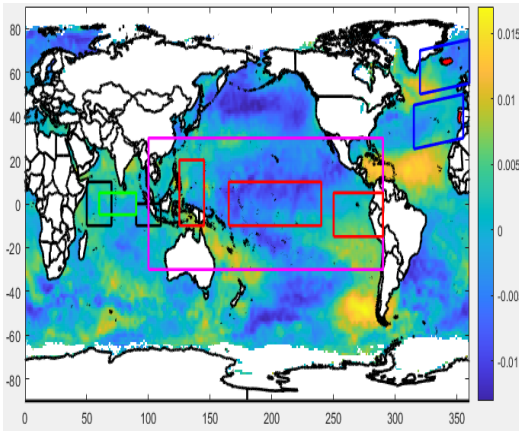

*(c) EOF3 of standardized SST for June shows weak patterns of DMI, EMI-MODOKI and NAO*

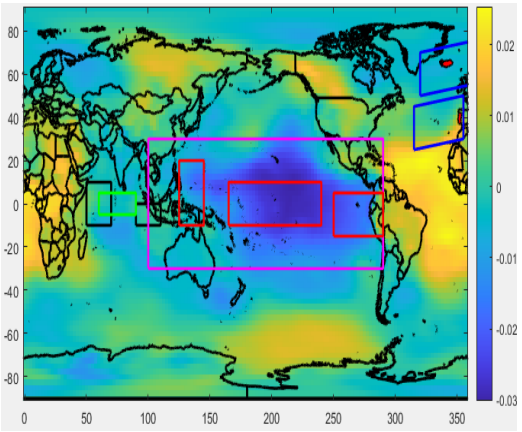

*(z) EOF3 of standardized SLP for June shows patterns of ENSO-MEI and AO though not very distinguished.*

FIGURE 3.19: EOFs of Standardized SST and SLP for June (1977-2017)[235].

Leading modes of ZW-Surface are shown in Figure 3.20(a), (b) and (c). EOF1(9%), EOF2(7%) and EOF3(6%) of ZW-Surface explain about 23% cumulative variability. As mentioned above, Equatorial Indian Ocean Zonal Wind Index (EQWIN), is highly correlated with the difference of Outgoing Longwave Radiation (OLR), in the Eastern Equatorial Indian Ocean (EEIO) and Western Equatorial Indian Ocean (WEIO) regions therefore the occurrence of Equatorial Indian Ocean Zonal Wind Index (EQWIN) can easily be detected by identifying the enhanced/suppressed convection (cloudiness) in Western Equatorial Indian Ocean (WEIO)/Eastern Equatorial Indian Ocean region.Empirical Orthogonal Function (EOF)s, of Outgoing Longwave Radiation (OLR), are shown in Figures 3.20(x), (y) and (z). EOF1 and EOF2 depict weak patterns, whereas EOF3 shows a moderate pattern of Equatorial Indian Ocean Zonal Wind Index (EQWIN).

From the Empirical Orthogonal Function (EOF), analysis as mentioned above, it is clear that patterns of North Atlantic Oscillation, (weak), Arctic Oscillation , (None), Atlantic Multi-decadal Oscillation (moderate), Dipole Mode Index (weak), Equatorial Indian Ocean Zonal Wind Index (strong), ENSO-MEI (moderate to strong), EMI-MODOKI (weak) and Pacific Decadal Oscillation (moderate to strong) are found in the three leading modes of June.

#### 3.3.5.4 Relationship of Region 1 Precipitation with SST Anomalies for June

The distribution of correlation coefficient between PCs (1, 2 and 3) and standardized surface Sea Surface Temperature (SST) June are shown in Figure 3.21. In tropical areas, PC-1 and PC-3 are negatively correlated with central-Eastern pacific, whereas they are positively correlated with western pacific (Figure 3.21(a) and (c)). This surface Sea Surface Temperature (SST), anomaly is indicative of linkages of precipitation with ENSO-MEI, but the correlation is mostly insignificant with some significant areas and may be considered as weak which is in line with the findings in Table 3.9. Figure 3.21(b) shows a positive correlation in the central area for EMI-MODOKI and a negative correlation in flank areas marked

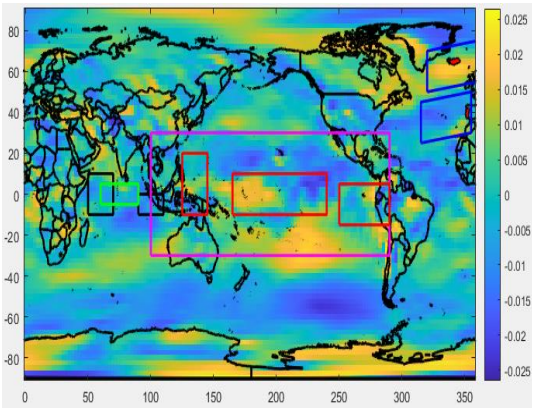

*(a) EOF1 Map of standardized ZW-Surface for June*

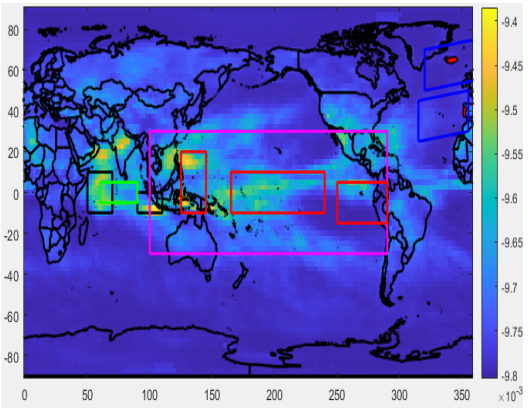

*(x) EOF1 Map of standardized OLR for June*

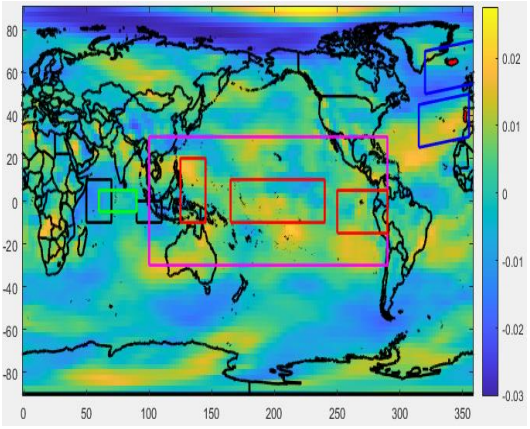

*(b) EOF2 Map of standardized ZW-Surface for June*

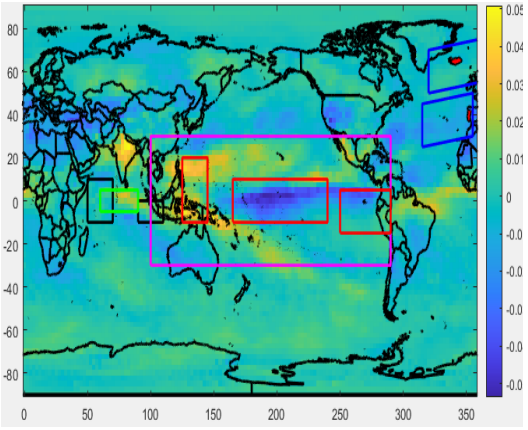

*(y) EOF2 Map of standardized OLR for June*

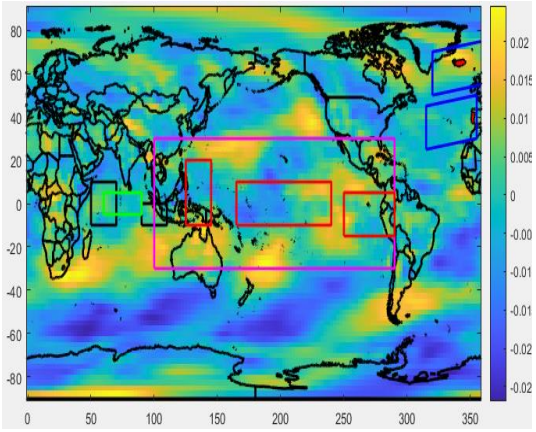

*(c) EOF3 Map of standardized ZW-Surface for June*

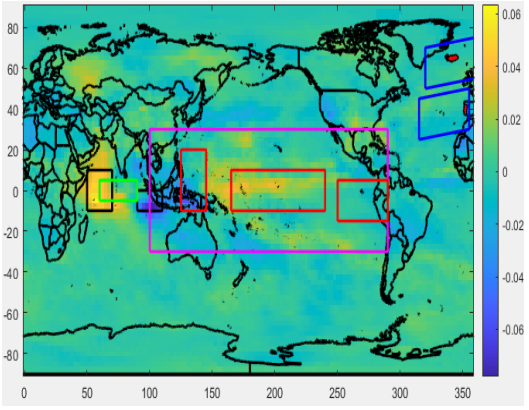

*(z) EOF3 Map of standardized OLR for June*

FIGURE 3.20: EOFs of Standardized ZW-Surface and OLR for June (1977-2017) [235].

by red boxes but with weak strength, which indicates weak linkages of PC2 with the EMI-MODOKI index. At mid and high latitudes, PC1 and PC2 are negatively and positively correlated with surface Sea Surface Temperature (SST)s analogous to the Pacific Decadal Oscillation (PDO), index (Figure 3.21(a) and 3.21(b)).

The correlation of PC1 with Pacific Decadal Oscillation (PDO) is considered moderate; with PC2, it is deemed to be strong. PC3 shows correlation analogous to Pacific Decadal Oscillation (PDO) pattern but not very significant.

In the tropical Indian Ocean, PC1 does not show any distinguishable positive/negative correlations in Western Equatorial Indian Ocean (WEIO)/Eastern Equatorial Indian Ocean (EEIO) region. Both PC2 and PC3 are positively/negatively correlated with Sea Surface Temperature (SST), in Western Equatorial Indian Ocean (WEIO)/Eastern Equatorial Indian Ocean (EEIO), but the correlation is weak.

These Sea Surface Temperature (SST), anomalies over Western Equatorial Indian Ocean (WEIO)/Eastern Equatorial Indian Ocean (EEIO), region is indicative of linkages with Dipole Mode Index (DMI) , but the correlation appears weak with some significant positive correlations.

In the Northern Atlantic Ocean, PC1 (Figure 3.21(a)) is correlated with Sea Surface Temperature (SST) anomalies. Analogous to the North Atlantic Oscillation (NAO) associated Sea Surface Temperature (SST) pattern, thus indicative of an association with North Atlantic Oscillation (NAO).

PC2 shows no correlation pattern similar to North Atlantic Oscillation (NAO) but the correlation is weak. Figure 3.21(c) shows a moderate positive correlation with Sea Surface Temperature (SST), in the Northern Atlantic, indicating Atlantic Multi-decadal Oscillation (AMO) linkage with PC3.

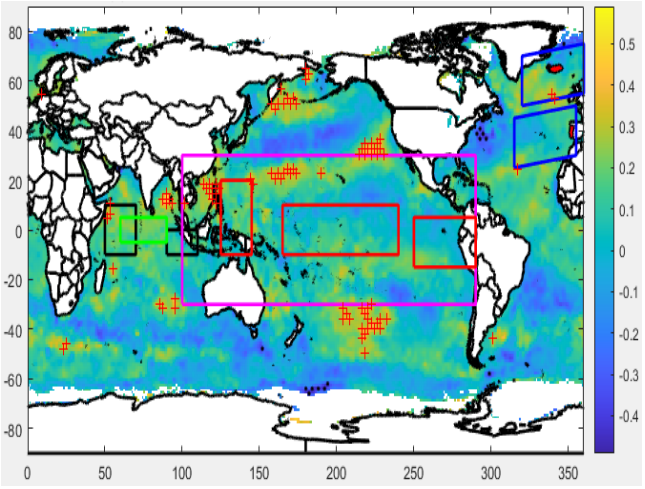


*(a) Correlation between PC1 precipitation and SST for June*

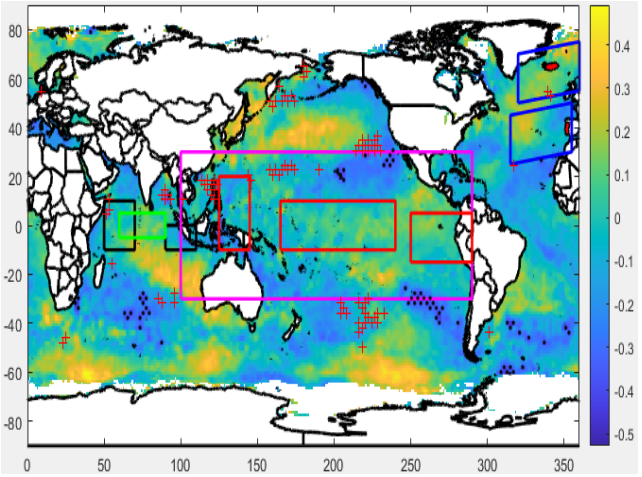


*(b) Correlation between PC2 precipitation and SST for June*

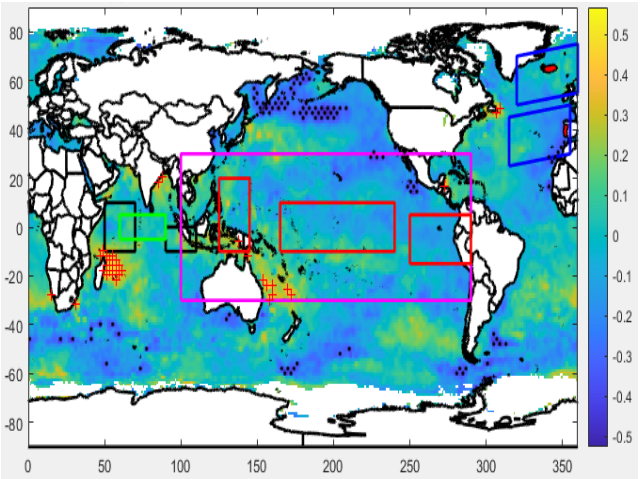


*(c) Correlation between PC3 precipitation and SST for June*

FIGURE 3.21: Correlation between PCs of Region1 precipitation and standardized SST for June (1977-2017)[235].

#### 3.3.5.5 Relationship of Region 1 Precipitation with Atmospheric Circulation Anomalies for June

The relationship of Region 1 precipitation with atmospheric circulations is studied by conducting the correlation analysis between PCs and atmospheric circulations SLP, GPH500. Figure 3.22 shows the distribution of correlation coefficient between PCs (1, 2, 3) and standardized SLP for June. In tropical regions, the Pacific warm pool shows some significant correlation with Region 1 precipitation. Responding to PC3, the Eastern-Central tropical region shows a negative correlation with SLP, whereas the western tropical region shows a positive correlation analogous to the ENSO pattern. Similarly, responding to PC1, the center tropical region shows a negatively correlates with SLP and a positive correlation in flank areas marked by red boxes. This surface SLP anomaly is indicative of linkages with ENSO-MODOKI, but the correlation is mostly insignificant with some significant areas. Responding to PC2, the central Indian and Pacific Ocean shows a negative correlation with some significant correlated areas.

In the Indian Ocean, responding to SLP, PC1 and PC3 show significant negative correlation while PC-2 shows weak negative/positive correlation at WEIO/EEIO regions to DMI Index. In the Northern Atlantic Ocean, high-pressure anomaly is present over Iceland, whereas a significant low-pressure anomaly is present over the Azores in response to correlation of PC1 with SLP. This surface Sea Level Pressure, anomaly is indicative of strong (-) NAO pattern. Responding to Sea Level Pressure (SLP), , PC2 is positively correlated with the Azores region and negatively correlated with the Iceland region, but the correlations remain insignificant (weak). This Sea Level Pressure, anomaly is indicative of +NAO mode. PC3 again shows a positive correlation with the Azores and a negative correlation with the Iceland with insignificant correlations (weak). Responding to SLP, PC1, PC2 and PC3 does not show any significant correlation analogous to AO pattern, although some positive and negative correlations are present in the Arctic region.

To understand the linkages of the observed signals of teleconnection including EMI-MODOKI, ENSO-MEI in the Pacific Ocean, DMI in the Indian Ocean, NAO, AO

in the Atlantic Ocean with Region 1 precipitation through atmospheric circulations, the correlation is performed between PCs (1, 2, 3) with GPH500 as shown in Figure 3.23. In response to correlations of PC1 with SLP and GPH500, Figure 3.22(a) shows positive surface pressure at Region 1, whereas Figure 3.22(x) depicts negative pressure anomaly (at GPH500) which is indicative of anti-cyclonic conditions with reduced precipitation. Negative/positive SLP anomaly at Azores/Iceland with its counterpart negative/positive anomaly at 500 hpa extending all the way to the Mediterranean and the Middle East Region, which is indicative of linkages with NAO.

Furthermore, in the tropical Pacific region, positive/negative/positive SLP anomaly with its counterpart negative/positive/negative GPH500 anomaly in EMI-MODOKI regions are not very supportive for teleconnection pattern of EMI-MODOKI Index. For PC2 correlations with responding SLP and GPH500, Figures 3.22(b) and (y) show that the pressure conditions at the surface are supportive of its counterpart pressure conditions at mid-altitude. Similarly, cyclonic condition exists in the Indian Ocean represented by negative SLP anomaly and positive mid-altitude anomaly at 500 hpa, which is indicative of enhance precipitation. Lastly, for PC3 correlations with SLP and GPH500, Figures 3.22(c) and (z) show anti-cyclonic conditions over Region 1 in response to anti-cyclonic conditions at SLP and cyclonic conditions at mid-heights over the tropical Indo-Pacific region and North Atlantic region, which is indicative of reduced precipitation.

To ascertain the linkages of atmospheric circulations with Region 1 precipitation, EOF modes of GPH500 are calculated. The target area is the 30S-90N and 0-360, where the teleconnection pattern under consideration is shaped. The corresponding time series of the three leading modes (G1, G2, G3), which explain 52% combined variability, are extracted. The correlation matrix between G1, G2, G3 with PCs of Region 1 precipitation (PC1, PC2, PC3) is shown in Table 3.15. The matrix is formulated to determine the PCs of GPH500, which have significant influence on the Region 1 precipitation through teleconnection via atmospheric circulations.

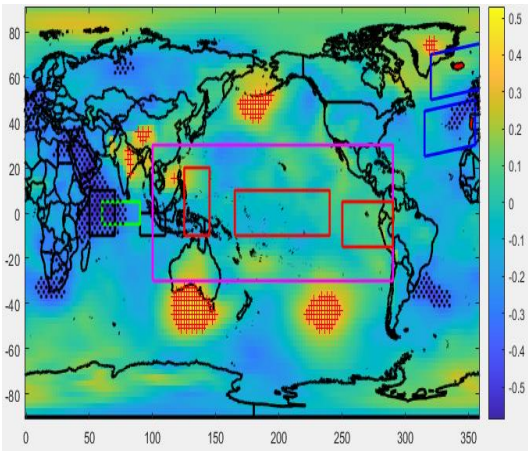

*(a) Correlation between PC1 of Region1 precipitation and standardized SLP for June*

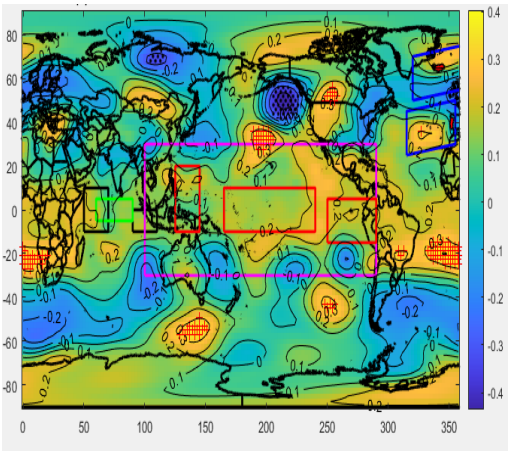

*(x) Correlation between PC1 of Region1 precipitation and standardized GPH500 for June*

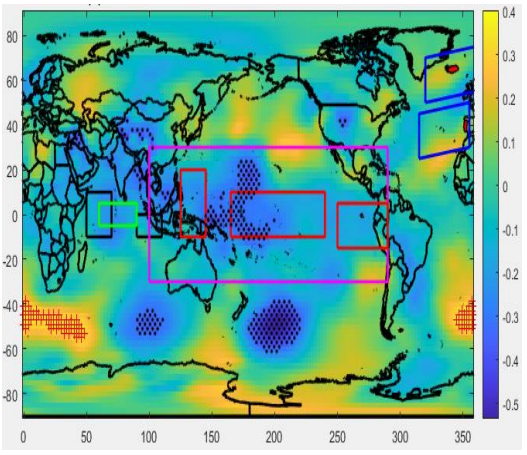

*(b) Correlation between PC2 of Region1 precipitation and standardized SLP for June*

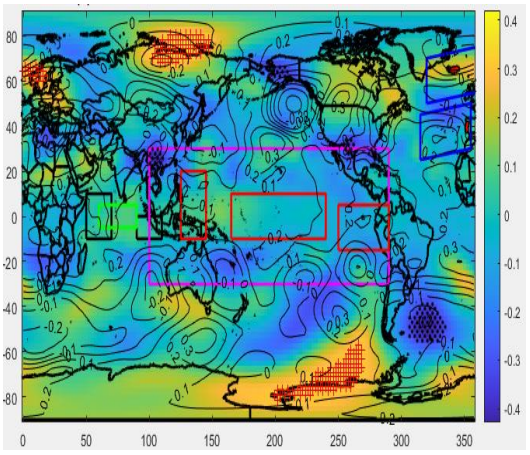

*(y) Correlation between PC2 of Region1 precipitation and standardized GPH500 for June*

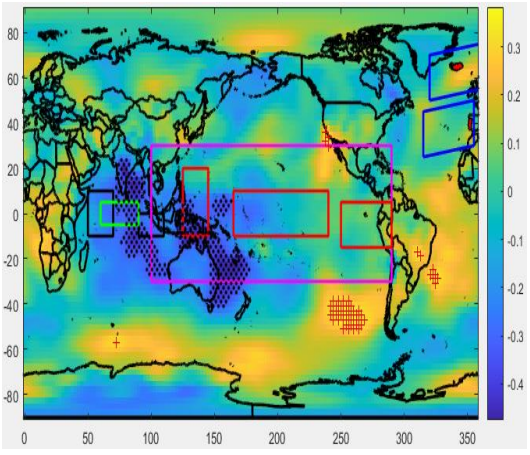

*(c) Correlation between PC3 of Region1 precipitation and standardized SLP for June*

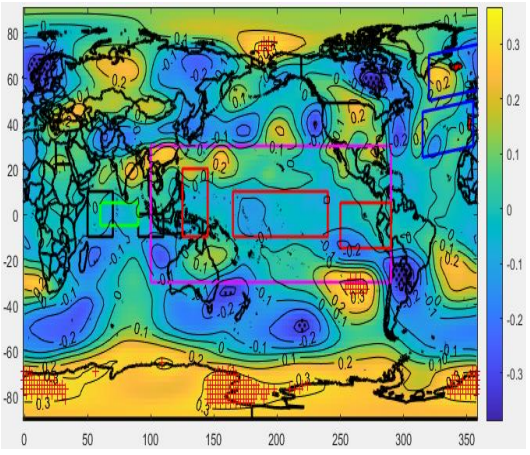

*(z) Correlation between PC3 of Region1 precipitation and standardized GPH500 for June*

FIGURE 3.22: Correlation between PCs of Region 1 Precipitation and Standardized SLP and GPH500 for June (1977-2017) [235].

Table 3.15 indicates that G1 and G2 have significant correlations with Region 1 precipitation PC2 only and are therefore considered for further analysis. The leading EOF modes (EOF1, EOF2) and the correlation of PCs of Region 1 precipitation (PC1, PC2) are shown in Figure 3.23.

TABLE 3.15: Correlation Matrix of p-value between PCs of GPH (G1, G2, G3) and PCs of Region1 precipitation (PC1, PC2 and PC3)

| | **R1JUNP-PC1** | | **R1JUNP-PC2** | | **R1JUNP-PC3** | |
|---|---|---|---|---|---|---|
| **GPH-Principal Components** | **Corrl. Coeff.** | **p-Value** | **Corrl. Coeff.** | **p-Value** | **Corrl. Coeff.** | **p-Value** |
| G1 | 0.0106 | 0.9476 | -0.3545 | **0.0230** | 0.2023 | 0.2047 |
| G2 | 0.2456 | 0.1217 | -0.3343 | **0.0327** | 0.0941 | 0.5585 |
| G3 | -0.1356 | 0.3979 | 0.1822 | 0.2543 | -0.1103 | 0.4925 |

Bold figures indicate a significant correlation at 10% confidence.

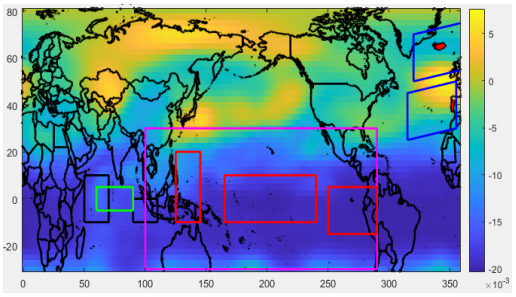

*(a) EOF1 of standardized GPH at 500 hpa in June.*

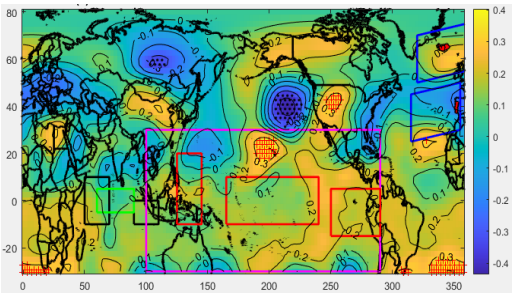

*(x) Correlation between PC1 of region1 precipitation and standardized GPH at 500 hpa for June*

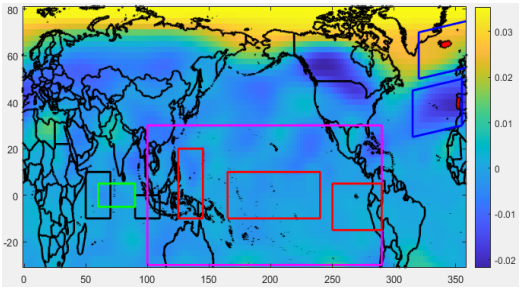

*(b) EOF2 of standardized GPH at 500 hpa in June.*

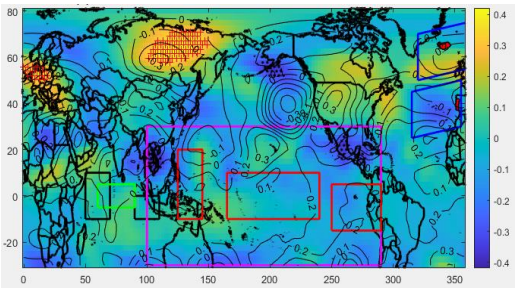

*(y) Correlation between PC2 of region1 precipitation and standardized GPH at 500 hpa for June*

FIGURE 3.23: EOF Modes of Standardized GPH at 500 hpa in June and Correlation with PCs of Region 1 Precipitation [235].

The correlation analysis is performed between the G1, G2 and climate indices to determine the influencing indices of Region 1 precipitation. The results are shown in Table 3.16. The result indicate that Region 1 precipitation is linked to AMO, EQWIN and EMI-MODOKI through atmospheric circulations.

TABLE 3.16: Correlation between PCs of GPH (G1, G2, G3) and Climate Indices

| | **G1** | | **G2** | |
|---|---|---|---|---|
| **Indices** | **Corrl. Coeff.** | **p-Value** | **Corrl. Coeff.** | **p-Value** |
| NAO | 0.0926 | 0.5648 | 0.0165 | 0.9184 |
| AO | 0.0586 | 0.7160 | 0.0282 | 0.8612 |
| AMO | -0.2212 | **0.1646** | -0.0865 | 0.5908 |
| DMI | -0.0652 | 0.6857 | -0.0676 | 0.6745 |
| EQWIN | 0.2216 | **0.1638** | 0.2609 | **0.0995** |
| ENSO-MEI | -0.0531 | 0.7416 | -0.1762 | 0.2704 |
| EMI-MODOKI | -0.2356 | **0.1382** | 0.0055 | 0.9725 |
| PDO | 0.1245 | 0.4379 | -0.0262 | 0.8706 |

Bold figures indicate significant correlation at 20% confidence.

#### 3.3.5.6 Relationship of Region 1 Precipitation with Surface Wind Anomalies for June

The distribution of correlation coefficient between PCs (1, 2 and 3) and standardized Zonal Winds at Surface (ZW-Surface) for the month of June is shown in Figure 3.24. As mentioned above, EQWIN being highly correlated to EQUINOO, correlations of PCs with OLR are calculated to identify the influence of the EQWIN index easily. In tropical Indian Ocean at WEIO and EEIO regions, OLR anomalies are significantly correlated with the PC1, PC3 of Region 1 precipitation which is indicative of correlation with surface zonal winds, whereas the association with

PC-2 remains insignificant and weak. This surface zonal wind anomaly is indicative of EQWIN significant positive correlation with R1JUNP (For the EQWIN index, the negative anomaly is to be multiplied by -1).

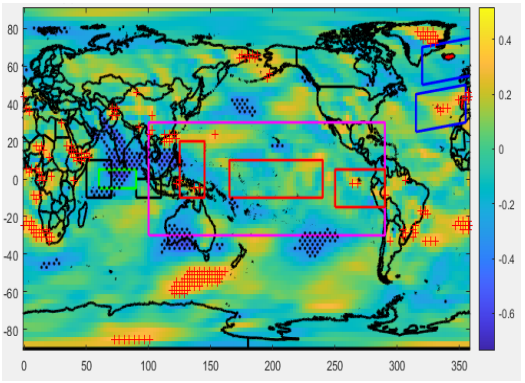

*(a) Correlation between PC1 of Region1 precipitation and Standardized ZW-Surface for June shows strong pattern of EQWIN.*

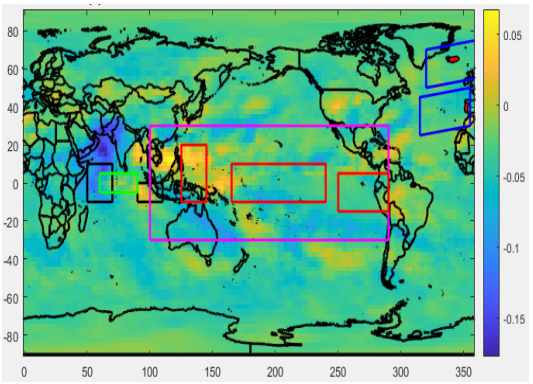

*(x) Correlation between PC1 of Region1 precipitation and Standardized OLR for June shows moderate pattern of EQUINOO*

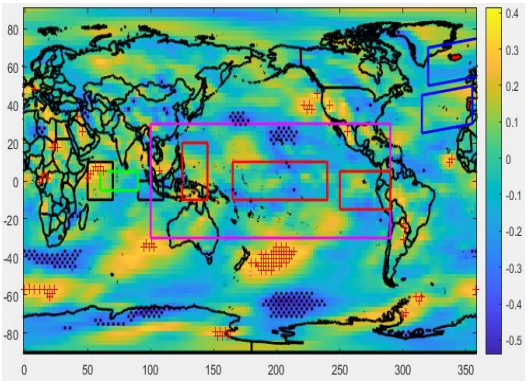

*(b) Correlation between PC2 of Region1 precipitation and Standardized ZW-Surface for June shows weak pattern of EQWIN*

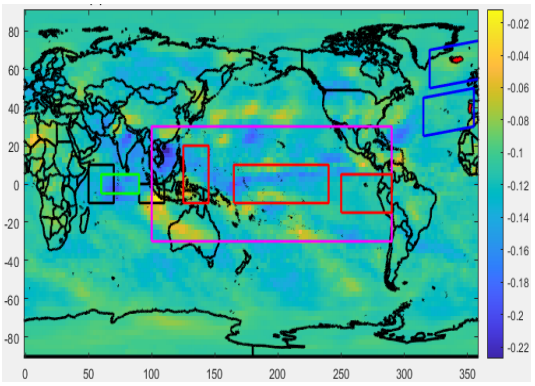

*(y) Correlation between PC2 of Region1 precipitation and Standardized OLR for June shows weak pattern of EQUINOO*

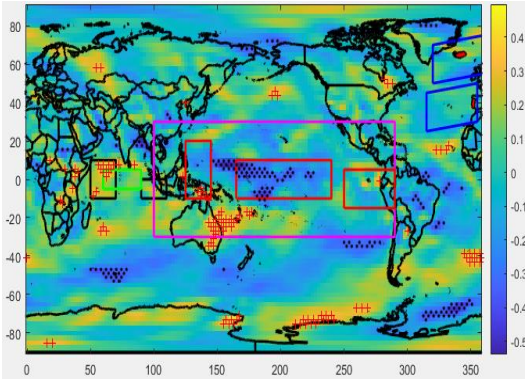

*(c) Correlation between PC3 of Region1 precipitation and Standardized ZW-Surface for June shows strong pattern of EQWIN*

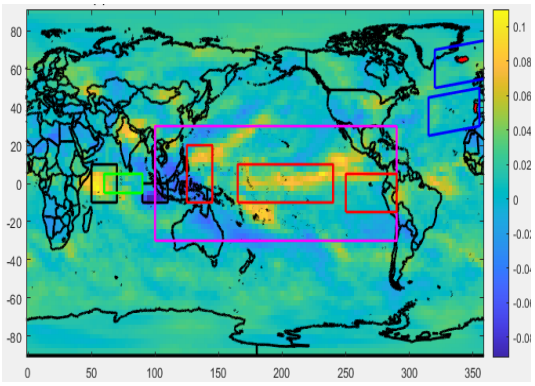

*(z) Correlation between PC3 of Region1 precipitation and Standardized OLR for June shows moderate pattern of EQUINOO*

FIGURE 3.24: EOFs of Standardized ZW-Surface for June (1977-2017) [235].

#### 3.3.5.7 Time-Lag Relationship of PCs with Climate Indices for June

The time-lag relationship for the correlation coefficient of PCs with the climate indices is also examined in this study. As mentioned earlier, the three most significant PCs of Region 1 precipitation are considered. Time-lag relationship of only those PC-climate indices relationship is considered which are most significant. The time-lag relationship indicates the climate indices NAO, AO, EQWIN and PDO are at their maximum significance level with the respective principal mode (PC) preceding to the month of June. AMO attains its maximum negative significance in January preceding June in the same year. The climate indices DMI, ENSO-MEI and ENSO-MODOKI attain their maximum significance in the preceding month of May. The time-lag relationship also shows that AMO, DMI, EQWIN and ENSO-MODOKI are positively correlated, whereas NAO, AO, ENSO-MEI and PDO are negatively correlated with their respective principal modes of precipitation.

#### 3.3.5.8 Result Analysis for June

The results obtained from all the above analyses are summarized in Table 3.17, along with the comparison with the previously obtained results of correlation and Partial Mann-Kendall analysis. Thus, from the analyses, it can be concluded that the influence of AO, DMI and EMI-MODOKI on Region 1 precipitation is insignificant (weak). The influence of NAO, AMO and ENSO-MEI may be considered as moderate. Lastly, the influence of Equatorial Indian Ocean Zonal Wind Index (EQWIN), and Pacific Decadal Oscillation (PDO), is significant up to 5% confidence (may be considered as strong). It is found that the Indian Summer Monsoon Rainfall (ISMR) is influenced by IOD [116, 228, 229]. As explained in sections 3.2.4.4 and 3.2.4.5, DMI and EQWIN are the Oceanic and atmospheric circulation indices that describe Indian Ocean Dipole (IOD). In this study, Equatorial Indian Ocean Zonal Wind Index (EQWIN), is found to be more correlated than Dipole Mode Index (DMI) having moderate to strong influence on June precipitation [228].

TABLE 3.17: Summary of Analysis Results for Region 1 precipitation and Climate Indices for June

| | | | | **Correlation b/w PCs and anomalies of** | | |
|---|---|---|---|---|---|---|
| **Indices** | **Partial Mann-Kendall** | **Correlation b/w PCs and Climate Indices** | **EOF Analysis** | **SST** | **Atmospheric Circulation** | **Zonal Winds and OLR** |
| NAO | Weak | Significant at 11.05% | Weak | Weak | Moderate | – |
| AO | Weak | Insignificant | Weak | – | – | – |
| AMO | Weak | Insignificant | moderate | Moderate | – | – |
| DMI | Weak | Insignificant | Weak | Weak | Weak | – |
| EQWIN | Strong | Significant at 0.4 % | Strong | Moderate | – | Moderate to Strong |
| ENSO-MEI | Weak | Insignificant | Strong | Weak | – | – |
| EMI-MODOKI | Strong | Insignificant | Weak | Weak | Weak | – |
| PDO | Weak | Significant at 4.57 % | Strong | Strong | – | – |

#### 3.3.5.9 Discussion of Results - June

**Insignificant effect of -AO, +DMI and +EMI-MODOKI**

The results indicate that AO, DMI, EMI-MODOKI and AMO remain insignificant. Chen et al. [313] suggest that AO climate pattern is mostly influenced by the **East Asian Winter Monsoon**. In **contrast**, both +DMI and +EMI-MODOKI are reported to influence the Indian summer monsoon rainfall (ISM). **Dandi, Ramu et al. [314]** suggest that El Nino Modoki modifies ISM rainfall by creating changes in the low-level circulation in north western Pacific. The weak positive rainfall

over the monsoon trough region is due to weak moisture convergence associated with the westward extension of cyclonic circulation in the northwestern Pacific strengthened by low pressure.

**Moderate effect of +AMO, -NAO and -ENSO-MEI**

NAO and ENSO-MEI both have a moderate effect on the precipitation of this region. The effect of NAO on the summer precipitation in Pakistan is not very well reported as per the previous studies, whereas ENSO-MEI, which is the multivariate index of ENSO representing the anomalous condition in the equatorial Pacific Ocean, influenced the interannual precipitation variability of this region through teleconnection by means of Walker circulation and Hadley circulation atmospheric bridges. The findings of this study are in **line with other studies such as [315, 316]**. Their work mutually agrees that the positive (negative) ENSO decreases (increases) the precipitation. Mahmood et al.[316] suggested that the opposite relationship between ENSO and ISM became weakened in the last decades. The weakening of the ENSO-ISM relationship might be due to the reinforcing positive phase of NAO and associated jet stream track patterns over the North Atlantic during recent decades. Goswami et al.[315] suggested that positive AMO positive tropospheric temperature anomaly over Eurasia produced stronger monsoon. It is also linked with increased La Nina type Pacific SST anomalies that cause stronger monsoon and stronger regional Hadley circulation. Thus, these two teleconnection mechanisms are complementary in regulating the monsoon.

**Significant Effect of +EQWIN and -PDO**

The positive phase of EQWIN has a significant effect on the precipitation in Baluchistan. +EQWIN is the index for the positive phase of EQUINOO, which is the atmospheric component of IOD in the Indian Ocean. Behera et al. [317], Ashok et al. [318, 319] and Hussain et al. [320] suggested that Positive IOD events are associated with the increased rainfall in Pakistan and India extending all the way to the Bay of Bengal during the monsoon season. The findings of the current study **confirm the work of all previous studies mentioned above [306-308]**. The moisture-loaded monsoon winds bring the moisture from the Indian Ocean and are responsible for the precipitation in the monsoon season. Charlotte

et al. [321] suggest that east winds are reinforced along the equator during strong EQUINOO and positive dipolar structure of SST between WEIO and EEIO is seen over the Indian Ocean, but the pattern is reversed for the negative phase of EQUINOO. Strong EQUINOO is correlated with the positive phase of monsoon and vice-versa. EQUINOO and Monsoon rainfall has a significant positive correlation, which **confirms** the results of the current study. The negative phase of PDO has a significant effect on the precipitation of Baluchistan. The negative phase of PDO is the extension of a cold region of La-Nina, southern oscillation along the west coast of continent USA on a decadal scale. Although La-Nina, that is the negative phase of ENSO, has affected this region moderately but -PDO is reported to have a significant effect on the precipitation variability of this region in decadal scale. The effect of cold phase of ENSO (La-Nina) is enhanced during the negative phase of PDO. Due to the extended effect of PDO extends in the tropical Pacific, the relation between the monsoon rainfall and El Nino-Southern Oscillation (ENSO) is altered. Krishnamurthy et al. [322], Roy et al. [323] suggests that during the positive PDO period, the impact of El Nino (La Nina) on the monsoon rainfall is enhanced (reduced). Depending on the phase of the PDO, this condition affects the trade winds and either strengthens or weakens the Walker circulation over the Pacific and Indian Oceans. The impact of PDO on monsoon rainfall is determined by the related Hadley circulation in the monsoon region.

## 3.4 Significance/Application of the study's Finding

The importance of the finding is that the two **climatic indices +EQWIN and +EMI-MODOKI, being most significant for the month of January, and +EQWIN and -PDO, being most significant for the month of June, can be used as the potential determinants in the regression modeling to predict the precipitation variability in this region**. They can be used as a baseline for further modeling and analysis by the climatologist and meteorologist.

The findings will be helpful for anticipating no or less precipitation in the month of January and downpours or extreme precipitation in June. The decision-maker, local and provincial governments, and disaster management authority can use it for issuing early warnings and weather alerts. They can also plan mitigation measures as extreme precipitation can cause **flash floods** due to the topography and rugged in Baluchistan. Flash floods are proven to be more catastrophic and dangerous by mother nature.

## 3.5 Summary

Baluchistan province receives about 60% of total provincial rainfall in the winter and spring months and nearly 30% in the monsoon season [145]. Decreasing trends in precipitation are observed in the months of January in Region 1, when the time series data is analyzed from 1977 to 2017 through Mann-Kendall test, which confirms that Baluchistan is receiving lesser rainfall since the past few decades. The change in trends under the influence of climatic indices is determined through PMK for January and June in Region 1. EQWIN, ENSO-MEI and EMI-MODOKI show moderate to strong influence on precipitation.

It is determined through correlation of time series of Region1 Precipitation (PCCs) and climate indices that NAO, AMO, EQWIN, EMI-MODOKI and PDO are influencing the precipitation in January and explain the maximum variability of the precipitation in January. EQWIN, EMI-MODOKI and AMO are positively correlated with principal modes of January precipitation up to 8% significance, whereas PDO and NAO are negatively correlated with the January precipitation but are insignificant (their significance is between 20% to 35%) and thus can be ignored.

North Atlantic Oscillation (NAO), was found out to be favorable for winter and spring precipitation over Pakistan as per previous studies, but its effect is determined as insignificant for January precipitation in the Region1 of Baluchistan. AMO is in its warmer phase since 1997 and it is observed that the strength of NAO and AO are weak during this phase of AMO. The decreasing precipitation

trend may be due to the weakening of NAO strength. Because during the past few decades, NAO is negatively affecting the precipitation in January.

Slightly increasing trends are found in the precipitation of June, when the time series data is analyzed from 1977 to 2017 through Mann-Kendall test. NAO, AMO, EQWIN, ENSO-MEI and PDO are found to be influencing the June precipitation as determined through correlation analysis between PCs and climate indices. AMO may be considered as positively correlated, whereas NAO and ENSO-MEI may be considered as negatively correlated, but their strengths are insignificant. PDO is negatively correlated to the principal modes of region1 precipitation at 5% significance which means that the negative phase of PDO is favorable for the precipitation of June; whereas EQWIN is positively correlated with June precipitation at 1% significance which means that the positive phase is favorable for June precipitation.

The average precipitation in June 2007 was high (86.4 mm) and during this year, PDO (0.09) and AMO (-0.08) were neutral, NAO (-3.339), ENSO-MEI (-0.215) were negative whereas EQWIN (0.66) was positive. This confirms the correlation findings as above and accounts for the slightly increasing trend in the June precipitation. The influencing climatic indices for January and June over the Region1 of Baluchistan as identified through EOF maps, PCA and correlation analyses can be used as the possible predictors of precipitation for further studies.

# Chapter 4

# Estimation of Potential Determinants Causing Precipitation Variability using Multi Linear Regression

## 4.1 Background

Climate study and frequent weather forecasting is a decisive, crucial, and robust topic around the globe. Numerous parameters contribute significantly to increase the forecasting precision. One of them is the advancement of statistical methods to increase the domain and accuracy of modeling [324]. Over the years, several models have been developed by using various techniques, but the authenticity of statistical methodology in predicting the weather parameters is well established and recognized. This is because of its accuracy, precision and authentic results. The multilinear models are among the most accepted and extensively used models. The reason is their simplicity and ease to use, in addition to their forecasting precision and accuracy. This doctoral study uses the Multiple Linear Regression (MLR) model to estimate the potential determinants causing precipitation variability in

Baluchistan province. Climate indices and large-scale circulations are responsible for the precipitation variability in the selected study area of the research. It was determined in chapter 3 through Mann-Kendall that January and June are the only months that have significant decreasing/increasing trends in precipitation. It is also determined in chapter 3 through correlation and through Empirical Orthogonal Function (EOF) pattern analysis that North Atlantic Oscillation (NAO), Atlantic Multi-decadal Oscillation (AMO),Equatorial Indian Ocean Zonal Wind Index (EQWIN), EMI-MODOKI and Pacific Decadal Oscillation (PDO) are influencing the precipitation and explain the maximum variability of the precipitation in January, whereas North Atlantic Oscillation (NAO), Atlantic Multi-decadal Oscillation (AMO),Equatorial Indian Ocean Zonal Wind Index (EQWIN), EMI-MODOKI and Pacific Decadal Oscillation (PDO) are found to be influencing the June precipitation. These climate indices are selected as predictor to predict the variability in precipitation through statistical modeling, which is the simplest way to address this uncertain natural phenomenon. This chapter focuses on developing an authentic, contemporary model for determining possible predictors of precipitation variability in Baluchistan province using MultiLinear Regression (MLR) analysis. MLR model is specified using a stepwise regression modeling approach to select the best model using performance indices and post residual estimation analyses to check the validity of all estimated equations.

## 4.2 Methodology

Multiple Linear Regression (MLR) is used to develop the model of the potential determinants (explanatory variables) causing the variability in precipitation trends (dependent variable). Multiple Linear Regression (MLR) can adequately adjust more than two explanatory variables at a time for predicting an equation. The procedure for performing the Multiple Linear Regression (MLR) is discussed in the subsequent section.

### 4.2.1 Data

The time series of monthly precipitation data (from 1977-2020) is used as the dependent variable in the MLR regression analysis. The observed monthly precipitation data over the study period (1977-2015) is ingested in multilinear regression analysis for the training of the model, whereas data from (2016-2020) is used for validation [210]. The climatic indices which are relevant to the study area such as Arctic Oscillation (AO), North Atlantic Oscillation (NAO), Atlantic Multi-Decadal Oscillation (AMO), Indian Ocean Dipole-Dipole mode index (IOD-DMI), Equatorial Indian Ocean Zonal Wind Index (IOD-EQWIN), El Nino Southern Oscillation-Multivariate ENSO Index (ENSO-MEI), El Nino Southern Oscillation-Multivariate ENSO-MODOKI and Pacific Decadal Oscillation (PDO) are considered as the independent variables [216, 325]. Additionally, large-scale circulations such as SST, SLP, ZW, GPH, RH and OLR are also considered as the independent variables [86, 325]. Data of climatic indices and the large-scale circulations at various pressure levels (200hpa, 300hpa, 500hpa and 800hpa) are acquired from the NCEP/NCAR reanalysis data set available at 2.5° resolution except for SST, which is at 1° resolution [212, 213].

### 4.2.2 Potential Determinants

The potential determinants are the climate indices and large-scale circulations, which cause the precipitation variability in the study area (Baluchistan) in the months with significant trends. Mann-Kendall test shows that January and June are the only months, which have significant decreasing/increasing trends in precipitation [138, 218]. It is also established through correlation analysis and empirical orthogonal function (EOF) pattern analysis that NAO, AMO, EQWIN, EMI-MODOKI and PDO are influencing the precipitation trend. It is found that they explain the maximum variability of the precipitation in January. NAO, AMO, EQWIN, ENSO-MEI and PDO are found to be influencing the June precipitation

as well [235]. These climate indices are selected as predictor to predict the variability in precipitation through empirical statistical modeling, which is the simplest way to address this uncertain natural phenomenon [216]. The current study is focused on creating an authentic, contemporary model for determining possible predictors of precipitation variability in Baluchistan province using MultiLinear Regression (MLR) analysis. MLR model is specified using stepwise regression modeling approach to the selection of best model using performance indices and post residual estimation analyses to check the validity of all estimated equations.

### 4.2.3 Multilinear Regression Analysis

Regression is a well-established statistical technique that uses the connection between two or more quantitative variables so that the resultant variable can be predicted. Regression analysis main aim is to evaluate the extent, the dependent variable (resultant) can be predicted from the independent variables [267-269, 281]. Regression analysis is extensively employed in business, social, interactive, behavioral sciences analysis and climate forecast [250]. Designing a regression model is a reiterative method that requires identifying efficient independent variables which significantly control and impact the entire process that is being studied to be modeled. Then running regression tool repeatedly to identify effective variables, removing the irrelevant variables until the best possible model is prepared [244-255]. Regression can be of different types, namely linear, logistic , lasso, polynomial and nonpolynomial.The residuals and post estimation test in ML were passed successfully. Confirming that the residuals are independent, and identically distributed. The basic assumption of OLS was satisfied concluding that the form of function which is linear is correctly selected for the analysis in this research. Linear regression analysis commonly uses two simple approaches Simple Linear Regression and Multiple Linear Regression.

Simple regression has only one predictor (X) and is of the form:

$$Y = \alpha_0 + \alpha_1 X \tag{4.1}$$

Where $\alpha_0$, $\alpha_1$ are regression coefficient and X is a predictor or regressor.

As the name indicate Multi-Linear Regression has more than two predictor or regressor.

Multiple regression model is of the form:

$$Y = \alpha_0 + \alpha_1 A_1 + \alpha_2 A_2 + \alpha_3 A_3 + \alpha_4 A_4 ... + e \tag{4.2}$$

where y = Response variable $\alpha_0, \alpha_1, \alpha_2, \alpha_3, \alpha_4$ are regression coefficients.

A1, A2, A3, A4 are the predictors or regressors or explanatory variables/ independent variables. And e is an unexplained portion of dependent variable with zero mean and constant variance. Error term 'e' include all those variables that cannot be taken into the model for various reasons and the average influence of these variables on the predictand is assumed to be trivial. Regression analysis mainly aims to explain the average response of Y in respond to the regressor, that is, how Y reacts to the changes in the X variables. Multiple regression fits a model to predict a dependent (Y) variable from two or more independent (X) variables. Multiple linear regression models are often used as approximating functions, that is, a true functional relationship between y and x1, x2, x3, ...xn is unknown, but over certain ranges of the regressor variables linear regression model is an adequate approximation to the true unknown function.

### 4.2.4 Specifying Regression Model

After selecting the dependent and independent variables, the next step is to specify the regression model. Specifying the regression model is the process of determining variables (independent) to include and exclude from the model and whether the modeling curvature and interaction effects are appropriate. While specifying the model, efforts are being made to include the independent variables that have an actual relationship with dependent variables and exclude those variables which

are not related. The appropriateness of the model is assessed using various statistical performance indices of regression and post estimation tests. The automatic selection procedure for specifying the regression model is step-wise regression (either General to Specific or Specific to General) and best subset regression. Using these automatic procedures, the best candidate model based on best performance indices and post estimation results are selected [259].

In the step-wise approach, t-test is used. At this stage, a variable is removed, which has the highest p-value than some predetermined value (say 0.05). Then performance indices are examined. If the value falls below the predetermined value, then the model fits the data well, if not, then another variable is removed from the set, which shows the higher p-value, and again the performance indices are examined. This process is continued till no more predictor p-value is greater than the predetermined significant value. Understandably, if there are no more predictors left whose p-value is greater than significant value, then the performance indices meet the criteria and hence it can be established that the model fits the data well [326].

### 4.2.5 Regression Model Performance Indices

As explained above, the model performance is assessed through performance indices to estimate the best model. Performance indices that will be assessed are briefly discussed below.

#### 4.2.5.1 Person Correlation Coefficient (R) or Multiple R

The Regression model has a number of different coefficients that are used for different scenarios. One of the best-known coefficient is the Pearson product-moment correlation coefficient, which is also known as Pearson correlation coefficient or simply the correlation coefficient. It is denoted as R. This coefficient is a single number, but it shows both the magnitude and direction of the linear relationship between the two continuous variables. Its value ranges from -1 to +1. The greater

the absolute value of the coefficient of correlation, the stronger the correlation. The coefficient of correlation having zero value represents no linear relationship among the variables. In other words, if one variable increases, there is no tendency in the other variable to either increase or decrease. The extreme values of -1 and +1 show a perfectly linear relationship where the change in one variable is accompanied by a perfectly consistent change in the other; however, it is practically not achievable. The sign of the coefficient correlation ship shows the direction of the relationship. If the coefficient of correlation is positive, it shows that when the value of one variable will increase, the value of the other variable will also tend to increase. A scatter plot with ascending slope indicates positive, relationships. Similarly, if the coefficient of correlation is negative, it shows that when the value of one variable decreases, the value of the other variable will also tend to decrease.A Scatter plot with descending slope indicate positive relationships [326-328]. If there are n observations in a time series, then the Pearson product-moment correlation coefficient can be used to estimate the correlation between model and observations with the help of the equation as follows:

$$R = \frac{\sum_{i=l}^{n}(x_i - \bar{x})(y_i - \bar{y})}{\sqrt{\sum_{i=l}^{n}(x_i - \bar{x})^2 \sum_{i=l}^{n}(y_i - \bar{y})^2}} \tag{4.3}$$

Where x(i) is the observed values and y(i) is the modeled value; x and y are the average values of observed and modeled value; respectively, as explained above. If correlation coefficient R is +1 then there is a perfect increasing linear relationship between estimated and observed predictand, and if R is -1 then there is decreasing linear relationship between estimated and observed predictand. A correlation coefficient of zero means that there is no linear relationship between the variables.

#### 4.2.5.2 Coefficient of Determination ($R^2$)

The coefficient of determination symbolized $R^2$ and uttered as R squared is one of the most valuable and key outputs of the regression analysis. It is also known as the Goodness of fit and is defined as the proportion of the variance in the

dependent variable that is predictable from the independent variable. It is most commonly used parameter in statistical analysis to evaluate the efficiency, accuracy and authenticity of a model. The coefficient of determination indicates the level variability of dependent variable explained in the model by the independent variable. Its values range from 0 to 1. $R^2$ having 0 values means that the dependent variable cannot be predicted from the independent variables. And $R^2$ having 1 value means the dependent variable can be predicted without error from the independent variable. The value of $R^2$ between 0 and 1 indicates the amount and level to which the dependent variable is predictable from the independent variables. For example, an $R^2$ of 0.30 indicates that 30 percent of the variance in Y is predictable from X; an $R^2$ of 0.50 indicates that 50 percent is predictable; and so on. A good model should have coefficient of determination as possible as nearer to unity. $R^2$ is always a positive value, and it cannot be negative [329].

The equation for computing the coefficient of determination with one independent variable is as follow:

$$R^2 = \left(\frac{\sum_{i=l}^{n}(y_i - \bar{y})(\hat{y}_i - \bar{y})}{\sqrt{\sum_{i=l}^{n}(y_i - \bar{y})^2 \sum_{i=l}^{n}(\hat{y}_i - \bar{y}_i)^2}}\right)^2 \tag{4.4}$$

#### 4.2.5.3 Adjusted R Squared (Adj $R^2$)

The adjusted $R^2$ is a revised version of $R^2$ that has been adopted because of the number of predictors in the model. The adjusted $R^2$ value increases only if the new term improves the model more than would be expected by chance. Similarly, $R^2$ value decreases when a predictor improves the model by less than expected by chance. The adjusted $R^2$ can be negative, but it is usually not. Adjusted $R^2$ has a value that is always less than that of $R^2$ [329].

One of the disadvantages of coefficient of determination $R^2$ is that it is an increasing function of the number of regressors. In other words, if one adds variables to the model, the values of $R^2$ will also increase. Sometimes the researcher is under the illusion that the higher the $R^2$, the better the model will be. To overcome

this misconception, it is recommended that adjusted $R^2$ may also be included and reported in the outputs. Adjusted $R^2$ measures explicitly a number of regressors included in the model. The word adjusted represents the adjustment for the degrees of freedom, which depend on the number of regressors (k) in the model. The adjusted $R^2$ imposed a penalty for adding more regressors. Besides other parameters to comparing regression models, adjusted $R^2$ is also used to compare two or more regression models with the same dependent variable.

The equation to compute adjusted $R^2$ is as follows:

$$R^2_{adj} = 1 - [\frac{(1 - R^2)(n - 1)}{n - k - 1}] \tag{4.5}$$

#### 4.2.5.4 Standard Error (SE)

The standard error (SE) is the amount of the variability of a statistic. The standard error of the regression (SE) and the coefficient of determination ($R^2$) explained above are two key goodness-of-fit measures for regression analysis. However, the most commonly reported and most well-known among the goodness-of-fit statistics is the coefficient of determination ($R^2$). The standard error (SE) of the regression is also a great parameter to report the statistical test in the reporting table. It is an estimate of the standard deviation of a sampling distribution. The standard error (SE) depends on three factors: the number of observations (n), the way the random sample is chosen and the number of observations in the sample.

SE: Standard error of the sample is given by
n: The number of observations in the sample.
$\sigma$: Sample standard deviation

$$SE = \frac{\sigma}{\sqrt{n}} \tag{4.6}$$

#### 4.2.5.5 Overall F -test

The F-test of overall significance indicates that whether the linear regression model provides a better fit than a model that contains no independent variable. In other words, it tests whether the model contains at least one significant independent variable. The F-test of overall significance is conducted with the following hypothesis statement:

1. **Hnul**: *The model with no independent variable (with the intercept only model) fits the data better or the model contains no significant independent variable.*

2. **Halt**: *The model with independent variables fits the data better than the intercept-only model or the model contains at least one significant independent variable.*

   The significance is checked against the confidence level of 0.05 (alpha level) for the following:
   i) If the p-value is smaller than 0.05, then the null hypothesis can be rejected in favor of the alternate hypothesis, which indicates that the model contains at least one significant independent variable.
   ii) If the p-value is greater than 0.05, then the null hypothesis cannot be rejected, which indicates that the model contains no significant independent variable.

### 4.2.6 Efficiency of Regression Model

The efficiency of the regression model is shown by adjusted $R^2$, which is also identified as variance explained or strength of determination (refer to Section 4.2.5.3). The overall $R^2$ value will be high if the model fits the data well, and the corresponding p-value will be low (p-value is the observed significance level which the null hypothesis is rejected). In addition to the overall p-value, multiple regressions also report an individual p-value for each independent variable. A small p-value in

the analysis shows that the particular independent variable significantly improves the fit of the model. It is determined by comparing the goodness-of-fit of the entire model to the goodness-of-fit when that independent variable is omitted. If the fit is much worse (overall $R^2$ value decreases), then that variable is omitted from the model. The p-value will be low, showing that the variable has a significant impact on the model.

### 4.2.7 Post Estimation Tests

Post estimation tests are applied on the residuals or on the error. Analysis of residuals plays an important role in validating the regression model. If the error term in the regression model satisfies the post estimation tests, then the model is considered effective. Since the performance indices tests for regression are also based on the assumptions, the conclusions resulting from these significance tests are called into question if the assumptions regarding error are not satisfied [200]. The post estimation tests on the residuals considered in the analysis are described below.

#### 4.2.7.1 Auto correlation (AR)-Test

In order to ensure that the residuals of the model are free from serial correlation, unbiased and non-spurious, the Auto Correlation test, commonly known as (AR) test, is conducted with the following hypothesis statements:

1. **Hnul**:*No serial correlation in the residuals.*
2. **Halt**:*Residuals are serially correlated.*

#### 4.2.7.2 Auto Regressive Conditional Heteroskedasticity (ARCH) Test

Heteroscedasticity can easily be understood as unequal spread of data samples. In the context of regression analysis, heteroscedasticity means the unequal spread

of the residuals or error term. Precisely, heteroscedasticity is a systematic change in the spread of residuals over the range of measured values. The Ordinary Least Squares (OLS) regression is based on the assumption that all residuals are homoscedastic, meaning these are drawn from a population that has a constant variance (equal spread). To make the model authentic and the result accurate, the residuals should have constant variance (homoscedastic).The ARCH test is applied to check the variance of residuals [250, 282]. The hypothesis of the test is as follows:

1. **Hnul**:*No heteroskedasticity in the residual.*
2. **Halt**:*Residuals are homoscedastic.*

## 4.3 Results and Analysis

The objective of this chapter is to find the potential determinants of precipitation variability in the study area using Multi-Linear Regression analysis. The dependent variable in the regression analysis is the time series precipitation data of Region 1 in Baluchistan, whereas the independent variables (regressors) are the potential determinants, including climatic indices and large-scale circulation. The domain for the analysis and selected pressure levels are discussed in subsequent paragraphs.

### 4.3.1 Domain for Analysis for Large-Scale Circulations

The climatic indices NAO, AO and AMO, are the anomalies associated with the Arctic and the Atlantic Ocean to the North of the Equator. The indices DMI and EQWIN are anomalies associated with the Indian Ocean to the North of -30S latitude, whereas ENSO-MEI, EMI-MODOKI and PDO are anomalies associated with the Pacific Ocean to the North of -30S latitude. Therefore, the domain for the analysis for large-scale circulations is selected as the -30S to 80N and 0 to 360.

### 4.3.2 Pressure Level for Analysis

The lowest most layer of the Earth's atmosphere is the troposphere which contains almost 85% of the mass of the atmosphere. The tropopause is the boundary between troposphere and the next layer of atmosphere, i.e., the stratosphere. The pressure at the tropopause is about 100 hpa and that at the surface of the Earth is about 1000 hpa. The troposphere extends to an average height of 12 km above the surface of the Earth. Most of the weather and clouds occur in the troposphere. The wind increases and the temperature decreases when it moves from the surface of the Earth to the tropopause. In practical meteorology, the most common and significant levels of the troposphere which are used for analysis of climate are at surface (1000 hpa), 850 hpa, 500 hpa, 300 hpa and 200 hpa. The 850 hpa and 500 hpa levels are known for clouds and precipitation changes, whereas 300 hpa and 200 hpa are levels where jet streams exist.

### 4.3.3 Predictands and Regressors

The climate indices pertinent to the study area are chosen through literature review and analysis. This has been discussed in detail in Chapter 3. The climatic indices, including DMI, EQWIN ENSO-MEI and ENSO-MODOKI (EMI) are considered for the first time. These have never been studied in the area prior to this study which is the novelty of this doctoral study. The climatic indices which are considered in the regression analysis as regressors are listed in Table 4.1. Additionally, the large-scale circulations such as Sea Surface Temperature (SST), Sea Level Pressure (SLP), Zonal Winds at surface (ZW-Surface) and Geo-potential Heights (GPH), Outgoing Longwave Radiation (OLR), and Relative Humidity (RH) at different pressure levels like (1000 hpa, 850 hpa, 500 hpa, 300 hpa and 200 hpa) are also considered and are tabulated in Table 4.1.

Table 4.1: Details of the Predictor used in MLR -Analysis

| **S.no** | **Attributes** | **Type** | **Description** | **Variable type** |
|---|---|---|---|---|
| 1 | Precipitation | Numeric | Monthly Precipitation | Predictor |
| 2 | NAO | Numeric | North Atlantic Oscillation | Regressor |
| 3 | AO | Numeric | Arctic Oscillation | Regressor |
| 4 | AMO | Numeric | Atlantic Multi-decadal Oscillation | Regressor |
| 5 | DMI | Numeric | Dipole Mode Index | Regressor |
| 6 | EQWIN | Numeric | Equatorial Indian Ocean Zonal Wind Index | Regressor |
| 7 | ENSO- MEI | Numeric | Multivariate ENSO Index | Regressor |
| 8 | ENSO-MODOKI | Numeric | ENSO Modoki Index | Regressor |
| 9 | PDO | Numeric | Pacific Decadal Oscillation | Regressor |
| 10 | NINO 3.4 | Numeric | EL NINO / LA NINA 3.4 Index | |
| 11 | ENSO SOI | Numeric | El Nino Southern Oscillation index | Regressor |
| 12 | SST | Numeric | Sea Surface Temperature | Regressor |
| 13 | SLP | Numeric | Sea Level Pressure | Regressor |
| 14 | OLR | Numeric | Outgoing Long Wave Radiation | Regressor |
| 15 | ZW-Surface | Numeric | Zonal Wind Surface | Regressor |

| | | | | |
|---|---|---|---|---|
| 16 | ZW200 | Numeric | ZonalWind at 200 hpa | Regressor |
| 17 | ZW300 | Numeric | ZonalWind at 300 hpa | Regressor |
| 18 | ZW500 | Numeric | ZonalWind at 500 hpa | Regressor |
| 19 | ZW850 | Numeric | ZonalWind at 850 hpa | Regressor |
| 20 | GPH200 | Numeric | Geo-potential Heights at 200 hpa | Regressor |
| 21 | GPH300 | Numeric | Geo-potential Heights at 300hap | Regressor |
| 22 | GPH500 | Numeric | Geo-potential Heights at 500 hpa | Regressor |
| 23 | GPH850 | Numeric | Geo-potential Heights at 850 hpa | Regressor |
| 24 | RH300 | Numeric | Relative humidity at 300 hpa | Regressor |
| 25 | RH500 | Numeric | Relative humidity at 500 hpa | Regressor |
| 26 | RH850 | Numeric | Relative humidity at 850 hpa | Regressor |
| 27 | VW-Surface | Numeric | Meridional Wind - Surface hpa | Regressor |
| 28 | VW200 | Numeric | Meridional Wind at 200 hpa | Regressor |
| 29 | VW300 | Numeric | Meridional Wind at 300 hpa | Regressor |
| 30 | VW500 | Numeric | Meridional Wind at 500 hpa | Regressor |
| 31 | VW850 | Numeric | Relative humidity at 850 hpa | Regressor |

The total number of independent variables thus selected is (thirty) 30 including, the constant term in the regression equation. Therefore, a total number of $2.653x10^{32}$ permutations (P=30!; factorial) are possible for specifying the regression model.

The best candidate regression model is then selected by using an automatic stepwise regression procedure based on the performance indices and post estimation tests

*AR test*

*ARCH test*

on residuals are performed. The null hypothesis and Alternate hypothesis of these test are also discussed in their respective sections. The analysis is performed by using Ox-metrics software.

### 4.3.4 Multi-Linear Collinearity

Multicollinearity in regression analysis refers to the degree to which independent variables are correlated. Multicollinearity exists when one independent variable is correlated with another independent variable, or one independent variable is correlated with a linear combination of two or more independent variables. Due to the presence of multicollinearity, the marginal contribution of that independent variable is influenced by other independent variables.

As a result, estimates for regression coefficients can be unreliable and the tests of significance for regression coefficients can be misleading. Therefore, multicollinearity among the independent variables must be checked [280]. The multicollinearity among all the (thirty) 30 regressors are calculated and tabulated in Table 4.2 to Table 4.5:

Table 4.2: Collinear Matrix of Climatic Indices January

| | **NAO** | **AO** | **AMO** | **ENSO-MEI** | **EMIM-ODOKI** | **EQWIN** | **IOD** | **PDO** | **ENSO-SOI** | **ENSO-SST** | **OLR** |
|---|---|---|---|---|---|---|---|---|---|---|---|
| NAO | 1.000 | | | | | | | | | | |
| AO | 0.777 | 1.000 | | | | | | | | | |
| AMO | 0.046 | 0.103 | 1.000 | | | | | | | | |
| ENSO-MEI | 0.117 | -0.068 | -0.406 | 1.000 | | | | | | | |
| EMI-MODOKI | -0.096 | 0.102 | 0.595 | -0.860 | 1.000 | | | | | | |
| EQWIN | -0.062 | -0.025 | -0.311 | 0.467 | -0.429 | 1.000 | | | | | |
| IOD | -0.220 | -0.297 | 0.138 | 0.141 | -0.002 | 0.189 | 1.000 | | | | |
| PDO | -0.173 | -0.284 | -0.264 | 0.421 | -0.471 | 0.046 | -0.124 | 1.000 | | | |
| ENSO-SOI | 0.058 | -0.164 | -0.372 | 0.965 | -0.853 | 0.417 | 0.192 | 0.442 | 1.000 | | |
| ENSO-SST | 0.059 | -0.158 | -0.384 | 0.960 | -0.860 | 0.444 | 0.209 | 0.419 | 0.997 | 1.000 | |
| OLR | 0.647 | 0.600 | 0.110 | 0.106 | -0.060 | 0.030 | -0.076 | -0.163 | 0.083 | 0.093 | 1.000 |

The collinearity matrix in Table 4.2 shows that although the novel index Equatorial Indian Ocean Zonal Wind Index (EQWIN), is not correlated with NAO and AO because the value is (-0.006 and 0.158). Hence, they can be used as the independent variables with no correlation in the regression equation for predicting possible predictors for precipitation variability in Baluchistan province.

TABLE 4.3: Collinear Matrix of Large-Scale Circulations January

| | **ZW-SUR** | **ZW-200** | **ZW-300** | **ZW-500** | **ZW-850** | **GPH-200** | **GPH-300** | **GPH-500** | **GPH-850** | **RH-300** | **RH-500** | **RH-850** |
|---|---|---|---|---|---|---|---|---|---|---|---|---|
| ZW-SUR | 1.000 | | | | | | | | | | | |
| ZW-200 | 0.230 | 1.000 | | | | | | | | | | |
| ZW-300 | 0.209 | 0.968 | 1.000 | | | | | | | | | |
| ZW-500 | 0.136 | 0.931 | 0.979 | 1.000 | | | | | | | | |
| ZW-850 | 0.004 | 0.748 | 0.789 | 0.879 | 1.000 | | | | | | | |
| GPH-200 | -0.188 | -0.162 | -0.043 | 0.050 | 0.206 | 1.000 | | | | | | |
| GPH-300 | -0.217 | -0.154 | -0.062 | 0.036 | 0.211 | 0.973 | 1.000 | | | | | |
| GPH-500 | -0.254 | -0.233 | -0.136 | -0.034 | 0.146 | 0.956 | 0.987 | 1.000 | | | | |
| GPH-850 | -0.283 | -0.411 | -0.287 | -0.188 | -0.027 | 0.836 | 0.850 | 0.913 | 1.000 | | | |
| RH-300 | 0.057 | 0.123 | 0.157 | 0.196 | 0.284 | 0.402 | 0.455 | 0.430 | 0.322 | 1.000 | | |
| RH-500 | 0.245 | 0.154 | 0.151 | 0.122 | 0.091 | -0.356 | -0.376 | -0.365 | -0.358 | 0.343 | 1.000 | |
| RH-850 | 0.229 | -0.077 | -0.143 | -0.186 | -0.243 | -0.524 | -0.557 | -0.560 | -0.546 | 0.000 | 0.663 | 1.000 |

Table 4.4: Collinear Matrix of Climatic Indices - June

| | **NAO** | **AO** | **AMO** | **ENSO-MEI** | **EMIM-ODOKI** | **EQWIN** | **IOD** | **PDO** | **ENSO-SOI** | **ENSO-SST** | **OLR** |
|---|---|---|---|---|---|---|---|---|---|---|---|
| NAO | 1.000 | | | | | | | | | | |
| AO | 0.656 | 1.000 | | | | | | | | | |
| AMO | -0.253 | 0.037 | 1.000 | | | | | | | | |
| ENSO-MEI | -0.022 | -0.212 | -0.351 | 1.000 | | | | | | | |
| EMIMO-DOKI | -0.060 | 0.165 | 0.501 | -0.821 | 1.000 | | | | | | |
| EQWIN | -0.006 | 0.158 | 0.093 | -0.203 | 0.090 | 1.000 | | | | | |
| IOD | -0.017 | -0.096 | -0.006 | 0.340 | -0.194 | 0.278 | 1.000 | | | | |
| PDO | -0.109 | 0.010 | -0.328 | 0.503 | -0.488 | -0.004 | -0.069 | 1.000 | | | |
| ENSO-SOI | 0.040 | -0.182 | -0.433 | 0.889 | -0.828 | -0.190 | 0.297 | 0.364 | 1.000 | | |
| ENSO-SST | -0.003 | -0.189 | -0.364 | 0.873 | -0.751 | -0.209 | 0.343 | 0.339 | 0.978 | 1.000 | |
| OLR | 0.263 | 0.067 | 0.135 | -0.336 | 0.362 | 0.042 | 0.177 | -0.477 | -0.240 | -0.221 | 1.000 |

TABLE 4.5: Collinear Matrix of Large-Scale Circulations - June

| | **ZW-SUR** | **ZW-200** | **ZW-300** | **ZW-500** | **ZW-850** | **GPH-200** | **GPH-300** | **GPH-500** | **GPH-850** | **RH-300** | **RH-500** | **RH-850** |
|---|---|---|---|---|---|---|---|---|---|---|---|---|
| ZW-SUR | 1.000 | | | | | | | | | | | |
| ZW-200 | 0.044 | 1.000 | | | | | | | | | | |
| ZW-300 | 0.064 | 0.985 | 1.000 | | | | | | | | | |
| ZW-500 | 0.098 | 0.958 | 0.978 | 1.000 | | | | | | | | |
| ZW-850 | 0.106 | 0.793 | 0.816 | 0.905 | 1.000 | | | | | | | |
| GPH-200 | -0.030 | 0.606 | 0.565 | 0.537 | 0.416 | 1.000 | | | | | | |
| GPH-300 | -0.039 | 0.534 | 0.492 | 0.469 | 0.370 | 0.969 | 1.000 | | | | | |
| GPH-500 | -0.011 | 0.485 | 0.446 | 0.424 | 0.333 | 0.943 | 0.990 | 1.000 | | | | |
| GPH-850 | 0.117 | 0.434 | 0.419 | 0.397 | 0.300 | 0.833 | 0.875 | 0.920 | 1.000 | | | |
| RH-300 | -0.086 | -0.137 | -0.152 | -0.144 | -0.105 | 0.162 | 0.224 | 0.226 | 0.128 | 1.000 | | |
| RH-500 | -0.089 | -0.093 | -0.089 | -0.076 | -0.031 | -0.415 | -0.507 | -0.529 | -0.495 | 0.203 | 1.000 | |
| RH-850 | 0.174 | -0.054 | -0.062 | -0.058 | -0.038 | -0.492 | -0.604 | -0.633 | -0.592 | 0.042 | 0.733 | 1.000 |

### 4.3.5 Selection of Regressors

The 30 regressors and the regression model would be specified using these regressors. The selection of the right regressors is crucial and challenging task. The regressors are selected keeping in view the following conditions:

a. Correlation of the regressors with the dependent variable (precipitation).

b. Avoid combining the variables having multicollinearity.

### 4.3.6 MLR Regression Results

Following the step-wise method and the approach for selection of regressors, the regression analysis is performed. The best regression model out of several permutations is presented in Table 4.6 and Table 4.7 for January and June. The independent variable along with their coefficients, t- stat and the p-value 5% significant level are also listed in Table 4.6 and Table 4.7.

Table 4.6: Regression Output for the Month of January

| **Regressors** | **Coefficients** | **Standard Error** | **t-Stat** | **p-value** |
|---|---|---|---|---|
| Intercept | 1.466 | 10.81 | 0.136 | 0.8929 |
| NAO | -6.175 | 1.591 | -3.88 | 0.0005 |
| AO | 8.610 | 2.452 | 3.51 | 0.0013 |
| RH-500 | 0.965 | 0.335 | 2.88 | 0.0070 |
| VWind-Surface | 6.299 | 3.475 | 1.81 | 0.0790 |
| EQWIN | 2.32 | 2.494 | 0.930 | 0.3590 |

Table 4.7: Regression Output for the Month of June

| **Regressors** | **Coefficients** | **Standard Error** | **t-Stat** | **p-value** |
|---|---|---|---|---|
| Intercept | -882.14 | 355.9 | -2.480 | 0.0190 |
| EQWIN | 6.050 | 1.990 | 3.04 | 0.0049 |
| RH850 | 1.484 | 0.482 | 3.08 | 0.0045 |
| EMI-MODOKI | 2.822 | 1.878 | 1.50 | 0.1434 |
| AO | -9.619 | 3.343 | -2.88 | 0.0073 |
| GPH850 | 0.577 | 0.263 | 2.19 | 0.0362 |
| ZW300 | -1.795 | 0.762 | -2.36 | 0.0252 |
| VWind300 | 0.8146 | 0.725 | 1.12 | 0.2704 |
| Airtemp200 | -1.494 | 2.243 | 0.66 | 0.5103 |

The p-value of all the predictors is less than 0.005 showing that all the predictors are highly significant at 5% confidence level.

#### 4.3.6.1 Performance Indices of Regression

As discussed above, the validity of the regression model is judged by the performance indices of regression. Most reported statistics in regression are Person Correlation Coefficient (R), Coefficient of Determination ($R^2$), Adjusted $R^2$ (Adj $R^2$), Sigma ($\sigma$) and Standard Error (SE). The statistics of these tests for January and June are listed in Tables 4.8.

TABLE 4.8: Regression Statistics for the Month of January and June

| **Regression Indices** | **January** | **June** |
|---|---|---|
| Correlation Coefficient (R) | 0.8301 | 0.8291 |
| Coefficient of Determination ($R^2$) | 0.6890 | 0.6873 |
| Adjusted $R^2$ | 0.6419 | 0.6040 |
| Standard Error | 20.0165 | 17.7586 |
| F test | 0.0001 | 0.001 |
| Observations | 39 | 39 |

The regression indices of January using MLR is found to have 0.6890 $R^2$, which means 68.90% variability in precipitation (dependent variable) is due to the independent variable listed in Table 4.6. Similarly, the regression indices of June using MLR is found to have 0.6873 $R^2$, which means 68.73% variably in precipitation (dependent variable) is due to the independent variable listed in Table 4.7.

#### 4.3.6.2 MLR Results- Post Estimation Residual Analysis

Post Estimation Residual Analysis are carried out to prove the efficiency of the predicted model. Auto correlation (AR) test and Auto Regressive Conditional Heteroskedasticity (ARCH) tests are performed on the residuals of the regression analysis for the month of January and June. The statistics found are listed in Table 4.9.

TABLE 4.9: Post Estimation Residual Analysis for the Month January and June

| **Post Estimation Residual Tests** | **January** | **June** |
|---|---|---|
| Auto correlation (AR) - test | 0.3905 | 0.0786 |
| Auto Regressive Conditional Heteroskedasticity (ARCH)- test | 0.6794 | 0.5335 |

- **Residual Analysis - January**

  **Auto correlation (AR)**

  test is 0.3905, as mentioned in Table 4.9. The AR test value is greater than the 5% significance level, i.e., $0.3905 > 0.05$, which indicates that the null hypothesis of no correlation cannot be rejected. Statistically, the alternate hypothesis is rejected, and the null hypothesis is accepted. This means that the residuals are free from serial correlation, which is desirable and the model is good to go.

  **Auto Regressive Conditional Heteroskedasticity (ARCH)**

  The ARCH test $= 0.6794 > 0.05$, which means one cannot reject the null hypothesis of no heteroskedasticity in the residuals; in other words, residual is homoscedastic which indicate that the model is good.

- **Residual Analysis - June**

  **Auto correlation (AR)**

  test is 0.0786 as mentioned in the Table 4.9. The AR test value is greater than the 5% significance level, i.e., $0.0786 > 0.05$, which indicates that the null hypothesis cannot be rejected. Statistically, the alternate hypothesis is rejected, and the null hypothesis is accepted. This means that the residuals are free from serial correlation, which is desirable and indicates that the model is good to go.

  **Auto Regressive Conditional Heteroskedasticity (ARCH)**

  The ARCH test $= 0.5335 > 0.05$, which means one cannot reject the null hypothesis of no heteroskedasticity in the residuals; in other words, residual are homoscedastic which indicate that the model is good.

#### 4.3.6.3 MLR Regression Equation

**January**

The regression outputs for January are shown in Table 4.6. using MLR techniques with precipitation as response variable NAO, AO, RH500 and VWind surface come out to be highly significant explanatory variables except EQWIN. EQWIN is the only explanatory variable that is not highly significant climate indices. The p-value of NAO, AO, RH500 and VWind surface is equal to or less than 0.05, which shows that the regressors are significant for a confidence level of 5%. However, the p-value of EQWIN is 0.3590. EQWIN is used as an explanatory variable in the model because EQWIN influences the precipitation in January and explain, the maximum variability of the precipitation in January. EQWIN is positive and highly correlated with principal modes of January precipitation up to 2% significance [235].The coefficient of determination $R^2$ is come out to be 0.6890, which indicates that 68.90% variation in precipitation can be estimated by explanatory variables in the regression equation precipitation for the of January. The regression equation for January is given by the following equation:

**Precipitation = 1.467 - 6.17*NAO + 8.61*AO + 0.96*RH500 + 6.29* VWind-Surface+2.32*EQWIN**

**June**

The regression outputs for June are shown in Table 4.7. With precipitation as a response variable and EQWIN, EMI-MODOKI, AO along with RH850, GPH850, ZWind300, VWind300 and Airtemp200 as the explanatory variables. The p-value of all the regressors is less than 0.05, which indicates that all the regressors are significant with a confidence level of 5%. Except for EMI-MODOKI, Vwind300 and Airtemp200. $R^2$ is come out to be 0.6873, which indicates that 68.73 % variation in precipitation can be estimated by explanatory variables using multiplelinear regression. EQWIN has a strong positive influence, EMI-MODOKI has a moderate positive influence, whereas AO has a strong negative influence on the precipitation variability of June [235]. The regression equation for the month of June is given by the following equation:

**Precipitation = -882.1 +6.05 *EQWIN + 1.48*RH850 + 2.83*EMI-MODOKI - 9.62*AO + 0.57*GPH850 -1.79*ZW300 + 0.81*VWind300 - 1.49*Airtemp200**

#### 4.3.6.4 Model Evaluation Statistics (Loss Error)

The predictability of the model is assessed by **Root Mean Squared Error (RMSE), Mean Absolute Error (MAE), Nash-Sutcliffe Efficiency (NSE), Percent Bias (PBIAS) and RMSE-observations Standard deviation Ratio (RSR)** [210, 212, 329, 330]. Root Mean Squared Error (RMSE) , Mean Absolute Error (MAE) are the most common and widely used error indices for model evaluations. These indices are widely used because they show errors in the units (or squared units) of the constituents of interest, which help in result analysis. RMSE and MAE values of 0 indicate a perfect fit. The lower the value, the better the model is. However, values less than half the standard deviation of the measured data are considered low values and good models.

Nash-Sutcliffe Efficiency (NSE) is a normalized statistic that determines the relative magnitude of the residual variance compared to the measured data variance. NSE shows how well the plot of observed versus estimated data fits the 1:1 line. NSE between 0.0 to 1.0 is generally viewed as acceptable levels of performance [329]. Percent Bias (PBIAS) measure the average tendency of the stimulated data to be larger or smaller than their observed counterpart. The optimal value of PBIAS is 0.0; the lower the magnitude value the accurate the model. Positive values show model underestimation bias and negative values indicate model overestimation bias. RSR is calculated as the ratio of the RMSE and standard deviation of measured data. The lower the RSR and RMSE, the better the model prediction results will be [329, 331].

The regression model is prepared by using the data in the training period from 1977 to 2015 and the values of predicted precipitation are obtained from the regression equation in the training period. The RMSE and MAE are then calculated to check the performance of model. The MLR model is further used for validation of the period from 2016 to 2020. The values of RMSE and MAE are then again

calculated for the validation period (2016-2020) to check the predictive performance of the model. Model evaluation statistics, namely NSE, PBIAS and RSR for over study period (1977-2020) for both January and June, are calculated and listed in Table 4.10. All the statistics are between 0.0 to 1.0, as recommended for a very good model [329, 331].

Therefore, the developed model is **very good with strong and accurate prediction power**. The comparison of RMSE and MAE for the training period and validation period are reported as loss errors in Table 4.10. The graph and histogram between the observed values and estimated/predicted values both for the training and validating period are shown in Figures 4.1 and 4.2 (for the months of January).

Similarly, graphs and histograms between the observed values and estimated/predicted values both for the training and validating period are shown in Figures 4.3 and 4.4 (for the months of June). The values of RMSE and MAE for the training period and validating period are more or less the same for the months of January and June, which shows the predictability of a good model [329]. The calculation for **RMSE, MAE, NSE, PBIAS and RSR for the months of January and June is attached in Annexure-B (B.1, B.2, B.5 & B.6)**.

TABLE 4.10: Model Evaluation Statistics for the Months of January and June

| **Loss Error for training period (1977-2015)** | **January** | **June** |
|---|---|---|
| Root Mean Square Error (RMSE) | 11.02 | 9.80 |
| Mean Absolute Error (MAE) | 8.37 | 7.61 |
| **Loss Error for validation period (2016-2020)** | **January** | **June** |
| Root Mean Square Error (RMSE) | 7.46 | 16.03 |
| Mean Absolute Error (MAE) | 6.13 | 13.92 |
| **Loss Error for the Entire study period (1977-2020)** | **January** | **June** |
| Nash-Sutcliffe Efficiency (NSE) | 0.7283 | 0.6087 |
| Percent Bias (PBAIS) | 0.86 | 7.92 |
| RMSE Standard-deviation Ratio (RSR) | 0.5618 | 0.5673 |

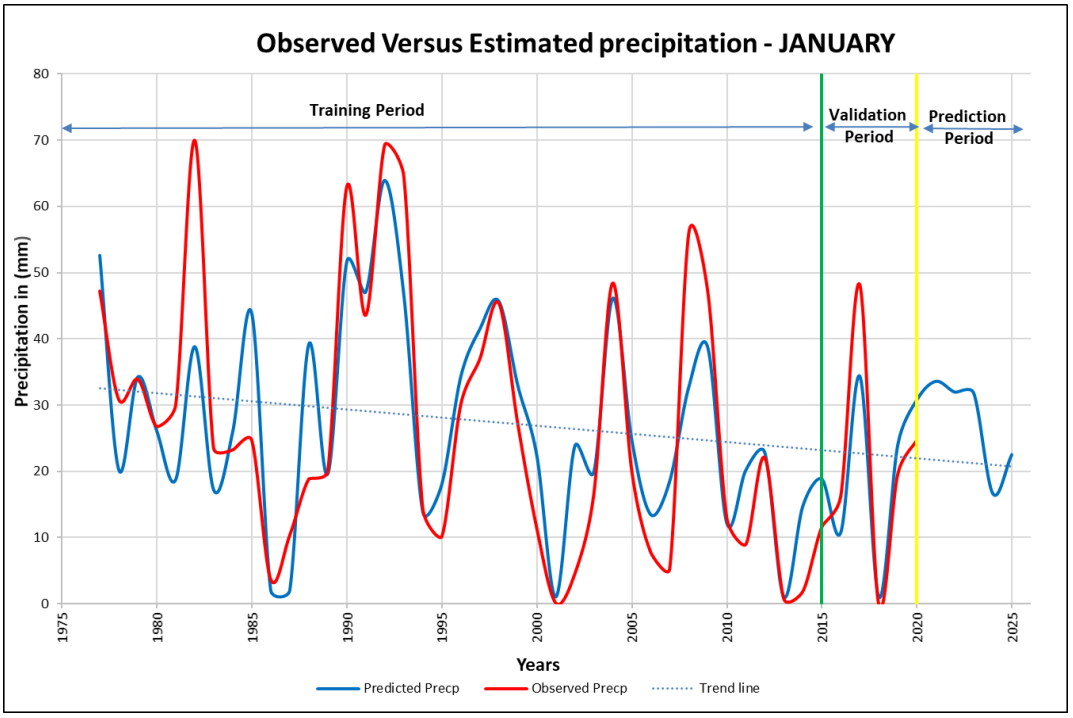


FIGURE 4.1: Observed versus Estimated Precipitation using MLR- JANUARY

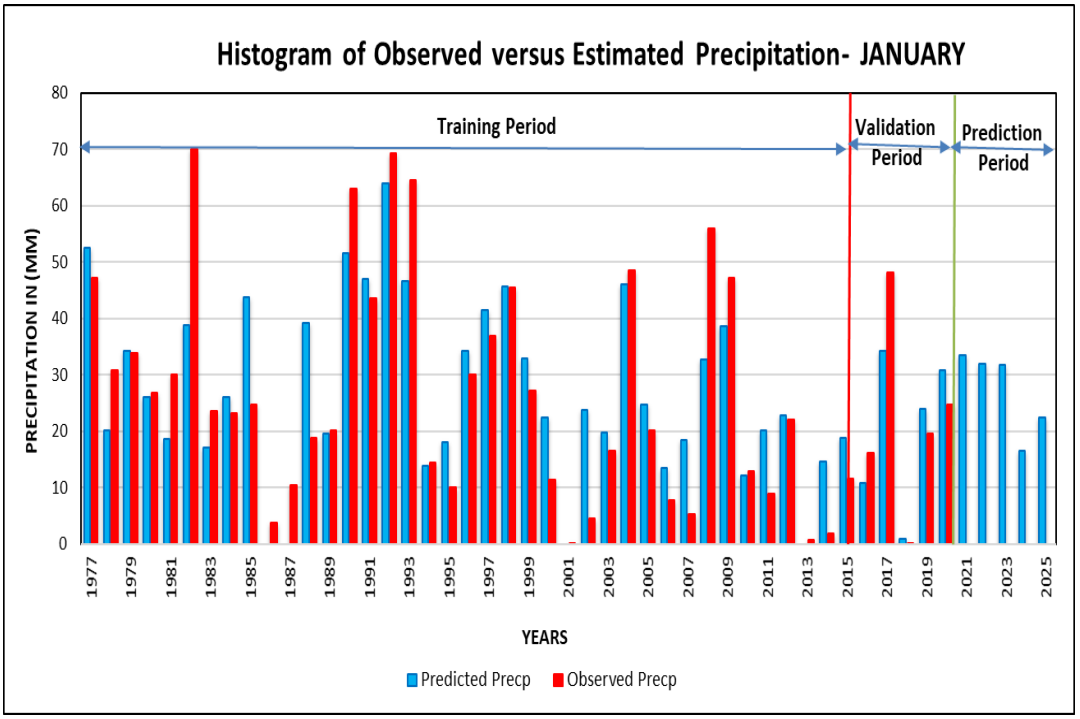


FIGURE 4.2: Histogram of Observed versus Estimated Precipitation using MLR- JANUARY

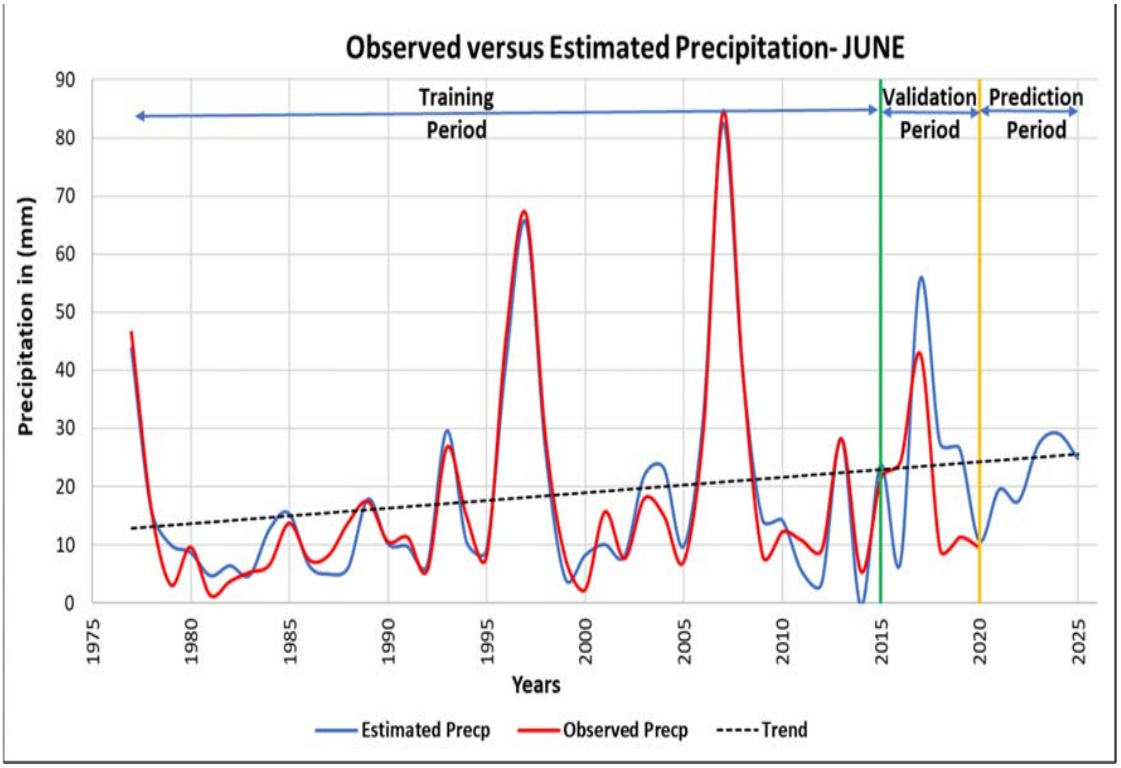


FIGURE 4.3: Observed versus Estimated Precipitation using MLR- JUNE

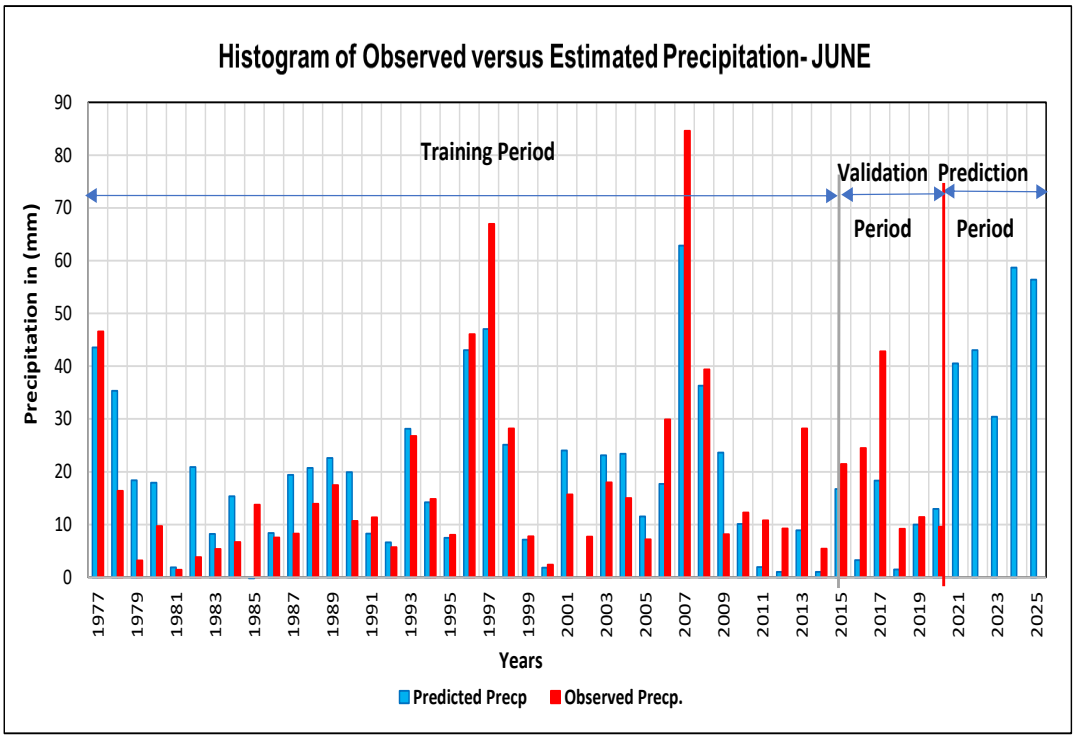


FIGURE 4.4: Histogram of Observed versus Estimated Precipitation using MLR- JUNE

## 4.4 Significance/Application of the Finding

The equation developed identify the novel index EQWIN, a new climatic index, besides other potential determinants. The climatic index EQWIN has a significant effect on the precipitation variation of January and shows a decreasing trend in January, so it is crucial to educate and prepare local inhabitants about the aspects of decrements in precipitation. Encourage locals to adopt and implement water consumption practices, store water by constructing small water reservoirs and dams. Promote rainwater harvesting and construction of recharge wells. Restore and revive the famous effective karez system in the province. The trend is increasing in June, which may cause unprecedented rainfall and due to the topography and rugged terrain of Baluchistan, this torrential rain can cause flash floods. Flash floods are proven to be more catastrophic and disastrous by mother nature. The timely intimation of the flash floods will be a great blessing for local inhabitants to save their precious lives, livestocks and other valuable belongings. This model has very good predicting power as, shown by the statistical error. It can give valuable information about the potential factors effecting the future trend of precipitation, which can be very useful to the local government, provincial government, agriculture department, provincial disaster management and metrological department for predicting dry spells or extreme, unprecedented torrential rainfall. The information can be helpful in planning crops or opt for re-cropping, ridge farming, and re-sowing. It should be noted that 90% of the grassland, shrubs and bushes in the study area are rain fed. The decrease in rainfall in the month of January will have a direct impact on these grasslands and on the livestock. The model prediction should be used to plan livestock, which is the second most common occupation of local dwellers. The livestock contributes 20% of the provincial Gross Domestic Product (GDP). The model output information will not only be useful for the livestock business but to other pertinent industries like leather, carpet and pharmaceutical that are the main consumer of livestock products. Baluchistan also fulfills the need and demand of leather and carpet industries in Pakistan by the sustainable supply of hide, skin and wool.

### 4.4.1 Comparative analysis with previous work

The findings and results of Multilinear Regression analysis are **consistent with the previous studies results**. These studies include research conducted by Gong et al. [90], Hall and Hanna [109], Afzal et al. [110] and Pinagle et al. [207] and Vishnu et al. [228], Midhuna and Dimir [229]. Francis and Gadgil [332] reported a strong association between the climate extremes (i.e., droughts and heavy rainfalls) of climate indices ENSO and EQWIN with Indian Summer Monsoon Rainfall (ISMR), which confirms the findings of current research. Although, no focused modeling has been done on the precipitation variability of Baluchistan. However, the studies performed by Iqbal and Athar in [216], Mahmood et al. [128], Dogar et al. [127] about the influence of climatic indices on Pakistan endorsed that NAO, AO and ENSO has a strong influence on the ISMR, consequently influencing the precipitation of study area as well.

## 4.5 Summary

The regression equation of precipitation formulated for January using MLR addresses about 68.90% variation in precipitation. **NAO, AO, RH500, VWind surface and EQWIN are identified as the potential determinants for the month of January**. NAO and AO came out to be highly significant predictors with a p-value of 0.0005 and 0.0013, respectively. The model is reasonably good as $R^2$=0.6890, which indicates that 68.90% variation in precipitation can be estimated by explanatory variables. The regressors in the regression model show that **NAO, AO and VWind-Surface** influence the precipitation in January, and explain the maximum variability of the precipitation in January whereas **EQWIN** has a weak influence on the precipitation. The direction and strength of the association (influence) are provided by the coefficient of regressors.

Root Mean Square Error (RMSE) and Mean Absolute Error (MAE) for January of the training period (1977-2015) are found to be 11.02 and 8.37 for the validation period (2016-2020) 7.46 and 6.13, respectively. The RMSE and MAE values show that the prediction performance of the model is outstanding. The NSE (0.72), PBIAS (0.86%) and RSR (0.56) for the month of **January** show that model is **good** with accurate and strong predicting potential.

Similarly,the Regression equation of precipitation for the month of June addresses about 68.73% variation in precipitation. **EWQIN, AO, EMI-MODOKI, along with RH850, GPH850, ZW300, VWind300 and Airtemp200 are identified as the potential determinants of the precipitation variability for the month of June**. **EQWIN** came out to be a highly significant predictor having a p-value of less than 0.05 for a confidence level of 5%.The coefficient of determination $R^2$ is equal to 0.6873, suggesting that 68.73% variation in precipitation can be estimated by explanatory variables. The model shows that **AO has strong and EMI-MODOKI** has a weak influence on precipitation. The direction and strength of the association (influence) of the regressors are provided by the coefficient of regressors. Root Mean Square Error (RMSE) and Mean Absolute Error (MAE) for June of the training period (1977-2015) are found to be 9.80, 7.61 and for the validation period (2016-2020) 16.03 and 13.92, respectively, which shows that model has good forecasting power. The NSE (0.60), PBIAS (7.92%) and RSR (0.56) for the months of **June** show that the model is robust with **good** predicting power.

# Chapter 5

# Estimation of Potential Determinant Causing Variability in Precipitation using Principal Component Regression (PCR) Analysis

## 5.1 Background

Modeling and prediction are very crucial in all aspects of modern life. Modeling of weather and climate are significant and has multiple positive influences on our social, economical and financial life pattern. There are number of complex phenomena, complicated processes, intricate development at global, regional, and zonal scale are going on in troposphere. These are not only linked but also create uncertainties, doubts, inaccuracies and complexity in the atmosphere during the prediction of weather and climate. Accurate and precise modeling of climate involves a large number of variables that may have multicollinearity within themselves. Most likely, there will always be inaccuracies and flaws in weather and

climate forecasting and that may exist due to several sources of errors present in modeling; like uncertain and complex nature of atmospheric conditions, a shortcoming of the numerical model, instrumental errors, huge dataset, data collection, discrete observations, and irregularly spaced weather stations especially in Baluchistan province.

In the case of modeling, sometimes, the artificial boundary condition increases the errors and uncertainties. Inadequacy of the numerical model consists in difficulty to represent the influence of all physical, chemical and biological factors in the state of the atmosphere and its evolution in time. It is found that a combination of variables that are correlated, in other words, variables having multicollinearity, never help in bringing out good results. Also, huge number of variables and insignificant variables in modeling or analysis techniques never improve the result prediction and accuracy. A solution is needed that can address and remove all the above-stated redundancy from the model and that solution is Principal Component Regression (PCR) analysis.

To create Principal Component Regression (PCR) model, Principal Components (PCs) are linearly combined using the regression technique. The Principal Component Regression (PCR) model overcomes the problems arising from the situations when the explanatory variables are close to being collinear [333]. In other words, Principal Components Regression (PCR) analysis is the best way to address multicollinearity issues in analysis.

The analysis that is performed in the previous chapter leads to the conclusion that January and June are the only two months that show a significant precipitation trend. Therefore, these two months (January and June) are considered to a develop regression models for finding potential determinants using Principal Component Regression (PCR) analysis technique in this chapter too.

## 5.2 Methodology

### 5.2.1 Data Used

It is found in chapter 3 that January and June are the only two months that show significant negative/positive trends in precipitation at the stations located in the Region 1 of Baluchistan. Therefore, the observed monthly precipitation of January and June for the period from 1977 to 2020 is used to prepare a regression model using Principal Component Regression (PCR) Analysis. The observed monthly precipitation data for the period (1977-2015) is ingested in principal component regression analysis for the **training** of the model, whereas data for the period (2016-2020) is used for **validation**. The precipitation is the dependent variable, whereas principal components of the large-scale circulation are the independent variables. Data of the large-scale circulations such as Sea Level Pressure (SLP), Sea Surface Temperature (SST), Geopotential Height (GPH) data at various pressure levels, Relative Humidity (RH) at various pressure levels, Zonal Winds (ZW) at various levels and Outgoing long Radiation (OLR) are acquired from the NCEP/N-CAR reanalysis dataset available at 2.5° resolution except for SST which is at 1° resolution [210, 212].

The lowest most layer of Earth's atmosphere is the troposphere, which contains almost 85% of the atmosphere's mass. The tropopause is the boundary between troposphere and the next layer of atmosphere, the Stratosphere. Pressure at the tropopause is about 100 hpa and that at the surface of Earth is about 1000 hpa. The troposphere extends to an average height of 12 km above the surface of the Earth. Most of the weather and clouds occurs in the troposphere. Wind increases and the temperature decreases when it moves from the surface of the earth to tropopause. In practical meteorology, the most common and significant levels of troposphere which are used for analysis of climate are at surface level: 850 hpa, 500 hpa, 300 hpa and 200 hpa. The 850 hpa and 500 hpa levels are known for clouds and precipitation changes, whereas 300 hpa and 200 hpa are levels where

jet streams exist. The matrix between large scale circulation and selected pressure levels are given in Table 5.1.

TABLE 5.1: Large-Circulations and Selected Pressure Levels Matrix

| **S.No** | **Large-Circulations** | **Surface** | **850hpa** | **500hpa** | **300hpa** | **200 hpa** |
|---|---|---|---|---|---|---|
| 1 | SST | √ | x | x | x | x |
| 2 | SLP | √ | x | x | x | x |
| 3 | OLR | √ | x | x | x | x |
| 4 | ZW | √ | √ | √ | √ | √ |
| 5 | GPH | x | √ | √ | √ | √ |
| 6 | RH | x | √ | √ | √ | x |

The precipitation data is used as predictand (dependent variable) in the PCR model. The predictors (independent variables) are the PCs of the SLP, SST, GPH at 200, 300, 500, 850 pressure levels, ZW at 200, 300, 500, 850 pressure levels, RH at 300, 500, 850 pressure levels and OLR for January and June. Therefore, there are 14 independent variables to be used in the PCR model. The methodology for conducting the PCR regression analysis is as described below:

### 5.2.2 Normalization of Precipitation data

The precipitation data for January and June is normalized and detrended. The normalization is done by deducting the mean from each of the observations of the time series data of precipitation [138].

### 5.2.3 Selecting the Domain for Analysis

The climatic indices NAO, AO and AMO, are the anomalies associated with the Arctic and the Atlantic Ocean to the North of the Equator [216]. The indices DMI and EQWIN are anomalies associated with the Indian Ocean to the North of -30S latitude, whereas ENSO-MEI, EMI-MODOKI and PDO are anomalies associated with the Pacific Ocean to the North of -30S latitude. Therefore, the domain for

the analysis for calculation of PCs through PCA is selected as the -30S to 80N and 0 to 360.

### 5.2.4 Calculation of Regressors (PCs)

Principal Components (PCs) are the linear grouping variables of the original variables acquired through Principal Component Analysis (PCA). PCA is a well established widely used statistical technique in the modern data analysis era. It is an easy and non-parametric technique for separating relevant data from humongous, superfluous, confusing data sets [82]. PCA explores the interrelationship among a set of variables; hence it has an edge on bivariate statistical techniques, which are used earlier. PCA detects patterns in data and presents the data in such a manner that its similarities and differences are highlighted. It has an advantage to compress the data by reducing the number of dimensions. PCA technique is best suited in analysing a large data set, selecting few components and explaining large percentage of the total variance with those selected few components. Principal components are selected in such a way that each successive PC explains a maximum of the remaining variance; the first selected PC explains the maximum proportion of the total variance, the second PC explains the maximum of the remaining variance, and so on. PCA is a non-parametric technique, so every type of data set can be used in it, and the resultant PCs require no adjustments. From one perspective, the fact that PCA is non-parametric (or plug-and-play), it can be considered a positive feature because the output is unique and independent of the user [333].

### 5.2.5 Selecting Leading Modes of PCs

The non-degeneracy of Eigen-spectrum is an important property and can be used for selecting leading modes of PCs. It helps in selecting the PCs that addresses the maximum variance, removing the redundant information from principal component analysis, make complex analysis simple, easy with improved prediction.

Although the inclusion of all the possible predictors in a regression model can maximize the coefficient of determination ($R^2$) and there can be a very high correlation among them (multicollinearity). Furthermore, the inclusion of too many predictors can introduce positive bias and can minimize the true predictive skill of a model. Hence, the Eigen-spectrum of predictors are made not only to select the most significant PCs but can also optimize $R^2$ proficiently [205, 242, 246].

### 5.2.6 Performing Regression

Selected PCs are then linearly combined in a regression model using Principal Component Regression analysis (PCR), which is defined as the statistical technique that uses a linear combination of the original variables known as Principal components (PCs) instead of using original variables. It is encouraged to use PCs in analysis instead of using original variables if there exists a possibility of correlation among the variables. PCA converts the original inter-correlated independent set of variables to an uncorrelated fresh group of variables (i.e., PCs). These PCs are useful not only to address the problem of multicollinearity among the original independent variables but also to differentiate the most significant variable to be used in the analysis. In other words, redundant and superfluous PCs are removed from the analysis.

### 5.2.7 Specifying Regression Model

Specifying the regression model is the process of determining the independent variables that will be used in the model. It helps to sort which variables to include and which to exclude from the model. It also supports finding whether the modeling curvature and interaction effects are appropriate. While specifying the model efforts are being made to include the independent variables which have an actual relationship with dependent variables and exclude those which are not related. The appropriateness of the model is assessed through the use of various statistical

performance indices of regression and post estimation tests. The automatic selection procedure for specifying the regression model is stepwise regression (either General to Specific or Specific to General) and best subset regression. Using these automatic procedures, the best candidate model based on the best performance indices and post estimation results are selected.

### 5.2.8 Regression Model Performance Indices

Model performance and robustness are assessed through performance indices. The most commonly reported indices that are used to evaluate the performance of the PCR model are Person Correlation Coefficient (R), Coefficient of Determination ($R^2$), Adjusted $R^2$ (Adj $R^2$), and Standard Error (SE), which are already discussed briefly in chapter 4.

### 5.2.9 Post Estimation Tests

Post Estimation tests are mostly performed on residuals because residual plays an important role in validating the regression model. If the error term in the regression model satisfies the post estimation tests, then the model is considered effective. The performance indices tests for regression are also based on the assumptions. Therefore the conclusions resulting from these significance tests are called into question if the assumptions regarding error are not satisfied. The post estimation tests performed on the residuals are described below.

#### 5.2.9.1 Auto correlation (AR)-Test

In order to ensure that the residuals of the model are free from serial correlation, unbiased and non-spurious auto correlation test, commonly known as (AR) Test, is conducted with the following hypothesis statements:

- **Hnul** :*No serial correlation in the residuals.*

- **Halt** :*Residuals are serially correlated.*

#### 5.2.9.2 Auto Regressive Conditional Heteroskedasticity (ARCH) Test

Heteroscedasticity can easily be understood as unequal spread of data samples. In the context of regression analysis heteroscedasticity means the unequal spread of the residuals or error term. Precisely, heteroscedasticity is a systematic change in the spread of residuals over the range of measured values. The ordinary least squares (OLS) regression is based on the assumption that all residuals are homoscedastic, meaning these are drawn from a population that has a constant variance (equal spread). To make the model authentic and the result accurate, the residuals should have a constant variance (homoscedastic). The ARCH test is applied to check the variance of residuals [263]. The hypothesis of test is as follows:

- **Hnul** :*No Heteroskedasticity in the residual.*
- **Halt** :*Residuals are Homoscedastic*

## 5.3 Results and Analysis

The objective of this chapter is to develop the model for finding potential determinants defining precipitation variability using the Principal Component Regression (PCR) technique. The dependent variable in the regression analysis is the time series precipitation data of Region 1 in Baluchistan. The precipitation data is normalized and detrended. The domain for analysis is the -30S to 80N and 0 to 360. The pressure levels of 850 hpa, 500 hpa, 300 hpa and 200 hpa are considered for GPH, ZW and RH, whereas SST, SLP, ZW and OLR are considered at the surface of the atmosphere in the troposphere. Principal Component (PCs) of Sea Surface Temperature (SST), Sea Level Pressure (SLP), Geopotential Height (GPH), Zonal Wind (ZW), Relative Humidity (RH) and Outgoing Longwave Radiation (OLR) are calculated using Principal Component Analysis (PCA).

### 5.3.1 Leading Modes

For each of the above independent variables (predictors), thirty nine (39) PCs are calculated. The uncertainty estimates of Eigenvalues spectrum of predictors Sea Surface Temperature (SST), Sea Level Pressure (SLP),Geo-potential Heights ( GPH) (at 200, 300, 500, 850 levels), Relative Humidity (RH) (at 300, 500, 850 levels), Zonal Winds (ZW) (at 200, 300, 500, 850 levels) and Outgoing Longwave Radiation (OLR), are calculated by thumb rule proposed by North et al. [308] and are shown in Figures 5.1, 5.2, 5.3 and 5.4 for January and June. Out these thirty nine (39) PCs, the number of significant patterns coming out of a Principal Component Analysis (PCA) or Empirical Orthogonal Function (EOF) Analysis are then considered for Principal Component Regression (PCR) analysis. The North's Rule of Thumb (North et al., 1982) is applied to determine this cutoff. Basically, the rule of thumb is that the difference between neighboring Lambdas (uncertainity estimates) must be greater than their associated errors.

From the above Eigenvalue spectrum analysis, the four (4) leading modes of the transformed (PCs) predictors are selected as the predictors to be used in the regression analysis both for the months of January and June [242, 273].

### 5.3.2 Details of Dependent and Independent Variables

The details of the dependent variable (predictands) and the independent variables (potential determinants) are shown in Table 5.2. The total number of independent variables thus selected are 61, including the constant term in the regression equation. Therefore, a total number of C (61!) = (5.07x10E83) factorial combinations are possible for specifying the regression model.

**The best candidate regression model is then selected using an automatic stepwise regression procedure based on the performance indices and post estimation tests on residuals.**

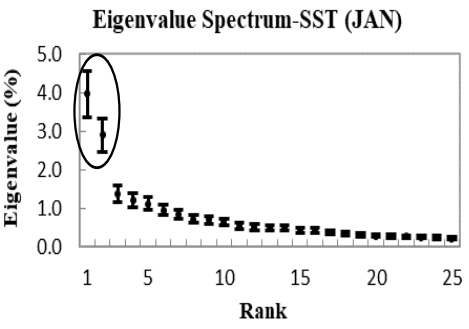


Showing two leading modes

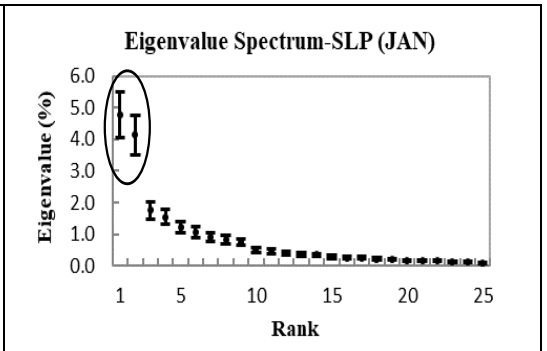


Showing two leading modes

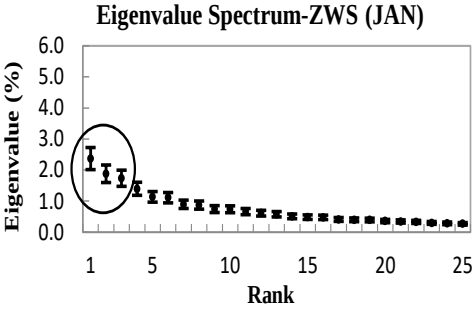


Showing three leading modes

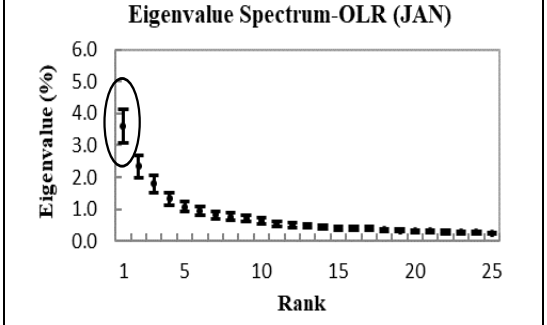


Showing One leading modes

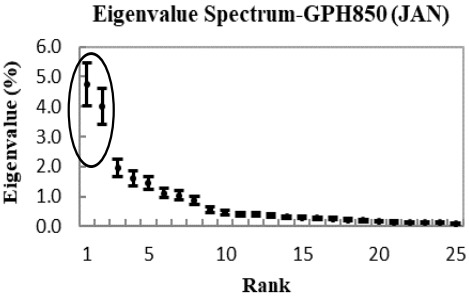


Showing two leading modes

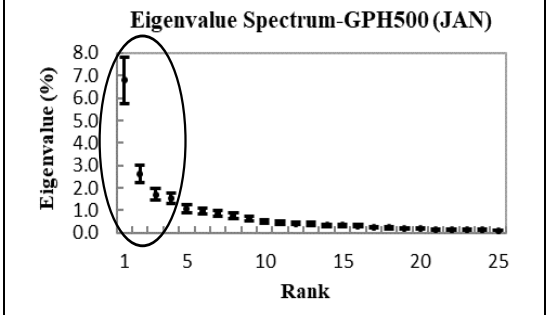


Showing Four leading modes

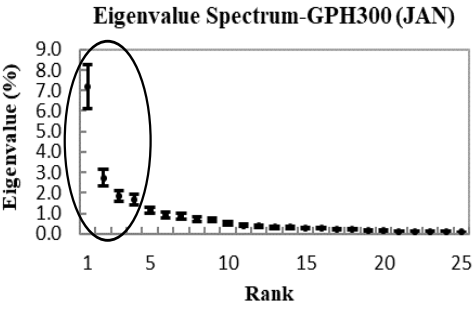


Showing Four leading modes

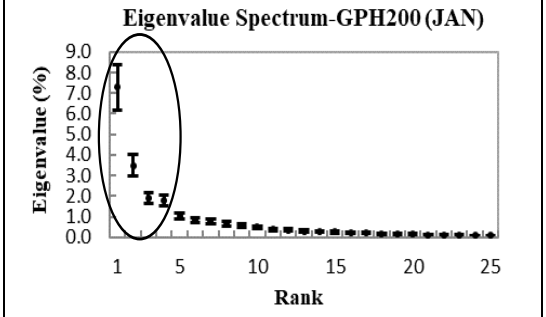


Showing Four leading modes

FIGURE 5.1: Eigenvalue Spectrum Modes of JANUARY

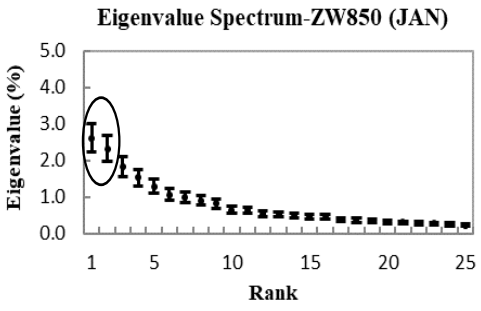


Showing Two leading modes

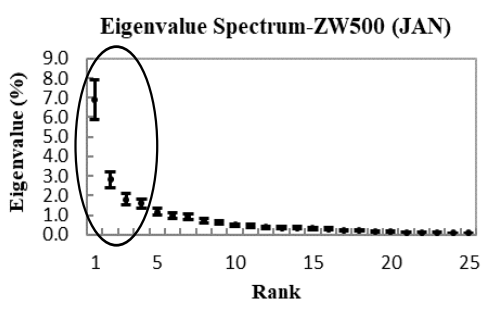


Showing Four leading modes

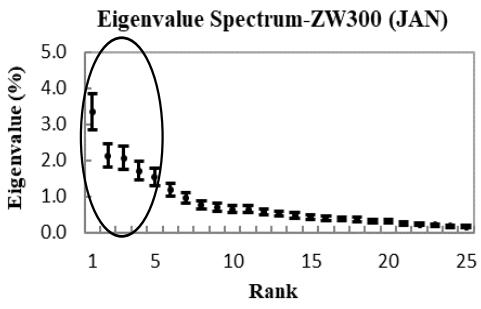


Showing Five leading modes

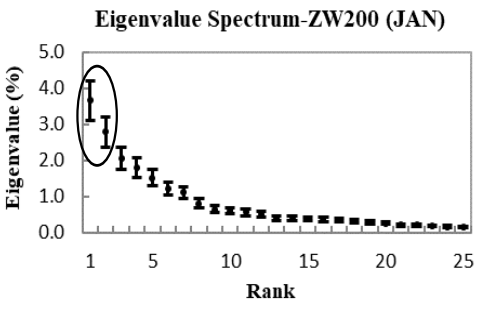


Showing Two leading modes

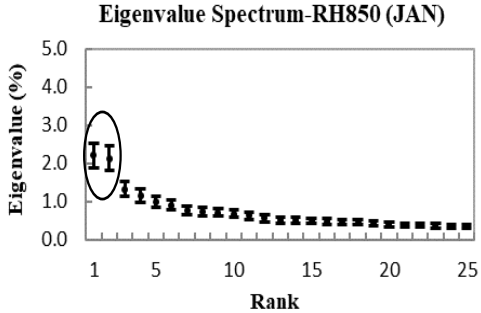


Showing Two leading modes

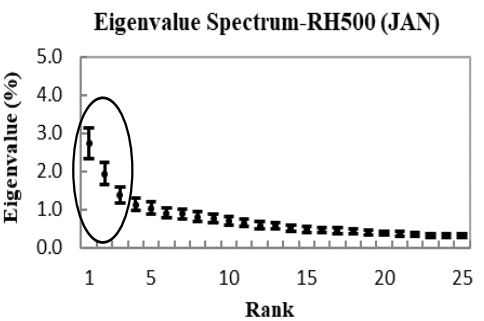


Showing Three leading modes

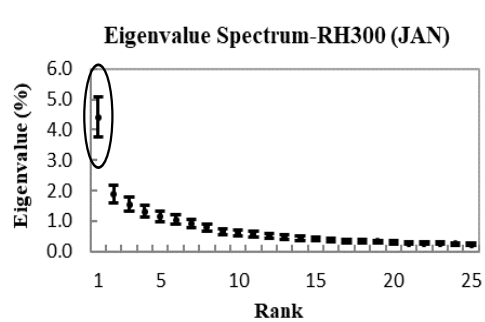


Showing One leading modes

Empty -Please ignore

FIGURE 5.2: Eigenvalue Spectrum Modes of JANUARY

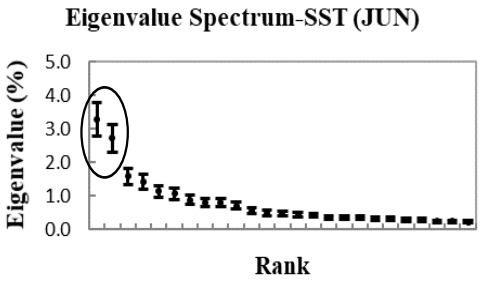


Showing two leading modes

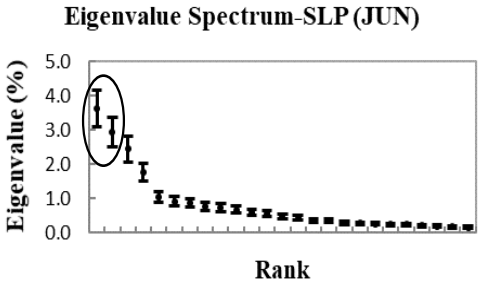


Showing two leading modes

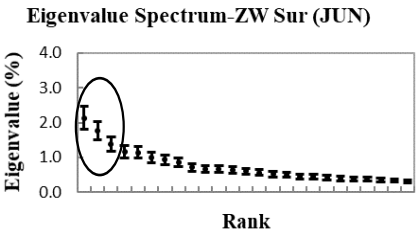


Showing three leading modes

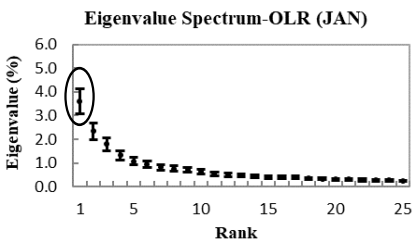


Showing One leading modes

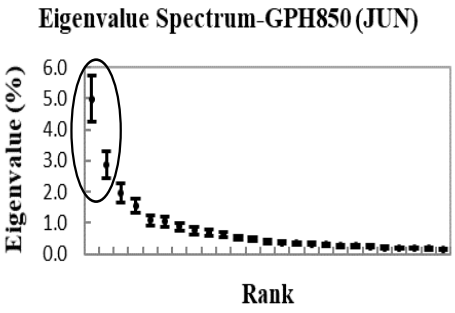


Showing two leading modes

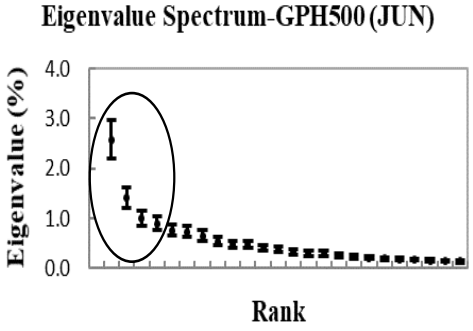


Showing Four leading modes

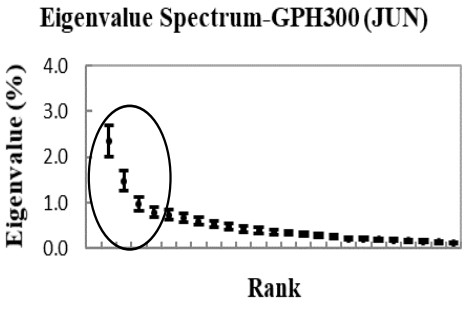


Showing Four leading modes

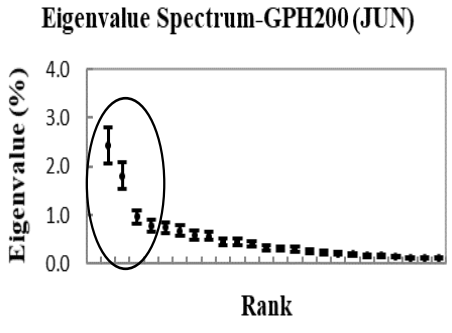


Showing Four leading modes

FIGURE 5.3: Eigenvalue Spectrum Modes of JUNE

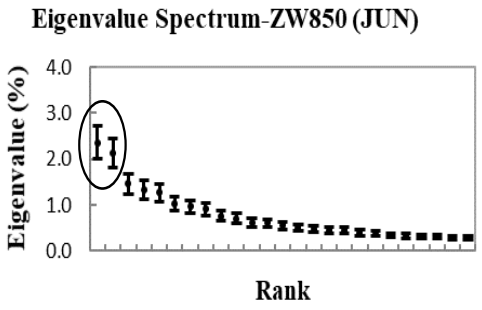


Showing Two leading modes

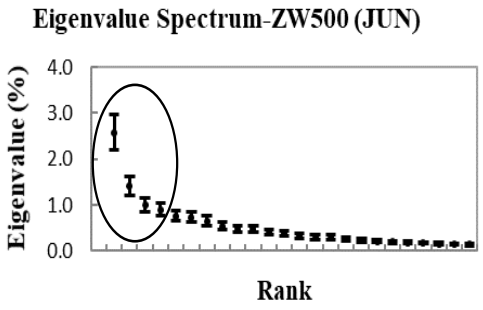


Showing Four leading modes

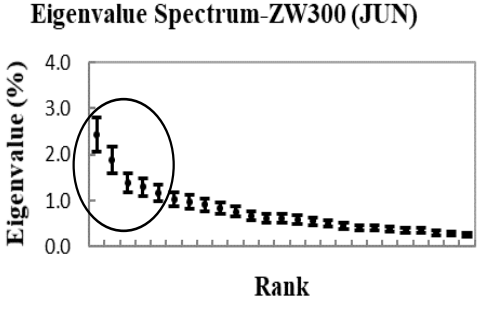


Showing Five leading modes

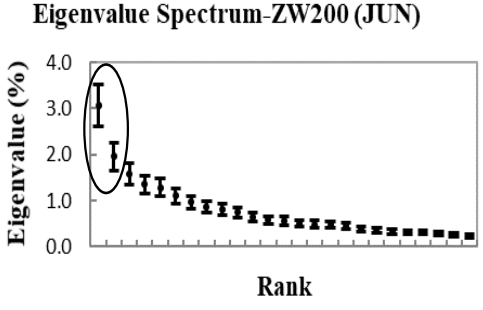


Showing Two leading modes

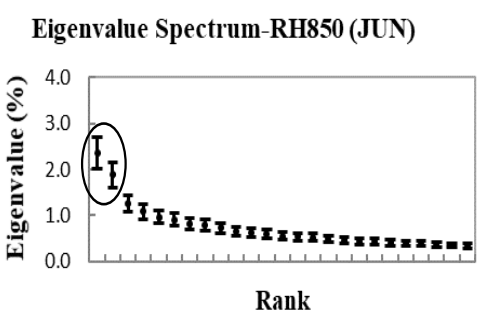


Showing Two leading modes

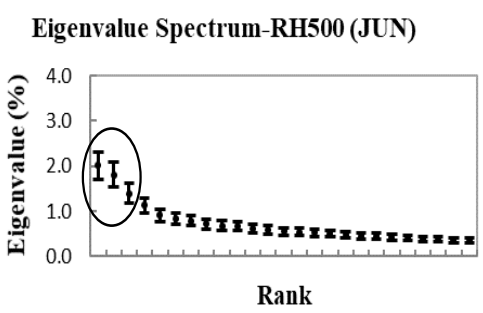


Showing Three leading modes

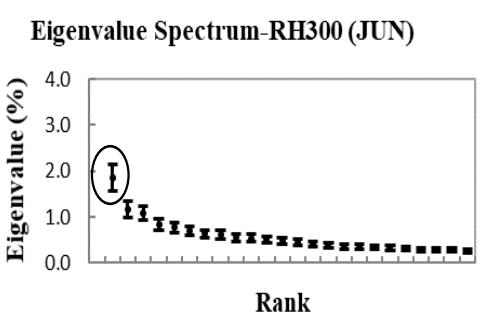


Showing One leading modes

Empty -Please ignore

FIGURE 5.4: Eigenvalue Spectrum Modes of JUNE

TABLE 5.2: Details of the Selected Dependent and Independent variables used in PCR-Analysis

| S.no | Attributes | Type | Description | Variable type |
|---|---|---|---|---|
| 1 | Year | Numeric | 1977-2015 (Study period) | Observation |
| 2 | Months | String | January, June | Observation |
| 3 | Precipitation | Numeric | Monthly Precipitation(Normalized) | Response |
| 4 | SST-PC1 | Numeric | Principal Component-1 of SST | Explanatory |
| 5 | SST-PC2 | Numeric | Principal Component-2 of SST | Explanatory |
| 6 | SST-PC3 | Numeric | Principal Component-3 of SST | Explanatory |
| 7 | SST-PC4 | Numeric | Principal Component-4 of SST | Explanatory |
| 8 | SLP-PC1 | Numeric | Principal Component-1 of SLP | Explanatory |
| 9 | SLP-PC2 | Numeric | Principal Component-2 of SLP | Explanatory |
| 10 | SLP-PC3 | Numeric | Principal Component-3 of SST | Explanatory |
| 11 | SLP-PC4 | Numeric | Principal Component-4 of SST | Explanatory |
| 12 | ZWS-PC1 | Numeric | Principal Component-1 of ZWS | Explanatory |
| 13 | ZWS-PC2 | Numeric | Principal Component-2 of ZWS | Explanatory |
| 14 | ZWS-PC3 | Numeric | Principal Component-3 of ZWS | Explanatory |
| 15 | ZWS-PC4 | Numeric | Principal Component-4 of ZWS | Explanatory |
| 16 | GPH850-PC1 | Numeric | Principal Component-1 of GPH850 | Explanatory |

| | | | | |
|---|---|---|---|---|
| 17 | GPH850-PC2 | Numeric | Principal Component-2 of GPH850 | Explanatory |
| 18 | GPH850-PC3 | Numeric | Principal Component-3 of GPH850 | Explanatory |
| 19 | GPH850-PC4 | Numeric | Principal Component-4 of GPH850 | Explanatory |
| 20 | GPH500-PC1 | Numeric | Principal Component-1 of GPH500 | Explanatory |
| 21 | GPH500-PC2 | Numeric | Principal Component-2 of GPH500 | Explanatory |
| 22 | GPH500-PC3 | Numeric | Principal Component-3 of GPH500 | Explanatory |
| 23 | GPH500-PC4 | Numeric | Principal Component-4 of GPH500 | Explanatory |
| 24 | GPH300-PC1 | Numeric | Principal Component-1 of GPH300 | Explanatory |
| 25 | GPH300-PC2 | Numeric | Principal Component-2 of GPH300 | Explanatory |
| 26 | GPH300-PC3 | Numeric | Principal Component-3 of GPH300 | Explanatory |
| 27 | GPH300-PC4 | Numeric | Principal Component-4 of GPH300 | Explanatory |
| 28 | GPH200-PC1 | Numeric | Principal Component-1 of GPH200 | Explanatory |
| 29 | GPH200-PC2 | Numeric | Principal Component-2 of GPH200 | Explanatory |
| 30 | GPH200-PC3 | Numeric | Principal Component-3 of GPH200 | Explanatory |
| 31 | GPH200-PC4 | Numeric | Principal Component-4 of GPH200 | Explanatory |
| 32 | ZW850-PC1 | Numeric | Principal Component-1 of ZW850 | Explanatory |
| 33 | ZW850-PC2 | Numeric | Principal Component-2 of ZW850 | Explanatory |
| 34 | ZW850-PC3 | Numeric | Principal Component-3 of ZW850 | Explanatory |

| | | | | |
|---|---|---|---|---|
| 35 | ZW850-PC4 | Numeric | Principal Component-4 of ZW850 | Explanatory |
| 36 | ZW500-PC1 | Numeric | Principal Component-1 of ZW500 | Explanatory |
| 37 | ZW500-PC2 | Numeric | Principal Component-2 of ZW500 | Explanatory |
| 38 | ZW500-PC3 | Numeric | Principal Component-3 of ZW500 | Explanatory |
| 39 | ZW500-PC4 | Numeric | Principal Component-4 of ZW500 | Explanatory |
| 40 | ZW300-PC1 | Numeric | Principal Component-1 of ZW300 | Explanatory |
| 41 | ZW300-PC2 | Numeric | Principal Component-2 of ZW300 | Explanatory |
| 42 | ZW300-PC3 | Numeric | Principal Component-3 of ZW300 | Explanatory |
| 43 | ZW300-PC4 | Numeric | Principal Component-4 of ZW300 | Explanatory |
| 44 | ZW200-PC1 | Numeric | Principal Component-1 of ZW200 | Explanatory |
| 45 | ZW200-PC2 | Numeric | Principal Component-2 of ZW200 | Explanatory |
| 46 | ZW200-PC3 | Numeric | Principal Component-3 of ZW00 | Explanatory |
| 47 | ZW200-PC4 | Numeric | Principal Component-4 of ZW200 | Explanatory |
| 48 | RH850-PC1 | Numeric | Principal Component-1 of RH850 | Explanatory |
| 49 | RH850-PC2 | Numeric | Principal Component-2 of RH850 | Explanatory |
| 50 | RH850-PC3 | Numeric | Principal Component-3 of RH850 | Explanatory |
| 51 | RH850-PC4 | Numeric | Principal Component-4 of RH850 | Explanatory |
| 52 | RH500-PC1 | Numeric | Principal Component-1 of RH500 | Explanatory |

| | | | | |
|---|---|---|---|---|
| 53 | RH500-PC2 | Numeric | Principal Component-2 of RH500 | Explanatory |
| 54 | RH500-PC3 | Numeric | Principal Component-3 of RH500 | Explanatory |
| 55 | RH500-PC4 | Numeric | Principal Component-4 of RH500 | Explanatory |
| 56 | RH300-PC1 | Numeric | Principal Component-1 of RH300 | Explanatory |
| 57 | RH300-PC2 | Numeric | Principal Component-2 of RH300 | Explanatory |
| 58 | RH300-PC3 | Numeric | Principal Component-3 of RH300 | Explanatory |
| 59 | RH300-PC4 | Numeric | Principal Component-4 of RH300 | Explanatory |
| 60 | OLR-PC1 | Numeric | Principal Component-4 of OLR | Explanatory |
| 61 | OLR-PC2 | Numeric | Principal Component-4 of OLR | Explanatory |
| 62 | OLR-PC3 | Numeric | Principal Component-4 of OLR | Explanatory |
| 63 | OLR-PC4 | Numeric | Principal Component-4 of OLR | Explanatory |

### 5.3.3 PCR Results - Performance Indices of Regression

One of the main objectives of PCR Regression is to describe the relationship between independent variables and a dependent variable. To comprehend the relationships between these variables and to understand the way changes in the independent variables related to the changes in the dependent variable linearly. Most reported statistics in regression are Correlation Coefficient (R), Coefficient of Determination ($R^2$), Adjusted ($R^2$), Sigma ($\sigma$) and Standard Error (SE) dependent variable, i.e., Precipitation SE (Prep). The model satisfactorily fulfilled all of the statistical stated requirements of a prediction model. The statistics of these tests for January and June are listed in Table 5.3.

TABLE 5.3: PCR Regression Statistics for the Month of January and June

| **Regression Statistics** | **January** | **June** |
|---|---|---|
| Correlation Coefficient (R) | 0.8991 | 0.9750 |
| Coefficient of Determination ($R^2$) | 0.8084 | 0.9531 |
| Adj $R^2$ | 0.7399 | 0.9151 |
| Sigma ($\sigma$) | 10.20 | 5.174 |
| Standard Error (SE) | 11.04 | 5.08 |
| F test | 0.0001 | 0.0001 |
| Observations | 39 | 39 |

**5.3.3.1 Regression Model Performance Indices of January** The Pearson correlation coefficient for January is 0.8991, which shows a strong and positive relationship between independent and dependent variables. The value of the coefficient of determination $R^2$= 0.80 highlights a very good fit of the regression line, which is further supported by Adjusted $R^2$ (Adj $R^2$ = 0.73). Sigma ($\sigma$) is another goodness of fit ($\sigma = 10.20$) as reported in the regression analysis to confirm the statistical authenticity and accuracy of the model. For a good quality model, Sigma should be less than the standard error of the dependent variable ($\sigma >$ SE-Prep), which is true also in the January model. All the statistics that are reported above confirm that the PCR regression analysis for the month of January has predicted

a good model. F-statistics = 10.20 > 0.00 (F stat > F critical) suggest a significance relationship between the independent and dependent variable for the overall model performance. In other words,the high explanatory power of the independent variables is observed for the dependent variable on a collective basis. The t-test ($p<0.05$) signified the effect of each of the independent variables on an individual basis. The results conclude that these individual independent variables possess significant explanatory power to predict the value of the dependent variable.

**5.3.3.2 Regression Model Performance Indices of June** The Pearson correlation coefficient for June is 0.975, which shows a strong and positive relationship between independent and dependent variables. The value of coefficient of determination $R^2 = 0.95$ highlights a very good fit of the regression line, which is further supported by Adjusted $R^2$ (Adj $R^2$) = 0.91. Sigma ($\sigma$) is another goodness of fit ($\sigma = 5.08$) as reported in the regression analysis to confirm the statistical authenticity and accuracy of the model. For better model, Sigma should be less than the standard error of the dependent variable ($\sigma >$ SE-Prep), which is true in the case of the current study. All the statistics that are reported above confirm that the PCR regression analysis for June is very good. F-statistics = 25.09 > 0.00 (F stat > F critical) suggest a significance relationship between the independent and dependent variable for the overall model performance. In other words,the high explanatory power of the independent variables is observed for the dependent variable on a collective basis. The t-test ($p < 0.05$) signifies the effect of each of the independent variables on an individual basis. The results conclude that these individual independent variables possess significant explanatory power to predict the value of the dependent variable.

### 5.3.4 PCR Results - Post Estimation Residual Analysis

Post Estimation Residual Analysis is carried out to prove the efficiency of the predicted model. Most reported post estimation tests are Auto correlation (AR) test, Auto Regressive Conditional Heteroskedasticity (ARCH)- test. These tests

are performed on the month of January and June. The statistics found are listed in tabular form below, followed by the illustration and conclusion drawn out of each test.

TABLE 5.4: Post Estimation Residual Analysis Table for January and June

| **Post Estimation Residual Tests** | **January** | **June** |
|---|---|---|
| Auto correlation (AR)test | 0.5502 | 0.0931 |
| Auto Regressive Conditional Heteroskedasticity (ARCH)test | 0.1921 | 1.7469 |

**Residual Analysis - January**

Auto correlation (AR) -test is 0.5502, as mentioned above in Table 5.4. The AR-test value is greater than the 5% significance level, i.e., 0.5502 greater than 0.05, which clearly indicates that the null hypothesis cannot be rejected. Statistically, the alternate hypothesis is rejected, and the null hypothesis is accepted. This means that the residuals are free from serial correlation, which is desirable and indicate good for estimation without any problem. Thereby estimated model is good and robust. ARCH test = 0.1921 greater 0.05, which means one cannot reject the null hypothesis (null is no heteroskedasticity in the residual) in other words, residuals are homoscedastic. Thereby estimated model equation is good.

**Residual Analysis - June**

AR test = 0.0931 greater than 0.05, which means one cannot reject the null hypothesis (null is no serial correlation in the residuals). In other words, residual are identical and independent. Thereby estimated model is good and accurate.
ARCH test = 1.7469 greater 0.05, which means one cannot reject the null hypothesis (null is no heteroskedasticity in the residual). In other words, residuals are homoscedastic. Thereby estimated model equation is accurate and powerful.

### 5.3.5 PCR Regression Equation

**January**

The regression equation for January by using Principal Component Regression is

found to have a coefficient of determination ($R^2$) = 0.8084 , which means that 80.84 % variablity in precipitation (dependent variable) is due to the independent variable mentioned in Table 5.5. The independent variables, along with their coefficients, t- stat and the p-value at 5% significant level are also listed in Table 5.5.

The p-value of all the predictors is less than 0.05, showing that **all the predictors (Atlantic Multi-decadal Oscillation (AMO), Equatorial Indian Ocean Zonal Wind Index (EQWIN), AIR TEMP850-PC3, GPH200-PC2, RHUM850-PC2, ZW200-PC3, ZW300-PC1, ZW500-PC2, VW500-PC1, SST-PC3) are highly significant at 5% significant level.** The t-stat is the ratio of the departure of the estimated value of the coefficient of a variable from its hypothesized value (which is zero) to its standard error and is used in hypothesis testing through student t-test.

The t-stat is compared against the critical value (2.026 in this case) based on significance value (=0.05) for a two-tailed distribution, degree of freedom (df=n-2=37) and is also used to determine p-value. The greater the departure,the higher will be the significance of that variable. The p-value is of all the predictors is less than 0.005 showing that all the predictors are highly significant at 5 % significant level.

For the **month of January, Equatorial Indian Ocean Zonal Wind Index (EQWIN), having t-stat value of 5.36 and Zonal Wind 500-PC2 with a value of -6.92, having the greatest departure, are the most significant variables**. The positive sign of the coefficient indicate that increase in the predictor will also increase the forecasting power of precipitation and the negative sign of the coefficient indicate vice versa.

TABLE 5.5: Residual Output for January

| | **Coefficients** | **Standard Error** | **t-stat** | **p-value** |
|---|---|---|---|---|
| Intercept | 24.9924 | 2.51 | 9.93 | 0.0000 |
| AMO | -34.0050 | 10.19 | -3.34 | 0.0024 |
| **EQWIN** | 10.0491 | 1.87 | **5.36** | 0.0000 |
| AIR-TEMP850-PC3 | -0.4621 | 0.13 | -3.44 | 0.0018 |
| GPH200-PC2 | 0.5556 | 0.24 | 2.29 | 0.0008 |
| RHUM850-PC2 | 0.6958 | 0.17 | 4.09 | 0.0003 |
| ZW200-PC3 | 0.5358 | 0.17 | 3.01 | 0.0000 |
| ZW300-PC1 | -1.6328 | 0.28 | -5.03 | 0.0000 |
| **ZW500-PC2** | -1.3774 | -0.19 | **-6.92** | 0.0000 |
| VW500-PC1 | 1.3816 | 0.27 | 5.04 | 0.0000 |
| SST-PC3 | 0.1969 | 0.09 | 2.15 | 0.0400 |

Estimated-Precipitation =Precp Jan =24.9924 - 34.0050*AMO + **10.0491*EQWIN** - 0.4621*AIR-TEMP850-PC3 + 0.5556*GPH200-PC2 + 0.6958*RHUM850-PC2+ 0.5358*ZW200-PC3 - 1.6328*ZW300-PC1 - **1.3774*ZW500-PC2** + 1.3816*VW500-PC1 + 0.1969*SST-PC3

**June**

The Regression equation for June using PCR is found to have $R^2 = 0.9531$, which means 95.31% variablity in precipitation (dependent variable) is due to the independent variable mentioned in Table 5.6. The independent variable, along with their coefficients, t-stat and the p-value at 5% significant level, are also listed in Table 5.6. The t-stat is the ratio of the departure of the estimated value of the coefficient of a variable from its hypothesized value (which is zero) to its standard error. It is used in hypothesis testing through student t-test. The t-stat is compared against the critical value (2.026 in this case) based on significance value (=0.05) for a two-tailed distribution, degree of freedom (df=n-2=37). It

is also used to determine p-value. The greater the departure, the higher will be the significance of that variable. The p-value is of all the predictors is less than 0.005 showing that all the predictors are highly significant at 5% significant level. For the **month of June, EQWIN (11.10) and RHUM300-PC4 (-11.20), having the greatest departure, are the most significant variables**. The positive sign of the co-efficient indicates that an increase in the predictor will also increase the forecasting power of precipitation and vice versa.

Table 5.6: Residual Output for June

| | **Coefficients** | **Standard Error** | **t-stat** | **p-value** |
|---|---|---|---|---|
| Intercept | 31.8157 | 2.3090 | 13.80 | 0.000 |
| ENSO-MEI | 16.5124 | 1.6580 | 9.96 | 0.000 |
| **EQWIN** | 9.8601 | 0.8891 | **11.10** | 0.000 |
| Air-Temp850-PC3 | 0.4434 | 0.106 | 4.18 | 0.000 |
| Air-Temp850-PC4 | -0.3181 | 0.106 | -3.13 | 0.005 |
| GPH200-PC2 | 0.5371 | 0.0923 | 5.82 | 0.000 |
| GPH300-PC3 | -0.2722 | 0.1161 | -2.34 | 0.029 |
| RHUM300-PC1 | 0.9695 | 0.1327 | 7.30 | 0.000 |
| RHUM300-PC3 | 0.5570 | 0.1001 | 5.57 | 0.000 |
| **RHUM300-PC4** | -1.6136 | 0.1443 | **-11.20** | 0.000 |
| ZW300-PC1 | -0.9800 | 0.1565 | -6.26 | 0.027 |
| ZW300-PC2 | 0.4471 | 0.0935 | 4.78 | 0.00 |
| ZW300-PC4 | -0.8064 | 0.1148 | -7.02 | 0.000 |
| VWIND300-PC4 | -0.2263 | 0.0807 | -2.81 | 0.010 |
| OLR-PC4 | -1.1898 | 0.5801 | -2.05 | 0.052 |
| ZW-SUR-PC4 | -0.3171 | 0.0900 | -3.52 | 0.002 |
| MW-SUR-PC4 | 0.7734 | 0.0951 | 8.13 | 0.000 |
| GPH500-PC2 | 0.2317 | 0.0746 | 3.11 | 0.005 |

Estimated Precipitation = Precp June = + 31.82 + 16.51*ENSO-MEI + **9.86* EQWIN** + 0.4434*Air-Temp850-PC3 - 0.3181*Air-Temp850-PC4 + 0.5371*GPH 200-PC2 - 0.2722*GPH300-PC3 + 0.9695*RHUM300-PC1 + 0.557*RHUM300-PC3 - **1.614*RHUM300-PC4** - 0.98*ZW300-PC1 + 0.4471*ZW300-PC2 - 0.8064* ZW300-PC4 - 0.2263*VWIND300-PC4 - 1.19*OLR-PC4 - 0.3171*ZW-SUR-PC4 + 0.7734*MW-SUR-PC4 + 0.2317*GPH500-PC2

### 5.3.6 Model Evaluation Statistics (Loss Error)

The predictability of the model is assessed by **Root Mean Squared Error (RMSE), Mean Absolute Error (MAE), Nash-Sutcliffe Efficiency (NSE), Percent Bias (PBIAS) and RMSE-observations Standard deviation Ratio (RSR)** [210, 212, 329, 330]. The PCR model is prepared by using the data in the training period from 1977 to 2015 and the values of predicted precipitation are obtained from the PC regression equation in the training period. RMSE and MAE are then calculated to check the performance of the PCR model. The PCR model is further used for validation of the period from 2016 to 2020. The values of RMSE and MAE are then again calculated for the validation period (2016-2020) to check the predictive performance of the model.

The model performance for both January and June months from (1977-2020) is also evaluated by reporting loss error, namely NSE, PBIAS and RSR. As explained in chapter 4, Nash-Sutcliffe Efficiency (NSE) is a normalized statistic that determines the relative magnitude of the residual variance with respect compared to the measured data variance. NSE show how well the plot of observed versus estimated data fits the 1:1 line. NSE between 0.0 to 1.0 is generally viewed as acceptable levels of performance. Percent Bias (PBIAS) measure the average tendency of the stimulated data to be larger or smaller than their observed counterpart. The optimal value of PBIAS is 0.0. The lower the magnitude value, of PBIAS the accurate the model. A positive value shows model underestimation bias and negative values indicate model overestimation bias [331]. RSR is calculated as the ratio of the RMSE and standard deviation of measured data. The lower the RSR and RMSE, the better the model Prediction [330].

These statistics are calculated and listed in Table 5.7. All the statistics, namely NSE, PBIAS (except which is converted in percentage for better interpretation) and RSR, are between 0.0 to 1.0 as recommended for a very good model [329-331]. Therefore, the developed model is **very good with strong and accurate prediction power** Comparison of RMSE and MAE for the training period and

validating period are reported as loss error in Table 5.7. Also, NSE, PBIAS and RSR for January and June (1977-2020) are reported as loss errors in Table 5.7.

TABLE 5.7: Loss Error for the Month January and June

| **Loss Error for training period (1977-2015)** | **January** | **June** |
|---|---|---|
| Root Mean Square Error (RMSE) | 7.99 | 3.79 |
| Mean Absolute Error (MAE) | 6.48 | 3.03 |
| **Loss Error for validation period (2016-2020)** | **January** | **June** |
| Root Mean Square Error (RMSE) | 26.95 | 14.44 |
| Mean Absolute Error (MAE) | 15.08 | 13.02 |
| **Loss Error for Entire study period (1977-2020)** | **January** | **June** |
| Nash-Sutcliffe Efficiency (NSE) | 0.6681 | 0.8751 |
| Percent Bias (PBAIS) | 5.47 | -3.79 |
| RMSE Standard-deviation Ratio (RSR) | 0.4077 | 0.2198 |

The graph and histogram between the observed values and estimated/predicted values, both for the training and validating period are shown in Figures 5.5 and 5.6 (for the month of January), respectively. Similarly, graphs and histograms between the observed values and estimated/predicted values both for the training and validating period are shown in Figures 5.7 and 5.8 (for the months of June), respectively. The values of Root Mean Squared Error (RMSE) and Mean Absolute Error (MAE) for the training period and validating period are more or less the same for the months of January and June, which shows the predictability of a good model [326-328].

**The calculation for Root Mean Squared Error, Mean Absolute Error, Nash-Sutcliffe Efficiency, Percent Bias and RMSE Standard-deviation Ratio for January and June is attached in Annexure-B (B.3, B.4, B.7 & B.8)**.

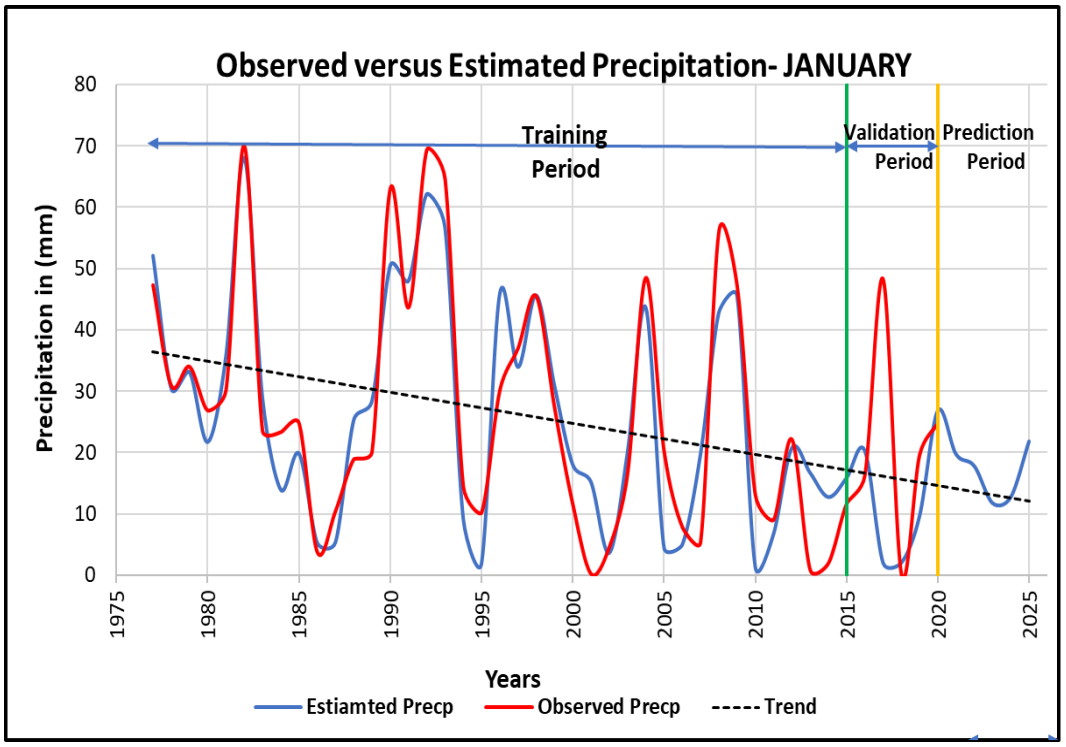


FIGURE 5.5: Observed versus Estimated Precipitation- JANUARY

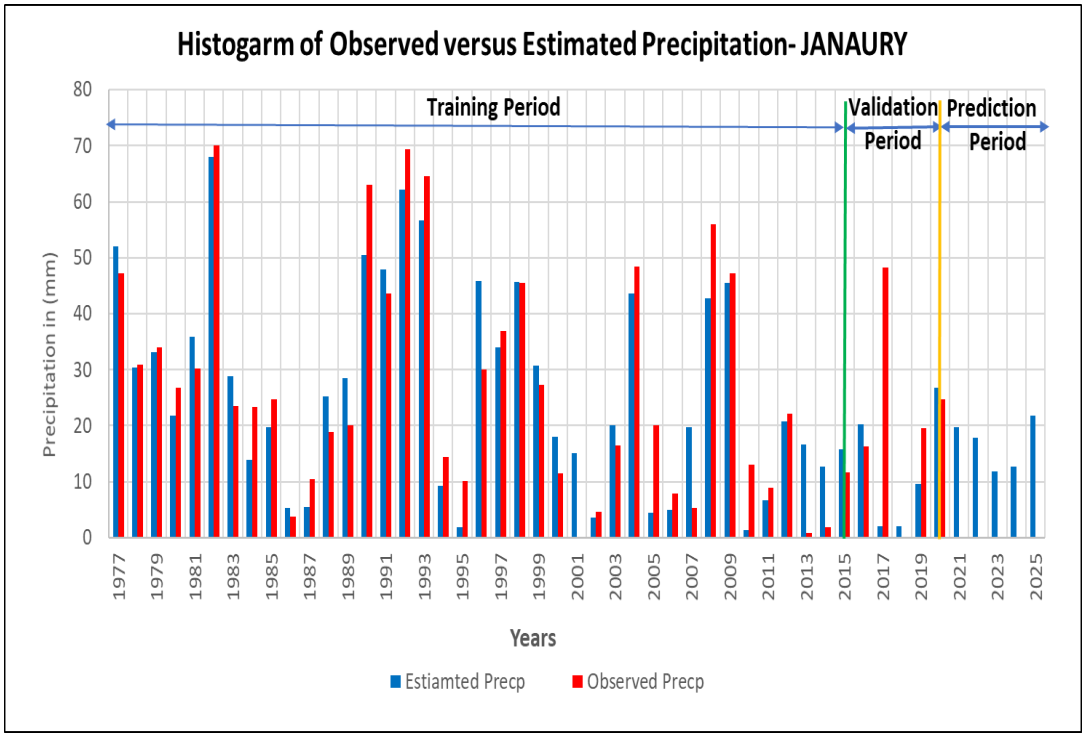


FIGURE 5.6: Histogram of Observed versus Estimated Precipitation- JANUARY

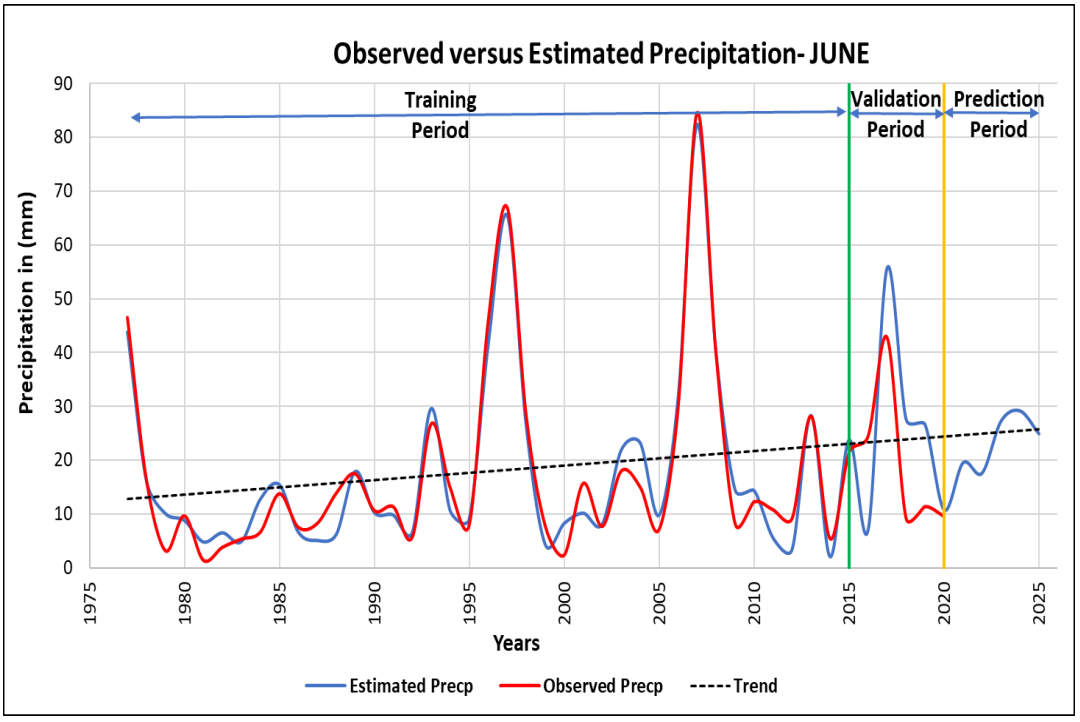


FIGURE 5.7: Observed versus Estimated Precipitation- JUNE

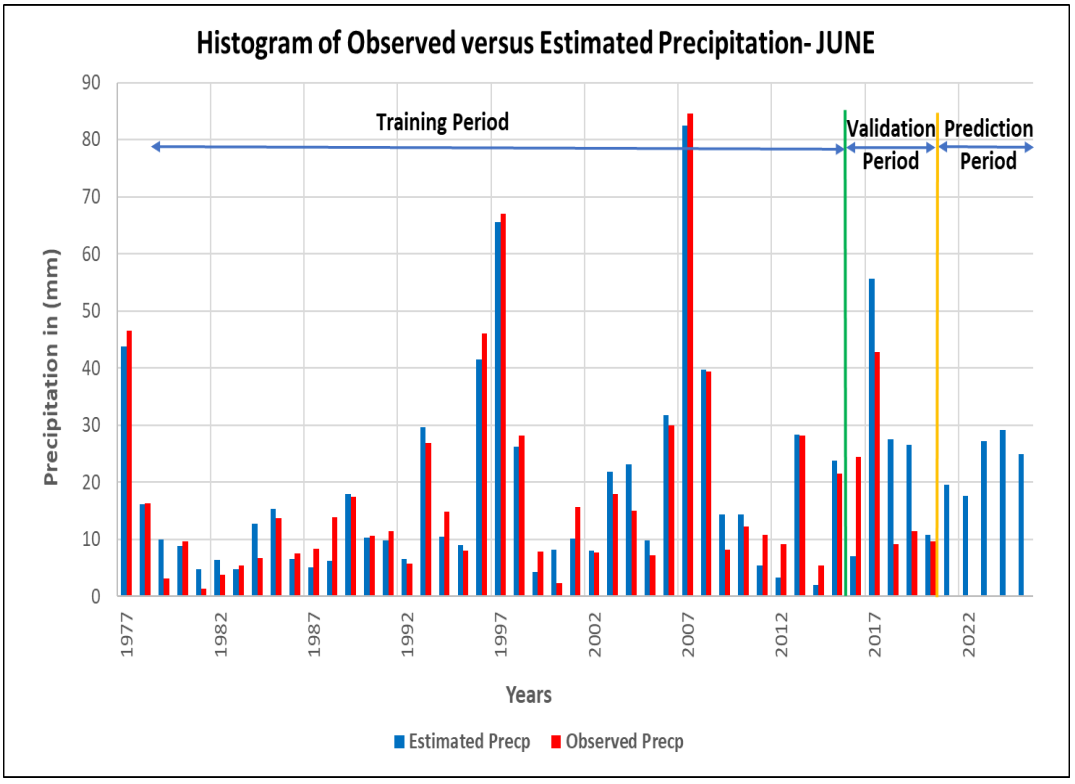


FIGURE 5.8: Histogram of Observed versus Estimated Precipitation- JUNE

### 5.3.7 Comparison of MLR and PCR Modeling Technique

The comparison of performance indices for both PCR and MLR are listed in Table 5.8. The performance indices show that PCR performs better than the MLR [210, 212]. The Pearson correlation coefficient (R) in PCR for January and June are better (0.8991 and 0.9750) as compared to (0.8301 and 0.8291) in MLR. Similarly, coefficient of determination and Adjusted R also have better values as compared to the MLR model. Standard errors in PCR are less as compared to MLR. The loss error (RMSE and MAE) of January model in PCR is not very good. It may be due to recurring droughts [57, 143]. Adnan et al. [212] also compared MLR and PCR models in their climate research over Pakistan. The study was foscused on predicting summer rainfall in Pakistan from Global Sea Surface Temperature and Sea Level Pressure.The study concludes that PCR model was better than MLR model.

Table 5.8: Comparison of PCR and MLR Technique

| | | **Modeling Using PCR technique** | | **Modeling Using MLR technique** | |
|---|---|---|---|---|---|
| **S.no** | **Description** | **January** | **June** | **January** | **June** |
| 1 | Pearson Correlation Coefficient (R) | 0.8991 | 0.9750 | 0.8301 | 0.8291 |
| 2 | Coefficient of Determination ($R^2$) | 0.8084 | 0.9506 | 0.6890 | 0.6873 |
| 3 | Adjusted R Square | 0.7399 | 0.9354 | 0.5419 | 0.6040 |
| 4 | Standard Error | 11.04 | 5.028 | 20.01 | 17.75 |
| 5 | Overall F test | 11.81 | 25.04 | 9.63 | 8.24 |
| 6 | Auto correlation (AR) Test | 0.5502 | 0.0939 | 0.0005 | 0.0786 |
| 7 | Auto Regressive Conditional Heteroskedasticity (ARCH) | 0.1921 | 1.7467 | 0.0786 | 0.5335 |

## 5.4 Significance/Application of the Finding

The model will give basic information to local inhabitants, provincial government, administration, National Disaster Management Authority (NDMA), Provincial Disaster Management Authority (PDMA) and Pakistan Metrological Department (PMD) to issue early flash flood warnings, take proactive measures in June due to unprecedented precipitation and dryness or drought alert in January due to less rain. This information can be helpful in planning crops or go for re-cropping (dual cropping), ridge farming, and re-sowing technique. As 90% of the grasslands, shrubs and bushes in Baluchistan are rain-fed. The livestock mostly depend on these grasslands. A decrease in rainfall in the month of January will have a direct impact on this grassland and on the livestock. The model will help them to look for an alternative or plan accordingly by storing food for the livestock, which is the second most common occupation of local dwellers. The livestock contributes 20% of the provincial Gross Domestic Product (GDP). The model output information will not only be helpful for the livestock business but to other related industries like leather, carpet, and pharmaceutical that are the leading consumer of livestock products. Baluchistan also fulfills the need and demand for leather tannery and carpet industries in Pakistan by providing a good and constant supply of hiding, skin, and wool.

### 5.4.1 Comparative analysis with previous work

The findings and results using Principal Component Regression (PCR) analysis are **in line with the previous studies performed by Adnan et al. [210, 212] that PCR technique is better than MLR technique due to its statistical results and robust prediction power**. Adnan et al. [212] selected two predictors, namely Sea Level Pressure (SLP) and Sea Surface Temperature (SST), to perform monsoon rainfall forecast with both Multiple Linear Regression (MLR) and Principal Component Regression (PCR) technique over Pakistan and

recommended PCR technique because of its superior results and strong predicting power.

## 5.5 Summary

The precipitation equation for January using the PCR Technique is as follows:

Estimated-Precipitation January =24.9924 - 34.0050*AMO + 10.0491*EQWIN - 0.4621*AIR-TEMP850-PC3 + 0.5556*GPH200-PC2 + 0.6958*RHUM850-PC2 + 0.5358*ZW200-PC3 - 1.6328*ZW300-PC1 - 1.3774*ZW500-PC2 + 1.3816*VWIND 500-PC1 + 0.1969*SST-PC3
with $R^2 = 0.8084$ means 80.84% variation in precipitation is due to the potential determinant mentioned in the equation.

Precipitation Equation for the month of June using PCR Technique is as follows:

Estimated-Precipitation June = + 31.82 + 16.51*ENSO-MEI + 9.86*EQWIN+ 0.4434*Air-Temp850-PC3 - 0.3181*Air-Temp850-PC4 + 0.5371*GPH200-PC2 - 0.2722*GPH300-PC3 + 0.9695*RHUM300-PC1 + 0.5570*RHUM300-PC3 - 1.614 RHUM300-PC4 - 0.9801*ZW300-PC1 + 0.4471*ZW300-PC2 - 0.8064*ZW300-PC4-0.2263*VWIND300-PC4 - 1.19*OLR-PC4 - 0.3171*ZW-SUR-PC4 + 0.7734 MW-SUR-PC4 + 0.2317*GPH500-PC2
with $R^2 = 0.9531$ means 95.31% variation in precipitation is due to the potential determinant mentioned in the equation.

Precipitation is a complex phenomenon and depends on numerous predicdant variables. In PCR analysis, there are 61 independent variables (including the constant term) depending on SST, SLP, ZW-Surface, GPH, RH at different levels are chosen. These variables possibly form total 5.07x10E83 combinations (61! factorial) for the regression equation. Out of the enormous variable data set, regression analysis is carried out by using selected principal component (PCs) instead of an enormous number of original variables and this is the most important feature of PCR technique. The PCR technique is come out with an excellent model having

the goodness of fit ($R^2$) 80.84% and 95.31% for January and June, respectively. Analysis, that is performed in the chapter adopting PCR techniques, concludes that EQWIN and ZWIND500-PC2 (January) and EQWIN and RHUM300-PC4 (June) are the most significant predictor in defining precipitation variability in Baluchistan. Post estimation residual analyses AR, ARCH (0.5502, 0.1921) for January and AR, ARCH (0.0931, 1.7469) for June is performed to check the validity of all estimated equations. Successfully being independent and identically distributed (i, i, d), the residuals guarantee the validity and robustness of estimated models for both months.

Root Mean Square Error (RMSE) and Mean Absolute Error (MAE)for the training period (1977-2015) for both January and June are found to be 7.99, 6.48, 3.79 and 3.03, respectively. Also, Root Mean Square Error (RMSE) and Mean Absolute Error (MAE) for the training period (2016-2020) for both January and June are found to be 26.9, 15.08, 14.44 and 13.02, respectively, which shows that model has good forecasting power. The NSE (0.6681), PBIAS (5.47%) and RSR (0.4077) for **January** show that the model is **very good** with accurate and strong predicting potential.

The NSE (0.87), PBIAS (-3.79%) and RSR (0.21) for **June**. Negative PBIAS indicate that the model is overestimating and positive PBIAS indicates that model is underestimating [334]. Overall, statistics show that it is a **very good** model with accurate and strong predicting potential. All the statistics, namely NSE, PBIAS (except which is expressed in percentage for better interpretation) and RSR, are between 0.0 to 1.0 as recommended for a **very good** model [329, 330]. The model that is developed by using the PCR technique has the goodness of fit ($R^2$) 80.84% and 95.31% for January and June, respectively.

# Chapter 6

# Conclusion and Future Work

## 6.1 Conclusions

### 6.1.1 Influence of Potential Determinants on Precipitation

Baluchistan receives its greater portion of the rainfall in the winter and spring months. The time series of precipitation data over the period of 1977 to 2017 is analyzed for 13 different stations in Baluchistan. Decreasing trends in precipitation are observed in the months of January in Region 1, whereas slight increasing trends are observed in June. Region 1 comprises stations located in Barakhan, Kalat, Khuzdar, Quetta and Zhob. The other regions of Baluchistan do not depict any trends and remain indifferent. The monthly trends in precipitation are detected through Mann-Kendall test.

The study confirms that Baluchistan is receiving lesser rainfall for the past few decades. The precipitation is influenced by large-scale circulations. The atmospheric variables which describe the large-scale circulations and climatic indices are the potential determinants. These variables are responsible for variation in precipitation. Partial Mann-Kendall (PMK), Empirical Orthogonal Functions analysis, Principal Component Analysis and correlation analysis are used to determine the potential determinants of precipitation variability. The change in trends under the

influence of climatic indices is determined through PMK for January and June in Region 1. It is determined through PMK analysis that EQWIN, ENSO-MEI and EMI-MODOKI show moderate to strong influence on precipitation for January, June and thus are the potential determinants.

The correlation of Principal Components of Region 1 Precipitation (PCs) and climate indices show that NAO, AMO, EQWIN, EMI-MODOKI and PDO influencing the precipitation in January and explain the maximum variability of the precipitation in January. EQWIN, EMI-MODOKI and AMO are positively correlated with the principal modes of January precipitation up to 8% significance, whereas PDO and NAO are negatively correlated with the January precipitation but are insignificant. NAO, AMO, EQWIN, ENSO-MEI and PDO are found to be influencing the June precipitation as determined through correlation analysis between PCs and climate indices. AMO may be considered as positively correlated, whereas NAO and ENSO-MEI may be considered as negatively correlated, but their strengths are insignificant to weak. PDO is negatively correlated to the principal modes of Region 1 precipitation at 5% significance which means that the negative phase of PDO is favourable for June precipitation, whereas EQWIN is positively correlated with June precipitation at 1% significance, which means that the positive phase is favourable for June precipitation.

The influencing climatic indices for January and June over the Region 1 of Baluchistan, as identified through PMK, EOF maps, PCA analysis and correlation analysis, are associated with precipitation variability and thus can be used as the possible predictors of precipitation. This study addresses three SDGs, namely SDG# 11: Sustainable Cities and Communities and SDG# 13: Climate Action.

### 6.1.2 SGD 11: Sustainable Cities and Communities

Baluchistan province mainly comprises of rugged terrains, hills, mountains, upper and lower highlands, making it more susceptible to devastating flash floods due to unprecedented torrential rains. Flash floods are proven to be more devasting

and catastrophic in nature. At the same time, the study area has gone through recurring droughts in the past few decades. The consecutive five years of drought (1998-2002) is one of the worst droughts in past the 50 years of history. The outcome of the research is in the form of two statistical precipitation models. The models will be helpful in giving early information about variation in precipitation. The extreme of which leads to flood and scarcity leads to drought in the area. This research will be useful for all stakeholders of the region in one way or another. For policymakers, it will render the latest insight about variations in precipitation trends rather than working on outdated information, thus, leading to better, resilient measures and action plan at the policy level.
Furthermore, provincial metrological department and disaster management authorities can prepare preventive, proactive plans accordingly. Also, local farmers, cultivators, agriculturalists and related industries can adopt the changing precipitation patterns, particularly in January and June. Plan the crops to gain benefit rather than blindly carrying on primitive agricultural practices. Re-cropping (also known as double cropping), resowing and mulching can be adopted by locals. Lastly, but most importantly, is this study can save precious lives and properties from drowning and washed away in flash floods. As flash floods are taken by surprise and are proven to be more catastrophic and devastating in nature. Hence, the research contributes to SDG-11 on multiple levels to create sustainable cities and communities.

### 6.1.3 SDG 13: Climate Action

The Global Climate Risk Index (GCRI) has placed Pakistan on the fifth position both in the long-term index and in the current year index, as among the most vulnerable country to climate change. Most alarmingly, Pakistan's vulnerability to climate change is increasing day by day also. This is because of Pakistan's geographical location, complex topography, dynamic climatology, and low coping capacity. It is of great importance for the study area to reduce disaster risk and achieve sustainable trade through Gwadar Port and CPEC. This can only be

possible if proper action is taken on time. This study is coherent with numerous other studies, and clearly indicates that there is an increase in precipitation trend in June, leading to extreme downpours and causing flash floods. Simultaneously, there is a decrease in precipitation trend in January that will effect crops and associated livelihood. The model will give rudimentary intimation and awareness about the trend and variation in precipitation pattern which can be used as a steer in adopting mitigation and adaptation techniques due to changing pattern by early warnings, weather alerts, cautionary notes, inkling of a flash flood, riverine flood landslides, mudslides other disasters including hydro-meteorological and geological hazards.

### 6.1.4 Modeling using Multi-Linear Regression Analysis (MLR)

The association of climatic indices and their influence on precipitation variability is determined using EOF, PCA and correlation analyses. The strength of association is then determined through the contemporary technique of Multi-Linear Regression Analysis. It is found that January and June are the only two months that show the significant trends and thus are considered for the development of the regression model. The regression equation of precipitation for January and June are formulated using MLR. The coefficient of determination of January and June are 68.09% and 68.73% respectively. The models are reasonably good as indicated by the $R^2 = 0.6890$ for January and $R^2 = 0.6873$ for June, which indicates that 68.90% and 68.73% variation in precipitation can be estimated by explanatory variables, respectively. NAO, AO, RH500, VWind surface and EQWIN are identified as the potential determinants for January. NAO and AO are found to be highly significant predictors with a p-value of 0.0005 and 0.0013, respectively, whereas EQWIN has a weak influence on the precipitation. EQWIN, AO, EMI-MODOKI, along with RH850, GPH850, UWind300, VWind300 and Airtemp200, are identified as the potential determinants of the precipitation variability for June. EQWIN came out to be a highly significant predictor having a p-value of less than

0.05 for a confidence level of 5%. The model shows that AO has strong and EMI-MODOKI has a weak influence on precipitation. The direction and strength of the association (influence) is provided by the coefficient of regressors. The RMSE, MAE, NES, PBIAS, RSR values also show that the prediction performance of the model is **VERY GOOD** for both January and June.

### 6.1.5 Modeling using Principal Component Regression Analysis (PCR)

Precipitation is a complex phenomenon and depends on a number of predicting variables. It is pretty common that these variables have multilinear collinearity among themselves. This problem is overcome using principal component analysis. The principal components are orthogonal to each other and do not have multicollinearity. Principal Component Regression eliminates the problem of multicollinearity among the variable themselves while doing the regression analysis. In this study, 61 independent variables (including the constant term) are considered for determining the prediction model for the precipitation to find out the potential determinants. These variables are dependent on SST, SLP, ZW-Surface, GPH, RH and Air Temperature at different levels. The Principal Component Regression (PCR) analysis is carried out by using selected principal component (four PCs) instead of an enormous number of original variables. The PCR technique yields a model with excellent goodness of fit of 80.84%, 95.31% for January and June, respectively. Post estimation residual analyses AR and ARCH tests for the month of January and June are performed to check the validity of the estimated regression equation, which also validate the results and confirm that the residuals are independent and identically distributed. Mean Absolute Error (MAE) and Root Mean Square Error (RMSE), Nash-Sutcliffe Efficiency (NSE), Percent Bias (PBIAS) and RMSE-observations Standard deviation Ratio (RSR) for both the months of January and June, show that the models has **very good** forecasting power.

It is concluded that AMO, EQWIN, along with AIR-TEMP850, SST, GPH200, RHUM850, UWIND200, UWIND300, UWIND500 and VWIND500 are identified as potential determinants for January, whereas ENSO-MEI, EQWIN along with Air-Temp850, GPH200, GPH500, GPH300, RHUM300, UWIND300, VWIND300, OLR, ZW-SUR and MW-SUR are identified as potential determinants for June. PCR analysis also concludes that, for January, EQWIN (t-stat 5.36) and ZW500-PC2 (t-stat -6.92) (having the greatest departure) are the most significant variables. Similarly, for June, EQWIN (t-stat 11.10) and RHUM300-PC4 (t-stat -11.20) (having the greatest departure) are the most significant variables.

### 6.1.6 Comparison of Modeling with MLR and PCR

The performance indices of regression show that **PCR performs better than MLR**. This is in line with previous studies conducted. Therefore, the PCR technique is recommended for modeling and forecasting to determine the variability of precipitation in Baluchistan under the influence of climatic indices and climate variables.

## 6.2 Trends and Potential Determinants

This study concludes that there is a decreasing trend of precipitation in the month of January and the slope of the trend is steep. Similarly, there is an increasing trend in June and the slope of the trend is mild. Since Baluchistan receives most of its rainfall in winter therefore, the decreasing trend is indicative of the water scarcity situation in Baluchistan, which may or may not be alleviated by an increasing trend in June having relatively lesser precipitation. This may be an **early warning to the authorities to take remedial measures preemptively to mitigate the drought situation if any**. It is concluded through PMK analysis, correlation analysis, EOF analysis, PCA analysis, MLR and PCR modeling that the climatic indices **EQWIN, ENSO-MEI and EMI-MODOKI along with**

**climate variables GPH, RH, UWIND and VWIND are the potential determinants causing the variability in the precipitation in Baluchistan which is the novelty of this study. These potential determinants may be used by the meteorologist in the weather prediction models for accurate forecasting**.

According to a WHO report in 2019, an unexpected spell of heavy rainfall in Lasbella district caused extreme flashflood on 20 th February 2019. This flood was unexpected and hit five districts just to share the catastrophe of Turbat district as an example. There were 150,000 affected people, 250-300 displaced, and 15 health facilities got damaged. Similarly, according to Dawn News (August 2020), torrential rain spell drown at least four people, many others were injured and over a dozen others went missing in different parts of the Baluchistan, due to torrential rains that lashed 22 districts of the province, caused flooding and damaged bridges and highways, cutting off Gwadar and some other areas with Quetta and rest of the country. Heavy flooding also damaged the main gas pipeline passing through the Bolan. History of the Baluchistan is filled with catastrophes of such flash floods and no concrete solution and policy have been developed yet. Such negligence may put CPEC and international trade at risk.

This precipitation model will be a **novel baseline model to implement for more accurate precipitation prediction**. The local government, provincial government, administration, and disaster management authority are planning, preparing, and working for disaster risk reduction at all levels. Global German watch, reporting agency (report 2020) clearly point out the lack of action taken to combat climate change risks. This research work has investigated the various potential determinants and their influences on precipitation patterns in the context of climate indices as well. Many more similar studies are the dire need of the situation as IPCC's reports has raised the alarm that further extreme precipitation events are projected to continue in future with even more intensity, frequency and impacts. This study can create awareness among local people regarding climate changes and will help to take proactive measures to be prepared and safe.

This prediction model will help the Pakistan Metrological Department (PMD) in alliance with National Disaster Management Authority (NDMA) to issue early flash flood warnings, travel alerts. This early warning will not only save crops, orchards, livestock, property, human lives but will also help to make the international and national trade route, highways safe from climate catastrophes like a landslide, mudslide. Since most of the CPEC (Eastern, Western and central route) passes through Baluchistan. Not to forget, the OBOR trade route is also under construction. Therefore, the model will be helpful by providing flash flood intimation due to unprecedented torrential rainfall and making national and international trade routes safe. This study can also be used as a baseline study to examine the impact of the anthropogenic activity on the precipitation pattern.

## 6.3 Impact on Policy Guidelines for Agriculture livestock and livelihood

Baluchistan province has enormous potential to emerge as a new vibrant economic center not only for Pakistan but also for Asia. The province is spread on 347,190 $Km^2$ with 77O km long most productive coastal belt along the Arabian Sea. The province has a bright future in **agriculture, farming, crop cultivation, livestock, fisheries, tourism, sea sport, gas coal, mineral treasure like copper, fluorite, gypsum gems and precious stones.** Baluchistan main industry is agriculture and farming. It is a well-established fact that precipitation plays a vital role in controlling a country's agriculture productivity. With 75% rural population in Baluchistan, about 68% are engaged in agriculture (i.e., 40 percent of Pakistan's total labour force). Unfortunately, out of which **81% of framers complain about the water scarcity in Baluchistan province. The present study and precipitation prediction model will be of great help to solve the problem of water scarcity by taking preventive measures to cope and combat the variations of precipitation trends**. The model will also be helpful to design a rainfed irrigation system, water resources

and reservoirs. The statistical model in this study points out decreasing precipitation trend in January (winter), which is also in line with previous studies. **It will also help crops planners to plan less water demanding crops, plan crop early, or use the month of January for mulching, ridge farming, relay cropping, and re- sowing. Rely on cropping (also known as double cropping) not only help farmers to increase their production, but it also helps in reducing Nitrogen leaching, increase carbon sequestration (i.e. removal of carbon dioxide from the atmosphere to slow or reverse atmospheric pollution and mitigate and reverse global warming)**. Since most of the farmers are not well-educated thus,the food and agriculture department should educate them to adopt new cropping techniques, get accustomed to changing precipitation patterns and get the maximum benefit from it.

Unprecedented torrential rainfall in rugged terrain of Baluchistan causes devastating flash flood loss and damage to agriculture, livestock and above all, loss of precious human life every year. According to the news report, the damages due to flooding in 2019 were close to 350 Million Rupees. **The increasing precipitation trend in June might cause flash floods in region stations like Barakhan, Kalat, Quetta, Khuzdar and Zhob. This prediction model will help National Disaster Management Authority (NDMA), Provincial Disaster Management Authority (PDMA) and Pakistan Metrological Department (PMD)** to issue early flash flood warnings. This early warning will not only save crops, orchards, livestock, property but will also save valuable human lives. **Therefore, the model will help policy makers to create proactive policy and educate local inhabitants accordingly. Due to the non-availability of basic data in the past, the policymakers and stakeholders could not effectively prepare a plan and infrastructure for the target region/area that are vulnerable to floods, landslide and mudslide, droughts and dryness**.

The tough weather, dry spell, recurring droughts of Baluchistan has adversely affected and reduced the cultivation, leaving most of the area to be used for rainfed

rangeland, grassland, shrubland for grazing of cattle. **These rangelands are responsible to fulfill about 90% of the food requirement for the livestock and cattle farm animals. Any variation in precipitation will directly affect the livestock and livelihood of this region. A good accurate precipitation model, like the one developed in the current study, will surely help and educate people to store food for grazing of cattle to maintain good and sustainable livelihood through good and sustainable livestock**. Baluchistan livestock contributes 20% to the provincial GDP and the provincial share in the country's total livestock population is about 40%. Moreover, leather, carpet and pharmaceutical industry are the main consumers of livestock products other than the consumption of meat by the general public. **The province caters to the needs and demands of the leather and carpet industries in Pakistan by sustaining the supply of hide, skins and wool to these sectors. Thus, a sustainable supply of livestock products is significant for the provincial and national economies**.

## 6.4 Comparative Analysis with Previous Studies

**Trend analysis** Naz et al. [57], Jamro et al. [58], Ahmed et al. [146], Hina et al. [149], Aamir et al. [138], Haroon et al. [150], Haider et al. [151], Bhatti et al. [197], Ashraf et al. [140] have reported increasing trend and dominating decreasing trend in Baluchistan. These findings are in perfect match with the result trend detection carried out in the study, in which an increasing trend by using Mann-Kendall was detected in June and a decreasing trend was found in January in Region 1 of Baluchistan. Numerous studies have reported in their conclusion that climatic indices, namely Pacific Decadal Oscillation (PDO), North Atlantic Oscillation (NAO), Atlantic Multidecadal Oscillation (AMO), El Nino Southern Oscillation (ENSO) and Indian Ocean Dipole (IOD) have significant inflence on precipitation of Pakistan. Iqbal and Athar [216] reported that AO, IOD, ENSO, NAO and PDO show a strong correlation with the monthly precipitation with Baluchistan, which confirms the finding of this study as well.

**Multi Linear Regression (MLR) Analysis** is one of the most commonly used techniques in climate for precipitation modeling. Kalra et al. [174, 195], Carrier et al. [193] used MLR for precipitation modeling. Kalra et al. [174] reported that oceanic-atmospheric oscillations significantly influence the precipitation pattern. The finding endorsed the result of our research in which oceanic-atmospheric oscillations indices are found to be the potential determinants causing variability in the precipitation pattern. The study also shows that indices in groups like Pacific Decadal Oscillation (PDO), North Atlantic Oscillation (NAO), Atlantic Multidecadal Oscillation (AMO), El Nino-Southern Oscillation (ENSO) are best for precipitation predictions in the Lower Colorado River Basin. This conclusion endorsed current research results too, which state that NAO, AO, EQWIN, EMI-MODOKI are the strong significant predictors for precipitation variation in Region 1 of Baluchistan. Another research performed by Carrier et al. [193] stated that oceanic-atmospheric oscillations including the El Nino-Southern Oscillation (ENSO), Pacific Decadal Oscillation (PDO), Atlantic Multidecadal (AMO), and North Atlantic Oscillation (NAO) influence the precipitation pattern and these indices also remarkably improved the precipitation predictability when useing as predictor in MLR modeling. The findings of Carrier et al. [193] are both illustrative and statistical in nature and fully support the result of this current study, which describes that NAO, AO, EQWIN are the potential determinants for the precipitation in January and EQWIN, EMI-MODOKI AO, are the potential determinants for the precipitation in June.

Principal Component Regression (PCR) Analysis Adnan et al. [212] performed monsoon rains forecast using both Multiple Linear Regression (MLR) and Principal Component Regression (PCR) methods, with two predictors Sea Level Pressure (SLP) and Sea Surface Temperature (SST). The study also compared the model performances based on statistical measures such as Root Mean Square Error (RMSE), Mean Absolute Error (MAE), bias and the Correlation Coefficient. This study also reported that PCR model is slightly better than that of the MLR model. Adnan et al. [212] results confirm and strengthen the finding of this research also which is based on the same modeling techniques (MLR and PCR), but

with different climate indices and climate parameters. In the end the present study compares the model on the basis of performance indices and found that the PCR is the better technique as compared to MLR as stated, in Adnan et al. [212]. In another research, Adnan et al. [210] studied the inter- and intra-annual variability of the monsoonal precipitation over Pakistan. The study focuses on the monsoon precipitation predictability using potential factors in linear statistical forecast model, principal component regression (PCR) analysis. The result reported through statistical measures such as mean BIAS, Mean Absolute Error (MAE), Root Mean Square Error (RMSE) and correlation coefficient (R) are around 14.92, 42.23, 60.65 and 0.75, respectively, suggested that the model exhibit robust predicting skills. The result in the above study validates the findings of the current research study, too, in which oceanic-atmospheric indices are used as potential determinants and prediction is carried out for five years using (PCR) analysis. The results of PCR analysis were reported through statistical measures, namely Mean Absolute Error (MAE), Root Mean Square Error (RMSE), Nash-Sutcliffe Efficiency (NSE), Percent Bias (PBIAS) and RMSE-observations Standard deviation Ratio (RSR). All statistical measures show the model has very good forecasting power for both months [329].

## 6.5 Future Work and Recommendations

- Trend analysis other than precipitation should be carried out like Flood, Glacial lake outburst Flood (GLOFs).
- Principal component regression (PCR) using other climate parameters like maximum and minimum precipitation, maximum and minimum temperature is recommended for future study.
- Data-Adaptive Principal Component Regression (DPCR) Artificial Neural Networking technique should be applied to further improve the model.

# Bibliography

[1] R. K. Pachauri, M. R. Allen, V. R. Barros, J. Broome, W. Cramer, R. Christ, et al., "Climate change 2014: synthesis report. Contribution of Working Groups I, II and III to the fifth assessment report of the Intergovernmental Panel", on *Climate Change*: IPCC, 2014.

[2] C. M. Eschliman, E. Kuster, J. Ripberger, and A. M. Wootten, "Preparing to adapt: are public expectations in line with climate projections?," *Climatic Change*, vol. 163, pp. 851-871, 2020.

[3] L. Guo, Z. Jiang, D. Chen, H. Le Treut, and L. Li, "Projected precipitation changes over China for global warming levels at 1.5° C and 2° C in an ensemble of regional climate simulations: impact of bias correction methods," *Climatic Change*, vol. 162, pp. 623-643, 2020.

[4] N. G. C. Change, "Vital signs of the planet," URL: https://climate. NASA. gov/vital-signs/global-temperature/[Accessed: 16-Aug- 2020], 2018.

[5] R. Leitold, J. R. Diez, and V. Tran, "Are we expecting too much from the private sector in flood adaptation? Scenario-based field experiments with small- and medium-sized firms in Ho Chi Minh City, Vietnam," *Climatic Change*, vol. 163, pp. 359-378, 2020.

[6] M. Zhang, H. Yu, A. D. King, Y. Wei, J. Huang, and Y. Ren, "Greater probability of extreme precipitation under 1.5° C and 2° C warming limits over East-Central Asia," *Climatic Change,* pp. 1-17, 2020.

[7] J. Bentz, "Learning about climate change in, with and through art," *Climatic Change*, vol. 162, pp. 1595-1612, 2020.

[8] E. Ser-Giacomi, G. JordSnchez, J. SotoNavarro, S. Thomsen, J. Mignot, F. Sevault, et al., "Impact of climate change on surface stirring and transport in the Mediterranean Sea," *Geophysical Research Letters*, vol. 47, no. 22, p. e2020GL089941, 2020.

[9] G. Cunningham, B. P. McCullough, and S. Hohensee, "Physical activity and climate change attitudes," *Climatic Change*, vol. 159, pp. 61-74, 2020.

[10] C. Wamsler, J. Alkan-Olsson, H. Bjrn, H. Falck, H. Hanson, T. Oskarsson, et al., "Beyond participation: when citizen engagement leads to undesirable outcomes for nature-based solutions and climate change adaptation," *Climatic Change*, vol. 158, pp. 235-254, 2020.

[11] L. Hughes, D. M. Konisky, and S. Potter, "Extreme weather and climate opinion: evidence from Australia," *Climatic Change*, vol. 163, pp. 723-743, 2020.

[12] A. Mjean, A. Pottier, S. Zuber, and M. Fleurbaey, "Catastrophic climate change, population ethics and intergenerational equity". *Climatic Change*, 163(2), pp. 873-890, 2020.

[13]J. Li, H.H. Hsu, W.C. Wang, K.J. Ha, T. Li, and A. Kitoh,, "East Asian climate under global warming: understanding and projection," *Springer*, 2018.

[14] P. W. Grez, C. Aguirre, L. Faras, M. Contreras-Lpez, and . Masotti, "Evidence of climate-driven changes on atmospheric, hydrological, and oceanographic variables along the Chilean coastal zone," *Climatic Change*, vol. 163, pp. 633-652, 2020.

[15] N. P. Kettle, J. E. Walsh, L. Heaney, R. L. Thoman, K. Redilla, and L. Carroll, "Integrating archival analysis, observational data, and climate projections to assess extreme event impacts in Alaska," *Climatic Change*, vol. 163, pp. 669-687, 2020.

[16] M. S. Mehboob, Y. Kim, J. Lee, M.-J. Um, A. Erfanian, and G. Wang, "Projection of vegetation impacts on future droughts over West Africa using a coupled RegCM-CLM-CN-DV," *Climatic Change*, vol. 163, pp. 653-668, 2020.

[17] B. Beckage, K. Lacasse, J. M. Winter, L. J. Gross, N. Fefferman, F. M. Hoffman, et al., "The Earth has humans, so why dont our climate models?," *Climatic Change*, vol. 163, pp. 181-188, 2020.

[18] J. Hussain, T. Khaliq, S. Asseng, U. Saeed, A. Ahmad, B. Ahmad, et al., "Climate change impacts and adaptations for wheat employing multiple climate and crop modelsin Pakistan," *Climatic Change,* vol. 163, pp. 253-266, 2020.

[19] A. Bichet, A. Diedhiou, B. Hingray, G. Evin, K. N. A. Browne, and K. Kouadio, "Assessing uncertainties in the regional projections of precipitation in CORDEX-AFRICA," *Climatic Change*, vol. 162, pp. 583-601, 2020.

[20] Q. Lin, Y. Wang, T. Glade, J. Zhang, and Y. Zhang, "Assessing the spatiotemporal impact of climate change on event rainfall characteristics influencing landslide occurrences based on multiple GCM projections in China," *Climatic Change*, pp. 1-19, 2020.

[21] D. Camuffo, A. della Valle, F. Becherini, and V. Zanini, "Three centuries of daily precipitation in Padua, Italy, 17132018: history, relocations, gaps, homogeneity and raw data," *Climatic Change*, pp. 1-20, 2020.

[22] P. B. de Amorim and P. B. Chaffe, "Towards a comprehensive characterization of evidence in synthesis assessments: the climate change impacts on the Brazilian water resources," *Climatic Change*, vol. 155, pp. 37-57, 2019.

[23] R. Mendelsohn, "The role of markets and governments in helping society adapt to a changing climate," *Climatic change,* vol. 78, pp. 203-215, 2006.

[24] S. E. Nicholson, C. Funk, and A. H. Fink, "Rainfall over the African continent from the 19th through the 21st century," *Global and planetary change*, vol. 165, pp. 114-127, 2018.

[25] J. Li and B. Wang, "Predictability of summer extreme precipitation days over eastern China," *Climate Dynamics*, vol. 51, pp. 4543-4554, 2018.

[26] M. F. Ismail, B. S. Naz, M. Wortmann, M. Disse, L. C. Bowling, and W. Bogacki, "Comparison of two model calibration approaches and their influence on future projections under climate change in the Upper Indus Basin," *Climatic Change*, pp. 1-20, 2020.

[27] S. A. Romshoo, J. Bashir, and I. Rashid, "Twenty-first century-end climate scenario of Jammu and Kashmir Himalaya, India, using ensemble climate models," *Climatic Change,* vol. 162, pp. 1473-1491, 2020.

[28] M. Sheikh, N. Manzoor, J. Ashraf, M. Adnan, D. Collins, S. Hameed, et al., "Trends in extreme daily rainfall and temperature indices over South Asia," *International Journal of Climatology*, vol. 35, pp. 1625-1637, 2015.

[29] V. Bharti, C. Singh, J. Ettema, and T. Turkington, "Spatiotemporal characteristics of extreme rainfall events over the Northwest Himalaya using satellite data," *International Journal of Climatology,* vol. 36, pp. 3949-3962, 2016.

[30] E. A. Albright and D. Crow, "Beliefs about climate change in the aftermath of extreme flooding," *Climatic Change*, vol. 155, pp. 1-17, 2019.

[31] P. Bubeck, L. Dillenardt, L. Alfieri, L. Feyen, A. H. Thieken, and P. Kellermann, "Global warming to increase flood risk on European railways," *Climatic Change,* vol. 155, pp. 19-36, 2019.

[32] W. Zhang, G. Villarini, and M. Wehner, "Contrasting the responses of extreme precipitation to changes in surface air and dew point temperatures," *Climatic change,* vol. 154, pp. 257-271, 2019.

[33] E. Weitkamp, L. McEwen, and P. Ramirez, "Communicating the hidden: toward a framework for drought risk communication in maritime climates," *Climatic Change,* vol. 163, pp. 831-850, 2020.

[34] D. J. Frame et al., "Climate change attribution and the economic costs of extreme weather events: a study on damages from extreme rainfall and drought," *Climatic Change*, pp. 1-17, 2020.

[35] A. M. Linke, F. D. Witmer, and J. OLoughlin, "Do people accurately report droughts? Comparison of instrument-measured and national survey data in Kenya," *Climatic Change,* vol. 162, pp. 1143-1160, 2020.

[36] E. O. Arceo-Gmez, D. Hernndez-Corts, and A. Lpez-Feldman, "Droughts and rural households wellbeing: evidence from Mexico," *Climatic Change,* vol. 162, pp. 1197-1212, 2020.

[37] N. Saddique, A. Khaliq, and C. Bernhofer, "Trends in temperature and precipitation extremes in historical (1961-1990) and projected (2061-2090) periods in a data scarce mountain basin, northern Pakistan," *Stochastic Environmental Research and Risk Assessment,* vol. 34, pp. 1441-1455, 2020.

[38] P. Webster, V. E. Toma, and H. M. Kim, "Were the 2010 Pakistan floods predictable?," *Geophysical research letters*, vol. 38, 2011.

[39] F. Viterbo, J. von Hardenberg, A. Provenzale, L. Molini, A. Parodi, O. O. Sy, et al., "High-resolution simulations of the 2010 Pakistan flood event: Sensitivity to parameterizations and initialization time," *Journal of Hydrometeorology,* vol. 17, pp. 1147-1167, 2016.

[40] R. Devkota, U. Bhattarai, L. Devkota, and T. N. Maraseni, "Assessing the past and adapting to future floods: a hydro-social analysis," *Climatic Change*, vol. 163, pp. 1065-1082, 2020.

[41] M. Zahid and G. Rasul, "Frequency of extreme temperature and precipitation events in Pakistan 1965-2009," *Science International,* vol. 23, pp. 313-319, 2011.

[42] S. Liu, W. Wu, X. Yang, P. Yang, and J. Sun, "Exploring drought dynamics and its impacts on maize yield in the Huang-Huai-Hai farming region of China," *Climatic Change*, vol. 163, pp. 415-430, 2020.

[43] M.A. Aun, A. Ghani, and M Adnan, and M.A. Latif, " Recognizing Rainfall Pattern for Pakistan using Computational Intelligence," *International Journal of Advanced Computer Science And Applications*, vol. 8(11), pp. 487-491,2017.

[44] M. Bas and A. Mahajan, "Contesting the climate: Security implications of geoengineering and counter-geoengineering," September, 2018.

[45] C. Eriksen, G. L. Simon, F. Roth, S. J. Lakhina, B. Wisner, C. Adler, et al., "Rethinking the interplay between affluence and vulnerability to aid climate change adaptive capacity," *Climatic Change*, vol. 162, pp. 25-39, 2020.

[46] W. G. Bastiaanssen and S. Ali, "A new crop yield forecasting model based on satellite measurements applied across the Indus Basin, Pakistan," *Agriculture, ecosystems & environment*, vol. 94, pp. 321-340, 2003.

[47] N. Radke, K. Keller, R. Yousefpour, and M. Hanewinkel, "Identifying decision-relevant uncertainties for dynamic adaptive forest management under climate change," *Climatic Change*, vol. 163, pp. 891-911, 2020.

[48] L. R. Mason, R. E. Green, C. Howard, P. A. Stephens, S. G. Willis, A. Aunins, et al., "Population responses of bird populations to climate change on two continents vary with species ecological traits but not with direction of change in climate suitability," *Climatic Change*, vol. 157, pp. 337-354, 2019.

[49] Z. Han, S. Huang, Q. Huang, Q. Bai, G. Leng, H. Wang, et al., "Effects of vegetation restoration on groundwater drought in the Loess Plateau, China," *Journal of Hydrology*, vol. 591, pp. 125566, 2020.

[50] L. Guo, N. P. Klingaman, M.-E. Demory, P. L. Vidale, A. G. Turner, and C. C. Stephan, "The contributions of local and remote atmospheric moisture fluxes to East Asian precipitation and its variability," *Climate Dynamics*, vol. 51, pp. 4139-4156, 2018.

[51] R. M. Cooke, "Uncertainty analysis comes to integrated assessment models for climate change and conversely," *Climatic change*, vol. 117, pp. 467-479, 2013.

[52] C. L. Franzke and H. T. i Sentelles, "Risk of extreme high fatalities due to weather and climate hazards and its connection to large-scale climate variability," *Climatic Change*, vol. 162, pp. 507-525, 2020.

[53] D. Eckstein, M. Winges, V. Knzel, and L. Schfer, "Global Climate Risk Index 2020: Who Suffers Most from Extreme Weather Events? Wether-Related Loss Events in 2018 and 1999 to 2018": *Germanwatch Nord-Sd Initiative* eV, 2019.

[54] D. Eckstein, V. Knzel, L. Schfer, and M. Winges, "Global climate risk index 2020," *Germanwatch Available at*: https://germanwatch. org/sites/germanwatch. org/files/20-2-01e% 20 Global, vol. 20, 2019.

[55] Q. U. Z. Chaudhry, Climate change profile of Pakistan: Asian Development Bank, 2017.

[56] UNDP. (2019). Environment & Climate Change — UNDP in Pakistan. Available: https://www.pk.undp.org/content/pakistan/en/home/environment -climate-change.html.[Accessed: 20-Aug-2020]

[57] F. Naz, G. H. Dars, K. Ansari, S. Jamro, and N. Y. Krakauer, "Drought Trends in Balochistan," *Water*, vol. 12, no. 2, 2020.

[58] S. Jamro, G. H. Dars, K. Ansari, and N. Y. Krakauer, "Spatio-temporal variability of drought in Pakistan using standardized precipitation evapotranspiration index," *Applied Sciences*, vol. 9, no. 21, p. 4588, 2019.

[59] M. Ashraf and J. K. Routray, "Perception and understanding of drought and coping strategies of farming households in north-west Balochistan," *International Journal of Disaster Risk Reduction*, vol. 5, pp. 49-60, 2013.

[60] H. Khozeymehnezhad, and. M.N Tahroudi, " Annual and seasonal distribution pattern of rainfall in Iran and neighboring regions, " *Arabian Journal of Geosciences*, vol. 12(8), p.271, 2019.

[61] H. Akbar and S. H. Gheewala, "Effect of climate change on cash crops yield in Pakistan," *Arabian Journal of Geosciences*, vol. 13, 2020.

[62] P. Dll, "Impact of climate change and variability on irrigation requirements: a global perspective," *Climatic change*, vol. 54, pp. 269-293, 2002.

[63] H. Ward. (2019).Pakistan: Distribution of gross domestic product (GDP) across economic sectors. Available: https://www.statista.com/statistics/383256/Pakistan-gdp-distribution-across-economic-sectors. [Accessed: 20-Aug-2020]

[64] Finance Division (2020). Finance Division —Government of Pakistan—. Available: http://www.finance.gov.pk. [Accessed: 20-Jan-2021]

[65] S. Piccolroaz, R. I. Woolway, and C. J. Merchant, "Global reconstruction of twentieth century lake surface water temperature reveals different warming trends depending on the climatic zone," *Climatic Change*, pp. 1-16, 2020.

[66] J. U. Khan, A. S. Islam, M. K. Das, K. Mohammed, S. K. Bala, and G. T. Islam, "Future changes in meteorological drought characteristics over Bangladesh projected by the CMIP5 multi-model ensemble," *Climatic Change*, vol. 162, pp. 667-685, 2020.

[67] R. Chhin, C. Oeurng, and S. Yoden, "Drought projection in the Indochina Region based on the optimal ensemble subset of CMIP5 models," *Climatic Change*, vol. 162, pp. 687-705, 2020.

[68] M. Enenkel, M. Brown, J. Vogt, J. McCarty, A. R. Bell, D. Guha-Sapir, et al., "Why predict climate hazards if we need to understand impacts? Putting humans back into the drought equation," *Climatic Change*, vol. 162, pp. 1161-1176, 2020.

[69] E. Tschumi and J. Zscheischler, "Countrywide climate features during recorded climate-related disasters," *Climatic change*, vol. 158, pp. 593-609, 2020.

[70] L. Xu, C. Zhang, N. Chen, H. Moradkhani, P. S. Chu, and X. Zhang, "Potential precipitation predictability decreases under future warming," *Geophysical Research Letters*, vol. 47, p. e2020GL090798, 2020.

[71] S. A. Wheeler, Y. Xu, and A. Zuo, "Modelling the climate, water and socio-economic drivers of farmer exit in the Murray-Darling Basin," *Climatic Change*, vol. 158, pp. 551-574, 2020.

[72] J. Shortridge, "Observed trends in daily rainfall variability result in more severe climate change impacts to agriculture," *Climatic Change*, vol. 157, pp. 429-444, 2019.

[73] UNDP, "Water security in Pakistan: Issues and challenges," *United Nations Development programme Pakistan*, vol. 3, 2016.

[74] S. Khair, R. Culas, and M. Hafeez, "The causes of groundwater decline in upland Balochistan region of Pakistan: Implication for water management policies," *in Australian Conference of Economists*, pp. 1-11, 2010.

[75] Kakar, Z., Shah, S. M., and Khan, M. A., "Scarcity of water resources in rural area of Quetta District; challenges and preparedness," *IOP Conference Series: Materials Science and Engineering*, vol. 414, no. 1, p. 012013. IOP Publishing, 2018.

[76] S. M. Hali. (2018). Water scarcity in Balochistan - Daily Times. Available: https://dailytimes.com.pk/250988/250988

[77] F. van Steenbergen, A. B. Kaisarani, N. U. Khan, and M. S. Gohar, "A case of groundwater depletion in Balochistan, Pakistan: Enter into the void," *Journal of Hydrology: Regional Studies*, vol. 4, pp. 36-47, 2015.

[78] WHO. (2019). Floods in Balochistan. Available: http://www.emro.who.int/pak/pakistan-infocus/floods-in-balochistan.html. [Accessed: 20-Aug-2020]

[79] Global (2020). China-Pakistan Economic Corridor (CPEC). Available: https://www.cpicglobal.com/pakistan-overview/cpec.[Accessed: 20-Aug-2020]

[80] SDGS. (2019). Sustainable Development Goals, Goal 13. Available: https://sdgs.un.org/goals/goal 13. [Accessed: 20-Aug-2020]

[81] SDGS. (2019). Sustainable Development Goals. Available: https://sdgs.un.org/goals/goal 11. [Accessed: 20-Aug-2020]

[82] D.J. Rees, A. Samiullah, F. Rehman,C.H. Kidd, J.D.H.Keatinge and S.H.Raza, "Precipitation and temperature regimes in upland Balochistan: their influence on rain-fed crop production," *Agricultural and forest meteorology*, vol. 52(3-4), pp.381-396, 1990.

[83] S. Adnan, K. Ullah, S. Gao, A. H. Khosa, and Z. Wang, "Shifting of agroclimatic zones, their drought vulnerability, and precipitation and temperature trends in Pakistan," *International Journal of Climatology*, vol. 37, pp. 529-543, 2017.

[84] S. Adnan, K. Ullah, and G. Shouting, "Investigations into precipitation and drought climatologies in South Central Asia with special focus on Pakistan over the period 1951-2010," *Journal of Climate*, vol. 29, pp. 6019-6035, 2016.

[85] S. Adnan, K. Ullah, and S. Gao, "Characterization of drought and its assessment over Sindh, Pakistan during 1951-2010," *Journal of Meteorological Research*, vol. 29, pp. 837-857, 2015.

[86] S. Liu and A. Duan, "Impacts of the global sea surface temperature anomaly on the evolution of circulation and precipitation in East Asia on a quasi-quadrennial cycle," *Climate Dynamics*, vol. 51, pp. 4077-4094, 2018.

[87] S. Kusunoki, "Future changes in precipitation over East Asia projected by the global atmospheric model MRI-AGCM3. 2," *Climate Dynamics*, vol. 51, pp. 4601-4617, 2018.

[88] Islamic Relief Pakistan. (2018). "Drought Study Report (Islamic Relief Pakistan in Collaboration with PDMA Baluchistan)". Available: https://www.humanitarianresponse.info/en/operations/pakistan/document/islamic-relief-balochistan-drought-study-report-2018.

[89] J.S. Deepa, C. Gnanaseelan, S. Mohapatra, J.S. Chowdary et al., " The tropical Indian Ocean decadal sea level response to the Pacific decadal oscillation forcing," *Climate Dynamics*, vol. pp.52(7-8), pp.5045-5058, 2019.

[90] Y. Gong, T. Li, and L. Chen, "Interdecadal modulation of ENSO amplitude by the Atlantic multi-decadal oscillation (AMO)," *Climate Dynamics*, vol. 55, pp. 2689-2702, 2020.

[91] F. O. Akinyemi and B. J. Abiodun, "Potential impacts of global warming levels 1.5 C and above on climate extremes in Botswana," *Climatic Change*, vol. 154, pp. 387-400, 2019.

[92] Riduna. (2019). "The Skeptical Science Effects Of Global Warming". Available: https://skepticalscience.com/Global-Warming-Effects.html.

[93] Effect of Global Warming (2020). Available: https://www.livescience.com/37057-global-warming-effects.html. [Accessed: 20-Aug-2020]

[94] L. Bodri, V. Cermak, and M. Kresl, "Trends in precipitation variability: Prague (the Czech Republic)," *Climatic Change*, vol. 72, pp. 151-170, 2005.

[95] A. Panda and N. Sahu, "Trend analysis of seasonal rainfall and temperature pattern in Kalahandi, Bolangir and Koraput districts of Odisha, India," *Atmospheric Science Letters*, vol. 20, p. e932, 2019.

[96] R. Marsooli and N. Lin, "Impacts of climate change on hurricane flood hazards in Jamaica Bay, New York," *Climatic Change*, pp. 1-19, 2020.

[97] R. Marsooli, N. Lin, K. Emanuel, and K. Feng, "Climate change exacerbates hurricane flood hazards along US Atlantic and Gulf Coasts in spatially varying patterns," *Nature communications*, vol. 10, pp. 1-9, 2019.

[98] O. Zolina, C. Simmer, K. Belyaev, A. Kapala, and S. Gulev, "Improving estimates of heavy and extreme precipitation using daily records from European rain gauges," *Journal of Hydrometeorology*, vol. 10, pp. 701-716, 2009.

[99] E. E. Aalbers, G. Lenderink, Van. Meijgard, E. and B. J. Van den Hurk, " Local-scale changes in mean and heavy precipitation in Western Europe, climate change or internal variability?" *Climate Dynamics*, vol. 50(11-12), pp.4745-4766, 2018.

[100] M. A. Khan, A. Tahir, N. Khurshid, M. Ahmed, and H. Boughanmi, "Economic Effects of Climate Change-induced Loss of Agricultural Production by 2050: A Case Study of Pakistan," *Sustainability*, vol. 12, p. 1216, 2020.

[101] A. Theobald, H. McGowan, and J. Speirs, "Teleconnection influence of precipitationbearing synoptic types over the Snowy Mountains region of southeast Australia," *International Journal of Climatology*, vol. 38, pp. 2743-2759, 2018.

[102] E. W. Kolstad, C. O. Wulff, D. I. Domeisen, and T. Woollings, "Tracing North Atlantic Oscillation forecast errors to stratospheric origins," *Journal of Climate*, vol. 33, pp. 9145-9157, 2020.

[103] S. Tietsche, M. Balmaseda, H. Zuo, C. Roberts, M. Mayer, and L. Ferranti, "The importance of North Atlantic Ocean transports for seasonal forecasts," *Climate Dynamics*, vol. 55, pp. 1995-2011, 2020.

[104] S. O. Krichak, J. S. Breitgand, S. Gualdi, and S. B. Feldstein, "Teleconnectionextreme precipitation relationships over the Mediterranean region," *Theoretical and Applied climatology*, vol. 117, pp. 679-692, 2014.

[105] P. Zhao, Y. Zhu, and R. Zhang, and "An AsianPacific teleconnection in summer tropospheric temperature and associated Asian climate variability " *Climate Dynamics*, 29(2-3), pp.293-303, 2007.

[106] S. Chen and B. Yu, "Projection of winter NPO-following winter ENSO connection in a warming climate: uncertainty due to internal climate variability," *Climatic Change*, vol. 162, pp. 723-740, 2020.

[107] G. J. Marshall, K. Jylh, S. Kivinen, M. Laapas, and A. V. Dyrrdal, "The role of atmospheric circulation patterns in driving recent changes in indices of

extreme seasonal precipitation across Arctic Fennoscandia," *Climatic Change*, pp. 1-19, 2020.

[108] N.-B. Chang, S. Imen, K. Bai, and Y. J. Yang, "The impact of global unknown teleconnection patterns on terrestrial precipitation across North and Central America," *Atmospheric Research*, vol. 193, pp. 107-124, 2017.

[109] R. J. Hall and E. Hanna, "North Atlantic circulation indices: links with summer and winter UK temperature and precipitation and implications for seasonal forecasting," *International Journal of Climatology*, vol. 38, pp. e660-e677, 2018.

[110] M. Afzal, M. Haroon, A. Rana, and A. Imran, "Influence of North Atlantic oscillations and Southern oscillations on winter precipitation of Northern Pakistan," *Pakistan Journal of Meteorology*, vol. 9, 2013.

[111] B. Myong. S.W. Yeh, J. Kim and M.C. Kafatos," Impacts of Pacific SSTs on atmospheric circulations leading to California winter precipitation variability, A diagnostic modeling, " *Atmospheres*,vol. 9(11), p.455, 2018.

[112] O. Alizadeh-Choobari, P. Adibi, and P. Irannejad, "Impact of the El NioSouthern Oscillation on the climate of Iran using ERA-Interim data," *Climate dynamics*, vol. 51, pp. 2897-2911, 2018.

[113] N. Xie, Y. Sun, and M. Gao, "The Influence of Five Teleconnection Patterns on Wintertime Extratropical Cyclones over Northwest Pacific," *Atmosphere*, vol. 11, p. 1248, 2020.

[114] S. Feldstein, "Atmospheric teleconnection patterns. Nonlinear and Stochastic *Climate Dynamics, CLE Franzke and TJ OKane, Eds," ed: Cambridge University Press*, 2017.

[115] X. Zhang, S. Zhong and Z.Wu, " Seasonal prediction of the typhoon genesis frequency over the Western North Pacific with a Poisson regression model," *Climate Dynamics*, vol. 51, p. 45854600, 2018.

[116] K. Ashok, Z. Guan, and T. Yamagata, "Impact of the Indian Ocean dipole on the relationship between the Indian monsoon rainfall and ENSO," *Geophysical Research Letters*, vol. 28, pp. 4499-4502, 2001.

[117] J. M. Wallace and D. S. Gutzler, "Teleconnections in the geopotential height field during the Northern Hemisphere winter," *Monthly weather review*, vol. 109, pp. 784-812, 1981.

[118] B. Yu, H. Lin, and N. Soulard, "A comparison of north american surface temperature and temperature extreme anomalies in association with various atmospheric teleconnection patterns," *Atmosphere*, vol. 10, p. 172, 2019.

[119] C. Hui and X.-T. Zheng, "Uncertainty in Indian Ocean Dipole response to global warming: the role of internal variability," *Climate Dynamics*, vol. 51, pp. 3597-3611, 2018.

[120] I. Mavilia, A. Bellucci, P. J. Athanasiadis, S. Gualdi, R. Msadek, and Y. Ruprich-Robert, "On the spectral characteristics of the Atlantic multidecadal variability in an ensemble of multi-century simulations," *Climate Dynamics*, vol. 51, pp. 3507-3520, 2018.

[121] D. Mukhin, A. Gavrilov, E. Loskutov, A. Feigin, and J. Kurths, "Nonlinear reconstruction of global climate leading modes on decadal scales," *Climate Dynamics*, vol. 51, pp. 2301-2310, 2018.

[122] R. Yadav, K. Rupa Kumar, and M. Rajeevan, "Increasing influence of ENSO and decreasing influence of AO/NAO in the recent decades over northwest India winter precipitation," *Journal of Geophysical Research: Atmospheres*, vol. 114, 2009.

[123] M. J. Butt and M. F. Iqbal, "Impact of climate variability on snow cover: a case study of northern Pakistan," *Pakistan Journal of Meteorology*, vol. 5, pp. 53-63, 2009.

[124] L. Hua, L. Chen, X. Rong, J. Su, L. Wang, T. Li, et al., "Impact of atmospheric model resolution on simulation of ENSO feedback processes: a coupled model study," *Climate Dynamics*, vol. 51, pp. 3077-3092, 2018.

[125] L. P. Garcia-Villada, M. G. Donat, O. Anglil, and A. S. Taschetto, "Temperature and precipitation responses to El Nio-Southern Oscillation in a hierarchy of datasets with different levels of observational constraints," *Climate Dynamics*, vol. 55, pp. 2351-2376, 2020.

[126] R. W.-K. Lee, C.-Y. Tam, S.-J. Sohn, and J.-B. Ahn, "Predictability of two types of El Nino and their climate impacts in boreal spring to summer in coupled models," *Climate Dynamics*, vol. 51, pp. 4555-4571, 2018.

[127] M. M. Dogar, F. Kucharski, and S. Azharuddin, "Study of the global and regional climatic impacts of ENSO magnitude using SPEEDY AGCM," *Journal of Earth System Science*, vol. 126, p. 30, 2017.

[128] A. Mahmood, T. M. A. Khan, and N. Faisal, "Correlation between multivariate ENSO index (MEI) and Pakistans summer rainfall," *Pakistan Journal of Meteorology*, vol. 1, 2004.

[129] I. Turki, B. Laignel, N. Laftouhi, Z. Nouaceur, and Z. Zamrane, "Investigating possible links between the North Atlantic Oscillation and rainfall variability in Marrakech (Morocco)," *Arabian Journal of Geosciences*, vol. 9, p. 243, 2016.

[130] A. R. WESTGARTHSMITH, D. B. Roy, M. Scholze, A. Tucker, and J. P. Sumpter, "The role of the North Atlantic Oscillation in controlling UK butterfly population size and phenology," *Ecological entomology*, vol. 37, pp. 221-232, 2012.

[131] Y. Huang and H. Wang, "A Possible Approach for Decadal Prediction of the PDO," *Journal of Meteorological Research*, vol. 34, pp. 63-72, 2020.

[132] T. DelSole and M. K. Tippett, "Predictability in a changing climate," *Climate Dynamics*, vol. 51, pp. 531-545, 2018.

[133] J. Neena, E. Suhas, and R. Murtugudde, "Boreal Spring El Nino Convective State and Its Impact on Monsoon Onset," *Geophysical Research Letters*, vol. 47, p. e2020GL090136, 2020.

[134] V. Krishnamurthy, "Intraseasonal oscillations in East Asian and South Asian monsoons," *Climate Dynamics*, vol. 51, pp. 4185-4205, 2018.

[135] K.-J. Ha, Y.-W. Seo, J.-Y. Lee, R. Kripalani, and K.-S. Yun, "Linkages between the South and East Asian summer monsoons: a review and revisit," *Climate Dynamics*, vol. 51, pp. 4207-4227, 2018.

[136] G. Feng, M. Zou, S. Qiao, R. Zhi, and Z. Gong, "The changing relationship between the December North Atlantic Oscillation and the following February East Asian trough before and after the late 1980s," *Climate Dynamics*, vol. 51, pp. 4229-4242, 2018.

[137] O. Rojas, Y. Li, and R. Cumani,"Understanding the drought impact of El Nino on the global agricultural areas," *An assessment using FAOs Agricultural Stress Index (ASI)", Food and Agriculture Organization of the United Nations.* Rome (Italy), pp. 1-52, 2014.

[138] E. Aamir and I. Hassan, "Trend analysis in precipitation at individual and regional levels in Baluchistan, Pakistan," *in IOP Conference Series: Materials Science and Engineering; IOP Publishing: Bristol*, UK, p. 012042, 2018.

[139] L. Chafik, J.E. Nilsen, and S. Dangendorf,"Impact of North Atlantic teleconnection patterns on Northern European sea level," *Journal of Marine Science and Engineering*, vol. 5, no. 3, pp. 1-23, 2017.

[140] M. Ashraf, J. K. Routray, and M. Saeed, "Determinants of farmers choice of coping and adaptation measures to the drought hazard in northwest Balochistan, Pakistan," *Natural hazards*, vol. 73, pp. 1451-1473, 2014.

[141] M. Ashraf and J. K. Routray, "Spatio-temporal characteristics of precipitation and drought in Balochistan Province, Pakistan," *Natural Hazards*, vol. 77, pp. 229-254, 2015.

[142] M. Ashraf and A. A. (2017). Sustainable Groundwater Management in Balochistan. Available: pcrwr.gov.pk.

[143] S. Adnan, K. Ullah, L. Shuanglin, S. Gao, A. H. Khan, and R. Mahmood, "Comparison of various drought indices to monitor drought status in Pakistan," *Climate Dynamics*, vol. 51, pp. 1885-1899, 2018.

[144] S.A Anjum, M.F Saleem,M.A Cheema,M.F Bilal,T. Khaliq ," An Assessment To Vulnerability Extent, Characteristics And Severity Of Drought Hazard In Pakistan," *Pakistan Journal of Science*. Jun 1; 64 (2), 2012.

[145] K.Ahmed, S. Shahid,S.b. Harun," Characterization of seasonal droughts in Balochistan Province, Pakistan," *stochastic environmental research and risk assessment*, 747-762, 2016. https://doi.org/10.1007/s00477-015-111

[146] K. Ahmed, Shamsuddin Shahid, Rawshan Othman Ali, SobriBin Haruna, Xiao-jun Wang ,"Evaluation of the performance of gridded precipitation products over Balochistan Province, Pakistan," *Desalination and Water Treatment* 2017. doi:l0.5004/dwt.2017.20859

[147] K. Ahmed, S. Shahid, E.S Chung, X.J Wang, and S.B Harun," Climate change uncertainties in seasonal drought severity-area-frequency curves: Case of arid region of Pakistan," *Journal of Hydrology*, 570, 473-485, 2019.

[148] H.Xie,C. Ringler,T. Zhu, and A. Waqas," Droughts in Pakistan: a spatiotemporal variability analysis using the Standardized Precipitation Index," *Water international* 38(5), 620-631, 2013.

[149] S.Hina,F. Saleem ," Historical analysis ( 1981-2017) of drought severity and magnitude over a predominantly arid region of Pakistan," *Climate Research* 78: 189-204, 2019. https://doi.org/10.3354/crO 1568

[150] M.A. Haroon, J. Zhang, and F. Yao," Drought monitoring and performance evaluation of MODIS-based drought severity index (DSI) over Pakistan," *Natural Hazards* 84(2), 1349-1366, 2016.

[151] S. Haider, S. Adnan,“ Classification and assessment of aridity over Pakistan provinces (1960-2009),” *International Journal of Environment* Dec 15;3(4):24-35, 2014.

[152] S. Haider, and K. Ullah,“ Historical and Projected Shift in Agro-Climatic Zones and Associated Variations of Daily Temperature and Precipitation Extremes using CORDEX-SA over Pakistan,” *Asia-Pacific Journal of Atmospheric Science* 15:1-5, 2021.

[153] H. Athar,“ Climate-related inter-annual variability and long-term influence on wheat yield across canal-irrigated areas of Punjab, Pakistan,” *Theoretical and Applied Climatology* vol. 143 :1195, 2021.

[154] S.S., Hassan and M.A Goheer ,“ Modeling and Monitoring Wheat Crop Yield Using Geospatial Techniques: A Case Study of Potohar Region, Pakistan. ” *Journal of the Indian Society of Remote Sensing.* 16:1-2,2021.

[155] S. Kreft, D. Eckstein, and I. Melchior, “Global climate risk index 2014,” *Who suffers most from extreme weather events*, vol. 1, pp. 1-28 2013.

[156] A. Rehman, L. Jingdong, Y. Du, R. Khatoon, S.A. Wang and S.K. Nisar, “ Flood disaster in Pakistan and its impact on agriculture growth (a review),” *Journal of Economics and Sustainable Development* 6(23), pp. 39-42, 2016.

[157] WHO. (2019). Floods in Balochistan — Pakistan-infocus — Pakistan - WHO EMRO. Available: http://www.emro.who.int/pak/pakistan-infocus/floods-in-balochistan.html.[Accessed: 20-May-2020]

[158] S.R. Kolusu, C. Siderius, M.C.Todd,“Sensitivity of projected climate impacts to climate model weighting: multi-sector analysis in eastern Africa,*Climatic Change* 164,36 2021. https://doi.org/10.1007/s10584-021-02991-8

[159] P. Maharana, R. Agnihotri, R. and Dimri, A.P,“Changing Indian monsoon rainfall patterns under the recent warming period 20012018,*Climate Dynamics* 2021. https://doi.org/10.1007/s00382-021-05823-8

[160] Prodhomme, C., Materia, S., Ardilouze, C. et al.,“ Seasonal prediction of European summer heatwaves, *Climate Dynamics* 2021. https://doi.org/10.1007/s00382-021-05828-3

[161] A. Duane, M. Castellnou, M. and L. Brotons,“Towards a comprehensive look at global drivers of novel extreme wildfire events,*Climatic Change* 165, 43, 2021. https://doi.org/10.1007/s10584-021-03066-4

[162] X.Wang, F.Xie, Z.Zhang “Complex network of synchronous climate events East Asia tree-ring data,*Climatic Change* 165, 54 2021. https://doi.org/10.1007/s10584-021-03008-0

[163] H. Antonson, P. Buckland, and R.A Nyqvist, R. A ,“society ill-equipped to deal with the effects of climate change on cultural heritage and landscape: a qualitative assessment of planning practices in transport infrastructure,*Climatic Change* 166, 18, 2021. https://doi.org/10.1007/s10584-021-03115-y

[164] M.D.P. Costa,K.A. Wilson, P.J. Dyer, P.J,“ Potential future climate-induced shifts in marine fish larvae and harvested fish communities in the subtropical southwestern Atlantic Ocean,*Climatic Change* 165, 66, 2021. https://doi.org/10.1007/s10584-021-03097-x

[165] E.A Neder,de Arajo Moreira, F. Dalla Fontana,“Urban adaptation index: assessing cities readiness to deal with climate change, *Climatic Change* 166, 16, 2021. https://doi.org/10.1007/s10584-021-03113-0

[166] O. Alcaraz,B.Sureda, A.TuronC. Ramrez, and M. Gebell,“ Equitable mitigation to achieve the 1.5 C goal in the Mediterranean Basin,*Climatic Change* 165, 62, 2021. https://doi.org/10.1007/s10584-021-03070-8

[167] A. Bourougaaoui, M.L. Ben Jama, M.L. and C. Robinet,“ Has North Africa turned too warm for a Mediterranean forest pest because of climate change?, *Climatic Change* 165, 46, 2021. https://doi.org/10.1007/s10584-021-03077-1

[168] R. Murali, A. Kuwar, A. and Nagendra,“ Whos responsible for climate change? Untangling threads of media discussions in India, Nigeria, Australia, and the USA *Climatic Change* 164, 51, 2021. https://doi.org/10.1007/s10584-021-03031-1

[169] T.R Shrum,“The salience of future impacts and the willingness to pay for climate change mitigation: an experiment in intergenerational framing,*Climatic Change* 165, 18, 2021. https://doi.org/10.1007/s10584-021-03002-6

[170] A. Mandel, T.Tiggeloven, D. Lincke, E. Koks, P. Ward, and J. Hinkel, ”Risks on global financial stability induced by climate change: the case of flood risks,*Climatic Change* 166, 4, 2021. https://doi.org/10.1007/s10584-021-03092-2

[171] K.A Cherkauer, L.C. Bowling,K.Byun, ”Climate change impacts and strategies for adaptation for water resource management in Indiana,*Climatic Change* 165, 21, 2021. https://doi.org/10.1007/s10584-021-02979-4

[172] K.A. Tamaddun, K. A. Kalra, A. Bernardez, and S. Ahmad, “Effects of ENSO on Temperature, Precipitation, and Potential Evapotranspiration of North India’s Monsoon: An Analysis of Trend and Entropy.” *Water* 11(2), 189, 2019.

[173] K.A. Tamaddun, A. Kalra,M. Bernardez , and S. Ahmad, “ Multi-scale Correlation between Western U.S. Snow Water Equivalent and ENSO/PDO Using Wavelet Analyses .” *Water Resources Management* 10.1007Is1 1269-017-1659-9, 2017.

[174] A.Kalra and S.Ahmad, “Estimating annual precipitation for the Colorado River Basin using oceanic-atmospheric oscillations.” *Water Resources Research* 48, W06527, 2012. doi:l 0.1029/2011WR010667.

[175] A.Kalra,S. Ahmad and A. Nayak , “ Increasing streamflow forecast lead time for snowmelt driven catchment based on large scale climate patterns, *Advances in Water Resources*, 53: 150-162, 2013.

[176] A.Kalra and S. Ahmad , " Using oceanic-atmospheric oscillations for long lead-time stream flow forecasting, *Water Resources Research*, 45, W0 3413, 2009.

[177] A.Kalra,L. Li, X. Li, and S.Ahmad, " Improving streamflow forecast lead time using oceanic-atmospheric oscillations for Kaidu River Basin, Xinjiang, China." *ASCE Journal of Hydrologic Engineering* 18(8): 1031-1040, 2013. doi: 10.1061/(ASCE)HE. 1943-5584.0000707.

[178] K.A Tamaddun, A. Kalra, and S.Ahmad, " Spatiotemporal Variation in the Continental US Streamflow in Association with Large-Scale Climate Signals Across Multiple Spectral Bands." *Water Resources Management* 2019. doi.org/l 0.1007/s l 1269-019-02217-8

[179] S.Sagarika ,A. Kalra, and S. Ahmad, " Pacific Ocean SST and Z500 climate variability and western U.S. seasonal streamflow." *International Journal of Climatology*, 36, 1515-1533, 2015. doi:10.1002/joc.4442.

[180] S. Bhandari, A. Kalra, K.A Tamaddun and S. Ahmad, " Relationship between Ocean Atmospheric Climate Variables and Regional Streamflow of the Conterminous United States." *Hydrology* 2018. doi: l0.3390/hydrology5020030.

[181] P. Pathak, A. Katra, K.W Lamb, W.P. Miller,S. Ahmad, R. Amerineni, and D.P Ponugoti, " Climatic variability of the Pacific and Atlantic Oceans and western US snowpack." *International Journal of Climatology*, 38(3), 1257-1269, 2018. doi:l 0.1002/joc.5241.

[182] S. Bukhary, A. Kalra, and S. Ahmad, " Incorporating Pacific Ocean Climate Information to Enhance the Tree-Ring based Streamflow Reconstruction Skill." *Journal of Water and Climate Change*.2020. doi .org/ I 0.2 l 66/wcc. 2020. 336.

[183] B. Thakur, A. Kalra A, S. Ahmad, K. Lamb and V. Lakshmi, " Bringing Statistical Learning Machines together for Hydro-climatological Predictions

-Case Study for Sacramento San Joaquin River Basin, California." *Journal of Hydrology: Regional Studies*, 2020. doi: I 0.1016/j.ejrh.2019.100651.

[184] K. Tamaddun, A. Kalra, S. Kumar and S Ahmad, " CMIP5 Models' Ability to Capture Observed Trends under the lnfluenc.e of Shifts and Persistence: An In-depth Study on the Colorado River Basin." *Journal of Applied Meteorology and Climatology*, 2019. doi.org/10.l 175/JAMC-D-18- 0251.l.

[185] P. Pathak,A. Kalra and S. Ahmad, "Temperature and Precipitation changes in the Midwestern United States: Implications for water management." *International Journal of Water Resources Development*, 33(6), 2017. 10.1080/07900627.2016.1238343.

[186] A. Kalra, S. Sagarika ,P.Pathak and S. Ahmad , " Hydro-climatological changes in the Colorado River Basin over a century." *Hydrological Sciences Journal* 10.1080/02626667.2017.

[187] K. Tamaddun, A.Katra, S.Ahmad, " Identification of Streamflow Changes across the Continental United States Using Variable Record Lengths." *Hydrology.* 3(2):24,2016. doi: I 0.3390/hydrology3020024.

[188] K. Tamaddun ,A. Kalra and S. Ahmad," Wavelet analysis of western U.S. streamflow with ENSO and PDO." *Journal of Water and Climate Change*, 8(1) 26-39,2017. doi: 10.2166/wcc.2016.162.

[189] C. Carrier, A. Kalra, and S. Ahmad, " Long-Range Precipitation Forecasts Using Paleoclimate Reconstructions in the Western United States, *Journal of Mountain Science.* 13(4):614-632,2016. doi:10.1007/s11629-014-3360-2.

[190] P. Pathak, A. Kalra, S. Ahmad and M. Bernardez, " Wavelet-aided analysis to estimate seasonal variability and dominant period icities in temperature, precipitation, and streamflow in the Midwestern United States." *Water Resources Management*, 10.1007Is11269-016-1445-0,2016.

[191] S. Sagarika,A. Kalra and S.Ahmad, " Interconnections between oceanic-atmospheric indices and variability in the U.S. streamflow,*Journal of Hydrology*, 525: 724-736,2015. 10.1016/j.jhydrol.2015.04.020.

[192] S. Sagarika ,A.Katra , and S. Ahmad, "Evaluating the effect of persistence on long-term trends and analyzi ng step changes in streamflows of the continental United States, *Journal of Hydrology*, 517:36-53. http://dx.d oi.org/ l 0.1016/j.jhydrol.2014.05.002,2014.

[193] C. Carrier,A. Kalra, and S. Ahmad, " Using Paleo Reconstructions to Improve Streamflow Forecast Lead-Time in the Western United States, *Journal of the American Water Resources Association (JAWRA)* 49(6): 1351-1366,2013. doi: 10.111l/jawra.12088.

[194] A. Katra, W.P Miller, K. W. Lamb, S. Ahmad,and T. Piechota, " Using large scale climatic patterns for improving long lead time streamflow forecasts for Gunnison and San Juan River Basins, *Hydrological Processes*, 27(11): 1543-1559, 2013.

[195] A. Kalra and S. Ahmad , " Evaluating changes and estimating seasonal precipitation for Colorado River Basin using stochastic non-parametric disaggregation technique, *Water Resources Research*, 47, W05555, 2011.

[196] A. Kumar and P. Sharma, "Impact of climate variation on agricultural productivity and food security in rural India," *Economics Discussion Papers*, 2013.

[197] A. S. Bhatti, G. Wang, W. Ullah, S. Ullah, D. Fiifi Tawia Hagan, I. Kwesi Nooni, et al., "Trend in Extreme Precipitation Indices Based on Long Term In Situ Precipitation Records over Pakistan," *Water*, vol. 12, p. 797, 2020.

[198] S. Salma, S. Rehman, and M. Shah, "Rainfall trends in different climate zones of Pakistan," *Pakistan Journal of Meteorology*, vol. 9, 2012.

[199] N. K. Arora and G. Rasul, " Impact of climate change on agriculture production and its sustainable solutions," *Environmental Sustainability*,Vol 2,p. 9596, 2019. https://doi.org/10.1007/s42398-019-00078-w.

[200] M. Latif and F. Syed, "Determination of summer monsoon onset and its related large-scale circulation characteristics over Pakistan," *Theoretical and Applied Climatology*, vol. 125, pp. 509-520, 2016.

[201] D. H. Burn and M. A. H. Elnur, "Detection of hydrologic trends and variability," *Journal of Hydrology*, vol. 255, pp. 107-122, 2002.

[202] C. Schr, N. Ban, E. M. Fischer, J. Rajczak, J. Schmidli, C. Frei, et al., "Percentile indices for assessing changes in heavy precipitation events," *Climatic Change*, vol. 137, pp. 201-216, 2016.

[203] K. Chaouche, L. Neppel, C. Dieulin, N. Pujol, B. Ladouche, E. Martin, et al., "Analyses of precipitation, temperature and evapotranspiration in a French Mediterranean region in the context of climate change," *Comptes Rendus Geoscience*, vol. 342, pp. 234-243, 2010.

[204] M. M. Dogar and T. Sato, "Analysis of climate trends and leading modes of climate variability for MENA region," *Journal of Geophysical Research: Atmospheres*, vol. 123, pp. 13,074-13,091, 2018.

[205] M. Latif, A. Hannachi, and F. Syed, "Analysis of rainfall trends over IndoPakistan summer monsoon and related dynamics based on CMIP5 climate model simulations," *International Journal of Climatology*, vol. 38, pp. e577-e595, 2018.

[206] M. Hanif, A. H. Khan, and S. Adnan, "Latitudinal precipitation characteristics and trends in Pakistan," *Journal of Hydrology*, vol. 492, pp. 266-272, 2013.

[207] S. M. Pingale, D. Khare, M. K. Jat, and J. Adamowski, "Trend analysis of climatic variables in an arid and semi-arid region of the Ajmer District,

Rajasthan, India," *Journal of Water and Land Development*, vol. 28, pp. 3-18, 2016.

[208] M. S. Khattak, M. Babel, and M. Sharif, "Hydro-meteorological trends in the upper Indus River basin in Pakistan," *Climate Research*, vol. 46, pp. 103-119, 2011.

[209] A. Aldahan, M.A. Al-Abri," Trend Detection in Annual Temperature and Precipitation Using MannKendall TestA Case Study to Assess Climate Change in Abu Dhabi, United Arab Emirates," *In Proceedings of 3rd International Sustainable Buildings Symposium (ISBS 2017)*: Volume 2 (Vol. 7, p. 3), 2018.

[210] M. Adnan, F. Khan, N. Rehman, S. Ali, S. S. Hassan, M. M. Dogar, et al., "Variability and Predictability of Summer Monsoon Rainfall over Pakistan," *Asia-Pacific Journal of Atmospheric Sciences*, pp. 1-9, 2020.

[211] S. Ali, B. Khalid, R. S. Kiani, R. Babar, S. Nasir, N. Rehman, et al., "Spatio-temporal variability of summer monsoon onset over Pakistan," *Asia-Pacific Journal of Atmospheric Sciences*, vol. 56, pp. 147-172, 2020.

[212] M. Adnan, N. Rehman, S. Ali, S. Mehmood, K. A. Mir, A. A. Khan, et al., "Prediction of summer rainfall in Pakistan from global seasurface temperature and sealevel pressure," *Weather*, vol. 72, pp. 76-84, 2017.

[213] F. Abbas, A. Ahmad, M. Safeeq, S. Ali, F. Saleem, H. M. Hammad, et al., "Changes in precipitation extremes over arid to semiarid and subhumid Punjab, Pakistan," *Theoretical and Applied climatology*, vol. 116, pp. 671-680, 2014.

[214] M. S. Hussain and S. Lee, "Long-term variability and changes of the precipitation regime in Pakistan," *Asia-Pacific Journal of Atmospheric Sciences*, vol. 50, pp. 271-282, 2014.

[215] K. Ahmed, Shamsuddin Shahid, Rawshan Othman Ali, SobriBin Haruna, Xiao-jun Wang ,"Evaluation of the performance of gridded precipitation products over Balochistan Province, Pakistan," *Desalination and Water Treatment* 2017. doi:l0.5004/dwt.2017.20859

[216] M. F. Iqbal and H. Athar, "Variability, trends, and teleconnections of observed precipitation over Pakistan," *Theoretical and Applied Climatology*, vol. 134, pp. 613-632, 2018.

[217] M. S. Hussain and S. Lee, "The regional and the seasonal variability of extreme precipitation trends in Pakistan," *Asia-Pacific Journal of Atmospheric Sciences*, vol. 49, pp. 421-441, 2013.

[218] A. Malik, A. Kumar, Q. B. Pham, S. Zhu, N. T. T. Linh, and D. Q. Tri, "Identification of EDI trend using Mann-Kendall and en-Innovative Trend methods (Uttarakhand, India)," *Arabian Journal of Geosciences*, vol. 13, pp. 1-15, 2020.

[219] I. Ahmad, D. Tang, T. Wang, M. Wang, and B. Wagan, "Precipitation trends over time using Mann-Kendall and spearmans rho tests in swat river basin, Pakistan," *Advances in Meteorology*, vol. 2015.

[220] C. Libiseller, "Comparison of methods for normalisation and trend testing of water quality data," *in 15th Annual Conference of The International Environmetrics Society*, 2004.

[221] C. Libiseller and A. Grimvall, "Performance of partial MannKendall tests for trend detection in the presence of covariates," Environmetrics: *The official journal of the International Environmetrics Society*, vol. 13, pp. 71-84, 2002.

[222] E. Hajani, A. Rahman, and E. Ishak, "Trends in extreme rainfall in the state of New South Wales, Australia," *Hydrological Sciences Journal*, vol. 62, pp. 2160-2174, 2017.

[223] S. Diatta, C. W. Diedhiou, D. M. Dione, and S. Sambou, "Spatial Variation and Trend of Extreme Precipitation in West Africa and Teleconnections with Remote Indices," *Atmosphere*, vol. 11, p. 999, 2020.

[224] J. A. Torres-Alavez, F. Giorgi, F. Kucharski, E. Coppola and L. Castro-Garca, " ENSO teleconnections in an ensemble of CORDEX-CORE regional simulations," *Climate Dynamics*, pp.1-17, 2021.

[225] O. Tomingas, "Relationship between atmospheric circulation indices and climate variability in Estonia," *Boreal Environment Research*, vol. 7, pp. 463-470, 2002.

[226] M. Vermeer and S. Rahmstorf, "Global sea level linked to global temperature," *Proceedings of the national academy of sciences*, vol. 106, pp. 21527-21532, 2009.

[227] H. Verworn, S. Krmer, M. Becker, and A. Pfister, "The impact of climate change on rainfall runoff statistics in the Emscher-Lippe region," *in Proceedings of the 11th International Conference on Urban Drainage*, 2008, pp. 1-10.

[228] S. Vishnu, P. Francis, S. Ramakrishna, and S. Shenoi, "On the relationship between the Indian summer monsoon rainfall and the EQUINOO in the CFSv2," *Climate Dynamics*, vol. 52, pp. 1263-1281, 2019.

[229] T.M. Midhuna and A.P. Dimir, " Impact of arctic oscillation on Indian winter monsoon,"*Meteorology and Atmospheric Physics*, vol. 131(4), pp. pp.1157-1167, 2019.

[230] M. M. Dogar, F. Kucharski, T. Sato, S. Mehmood, S. Ali, Z. Gong, et al., "Towards understanding the global and regional climatic impacts of Modoki magnitude," *Global and Planetary Change*, vol. 172, pp. 223-241, 2019.

[231] P. Hu, G. Feng, M. M. Dogar, J. Cheng, and G. Zhiqiang, "Joint Effect of East Asia/Pacific and Eurasian Teleconnections on the Summer Precipitation Pattern in North Asia," *Journal of Meteorological Research*, vol. 34, pp. 1-16, 2020.

[232] H. Athar, "Teleconnections and variability in observed rainfall over Saudi Arabia during 1978-2010," *Atmospheric Science Letters*, vol. 16, pp. 373-379, 2015.

[233] W. Zhang, Z. Wang, M. F. Stuecker, A. G. Turner, F.-F. Jin, and X. Geng," "Impact of ENSO longitudinal position on teleconnections to the NAO." *Climate Dynamics* vol. 52, no. 1, pp. 257-274, 2019/01/01 2019.

[234] H. Liu, K. Duan, M. Li, P. Shi, J. Yang, X.Zhang, J. Sun ," Impact of the north Atlantic oscillation on the dipole oscillation of summer precipitation over the central and eastern Tibetan Plateau." *International Journal of Climatology* 35: 4539-4546,2015.

[235] E. Aamir and I. Hassan, "The impact of climate indices on precipitation variability in Baluchistan, Pakistan," Tellus A: *Dynamic Meteorology and Oceanography*, vol. 72, pp. 1-46, 2020.

[236] L. Krishnamurthy, V. Krishnamurthy ,"Teleconnections of Indian monsoon rainfall with AMO and Atlantic tripole." *Climate Dynamics* 46:2269-2285, 2016.

[237] J. Li, J. Li, T. Li, and T. F. Au, "351-year tree ring reconstruction of the Gongga Mountains winter minimum temperature and its relationship with the Atlantic Multidecadal Oscillation,*Climatic Change* vol. 165, no. 3, p. 49, 2021.

[238] M. S Hussain, S. Kim, S. Lee S ," On the relationship between Indian ocean dipole events and the precipitation of Pakistan." *Theoretical and Applied Climatology.* https://doi.org/10.1007/s00704-016-1902-y, 2016.

[239] C. R Wu ," Interannual modulation of the Pacific decadal oscillation(PDO) on the low-latitude western North Pacific." *Prog Oceanogr* 110:4958, 2013.

[240] G. Meyers G, P. McIntosh,L. Pigot,M Pook ,"The years of El Nino, LaNina, and interactions with the tropical Indian ocean." *Journal of Climatology* 20: 2872-2880, 2007.

[241] F. Cannon, L.M Carvalho, C. Jones, J. Norris ,“ Winter westerly disturbance dynamics and precipitation in the western Himalaya and Karakoram: a wave-tracking approach.” *Theoretical and Applied Climatology* 125:2744.2016(b).

[242] A. Hannachi, I. Jolliffe, and D. Stephenson, “Empirical orthogonal functions and related techniques in atmospheric science: A review,” *International Journal of Climatology: A Journal of the Royal Meteorological Society*, vol. 27, pp. 1119-1152, 2007.

[243] H. Hefaidh and D. Mbarek, “Using Fuzzy-Improved Principal Component Analysis (PCA-IF) for Ranking of Major Accident Scenarios,” *Arabian Journal for Science and Engineering*, vol. 45, pp. 2235-2245, 2020.

[244] S. Huang, J. Ye, T. Wang, L. Jiang, X. Wu, and Y. Li, “Extracting refined low-rank features of robust PCA for human action recognition,” *Arabian Journal for Science and Engineering*, vol. 40, pp. 1427-1441, 2015.

[245] M. A. Haroon and G. Rasul, “Principal component analysis of summer rainfall and outgoing long-wave radiation over Pakistan,” *Pakistan Journal of Meteorology*, vol. 5, pp. 109-114, 2009.

[246] M. Latif, F. Syed, and A. Hannachi, “Rainfall trends in the South Asian summer monsoon and its related large-scale dynamics with focus over Pakistan,” *Climate Dynamics*, vol. 48, pp. 3565-3581, 2017.

[247] I. Roy and R. G. Tedeschi, “Influence of ENSO on regional indian summer monsoon precipitationlocal atmospheric influences or remote influence from pacific,” *Atmosphere*, vol. 7, p. 25, 2016.

[248] F. Syed, F. Giorgi, J.S Pal, K. Keay,“Regional climate model simulation of winter climate over central-southwest Asia, with emphasison NAO and ENSO effects.” *International Journal Climatology* 30: 220-235, 2010.

[249] K.A. Tamaddun, K. A. Kalra, A. Bernardez, and S. Ahmad, “Effects of ENSO on Temperature, Precipitation, and Potential Evapotranspiration of

North India's Monsoon: An Analysis of Trend and Entropy." *Water* 11(2), 189, 2019.

[250] P. S. Dutta and H. Tahbilder, "Prediction of rainfall using data mining technique over Assam," *Indian Journal of Computer Science and Engineering (IJCSE)*, vol. 5, pp. 85-90, 2014.

[251] D.M. Nielsen, A.L Belm, E. Marton, and M. Cataldi, " Dynamics-based regression models for the South Atlantic Convergence Zone," *Climate Dynamics*, vol. 52(9-10), pp. 5527-5553, 2019.

[252] D. Ramesh and B. V. Vardhan, "Analysis of crop yield prediction using data mining techniques," *International Journal of research in engineering and technology*, vol. 4, pp. 47-473, 2015.

[253] B. Ristic and N. Okello, "Sensor registration in ECEF coordinates using the MLR algorithm," *in Proceedings of the Sixth International Conference of Information Fusion*, pp. 135-142, 2003.

[254] S. J. Gaffney, A.W. Robertson, P. Smith, S. J Camargo and M. Ghil, " Probabilistic clustering of extratropical cyclones using regression mixture models," *Climate dynamics*, vol. 29(4), pp. 423-440, 2007.

[255] W. T. Zaw and T. T. Naing, "Modeling of rainfall prediction over Myanmar using polynomial regression," *International Conference on Computer Engineering and Technology* pp. 316-320, 2009.

[256] M. R. Grose, S. Foster, J. S. Risbey, S. Osbrough, and L. Wilson, " Using indices of atmospheric circulation to refine southern Australian winter rainfall climate projections " *Climate Dynamics*, vol.53(9-10), pp.5481-5493, 2019.

[257] P. Wuttichaikitcharoen and M.S. Babel," Principal component and multiple regression analyses for the estimation of suspended sediment yield in ungauged basins of Northern Thailand," *Water*, vol.6(8), pp.2412-2435, 2014.

[258] L. Yu, Z. Wu, and R. Zhang, " Partial least regression approach to forecast the East Asian winter monsoon using Eurasian snow cover and sea surface

temperature," *Climate Dynamics*, vol.51, p.45734584, 2018. https://doi.org/10 .1007/s00382-017-3757-z

[259] A. Arora. S.A., Rao, " Assessment of prediction skill in equatorial Pacific Ocean in high resolution model of CFS," *Climate Dynamics*, vol.51, 33893403 2018. https://doi.org/10.1007/s00382-018-4084-8

[260] I. M. M. Ghani and S. Ahmad, "Comparison methods of multiple linear regressions in fish landing," *Australian Journal of Basic and Applied Sciences*, vol. 5, pp. 25-30, 2011.

[261] S. K. Bhagat, T. Tiyasha, T. M. Tung, R. R. Mostafa, and Z. M. Yaseen, "Manganese (Mn) removal prediction using extreme gradient model," *Ecotoxicology and Environmental Safety*, vol. 204, p.111059, 2020.

[262] M. Niazian, S. A. Sadat-Noori, and M. Abdipour, "Artificial neural network and multiple regression analysis models to predict essential oil content of ajowan (Carum copticum L.)," *Journal of Applied Research on Medicinal and Aromatic Plants*, vol. 9, pp. 124-131, 2018.

[263] N. Zeb, M. F. Khokhar, A. Pozzer, and S. A. Khan, "Exploring the temporal trends and seasonal behaviour of tropospheric trace gases over Pakistan by exploiting satellite observations," *Atmospheric Environment*, vol. 198, pp. 279-290, 2019.

[264] Y. Pal, "Sugarcane weather relationship for north-west region U.P.," *G.B.P.U.A & T., Pantnagar*, 1995.

[265] D. A. Vaccari and J. Levri, "Multivariable empirical modeling of ALS systems using polynomials," *Life Support & Biosphere Science*, vol. 6, pp. 265-271, 1999.

[266] H. Hassani, M. Zokaei, and A. Amidi, "A new approach to polynomial regression and its application to physical growth of human height," *in Proceeding of Hawaii International Conference on Statistics, Mathematics and Related Fields*, 2003.

[267] N. Sen, "New forecast models for Indian south-west Monsoon season Rainfall," *Current Science*, vol. 84, pp. 1290-1292, 2003.

[268] N. Singhrattna, B. Rajagopalan, M. Clark, and K. Krishna Kumar, "Seasonal forecasting of Thailand summer monsoon rainfall," *International Journal of Climatology: A Journal of the Royal Meteorological Society*, vol. 25, pp. 649-664, 2005.

[269] K. T. Sohn, J. H. Lee, S. H. Lee, and C. S. Ryu, "Statistical prediction of heavy rain in South Korea," *Advances in Atmospheric Sciences*, vol. 22, pp. 703-710, 2005.

[270] W. T. Zaw and T. T. Naing, "Empirical statistical modeling of rainfall prediction over Myanmar," *World Academy of Science, Engineering and Technology*, vol. 2, pp. 500-504, 2008.

[271] M. D. Anderson, K. Sharfi, and S. E. Gholston, "Direct demand forecasting model for small urban communities using multiple linear regression," *Transportation research record*, vol. 1981, pp. 114-117, 2006.

[272] Y. Radhika and M. Shashi, "Atmospheric temperature prediction using support vector machines," *International journal of Computer Theory and Engineering*, vol. 1, p. 55, 2009.

[273] X. Chen, C. Chen, and L. Jin, "Principal component analyses in anthropological genetics," *Advances in Anthropology*, vol. 1, p. 9, 2011.

[274] A. Gomes Da Silva, and C. Moises Santos E Silva "Improving regional dynamic downscaling with multiple linear regression model using components principal analysis: precipitation over Amazon and Northeast Brazil," *Advances in Meteorology*, vol. 2014, 2014. doi:10.1155/2014/928729

[275] R. Cai, J. D. Mullen, J. C. Bergstrom, W. D. Shurley, and M. E. Wetzstein, "Using a climate index to measure crop yield response," *Journal of Agricultural and Applied Economics*, vol. 45, pp. 719-737, 2013.

[276] C. Chaleeraktrakoon and U. Khwanket, "A statistical downscaling model for extreme daily rainfalls at a single site," *in World Environmental and Water Resources Congress 2013: Showcasing the Future*, pp. 1058-1067, 2013.

[277] J. Kim, H. S. Oh, Y. Lim, and H. S. Kang, "Seasonal precipitation prediction via dataadaptive principal component regression," *International Journal of Climatology*, vol. 37, pp. 75-86, 2017.

[278] B. Pandey, M. Agrawal, and S. Singh, "Assessment of air pollution around coal mining area: emphasizing on spatial distributions, seasonal variations and heavy metals, using cluster and principal component analysis," *Atmospheric pollution Research*, vol. 5, pp. 79-86, 2014.

[279] J. T. Kellow, "Using principal components analysis in program evaluation: some practical considerations," *Journal of MultiDisciplinary Evaluation*, vol. 5, pp. 89-107, 2006.

[280] B. D. Fekedulegn, Coping with multicollinearity: An example on application of principal components regression in dendroecology vol. 721: US Department of Agriculture, Forest Service, Northeastern Research Station, 2002.

[281] A. Ul-Saufie, A. Yahya, and N. Ramli, "Improving multiple linear regression model using principal component analysis for predicting PM10 concentration in Seberang Prai, Pulau Pinang," *International Journal of Environmental Sciences*, vol. 2, pp. 403-410, 2011.

[282] M. Haque, A. Rahman, D. Hagare, and G. Kibria, "Principal component regression analysis in water demand forecasting: An application to the Blue Mountains, NSW, Australia," *Journal of Hydrology and Environment.* Res, vol. 1, pp. 49-59, 2013.

[283] R. Yadav, B. Sisodia, and S. Kumar, "Application of principal component analysis in developing statistical models to forecast crop yield using weather variables," *MAUSAM*, vol. 65, pp. 357-360, 2014.

[284] M. S. Gadiwala and F. Burke, "Climate change and precipitation in Pakistan-a meteorological prospect," *International Journal of Economic and Environmental Geology*, pp. 10-15, 2019.

[285] N. M. Razali and Y. B. Wah, "Power comparisons of shapiro-wilk, kolmogorov-smirnov, lilliefors and anderson-darling tests," *Journal of statistical Modeling and Analytics*, vol. 2, pp. 21-33, 2011.

[286] Y. Yang,T.Y Gan, and X. Tan, "Recent changing characteristics of dry and wet spells in Canada, *Climatic Change*, 165(3), pp.1-21, 2021.

[287] He, W., Xie, X., Mei, Y. et al,"Decreasing predictability as a precursor indicator for abrupt climate change, *Climate Dynamics* 56, 38993908 2021. https://doi.org/10.1007/s00382-021-05676-1

[288] K.S. Liu,J.C.L. Chan, and H. Kubota,"Meridional oscillation of tropical cyclone activity in the western North Pacific during the past 110 years,*Climatic Change* 164, 23 2021. https://doi.org/10.1007/s10584-021-02983-8

[289] La. Sorte, F.A., Johnston, A. and Ault, T.R,"Global trends in the frequency and duration of temperature extremes,*Climatic Change* 166, 1, 2021. https://doi.org/10.1007/s10584-021-03094-0

[290]van Oldenborgh, G.J., van der Wiel, K., Kew, S,"Pathways and pitfalls in extreme event attribution,*Climatic Change* 166, 13, 2021. https://doi.org/10.1007/s10584-021-03071-7

[291] Y. Zahan, R. Mahanta, P.V Rajesh,"Impact of climate change on North-East India (NEI) summer monsoon rainfall, *Climatic Change* 164, 2, 2021. https://doi.org/10.1007/s10584-021-02994-5

[292] X. Kuang, F. Schenk, R. Smittenberg, R.," Seasonal evolution differences of east Asian summer monsoon precipitation between Blling-Allerd and younger Dryas periods,*Climatic Change* 165, 19, 2021. https://doi.org/10.1007/s10584-021-03025-z

[293] G. Zanchetta,M.Bini, K. Bloomfield,"Beyond one-way determinism: San Fredianos miracle and climate change in Central and Northern Italy in late antiquity,*Climatic Change* 165, 25, 2021. https://doi.org/10.1007/s10584-021-03043-x

[294] Y.Liu, Z.Hao, X. Zhang, "Intercomparisons of multiproxy-based gridded precipitation datasets in Monsoon Asia: cross-validation and spatial patterns with different phase combinations of multidecadal oscillations,*Climatic Change* 165, 31, 2021. https://doi.org/10.1007/s10584-021-03072-6

[295] Z. Weiwei, Y. Yuda, and M. Zhimin, " Multiple movement characteristics of the Meiyu rain belt in East Asia: reconstructing historical data on the southern margin from 1861 to 2017,*Climatic Change* 165, 20, 2021. https://doi.org/10.1007/s10584-021-03007-1

[296] L. A. Alejo, V. B. Ella, R. M. Lampayan, and A. A. Delos Reyes, "Assessing the impacts of climate change on irrigation diversion water requirement in the Philippines,*Climatic Change* vol. 165, no. 3, p. 58, 2021.

[297] V. Trouet, J. Esper, N. E. Graham, A. Baker, J. D. Scourse, and D. C. Frank, "Persistent positive North Atlantic Oscillation mode dominated the medieval climate anomaly," *science*, vol. 324, pp. 78-80, 2009.

[298] Artic Oscillation (2013). Available: https://frontierscientists.com/2013/06/under-pressure-arctic-extreme-weather.[Accessed: 16-Mar-2020]

[299] D. Bahm. (2017). The Atlantic Multidecadal Oscillation (Amo): An Explanation and Analysis of Its Current State. Available:https:www.cyclonicfury.com/2017/06/29/atlantic-multidecadal-oscillation-amo-explanation-analysis-current-state.[Accessed: 16-Mar-2020]

[300] Woods Hole Oceanographic Institution (2020). Indian Ocean Dipole. Available: https://www.whoi.edu/multimedia/indian-ocean-dipole-2/.[Accessed: 16-Mar-2020]

[301] F. Pavanathara and S. Gadgil, "A note on new indices for the equatorial Indian Ocean oscillation, *Journal of Earth System Science* vol. 122, pp. 1005-1011, 08/01 2013.

[302] D. Olbers, *The Earth System* http://www.awi.defileadminuseruploadResearch/ResearchDivisions/ClimateSciences/ClimateDynamicsnew/Publications/earthsystemolbers.pdf, 03/01, 2012.[Accessed: 16-Mar-2020]

[303] C. EDWIN PINTO U., "El Nio, La Nia, ENSO, ENSO, El Nio Modoki, El Nio Canonico, El Nio Extraordinario, El Nio Godzilla, El Nio Costero, El Nio Oriental What do they really consist of and how do they affect Ecuador?", Inocar.mil.ec, 2021. [Online]. Available: https://www.inocar.mil.ec/web/index.php/articulos/770-el-nino-la-nina-enso-enos-el-nino-modoki-el-nino-canonico-el-nino-extraordinario-el-nino-godzilla-el-nino-costero-el-nino-oriental-en-que-consisten-realmente-y-como-afectan-al-ecuador. [Accessed: 16-Mar-2020].

[304] "ENSO and Pacific Decadal Oscillation: their effects on basins of the Puget Sound estuary," *University of Washington School of Oceanography* Seattle, WA.

[305] H. Chervenkov and K. Slavov, "TheilSen Estimator vs. Ordinary Least SquaresTrend Analysis for Selected ETCCDI Climate Indices," *Comptes rendus de lAcadmie bulgare des Sciences*, vol. 72, 2019.

[306] Y. Zhang, T. Liu, K. Li, and J. Zhang, "Improved visual correlation analysis for multidimensional data," *Journal of Visual Languages & Computing*, vol. 41, pp. 121-132, 2017.

[307] S. Yue, P. Pilon, and G. Cavadias, "Power of the MannKendall and Spearman's rho tests for detecting monotonic trends in hydrological series," *Journal of hydrology*, vol. 259, pp. 254-271, 2002.

[308] G. R. North, T. L. Bell, R. F. Cahalan, and F. J. Moeng, "Sampling errors in the estimation of empirical orthogonal functions," *Monthly Weather Review*, vol. 110, pp. 699-706, 1982.

[309] H.Azmat, "The influence of La-Nina phenomena on Pakistans precipitation, *Pakistan Journal of Meteorology* 1.1: 23-31, 2004.

[310] M. Adnan,N. Rehman N,MM. Sheikh,A. A. Khan, K.A Mir, M.A Khan , " Influence of natural forcing phenomena on precipitation of Pakistan, *Pakistan Journal of Meteorology* Vol. Jan;12(24), 2016.

[311] A. Chakraborty, S.K. Behera, M. Mujumdar, R. Ohba and T. Yamagata , " Diagnosis of tropospheric moisture over Saudi Arabia and influences of IOD and ENSO, *Monthly Weather Review* 134(2), pp.598-617, 2006.

[312] K. Ashok, S.K. Behera, S.A. Rao, H. Weng and T. Yamagata, " El Nino Modoki and its possible teleconnection, *Journal of Geophysical Research Oceans* 112(C11), 2007.

[313] D. Chen,J. Sun, andY. Gao, " Effects of AO on the interdecadal oscillating relationship between the ENSO and East Asian winter monsoon. , *International Journal of Climatology* 40(10), pp.4374-4383, 2020.

[314] Dandi, A. Ramu, S. Jasti, Chowdary,A. Prasanth, Pillai,NS. Sradhara Sidhan, and SSVS. Ramakrishna , "Impact of El Nio Modoki on Indian summer monsoon rainfall: Role of western north Pacific circulation in observations and CMIP5 models, *International Journal of Climatology* 40, no.4: 2117-2133, 2020.

[315] Goswami,N. Bhupendra , M. S. Madhusoodanan, C. P. Neema, and Debasis Sengupta, "A physical mechanism for North Atlantic SST influence on the Indian summer monsoon, *Geophysical Research Letters* 33, no. 2, 2006

[316] A. Mahmood, T.M Khan, N. Faisal, "Relationship between El Nino and summer monsoon rainfall over Pakistan, *Pakistan Journal of Marine Sciences* ;15(2):161-78, 2006.

[317] S.K. Behera, R. Krishnan, and T. Yamagata, "Unusual oceanatmosphere conditions in the tropical Indian Ocean during 1994, *Geophysical Research Letters* 26, no.19:3001-3004, 1999.

[318] K. Ashok,Z. Guan, and T. Yamagata, "Impact of the Indian Ocean dipole on the relationship between the Indian monsoon rainfall and ENSO, *Geophysical Research Letters* 28(23), pp.4499-4502, 2001.

[319] K. Ashok,Z. Guan,N.H. Saji, and T. Yamagata, "Individual and combined influences of ENSO and the Indian Ocean dipole on the Indian summer monsoon, *Journal of Climate* 17(16), pp.3141-3155, 2004.

[320] M.S. Hussain, S.Kim , S.Lee, " On the relationship between Indian Ocean Dipole events and the precipitation of Pakistan, *Theoretical and Applied Climatology* Oct; 130(1):673-85, 2017.

[321] B. Charlotte, V. Dhanya, and B. Mathew, "EQUINOO: The entity and validity of this oscillation to Indian monsoon, *International Joournal of Engineering and Science* 1.11 45-54, 2012.

[322] L. Krishnamurthy and V.J. Krishnamurthy , " Influence of PDO on South Asian summer monsoon and monsoonENSO relation, *Climate Dynamics* ;42(9-10):2397-410, 2014.

[323] S.S. Roy, G.B. Goodrich, R.C. Balling , " Influence of El Nino/southern oscillation, Pacific decadal oscillation, and local sea-surface temperature anomalies on peak season monsoon precipitation in India, *Climate Research*; 25(2):171-8, 2003.

[324] J. Chen and X. J. Zhang, "Challenges and potential solutions in statistical downscaling of precipitation,*Climatic Change* 165,63 2021. https://doi.org/10.1007/s10584-021-03083-3

[325] Y. Jin, X. Rong, and Z. Liu, "Potential predictability and forecast skill in ensemble climate forecast: a skill-persistence rule," *Climate dynamics*, vol. 51, pp. 2725-2742, 2018.

[326] T. Suryanarayana and P. Mistry, Principal component regression for crop yield estimation: Springer, 2016.

[327] S. Ray, "Seven Types of Regression Techniques you should know," ed, 2015.

[328] M. Bland, "Statistics Notes in the British Medical Journal," ed, 2018.

[329] D.N Moriasi, J.G Arnold, Van Liew, M. W. Bingner, R. L. Harmel, T. L.Veith, " Model evaluation guidelines for systematic quantification of accuracy in watershed simulations," *Transactions of the ASABE* , 50(3),pp.885-900, 2007.

[330] J. Singh ,H.V Knapp,J.G Arnold,M. Demissie," Hydrological modeling of the Iroquois river watershed using HSPF and SWAT 1. JAWRA," *Journal of the American Water Resources Association*, Apr; 41(2): 343-60, 2005.

[331] J.E. Nash and J.V. Sutcliffe,"River flow forecasting through conceptual models Part 1. " *Journal of Hydrology* 10(3): 282-290, 1970.

[332] P.A Francis, S.Gadgil,"A note on new indices for the equatorial Indian Ocean oscillation," *Journal of Earth System Science.* Aug 1;122(4):1005-11, 2013.

[333] S. Kumar and E. A. Chauhan, "A survey on image feature selection techniques," *International Journal of Computer Science and Information Technologies (IJCSIT)*, vol. 5, pp. 6449-6452, 2014.

[334] H.V, Gupta and P.O, Yaop,"Status of automatic calibration fro hydrologic models:Comprasion with multilevel expert calibration." *Journal of Hydrologic Enginering.* 4(2):135-143, 1999.

# Annexure A

| | | Precipitatoin Data - Barakhan (1977 to 2017) | | | | | | | | | | | |
|---|---|---|---|---|---|---|---|---|---|---|---|---|---|
| | | Jan | Feb | Mar | Apr | May | Jun | Jul | Aug | Sep | Oct | Nov | Dec |
| S. No | Years | BarakhanJan | BarakhanFeb | BarakhanMar | BarakhanApr | BarakhanMay | BarakhanJun | BarakhanJul | BarakhanAug | BarakhanSep | BarakhanOct | BarakhanNov | BarakhanDec |
| 1 | 1977 | 64.1 | 0.0 | 3.5 | 71.9 | 14.0 | 94.8 | 85.1 | 15.4 | 108.6 | 1.0 | 21.9 | 1.8 |
| 2 | 1978 | 13.0 | 64.3 | 25.2 | 36.8 | 0.7 | 53.2 | 276.7 | 57.3 | 53.6 | 0.0 | 21.2 | 0.0 |
| 3 | 1979 | 19.5 | 40.9 | 91.7 | 29.4 | 31.7 | 15.7 | 177.6 | 65.7 | 42.8 | 2.1 | 7.4 | 21.7 |
| 4 | 1980 | 20.4 | 3.6 | 57.5 | 6.9 | 9.3 | 11.4 | 215.5 | 29.1 | 12.2 | 15.3 | 5.7 | 0.0 |
| 5 | 1981 | 16.3 | 15.9 | 52.5 | 10.9 | 61.5 | 6.2 | 80.0 | 58.3 | 17.6 | 6.5 | 2.3 | 0.0 |
| 6 | 1982 | 19.2 | 52.7 | 47.6 | 20.2 | 25.6 | 19.1 | 66.6 | 65.6 | 0.1 | 18.5 | 17.3 | 38.3 |
| 7 | 1983 | 0.0 | 28.8 | 5.7 | 131.3 | 27.7 | 15.7 | 81.5 | 137.0 | 73.6 | 0.3 | 0.0 | 5.8 |
| 8 | 1984 | 11.4 | 0.0 | 24.5 | 23.1 | 0.0 | 9.7 | 180.6 | 294.3 | 70.4 | 0.0 | 0.0 | 0.0 |
| 9 | 1985 | 1.8 | 0.0 | 36.7 | 40.6 | 13.2 | 61.0 | 103.8 | 52.5 | 17.4 | 8.2 | 0.0 | 0.4 |
| 10 | 1986 | 3.6 | 22.4 | 14.2 | 13.1 | 18.4 | 12.5 | 23.4 | 129.1 | 6.2 | 0.0 | 1.4 | 0.0 |
| 11 | 1987 | 3.4 | 20.9 | 75.8 | 18.2 | 40.9 | 11.5 | 68.3 | 136.8 | 0.0 | 0.0 | 0.0 | 0.0 |
| 12 | 1988 | 18.0 | 12.3 | 55.9 | 9.8 | 1.4 | 51.0 | 65.5 | 31.9 | 12.7 | 0.0 | 14.1 | 5.2 |
| 13 | 1989 | 8.9 | 0.7 | 137.6 | 5.8 | 0.6 | 51.5 | 136.5 | 102.8 | 24.4 | 0.0 | 3.6 | 22.7 |
| 14 | 1990 | 18.3 | 51.8 | 24.9 | 54.1 | 27.2 | 42.1 | 64.0 | 155.5 | 36.0 | 0.0 | 14.5 | 2.5 |
| 15 | 1991 | 1.8 | 30.0 | 24.2 | 66.6 | 21.9 | 12.3 | 16.2 | 39.0 | 86.2 | 0.0 | 1.0 | 12.6 |
| 16 | 1992 | 50.9 | 37.0 | 31.7 | 56.5 | 38.7 | 24.4 | 144.3 | 145.1 | 47.2 | 23.0 | 4.3 | 2.2 |
| 17 | 1993 | 30.0 | 3.5 | 26.0 | 45.8 | 20.9 | 108.0 | 131.4 | 70.7 | 76.2 | 0.0 | 0.0 | 0.0 |
| 18 | 1994 | 2.3 | 56.8 | 9.4 | 30.9 | 7.0 | 17.8 | 229.1 | 96.7 | 135.5 | 2.3 | 2.1 | 11.7 |
| 19 | 1995 | 17.9 | 9.8 | 8.8 | 134.1 | 0.0 | 37.1 | 136.4 | 69.6 | 30.0 | 7.0 | 0.0 | 9.0 |
| 20 | 1996 | 12.2 | 9.0 | 17.0 | 43.0 | 10.0 | 140.9 | 113.2 | 36.0 | 17.7 | 0.0 | 0.0 | 2.0 |
| 21 | 1997 | 19.8 | 3.6 | 64.5 | 67.0 | 98.1 | 170.3 | 122.7 | 31.8 | 10.0 | 144.4 | 26.0 | 2.6 |
| 22 | 1998 | 2.0 | 12.5 | 48.1 | 28.1 | 30.6 | 40.1 | 50.8 | 55.6 | 21.1 | 10.0 | 0.0 | 0.0 |
| 23 | 1999 | 26.7 | 25.5 | 0.0 | 0.0 | 19.0 | 25.3 | 95.2 | 129.6 | 19.6 | 8.0 | 0.0 | 0.0 |
| 24 | 2000 | 8.2 | 14.5 | 4.0 | 2.0 | 6.0 | 6.6 | 63.7 | 48.5 | 25.8 | 0.0 | 0.0 | 4.4 |
| 25 | 2001 | 0.0 | 16.0 | 7.0 | 31.0 | 10.0 | 50.7 | 90.0 | 76.7 | 35.7 | 0.0 | 0.0 | 8.0 |
| 26 | 2002 | 0.0 | 10.5 | 9.0 | 5.0 | 0.0 | 9.6 | 15.0 | 26.0 | 6.0 | 5.0 | 9.0 | 3.0 |
| 27 | 2003 | 0.5 | 6.0 | 55.0 | 7.0 | 37.0 | 89.0 | 39.5 | 102.5 | 14.0 | 0.0 | 0.0 | 0.0 |
| 28 | 2004 | 46.6 | 7.0 | 0.0 | 2.5 | 6.0 | 57.0 | 53.0 | 74.0 | 3.0 | 15.0 | 13.0 | 11.0 |
| 29 | 2005 | 5.0 | 82.0 | 7.0 | 7.0 | 38.0 | 20.0 | 173.0 | 167.0 | 9.0 | 0.0 | 0.0 | 0.0 |
| 30 | 2006 | 0.0 | 4.0 | 28.0 | 17.0 | 151.0 | 79.0 | 191.0 | 96.0 | 110.0 | 47.0 | 11.0 | 50.0 |
| 31 | 2007 | 0.0 | 60.6 | 36.0 | 11.0 | 3.5 | 52.0 | 120.0 | 54.0 | 42.0 | 0.0 | 1.0 | 8.0 |
| 32 | 2008 | 14.0 | 9.0 | 18.0 | 41.0 | 63.0 | 99.0 | 47.0 | 57.0 | 13.0 | 0.0 | 0.0 | 36.0 |
| 33 | 2009 | 23.0 | 14.0 | 3.0 | 12.0 | 21.0 | 31.0 | 146.0 | 0.5 | 0.0 | 0.0 | 0.0 | 2.0 |
| 34 | 2010 | 2.0 | 3.0 | 48.0 | 6.0 | 23.0 | 46.0 | 110.0 | 140.0 | 81.0 | 11.0 | 0.0 | 0.0 |
| 35 | 2011 | 6.0 | 27.0 | 34.0 | 40.0 | 6.0 | 49.0 | 138.0 | 81.1 | 14.1 | 18.0 | 0.0 | 1.0 |
| 36 | 2012 | 4.0 | 0.1 | 1.0 | 119.1 | 5.0 | 13.1 | 138.1 | 30.2 | 51.0 | 1.0 | 0.0 | 4.0 |
| 37 | 2013 | 0.0 | 78.1 | 44.0 | 68.2 | 2.1 | 76.0 | 58.1 | 47.3 | 23.2 | 13.2 | 22.0 | 0.0 |
| 38 | 2014 | 0.0 | 18.0 | 31.2 | 35.0 | 73.0 | 23.0 | 169.2 | 107.0 | 44.2 | 0.0 | 0.0 | 0.0 |
| 39 | 2015 | 11.0 | 5.1 | 46.0 | 25.0 | 24.3 | 63.4 | 35.0 | 128.0 | 7.0 | 16.0 | 1.0 | 0.0 |
| 40 | 2016 | 1.0 | 0.0 | 22.0 | 41.5 | 16.0 | 50.2 | 110.1 | 168.6 | 11.1 | 0.0 | 0.0 | 0.0 |
| 41 | 2017 | 35.0 | 7.0 | 6.0 | 4.0 | 8.0 | 128.0 | 85.0 | 60.0 | 25.0 | 0.0 | 0.0 | 0.0 |
| | | **13.1** | **21.1** | **31.3** | **34.6** | **24.7** | **48.2** | **108.4** | **84.6** | **35.0** | **9.1** | **4.9** | **6.5** |

FIGURE A.1: Data Source: Courtesy of PMD

| | | Precipitatoin Data - Dalbandin (1977 to 2017) | | | | | | | | | | | |
|---|---|---|---|---|---|---|---|---|---|---|---|---|---|
| | | Jan | Feb | Mar | Apr | May | Jun | Jul | Aug | Sep | Oct | Nov | Dec |
| S. No | Years | DalabandinJan | DalabandinFeb | DalabandinMar | DalabandinApr | DalabandinMay | DalabandinJun | DalabandinJul | DalabandinAug | DalabandinSep | DalabandinOct | DalabandinNov | DalabandinDec |
| 1 | 1977 | 46.1 | 0.0 | 0.8 | 5.3 | 0.8 | 0.5 | 0.0 | 2.0 | 0.0 | 0.0 | 2.1 | 4.0 |
| 2 | 1978 | 0.0 | 5.1 | 4.0 | 1.0 | 0.0 | 0.0 | 32.0 | 0.0 | 0.0 | 0.0 | 10.0 | 1.0 |
| 3 | 1979 | 37.0 | 52.0 | 22.0 | 3.0 | 2.0 | 5.0 | 0.0 | 0.0 | 0.0 | 0.0 | 0.0 | 38.2 |
| 4 | 1980 | 18.0 | 1.0 | 56.5 | 1.0 | 0.0 | 0.0 | 0.0 | 0.0 | 0.0 | 24.0 | 4.2 | 7.0 |
| 5 | 1981 | 28.0 | 17.2 | 2.6 | 4.3 | 2.3 | 0.0 | 0.0 | 0.0 | 0.0 | 4.0 | 0.0 | 0.0 |
| 6 | 1982 | 13.5 | 60.7 | 71.6 | 10.7 | 6.6 | 0.0 | 0.0 | 0.0 | 0.0 | 10.2 | 8.9 | 21.5 |
| 7 | 1983 | 10.0 | 21.9 | 23.9 | 21.7 | 11.5 | 0.5 | 0.6 | 14.3 | 0.0 | 0.0 | 0.0 | 8.6 |
| 8 | 1984 | 3.2 | 0.0 | 33.9 | 0.0 | 0.0 | 0.0 | 0.0 | 0.0 | 0.0 | 0.0 | 0.0 | 5.8 |
| 9 | 1985 | 19.2 | 0.0 | 0.0 | 5.8 | 0.0 | 0.0 | 0.0 | 0.0 | 0.0 | 0.0 | 0.0 | 0.8 |
| 10 | 1986 | 9.6 | 22.2 | 0.0 | 0.0 | 0.0 | 8.8 | 0.0 | 2.7 | 0.0 | 0.0 | 13.1 | 4.2 |
| 11 | 1987 | 1.7 | 21.1 | 81.5 | 0.0 | 1.7 | 0.3 | 0.0 | 0.0 | 0.0 | 0.0 | 0.0 | 0.0 |
| 12 | 1988 | 9.0 | 2.8 | 12.8 | 0.0 | 0.0 | 0.0 | 5.5 | 0.0 | 4.0 | 0.0 | 0.0 | 0.5 |
| 13 | 1989 | 1.6 | 21.2 | 14.3 | 0.9 | 5.2 | 0.0 | 0.0 | 0.0 | 0.0 | 0.0 | 2.7 | 11.9 |
| 14 | 1990 | 55.6 | 61.3 | 7.0 | 6.5 | 0.0 | 0.0 | 0.0 | 1.8 | 0.0 | 0.0 | 12.4 | 14.6 |
| 15 | 1991 | 11.0 | 21.8 | 69.7 | 3.0 | 4.2 | 0.0 | 0.0 | 0.0 | 0.0 | 0.0 | 2.6 | 6.8 |
| 16 | 1992 | 20.4 | 1.3 | 11.3 | 33.5 | 4.3 | 0.0 | 0.0 | 2.8 | 0.0 | 10.0 | 0.0 | 20.8 |
| 17 | 1993 | 47.6 | 0.0 | 19.7 | 0.0 | 0.0 | 2.2 | 0.0 | 0.0 | 0.0 | 0.0 | 0.0 | 0.0 |
| 18 | 1994 | 15.0 | 30.2 | 18.6 | 7.5 | 3.2 | 0.0 | 6.4 | 0.0 | 0.0 | 3.5 | 0.0 | 3.1 |
| 19 | 1995 | 2.0 | 9.6 | 25.0 | 15.8 | 0.0 | 0.0 | 16.4 | 0.0 | 0.0 | 0.0 | 3.2 | 81.6 |
| 20 | 1996 | 32.0 | 60.9 | 24.5 | 0.0 | 0.0 | 2.2 | 0.0 | 0.0 | 0.0 | 0.0 | 0.0 | 3.5 |
| 21 | 1997 | 39.1 | 3.0 | 16.0 | 4.0 | 6.4 | 0.0 | 0.0 | 0.0 | 0.0 | 8.3 | 42.9 | 1.6 |
| 22 | 1998 | 31.1 | 2.0 | 35.7 | 2.0 | 0.0 | 0.0 | 0.0 | 0.0 | 0.0 | 4.0 | 0.0 | 0.0 |
| 23 | 1999 | 26.0 | 40.7 | 8.2 | 0.0 | 0.0 | 0.0 | 0.0 | 0.0 | 0.0 | 0.0 | 0.0 | 0.0 |
| 24 | 2000 | 3.0 | 0.0 | 0.0 | 0.0 | 0.0 | 0.0 | 0.0 | 0.0 | 0.0 | 0.0 | 0.0 | 0.5 |
| 25 | 2001 | 0.0 | 0.0 | 14.3 | 18.0 | 0.0 | 0.0 | 0.0 | 0.0 | 0.0 | 0.0 | 0.0 | 0.0 |
| 26 | 2002 | 0.0 | 0.0 | 0.0 | 2.0 | 0.0 | 0.0 | 0.0 | 0.0 | 0.0 | 0.0 | 5.0 | 0.0 |
| 27 | 2003 | 36.0 | 1.7 | 35.3 | 13.5 | 0.0 | 0.0 | 87.4 | 0.0 | 0.0 | 0.0 | 0.0 | 0.0 |
| 28 | 2004 | 16.2 | 0.0 | 0.0 | 0.0 | 0.0 | 0.0 | 0.0 | 0.0 | 0.0 | 0.0 | 0.0 | 70.0 |
| 29 | 2005 | 0.0 | 45.1 | 75.4 | 6.2 | 0.0 | 0.0 | 0.0 | 0.0 | 0.0 | 0.0 | 0.0 | 0.0 |
| 30 | 2006 | 0.0 | 6.0 | 5.2 | 1.0 | 0.0 | 0.0 | 0.0 | 0.0 | 1.2 | 0.0 | 11.1 | 42.6 |
| 31 | 2007 | 7.2 | 20.1 | 16.8 | 5.5 | 0.0 | 103.2 | 0.0 | 0.0 | 0.0 | 0.0 | 0.0 | 1.0 |
| 32 | 2008 | 70.0 | 2.0 | 0.0 | 0.0 | 0.0 | 0.0 | 0.0 | 1.7 | 0.0 | 0.0 | 0.0 | 9.0 |
| 33 | 2009 | 6.9 | 18.0 | 1.0 | 8.5 | 0.0 | 0.0 | 4.0 | 0.0 | 0.0 | 0.0 | 0.0 | 24.0 |
| 34 | 2010 | 4.0 | 9.0 | 0.0 | 0.0 | 4.0 | 0.0 | 0.0 | 0.0 | 0.0 | 3.0 | 0.0 | 0.0 |
| 35 | 2011 | 3.4 | 47.8 | 5.1 | 0.0 | 2.0 | 0.0 | 0.0 | 0.0 | 0.0 | 11.0 | 0.0 | 0.0 |
| 36 | 2012 | 19.5 | 2.0 | 0.0 | 1.6 | 0.0 | 0.0 | 0.0 | 0.0 | 0.0 | 0.0 | 0.0 | 1.0 |
| 37 | 2013 | 0.0 | 31.1 | 49.1 | 0.2 | 0.0 | 0.0 | 0.0 | 2.0 | 0.0 | 0.0 | 7.0 | 1.0 |
| 38 | 2014 | 14.1 | 8.1 | 23.2 | 9.3 | 0.0 | 0.1 | 0.0 | 0.0 | 0.0 | 0.0 | 0.0 | 0.0 |
| 39 | 2015 | 0.2 | 11.1 | 13.1 | 1.9 | 0.1 | 1.8 | 0.0 | 0.0 | 0.0 | 12.1 | 0.0 | 0.0 |
| 40 | 2016 | 0.2 | 0 | 41.6 | 4.2 | 0 | 0.1 | 0 | 0 | 0 | 0 | 0 | 0 |
| 41 | 2017 | 32.1 | 0.03 | 0.03 | 0 | 0 | 0 | 0 | 0 | 0 | 0 | 1.01 | 0 |
| | | **16.8** | **16.0** | **20.5** | **4.8** | **1.3** | **3.0** | **3.7** | **0.7** | **0.1** | **2.2** | **3.1** | **9.4** |

FIGURE A.2: Data Source: Courtesy of PMD

| | | Precipitatoin Data - Jiwani (1977 to 2017) | | | | | | | | | | | |
|---|---|---|---|---|---|---|---|---|---|---|---|---|---|
| | | Jan | Feb | Mar | Apr | May | Jun | Jul | Aug | Sep | Oct | Nov | Dec |
| S.no | Years | JiwaniJan | JiwaniFeb | JiwaniMar | JiwaniApr | JiwaniMay | JiwaniJun | JiwaniJul | JiwaniAug | JiwaniSep | JiwaniOct | JiwaniNov | JiwaniDec |
| 1 | 1977 | 50.5 | 7.1 | 0.0 | 0.0 | 0.0 | 12.9 | 0.0 | 3.8 | 0.0 | 0.0 | 17.2 | 5.0 |
| 2 | 1978 | 0.0 | 18.5 | 0.0 | 0.0 | 0.0 | 0.0 | 30.0 | 0.0 | 0.0 | 0.0 | 0.0 | 33.0 |
| 3 | 1979 | 23.7 | 18.0 | 0.0 | 0.0 | 0.0 | 0.1 | 0.0 | 0.0 | 0.0 | 1.0 | 0.0 | 97.0 |
| 4 | 1980 | 22.4 | 0.2 | 8.0 | 0.0 | 0.0 | 0.0 | 0.0 | 0.0 | 0.0 | 4.0 | 0.0 | 0.0 |
| 5 | 1981 | 0.2 | 0.0 | 21.7 | 15.0 | 0.0 | 0.0 | 0.0 | 0.0 | 0.0 | 0.0 | 0.0 | 12.8 |
| 6 | 1982 | 139.0 | 172.9 | 6.0 | 8.9 | 5.4 | 0.0 | 0.0 | 0.0 | 0.0 | 0.0 | 7.0 | 47.2 |
| 7 | 1983 | 6.2 | 69.5 | 2.7 | 14.7 | 0.0 | 0.0 | 0.0 | 29.8 | 0.0 | 0.0 | 0.0 | 19.0 |
| 8 | 1984 | 96.5 | 0.0 | 16.0 | 0.0 | 0.0 | 0.0 | 0.0 | 1.0 | 0.0 | 0.0 | 0.0 | 0.8 |
| 9 | 1985 | 12.6 | 0.0 | 7.2 | 0.0 | 0.0 | 0.0 | 0.0 | 0.0 | 0.0 | 0.0 | 0.0 | 12.0 |
| 10 | 1986 | 0.0 | 265.5 | 6.0 | 0.0 | 0.0 | 6.0 | 0.0 | 13.7 | 0.0 | 0.0 | 35.0 | 2.1 |
| 11 | 1987 | 0.0 | 154.0 | 26.5 | 5.0 | 0.0 | 0.0 | 0.0 | 0.0 | 0.0 | 0.0 | 0.0 | 9.0 |
| 12 | 1988 | 0.2 | 28.0 | 0.0 | 0.0 | 0.0 | 0.0 | 0.0 | 0.0 | 0.0 | 0.0 | 0.0 | 0.0 |
| 13 | 1989 | 0.0 | 0.7 | 33.3 | 0.0 | 0.0 | 0.0 | 0.0 | 0.0 | 0.0 | 0.0 | 0.0 | 142.8 |
| 14 | 1990 | 12.4 | 30.0 | 0.0 | 0.0 | 0.0 | 0.0 | 0.0 | 0.0 | 0.0 | 0.0 | 14.2 | 0.0 |
| 15 | 1991 | 22.5 | 0.0 | 74.8 | 1.2 | 0.0 | 0.0 | 0.0 | 0.0 | 0.0 | 0.0 | 6.5 | 0.4 |
| 16 | 1992 | 32.5 | 20.0 | 12.1 | 0.0 | 0.0 | 0.0 | 0.0 | 0.0 | 0.0 | 0.0 | 0.0 | 32.0 |
| 17 | 1993 | 25.0 | 0.0 | 2.0 | 0.0 | 0.0 | 0.0 | 0.0 | 0.0 | 0.0 | 0.0 | 0.0 | 0.0 |
| 18 | 1994 | 18.7 | 0.0 | 0.0 | 50.0 | 0.0 | 0.0 | 28.5 | 11.0 | 0.0 | 0.0 | 0.0 | 2.4 |
| 19 | 1995 | 0.0 | 32.0 | 52.0 | 0.0 | 0.0 | 0.0 | 39.7 | 0.0 | 0.0 | 0.0 | 0.0 | 113.8 |
| 20 | 1996 | 19.2 | 0.0 | 7.0 | 0.0 | 0.0 | 0.0 | 0.0 | 0.0 | 0.0 | 0.0 | 0.0 | 25.7 |
| 21 | 1997 | 27.1 | 0.0 | 64.3 | 0.0 | 0.0 | 7.0 | 1.3 | 3.8 | 0.0 | 39.4 | 24.4 | 116.3 |
| 22 | 1998 | 26.0 | 28.0 | 0.0 | 0.0 | 0.0 | 0.0 | 0.9 | 0.0 | 0.0 | 0.0 | 0.0 | 0.0 |
| 23 | 1999 | 0.0 | 7.1 | 16.9 | 0.0 | 0.0 | 0.0 | 0.0 | 0.0 | 0.0 | 0.0 | 0.0 | 0.0 |
| 24 | 2000 | 0.0 | 0.0 | 0.0 | 0.0 | 0.0 | 0.0 | 0.0 | 0.0 | 0.0 | 0.0 | 0.0 | 6.0 |
| 25 | 2001 | 0.0 | 0.0 | 0.0 | 0.0 | 0.0 | 0.0 | 9.0 | 0.0 | 0.0 | 0.0 | 0.0 | 0.0 |
| 26 | 2002 | 0.0 | 0.0 | 0.0 | 0.0 | 0.0 | 0.0 | 0.0 | 7.5 | 0.0 | 0.0 | 17.6 | 0.0 |
| 27 | 2003 | 47.3 | 0.2 | 0.0 | 0.4 | 0.0 | 0.0 | 14.5 | 3.4 | 0.0 | 0.0 | 0.0 | 0.0 |
| 28 | 2004 | 55.0 | 0.0 | 0.0 | 0.0 | 0.0 | 0.0 | 0.0 | 0.0 | 0.0 | 0.0 | 0.0 | 41.0 |
| 29 | 2005 | 50.0 | 3.2 | 120.0 | 0.0 | 0.0 | 0.0 | 0.0 | 0.0 | 0.0 | 0.0 | 0.0 | 0.0 |
| 30 | 2006 | 0.0 | 21.0 | 1.0 | 0.0 | 0.0 | 0.0 | 0.0 | 0.0 | 0.0 | 0.0 | 0.0 | 72.0 |
| 31 | 2007 | 0.0 | 0.0 | 0.0 | 0.0 | 0.0 | 92.0 | 0.0 | 0.0 | 0.0 | 0.0 | 0.0 | 0.0 |
| 32 | 2008 | 16.0 | 0.0 | 0.0 | 0.0 | 0.0 | 0.0 | 0.0 | 9.0 | 0.0 | 0.0 | 0.0 | 28.0 |
| 33 | 2009 | 113.0 | 0.0 | 0.0 | 10.0 | 0.0 | 0.0 | 0.0 | 0.0 | 0.0 | 0.0 | 0.0 | 11.0 |
| 34 | 2010 | 9.0 | 0.0 | 0.0 | 0.0 | 0.0 | 194.0 | 0.0 | 0.0 | 0.0 | 0.0 | 0.0 | 0.0 |
| 35 | 2011 | 2.0 | 2.0 | 0.0 | 0.0 | 0.0 | 0.0 | 0.0 | 0.0 | 0.0 | 0.0 | 0.0 | 0.0 |
| 36 | 2012 | 20.0 | 0.0 | 0.0 | 0.0 | 0.0 | 0.0 | 0.0 | 0.0 | 0.0 | 0.0 | 0.0 | 0.0 |
| 37 | 2013 | 0.0 | 33.0 | 0.0 | 45.0 | 0.0 | 0.0 | 0.0 | 13.0 | 0.0 | 0.0 | 24.0 | 0.0 |
| 38 | 2014 | 39.0 | 6.0 | 4.0 | 0.0 | 0.0 | 0.0 | 0.0 | 0.0 | 0.0 | 0.0 | 0.0 | 0.0 |
| 39 | 2015 | 19.0 | 5.0 | 85.0 | 0.0 | 0.0 | 0.0 | 0.0 | 0.0 | 0.0 | 2.0 | 0.0 | 0.0 |
| 40 | 2016 | 0 | 0 | 15 | 0 | 0 | 0 | 0 | 0 | 0 | 0 | 0 | 0 |
| 41 | 2017 | 33 | 0 | 3 | 0 | 0 | 0 | 0 | 0 | 0 | 0 | 0 | 0 |
| | | **22.9** | **22.5** | **14.3** | **3.7** | **0.1** | **7.6** | **3.0** | **2.3** | **0.0** | **1.1** | **3.6** | **20.2** |

FIGURE A.3: Data Source: Courtesy of PMD

| | | Precipitatoin Data - Kalat (1977 to 2017) | | | | | | | | | | | |
|---|---|---|---|---|---|---|---|---|---|---|---|---|---|
| | | Jan | Feb | Mar | Apr | May | Jun | Jul | Aug | Sep | Oct | Nov | Dec |
| S.no | Years | Kalat Jan | Kalat Feb | Kalat Mar | Kalat Apr | Kalat May | Kalat Jun | Kalat Jul | Kalat Aug | Kalat Sep | Kalat Oct | Kalat Nov | Kalat Dec |
| 1 | 1977 | 11.1 | 0.9 | 0.0 | 3.4 | 0.0 | 7.6 | 0.0 | 3.0 | 0.0 | 0.0 | 0.0 | 0.0 |
| 2 | 1978 | 17.5 | 33.1 | 2.8 | 21.5 | 0.0 | 0.0 | 47.9 | 0.0 | 0.0 | 0.0 | 0.0 | 0.0 |
| 3 | 1979 | 0.0 | 14.2 | 0.0 | 0.0 | 0.0 | 0.0 | 0.0 | 0.0 | 0.0 | 0.0 | 0.0 | 0.0 |
| 4 | 1980 | 9.4 | 0.0 | 0.0 | 0.0 | 0.0 | 0.0 | 0.0 | 0.0 | 0.0 | 25.0 | 0.0 | 16.7 |
| 5 | 1981 | 0.0 | 0.0 | 0.0 | 0.0 | 0.0 | 0.0 | 16.5 | 0.0 | 0.0 | 6.0 | 0.5 | 15.2 |
| 6 | 1982 | 97.7 | 103.1 | 117.5 | 14.9 | 10.9 | 0.0 | 5.5 | 33.1 | 0.0 | 55.0 | 12.8 | 96.4 |
| 7 | 1983 | 36.7 | 43.8 | 30.1 | 65.7 | 24.3 | 0.0 | 20.2 | 114.3 | 5.1 | 0.0 | 0.2 | 31.8 |
| 8 | 1984 | 32.2 | 10.5 | 19.8 | 0.0 | 0.0 | 0.0 | 3.6 | 5.2 | 0.0 | 0.0 | 0.2 | 11.7 |
| 9 | 1985 | 35.2 | 0.0 | 4.8 | 34.3 | 0.2 | 0.0 | 24.3 | 42.6 | 0.0 | 0.0 | 0.0 | 25.1 |
| 10 | 1986 | 8.8 | 55.6 | 48.4 | 4.6 | 0.0 | 1.1 | 18.7 | 75.8 | 0.0 | 0.0 | 10.6 | 2.3 |
| 11 | 1987 | 21.7 | 19.3 | 88.6 | 1.2 | 15.2 | 1.7 | 0.0 | 10.6 | 0.0 | 0.0 | 0.0 | 0.0 |
| 12 | 1988 | 18.0 | 11.4 | 61.7 | 5.9 | 0.0 | 0.5 | 90.1 | 0.0 | 0.1 | 0.0 | 0.0 | 5.4 |
| 13 | 1989 | 31.3 | 14.4 | 97.9 | 1.3 | 0.0 | 3.2 | 67.1 | 3.3 | 0.0 | 0.0 | 7.4 | 29.4 |
| 14 | 1990 | 88.6 | 105.6 | 50.5 | 13.4 | 3.2 | 0.2 | 0.0 | 13.0 | 0.0 | 0.0 | 6.3 | 28.3 |
| 15 | 1991 | 60.2 | 70.1 | 73.1 | 19.1 | 0.0 | 0.0 | 0.2 | 0.1 | 0.2 | 0.0 | 13.4 | 14.7 |
| 16 | 1992 | 76.6 | 56.2 | 27.9 | 31.5 | 16.2 | 0.0 | 52.8 | 16.4 | 0.0 | 4.6 | 0.0 | 14.7 |
| 17 | 1993 | 78.5 | 9.9 | 20.4 | 8.8 | 1.2 | 0.0 | 3.8 | 0.5 | 0.0 | 0.0 | 0.0 | 0.0 |
| 18 | 1994 | 0.5 | 32.3 | 1.6 | 4.7 | 7.1 | 0.0 | 58.3 | 24.9 | 13.7 | 0.0 | 1.4 | 1.3 |
| 19 | 1995 | 1.4 | 39.0 | 3.5 | 30.3 | 0.0 | 0.0 | 26.8 | 3.7 | 0.0 | 0.0 | 3.0 | 122.5 |
| 20 | 1996 | 57.8 | 93.0 | 26.0 | 9.9 | 10.7 | 9.2 | 0.0 | 0.0 | 0.6 | 5.2 | 0.0 | 24.2 |
| 21 | 1997 | 72.2 | 5.0 | 12.6 | 6.0 | 0.0 | 72.0 | 74.6 | 11.5 | 0.0 | 104.9 | 72.1 | 546.0 |
| 22 | 1998 | 125.8 | 26.0 | 105.0 | 0.0 | 0.0 | 30.5 | 30.0 | 0.0 | 0.0 | 0.0 | 0.0 | 54.6 |
| 23 | 1999 | 38.0 | 50.5 | 19.0 | 0.0 | 49.0 | 13.0 | 6.0 | 0.0 | 2.3 | 0.0 | 7.5 | 0.0 |
| 24 | 2000 | 20.7 | 45.9 | 0.0 | 0.0 | 1.0 | 0.0 | 0.0 | 12.2 | 1.2 | 0.0 | 10.0 | 0.0 |
| 25 | 2001 | 0.7 | 21.7 | 8.0 | 16.7 | 0.0 | 7.2 | 14.2 | 5.0 | 0.0 | 0.0 | 0.0 | 12.0 |
| 26 | 2002 | 17.6 | 13.2 | 45.5 | 5.0 | 0.0 | 0.0 | 0.0 | 7.0 | 0.0 | 0.0 | 22.5 | 18.0 |
| 27 | 2003 | 21.0 | 38.0 | 21.0 | 1.0 | 0.0 | 0.0 | 68.0 | 0.0 | 0.0 | 0.0 | 0.0 | 0.0 |
| 28 | 2004 | 75.4 | 3.0 | 0.0 | 0.0 | 0.0 | 1.4 | 0.0 | 0.0 | 0.0 | 0.0 | 2.0 | 13.0 |
| 29 | 2005 | 21.0 | 168.2 | 45.2 | 0.0 | 7.9 | 3.5 | 0.0 | 0.0 | 0.0 | 0.0 | 0.0 | 0.0 |
| 30 | 2006 | 10.6 | 3.1 | 18.6 | 2.0 | 0.0 | 0.0 | 9.6 | 32.2 | 0.0 | 0.0 | 14.2 | 72.9 |
| 31 | 2007 | 14.5 | 70.5 | 36.7 | 14.0 | 0.0 | 95.8 | 11.1 | 10.6 | 0.0 | 0.0 | 0.0 | 1.1 |
| 32 | 2008 | 133.4 | 13.0 | 0.0 | 3.0 | 2.0 | 2.0 | 4.5 | 33.5 | 0.0 | 0.0 | 0.0 | 29.0 |
| 33 | 2009 | 71.9 | 13.0 | 30.7 | 10.1 | 2.0 | 0.0 | 9.0 | 3.0 | 0.0 | 0.0 | 0.0 | 37.0 |
| 34 | 2010 | 2.0 | 28.0 | 7.0 | 4.0 | 3.0 | 0.0 | 2.0 | 1.0 | 0.0 | 0.0 | 0.0 | 0.0 |
| 35 | 2011 | 9.0 | 106.0 | 74.0 | 43.0 | 1.0 | 0.0 | 0.0 | 53.0 | 147.0 | 3.0 | 10.0 | 3.0 |
| 36 | 2012 | 42.0 | 25.0 | 20.0 | 52.0 | 1.0 | 0.0 | 0.0 | 0.0 | 19.0 | 0.0 | 0.0 | 15.0 |
| 37 | 2013 | 0.0 | 133.1 | 41.0 | 12.0 | 0.0 | 12.0 | 4.0 | 36.0 | 0.0 | 0.0 | 9.0 | 0.0 |
| 38 | 2014 | 7.0 | 63.0 | 42.0 | 11.3 | 2.0 | 0.0 | 0.0 | 0.0 | 0.0 | 0.0 | 26.0 | 0.0 |
| 39 | 2015 | 0.0 | 0.0 | 1.4 | 0.0 | 0.0 | 0.0 | 0.0 | 0.0 | 0.0 | 1.1 | 0.1 | 0.0 |
| 40 | 2016 | 8 | 0 | 70 | 0 | 0 | 12 | 0 | 0 | 0 | 0 | 0 | 0 |
| 41 | 2017 | 49 | 10 | 0 | 0 | 0 | 0 | 0 | 0 | 0 | 0 | 7 | 0 |
| | | **34.7** | **37.8** | **31.0** | **11.0** | **3.9** | **6.7** | **16.3** | **13.4** | **4.6** | **5.0** | **5.8** | **30.3** |

FIGURE A.4: Data Source: Courtesy of PMD

| | | Precipitatoin Data - Khuzdar (1977 to 2017) | | | | | | | | | | | |
|---|---|---|---|---|---|---|---|---|---|---|---|---|---|
| | | Jan | Feb | Mar | Apr | May | Jun | Jul | Aug | Sep | Oct | Nov | Dec |
| S.no | Years | KhuzdarJan | KhuzdarFeb | KhuzdarMar | KhuzdarApr | KhuzdarMay | KhuzdarJun | KhuzdarJul | KhuzdarAug | KhuzdarSep | KhuzdarOct | KhuzdarNov | KhuzdarDec |
| 1 | 1977 | 29.6 | 0.0 | 0.0 | 9.4 | 57.3 | 108.2 | 15.2 | 24.9 | 6.1 | 0.0 | 1.8 | 17.2 |
| 2 | 1978 | 16.5 | 31.9 | 9.6 | 22.0 | 0.0 | 23.7 | 108.3 | 43.9 | 10.0 | 0.0 | 17.5 | 0.0 |
| 3 | 1979 | 1.5 | 102.7 | 123.4 | 3.1 | 0.6 | 0.3 | 16.0 | 34.1 | 0.0 | 19.2 | 1.1 | 33.9 |
| 4 | 1980 | 9.4 | 6.4 | 78.1 | 4.8 | 4.1 | 10.4 | 2.0 | 0.0 | 10.9 | 22.9 | 26.8 | 16.7 |
| 5 | 1981 | 3.1 | 46.6 | 46.4 | 15.0 | 13.1 | 0.9 | 45.2 | 72.9 | 5.1 | 2.0 | 0.0 | 0.0 |
| 6 | 1982 | 25.0 | 76.8 | 34.0 | 21.5 | 27.8 | 0.0 | 13.3 | 87.1 | 0.0 | 50.2 | 1.7 | 69.4 |
| 7 | 1983 | 16.9 | 31.5 | 3.7 | 9.8 | 36.4 | 10.7 | 42.1 | 112.4 | 38.6 | 5.1 | 0.0 | 30.1 |
| 8 | 1984 | 10.5 | 0.5 | 10.9 | 7.5 | 0.0 | 0.0 | 13.3 | 222.9 | 0.0 | 0.0 | 0.0 | 2.7 |
| 9 | 1985 | 17.2 | 0.0 | 7.5 | 45.7 | 0.9 | 7.9 | 63.7 | 44.3 | 0.0 | 0.0 | 0.0 | 1.3 |
| 10 | 1986 | 0.0 | 30.9 | 15.9 | 0.0 | 0.0 | 14.9 | 55.5 | 118.5 | 0.0 | 0.0 | 3.0 | 0.0 |
| 11 | 1987 | 3.6 | 25.7 | 60.3 | 0.1 | 88.2 | 8.7 | 0.0 | 30.5 | 0.8 | 0.0 | 0.0 | 0.0 |
| 12 | 1988 | 12.9 | 17.1 | 8.7 | 3.8 | 0.0 | 9.8 | 197.8 | 80.9 | 6.3 | 0.0 | 7.0 | 3.6 |
| 13 | 1989 | 1.2 | 1.4 | 76.5 | 0.0 | 0.0 | 21.5 | 75.8 | 89.8 | 0.0 | 0.0 | 25.0 | 28.8 |
| 14 | 1990 | 20.7 | 55.7 | 4.0 | 8.7 | 14.8 | 0.8 | 10.0 | 53.5 | 3.1 | 0.0 | 9.3 | 25.0 |
| 15 | 1991 | 20.8 | 53.2 | 29.5 | 29.0 | 10.0 | 0.0 | 0.0 | 58.9 | 25.0 | 0.0 | 1.2 | 2.2 |
| 16 | 1992 | 149.9 | 75.7 | 9.2 | 41.3 | 0.0 | 0.0 | 100.2 | 57.2 | 0.0 | 2.2 | 0.5 | 8.6 |
| 17 | 1993 | 29.8 | 22.6 | 17.5 | 6.0 | 8.3 | 4.6 | 23.1 | 35.0 | 11.6 | 0.0 | 0.0 | 0.0 |
| 18 | 1994 | 5.0 | 69.2 | 6.6 | 64.5 | 12.9 | 2.4 | 190.7 | 150.3 | 41.0 | 0.0 | 0.0 | 52.1 |
| 19 | 1995 | 17.5 | 21.3 | 6.6 | 73.9 | 2.1 | 3.1 | 368.0 | 51.0 | 0.0 | 4.7 | 0.2 | 29.8 |
| 20 | 1996 | 31.2 | 54.0 | 10.0 | 0.0 | 68.2 | 63.3 | 20.0 | 2.6 | 1.0 | 0.0 | 0.0 | 12.0 |
| 21 | 1997 | 29.6 | 0.0 | 71.5 | 9.1 | 0.3 | 18.5 | 73.5 | 18.0 | 9.0 | 87.0 | 34.5 | 6.0 |
| 22 | 1998 | 20.0 | 0.0 | 59.0 | 37.0 | 4.0 | 46.0 | 44.0 | 0.0 | 6.0 | 4.5 | 0.0 | 0.0 |
| 23 | 1999 | 11.0 | 57.0 | 18.0 | 0.0 | 20.0 | 0.0 | 0.0 | 24.0 | 15.0 | 25.0 | 0.0 | 0.0 |
| 24 | 2000 | 9.6 | 22.2 | 0.0 | 0.0 | 29.0 | 0.0 | 27.7 | 35.1 | 0.0 | 0.0 | 4.3 | 5.3 |
| 25 | 2001 | 0.0 | 1.2 | 0.0 | 36.1 | 0.0 | 1.7 | 48.4 | 72.4 | 2.5 | 0.0 | 0.0 | 3.0 |
| 26 | 2002 | 0.0 | 9.2 | 3.4 | 1.5 | 0.0 | 0.0 | 2.0 | 2.0 | 0.0 | 0.0 | 17.7 | 16.5 |
| 27 | 2003 | 14.5 | 15.3 | 18.2 | 12.7 | 3.0 | 0.0 | 111.9 | 20.6 | 0.0 | 0.0 | 2.7 | 0.0 |
| 28 | 2004 | 21.2 | 0.0 | 0.0 | 0.0 | 4.4 | 3.4 | 21.7 | 31.2 | 8.4 | 0.0 | 0.0 | 2.0 |
| 29 | 2005 | 8.3 | 104.8 | 68.5 | 17.7 | 62.0 | 3.8 | 38.3 | 35.9 | 43.8 | 0.0 | 0.0 | 0.0 |
| 30 | 2006 | 3.1 | 4.8 | 25.0 | 9.0 | 10.2 | 24.6 | 30.8 | 39.9 | 8.1 | 28.9 | 3.2 | 81.0 |
| 31 | 2007 | 0.0 | 23.8 | 36.5 | 3.9 | 0.0 | 137.2 | 35.3 | 35.1 | 1.3 | 0.0 | 0.0 | 1.2 |
| 32 | 2008 | 14.4 | 10.0 | 0.0 | 22.7 | 6.6 | 18.7 | 43.9 | 67.8 | 8.4 | 0.0 | 0.0 | 109.7 |
| 33 | 2009 | 50.8 | 7.3 | 21.2 | 1.8 | 0.0 | 0.0 | 29.0 | 59.3 | 6.7 | 0.0 | 0.0 | 41.0 |
| 34 | 2010 | 4.8 | 8.8 | 0.0 | 7.7 | 19.5 | 3.5 | 25.7 | 89.0 | 0.2 | 0.0 | 0.0 | 0.0 |
| 35 | 2011 | 7.9 | 44.1 | 86.7 | 64.6 | 14.2 | 0.0 | 31.0 | 88.4 | 30.4 | 0.5 | 0.0 | 2.2 |
| 36 | 2012 | 15.0 | 3.0 | 20.0 | 25.2 | 25.0 | 2.0 | 5.4 | 51.0 | 35.0 | 0.0 | 0.0 | 0.1 |
| 37 | 2013 | 0.0 | 133.0 | 46.0 | 46.7 | 0.2 | 16.8 | 37.5 | 187.5 | 0.0 | 0.0 | 13.5 | 0.0 |
| 38 | 2014 | 0.0 | 75.3 | 60.1 | 0.0 | 22.0 | 0.0 | 0.0 | 2.7 | 0.0 | 0.0 | 0.0 | 0.0 |
| 39 | 2015 | 10.0 | 10.0 | 28.2 | 7.4 | 2.0 | 25.8 | 15.2 | 32.2 | 0.0 | 13.4 | 6.1 | 0.0 |
| 40 | 2016 | 0 | 0 | 66.6 | 1 | 2.1 | 37.1 | 37.6 | 43.5 | 37 | 0 | 0 | 0 |
| 41 | 2017 | 32 | 12 | 15 | 0 | 8 | 47 | 78.8 | 14.7 | 0 | 0 | 0 | 0 |
| | | **16.5** | **30.9** | **29.3** | **16.3** | **14.1** | **16.5** | **51.2** | **56.6** | **9.1** | **6.5** | **4.3** | **14.7** |

FIGURE A.5: Data Source: Courtesy of PMD

| | | Precipitatoin Data - Lasbella (1977 to 2017) | | | | | | | | | | | |
|---|---|---|---|---|---|---|---|---|---|---|---|---|---|
| | | Jan | Feb | Mar | Apr | May | Jun | Jul | Aug | Sep | Oct | Nov | Dec |
| S.no | Years | Lasbella Jan | Lasbella Feb | Lasbella Mar | Lasbella Apr | Lasbella May | Lasbella Jun | Lasbella Jul | Lasbella Aug | Lasbella Sep | Lasbella Oct | Lasbella Nov | Lasbella Dec |
| 1 | 1977 | 10.9 | 4.0 | 0.7 | 3.4 | 12.5 | 28.4 | 262.4 | 20.8 | 89.0 | 2.6 | 2.2 | 0.0 |
| 2 | 1978 | 8.3 | 7.5 | 0.7 | 1.6 | 12.5 | 3.9 | 252.6 | 189.6 | 0.0 | 2.5 | 2.5 | 0.0 |
| 3 | 1979 | 1.4 | 73.5 | 0.7 | 1.6 | 12.5 | 3.2 | 0.0 | 182.1 | 0.0 | 3.9 | 1.0 | 5.0 |
| 4 | 1980 | 0.0 | 2.6 | 6.8 | 1.6 | 12.5 | 49.5 | 4.6 | 0.0 | 0.0 | 17.9 | 12.8 | 51.6 |
| 5 | 1981 | 0.2 | 25.6 | 66.4 | 5.6 | 12.3 | 3.6 | 43.6 | 24.4 | 0.0 | 0.6 | 0.0 | 0.6 |
| 6 | 1982 | 0.0 | 12.3 | 8.6 | 14.1 | 24.1 | 0.0 | 8.6 | 16.3 | 0.0 | 0.0 | 0.0 | 5.5 |
| 7 | 1983 | 6.0 | 23.9 | 0.0 | 4.1 | 0.2 | 0.1 | 48.0 | 115.8 | 48.4 | 0.0 | 0.0 | 0.0 |
| 8 | 1984 | 0.3 | 0.0 | 0.7 | 0.0 | 0.0 | 0.0 | 50.0 | 88.6 | 3.0 | 0.0 | 0.0 | 0.0 |
| 9 | 1985 | 0.0 | 0.0 | 0.0 | 42.0 | 22.0 | 23.0 | 56.5 | 0.0 | 0.0 | 0.0 | 0.0 | 0.0 |
| 10 | 1986 | 0.0 | 6.0 | 1.5 | 0.0 | 0.0 | 4.7 | 1.2 | 19.0 | 0.0 | 0.0 | 15.0 | 0.0 |
| 11 | 1987 | 0.0 | 0.7 | 3.0 | 0.0 | 94.0 | 8.0 | 0.0 | 0.0 | 0.0 | 0.0 | 0.0 | 0.0 |
| 12 | 1988 | 0.0 | 0.0 | 0.0 | 25.0 | 0.0 | 0.0 | 130.8 | 26.8 | 0.0 | 0.0 | 0.0 | 0.0 |
| 13 | 1989 | 2.0 | 0.0 | 4.0 | 0.0 | 0.0 | 17.6 | 90.0 | 6.3 | 0.0 | 0.0 | 18.0 | 15.8 |
| 14 | 1990 | 0.0 | 24.3 | 23.5 | 0.0 | 0.0 | 8.0 | 0.0 | 61.1 | 0.0 | 0.0 | 3.0 | 0.0 |
| 15 | 1991 | 9.0 | 26.0 | 5.0 | 7.0 | 0.0 | 0.0 | 0.0 | 9.5 | 0.0 | 0.0 | 0.0 | 0.0 |
| 16 | 1992 | 23.0 | 4.6 | 50.0 | 0.0 | 16.0 | 0.0 | 78.0 | 79.2 | 0.0 | 22.0 | 0.0 | 0.0 |
| 17 | 1993 | 4.0 | 17.3 | 0.0 | 27.6 | 25.0 | 0.0 | 26.0 | 0.0 | 0.0 | 0.0 | 0.0 | 0.0 |
| 18 | 1994 | 0.0 | 0.0 | 0.0 | 15.0 | 21.0 | 0.0 | 151.1 | 156.9 | 62.6 | 0.0 | 0.0 | 19.5 |
| 19 | 1995 | 3.7 | 0.0 | 0.0 | 0.0 | 1.0 | 0.8 | 192.6 | 0.0 | 0.0 | 7.5 | 0.0 | 0.0 |
| 20 | 1996 | 4.5 | 45.5 | 6.5 | 4.5 | 80.8 | 7.5 | 18.0 | 2.5 | 0.0 | 0.0 | 0.0 | 0.0 |
| 21 | 1997 | 21.5 | 0.0 | 47.6 | 1.0 | 34.0 | 77.0 | 0.0 | 63.0 | 10.0 | 50.0 | 4.2 | 0.0 |
| 22 | 1998 | 5.0 | 4.5 | 15.0 | 9.0 | 0.0 | 2.0 | 13.0 | 19.0 | 0.0 | 13.0 | 0.0 | 0.0 |
| 23 | 1999 | 0.0 | 50.0 | 25.0 | 0.0 | 29.0 | 0.0 | 0.0 | 0.0 | 0.0 | 0.0 | 0.0 | 0.0 |
| 24 | 2000 | 26.0 | 0.0 | 0.0 | 0.0 | 8.0 | 0.0 | 0.7 | 3.0 | 0.0 | 0.0 | 0.0 | 0.0 |
| 25 | 2001 | 0.0 | 0.0 | 0.0 | 8.0 | 6.0 | 14.1 | 140.9 | 54.0 | 0.0 | 0.0 | 0.0 | 0.0 |
| 26 | 2002 | 0.0 | 0.7 | 0.0 | 0.0 | 0.0 | 0.0 | 0.0 | 0.0 | 8.0 | 0.0 | 0.0 | 0.0 |
| 27 | 2003 | 25.0 | 35.0 | 7.0 | 0.0 | 39.0 | 13.0 | 353.7 | 1.9 | 0.0 | 0.0 | 0.0 | 0.0 |
| 28 | 2004 | 3.8 | 0.0 | 0.0 | 0.0 | 0.0 | 15.5 | 4.2 | 0.0 | 0.0 | 0.0 | 0.0 | 1.3 |
| 29 | 2005 | 8.0 | 68.2 | 5.5 | 20.0 | 48.7 | 47.8 | 0.0 | 0.0 | 9.4 | 0.0 | 0.0 | 0.0 |
| 30 | 2006 | 0.0 | 0.0 | 0.0 | 3.2 | 20.0 | 0.2 | 8.2 | 63.1 | 15.4 | 17.5 | 0.0 | 53.9 |
| 31 | 2007 | 0.0 | 5.2 | 31.0 | 23.2 | 45.0 | 16.1 | 39.4 | 35.8 | 0.0 | 0.0 | 0.0 | 0.0 |
| 32 | 2008 | 7.3 | 0.0 | 0.0 | 0.0 | 9.7 | 12.3 | 10.0 | 87.6 | 2.5 | 0.0 | 0.0 | 124.5 |
| 33 | 2009 | 13.6 | 7.8 | 30.7 | 5.7 | 0.0 | 9.8 | 13.1 | 3.1 | 0.0 | 0.0 | 0.0 | 19.8 |
| 34 | 2010 | 1.5 | 6.9 | 0.0 | 0.0 | 0.0 | 13.0 | 59.0 | 36.7 | 0.0 | 0.0 | 0.0 | 0.0 |
| 35 | 2011 | 0.0 | 14.2 | 4.0 | 4.0 | 11.5 | 0.0 | 9.1 | 100.0 | 66.2 | 0.0 | 0.0 | 0.0 |
| 36 | 2012 | 0.0 | 1.0 | 0.0 | 29.0 | 51.8 | 13.0 | 4.0 | 0.0 | 21.2 | 66.0 | 0.0 | 0.0 |
| 37 | 2013 | 0.1 | 0.4 | 36.0 | 25.0 | 13.0 | 4.0 | 39.0 | 49.3 | 1.2 | 0.0 | 2.0 | 0.0 |
| 38 | 2014 | 0.2 | 0.0 | 14.0 | 18.5 | 62.1 | 39.1 | 47.0 | 0.1 | 12.0 | 0.0 | 16.0 | 0.0 |
| 39 | 2015 | 2.0 | 0.1 | 2.0 | 0.2 | 23.0 | 10.1 | 0.1 | 42.3 | 0.0 | 3.0 | 0.0 | 0.0 |
| 40 | 2016 | 0 | 0 | 15.4 | 0.1 | 30.6 | 0.1 | 0 | 37.2 | 0 | 0 | 0 | 0 |
| 41 | 2017 | 9 | 0.01 | 14.02 | 5 | 30.02 | 13.02 | 25.02 | 15.02 | 5 | 0 | 1 | 0 |
| | | **4.8** | **11.4** | **10.4** | **7.4** | **19.7** | **11.2** | **53.2** | **39.3** | **8.6** | **5.0** | **1.9** | **7.3** |

FIGURE A.6: Data Source: Courtesy of PMD

| | | Precipitatoin Data - Nokkundi (1977 to 2017) | | | | | | | | | | | |
|---|---|---|---|---|---|---|---|---|---|---|---|---|---|
| | | Jan | Feb | Mar | Apr | May | Jun | Jul | Aug | Sep | Oct | Nov | Dec |
| S.no | Years | NokkundiJan | NokkundiFeb | NokkundiMar | NokkundiApr | NokkundiMay | NokkundiJun | NokkundiJul | NokkundiAug | NokkundiSep | NokkundiOct | NokkundiNov | NokkundiDec |
| 1 | 1977 | 13.2 | 0.0 | 0.0 | 0.0 | 0.0 | 0.0 | 4.0 | 0.0 | 0.0 | 0.0 | 1.0 | 0.0 |
| 2 | 1978 | 0.0 | 1.7 | 0.4 | 1.5 | 0.0 | 0.0 | 1.2 | 0.0 | 0.0 | 0.0 | 1.9 | 0.0 |
| 3 | 1979 | 0.0 | 24.8 | 2.7 | 1.6 | 0.0 | 0.0 | 0.0 | 0.0 | 0.0 | 0.0 | 0.0 | 7.2 |
| 4 | 1980 | 0.0 | 0.0 | 24.6 | 0.0 | 4.0 | 0.0 | 0.0 | 0.0 | 0.0 | 8.3 | 0.0 | 2.0 |
| 5 | 1981 | 8.1 | 3.3 | 6.9 | 0.0 | 1.2 | 0.0 | 0.0 | 0.0 | 0.0 | 0.0 | 0.0 | 0.0 |
| 6 | 1982 | 4.7 | 19.9 | 70.5 | 24.8 | 0.0 | 0.0 | 0.0 | 0.0 | 0.0 | 0.4 | 1.1 | 1.6 |
| 7 | 1983 | 9.9 | 12.8 | 9.8 | 3.0 | 0.9 | 0.0 | 0.0 | 10.5 | 0.0 | 0.0 | 0.0 | 2.6 |
| 8 | 1984 | 3.8 | 0.0 | 11.2 | 1.0 | 0.0 | 0.0 | 0.0 | 0.0 | 0.0 | 0.0 | 0.0 | 0.0 |
| 9 | 1985 | 17.8 | 0.0 | 0.0 | 1.3 | 0.0 | 0.0 | 0.0 | 0.0 | 0.0 | 0.0 | 0.0 | 1.4 |
| 10 | 1986 | 4.3 | 5.3 | 1.6 | 0.0 | 0.0 | 0.0 | 0.0 | 0.2 | 0.0 | 0.0 | 0.6 | 0.1 |
| 11 | 1987 | 0.0 | 0.6 | 1.3 | 0.0 | 0.4 | 0.0 | 0.0 | 0.0 | 0.0 | 0.0 | 0.0 | 0.6 |
| 12 | 1988 | 7.2 | 1.4 | 0.0 | 0.6 | 0.0 | 0.0 | 0.0 | 0.0 | 0.0 | 0.0 | 0.0 | 0.0 |
| 13 | 1989 | 0.0 | 6.2 | 0.0 | 0.0 | 0.0 | 0.0 | 0.0 | 0.0 | 0.0 | 0.0 | 0.0 | 0.5 |
| 14 | 1990 | 1.0 | 46.2 | 0.0 | 0.0 | 0.0 | 0.0 | 0.0 | 0.0 | 0.0 | 0.0 | 0.0 | 0.0 |
| 15 | 1991 | 0.0 | 0.6 | 19.0 | 0.0 | 0.0 | 0.0 | 0.0 | 0.0 | 0.0 | 0.0 | 0.0 | 0.0 |
| 16 | 1992 | 0.0 | 0.0 | 0.0 | 0.0 | 0.0 | 0.0 | 0.0 | 0.0 | 0.0 | 0.0 | 0.0 | 0.0 |
| 17 | 1993 | 0.0 | 0.0 | 0.0 | 0.0 | 0.0 | 0.0 | 0.0 | 0.0 | 0.0 | 0.0 | 0.0 | 0.0 |
| 18 | 1994 | 0.0 | 24.0 | 17.7 | 3.5 | 0.0 | 0.0 | 10.0 | 0.0 | 0.0 | 0.0 | 0.0 | 2.3 |
| 19 | 1995 | 0.0 | 1.4 | 8.8 | 0.0 | 0.0 | 0.6 | 12.4 | 0.0 | 0.0 | 0.0 | 0.0 | 5.4 |
| 20 | 1996 | 30.0 | 35.0 | 8.0 | 0.0 | 0.0 | 0.0 | 0.0 | 0.0 | 0.0 | 0.0 | 0.0 | 0.0 |
| 21 | 1997 | 54.0 | 0.0 | 6.8 | 0.0 | 2.0 | 0.0 | 0.0 | 0.0 | 0.0 | 1.0 | 5.0 | 5.0 |
| 22 | 1998 | 0.0 | 0.0 | 11.0 | 0.0 | 0.0 | 0.0 | 0.0 | 0.0 | 0.0 | 0.0 | 0.0 | 0.0 |
| 23 | 1999 | 0.0 | 16.5 | 2.0 | 0.0 | 0.0 | 0.0 | 0.0 | 0.0 | 0.0 | 0.0 | 0.0 | 0.0 |
| 24 | 2000 | 0.0 | 0.0 | 3.4 | 0.0 | 0.0 | 0.0 | 0.0 | 0.0 | 0.0 | 0.0 | 0.0 | 2.1 |
| 25 | 2001 | 0.0 | 6.7 | 2.7 | 0.0 | 0.0 | 0.0 | 0.0 | 0.0 | 0.0 | 0.0 | 0.0 | 0.0 |
| 26 | 2002 | 2.8 | 0.4 | 0.0 | 0.0 | 0.0 | 0.0 | 0.0 | 0.0 | 0.0 | 0.0 | 2.2 | 0.0 |
| 27 | 2003 | 0.0 | 2.5 | 5.2 | 0.0 | 0.0 | 0.0 | 0.0 | 0.0 | 0.0 | 0.0 | 0.0 | 0.0 |
| 28 | 2004 | 0.4 | 0.0 | 0.0 | 0.0 | 0.0 | 0.0 | 0.0 | 0.0 | 0.0 | 0.0 | 0.0 | 31.8 |
| 29 | 2005 | 0.0 | 94.0 | 93.6 | 0.0 | 0.0 | 0.0 | 0.0 | 0.0 | 0.0 | 0.0 | 0.0 | 0.0 |
| 30 | 2006 | 0.0 | 0.0 | 1.0 | 0.0 | 1.0 | 0.0 | 0.0 | 0.0 | 0.0 | 0.0 | 0.0 | 5.2 |
| 31 | 2007 | 3.0 | 7.0 | 4.0 | 13.0 | 0.0 | 80.0 | 0.0 | 0.0 | 0.0 | 0.0 | 0.0 | 0.0 |
| 32 | 2008 | 75.0 | 0.0 | 0.0 | 0.0 | 0.0 | 0.0 | 0.0 | 0.0 | 0.0 | 0.0 | 0.0 | 2.3 |
| 33 | 2009 | 33.4 | 0.0 | 0.0 | 6.9 | 0.0 | 0.0 | 0.0 | 0.0 | 0.0 | 1.0 | 0.0 | 6.0 |
| 34 | 2010 | 2.5 | 7.5 | 0.0 | 0.0 | 0.0 | 0.0 | 0.0 | 0.0 | 0.0 | 0.7 | 0.0 | 0.0 |
| 35 | 2011 | 0.0 | 51.0 | 8.5 | 0.0 | 0.0 | 0.0 | 0.0 | 0.0 | 0.0 | 9.0 | 0.0 | 0.0 |
| 36 | 2012 | 2.0 | 1.1 | 0.0 | 2.0 | 0.0 | 0.0 | 0.0 | 0.0 | 0.0 | 0.0 | 0.0 | 7.0 |
| 37 | 2013 | 0.1 | 0.7 | 8.0 | 30.0 | 0.0 | 0.0 | 0.0 | 0.0 | 0.0 | 0.0 | 13.1 | 0.0 |
| 38 | 2014 | 8.0 | 8.0 | 4.5 | 1.5 | 0.2 | 0.2 | 0.0 | 0.0 | 0.0 | 0.0 | 0.0 | 0.0 |
| 39 | 2015 | 27.0 | 0.1 | 8.3 | 0.8 | 0.1 | 0.0 | 0.0 | 0.0 | 0.0 | 0.1 | 0.0 | 0.0 |
| 40 | 2016 | 0.1 | 0 | 11.7 | 0.4 | 0 | 0 | 2 | 0 | 0 | 0 | 0 | 0 |
| 41 | 2017 | 13.1 | 13.7 | 3.01 | 0 | 0.01 | 0 | 0 | 0 | 0 | 0 | 1.01 | 0 |
| | | **7.8** | **9.6** | **8.7** | **2.2** | **0.2** | **2.0** | **0.7** | **0.3** | **0.0** | **0.5** | **0.6** | **2.0** |

FIGURE A.7: Data Source: Courtesy of PMD

| | | Precipitatoin Data - Ormara (1977 to 2017) | | | | | | | | | | | |
|---|---|---|---|---|---|---|---|---|---|---|---|---|---|
| | | Jan | Feb | Mar | Apr | May | Jun | Jul | Aug | Sep | Oct | Nov | Dec |
| S.no | Years | OrmaraJan | OrmaraFeb | OrmaraMar | OrmaraApr | OrmaraMay | OrmaraJun | OrmaraJul | OrmaraAug | OrmaraSep | OrmaraOct | OrmaraNov | OrmaraDec |
| 1 | 1977 | 36.1 | 0.0 | 0.0 | 0.0 | 0.0 | 8.6 | 11.2 | 4.8 | 0.0 | 31.0 | 0.0 | 16.5 |
| 2 | 1978 | 0.0 | 0.0 | 0.0 | 0.0 | 0.0 | 0.0 | 185.2 | 60.2 | 0.0 | 0.0 | 0.0 | 0.0 |
| 3 | 1979 | 48.3 | 26.4 | 0.0 | 0.0 | 0.0 | 0.0 | 0.0 | 0.0 | 0.0 | 10.2 | 0.0 | 25.4 |
| 4 | 1980 | 40.7 | 0.0 | 0.0 | 0.0 | 0.0 | 0.0 | 0.0 | 0.0 | 0.0 | 39.0 | 0.0 | 10.1 |
| 5 | 1981 | 0.0 | 49.0 | 77.4 | 0.0 | 0.0 | 0.0 | 0.0 | 0.0 | 0.0 | 0.0 | 0.0 | 0.0 |
| 6 | 1982 | 0.3 | 77.4 | 11.4 | 0.0 | 0.0 | 0.0 | 0.0 | 0.0 | 0.0 | 0.5 | 0.6 | 4.4 |
| 7 | 1983 | 9.3 | 14.3 | 8.4 | 2.9 | 1.1 | 0.0 | 0.2 | 11.3 | 0.0 | 0.1 | 0.0 | 2.8 |
| 8 | 1984 | 3.0 | 0.6 | 11.0 | 0.5 | 0.2 | 0.0 | 0.0 | 0.0 | 0.0 | 0.2 | 0.0 | 0.0 |
| 9 | 1985 | 15.3 | 0.0 | 0.2 | 0.3 | 0.3 | 0.0 | 0.0 | 0.0 | 0.0 | 0.1 | 0.0 | 0.6 |
| 10 | 1986 | 3.3 | 6.0 | 2.5 | 0.0 | 0.3 | 0.0 | 0.0 | 0.0 | 0.0 | 0.1 | 1.2 | 0.4 |
| 11 | 1987 | 0.0 | 2.4 | 7.6 | 0.0 | 0.6 | 0.0 | 0.0 | 0.0 | 0.0 | 0.1 | 0.0 | 1.3 |
| 12 | 1988 | 7.2 | 1.5 | 0.0 | 0.7 | 0.3 | 0.0 | 0.3 | 0.0 | 0.0 | 0.1 | 0.0 | 0.0 |
| 13 | 1989 | 0.0 | 7.1 | 1.8 | 0.0 | 0.3 | 0.0 | 0.0 | 0.0 | 0.0 | 0.1 | 0.0 | 2.1 |
| 14 | 1990 | 5.4 | 44.3 | 0.0 | 0.0 | 0.3 | 0.0 | 0.0 | 0.0 | 0.0 | 0.2 | 0.0 | 0.0 |
| 15 | 1991 | 1.1 | 8.2 | 23.2 | 0.0 | 0.3 | 0.0 | 0.0 | 0.0 | 0.0 | 0.1 | 3.7 | 0.0 |
| 16 | 1992 | 0.7 | 1.4 | 3.7 | 0.7 | 1.0 | 0.0 | 0.0 | 0.0 | 0.2 | 1.1 | 0.0 | 2.2 |
| 17 | 1993 | 3.2 | 0.0 | 0.0 | 0.4 | 0.3 | 0.0 | 0.0 | 0.0 | 0.0 | 0.1 | 0.0 | 0.0 |
| 18 | 1994 | 1.2 | 23.6 | 15.8 | 4.9 | 0.2 | 0.0 | 9.0 | 3.0 | 0.0 | 0.7 | 0.0 | 1.4 |
| 19 | 1995 | 0.0 | 0.9 | 8.4 | 0.2 | 0.4 | 0.9 | 11.8 | 0.0 | 0.0 | 0.1 | 0.0 | 9.8 |
| 20 | 1996 | 54.5 | 0.0 | 12.0 | 0.0 | 1.7 | 0.0 | 0.0 | 0.0 | 0.0 | 0.0 | 0.0 | 2.4 |
| 21 | 1997 | 40.7 | 0.0 | 48.5 | 0.0 | 0.0 | 0.0 | 24.0 | 0.0 | 0.0 | 0.0 | 0.0 | 0.0 |
| 22 | 1998 | 0.0 | 0.0 | 0.0 | 0.0 | 0.0 | 0.0 | 0.0 | 0.0 | 0.0 | 0.0 | 0.0 | 0.0 |
| 23 | 1999 | 3.0 | 0.0 | 0.0 | 0.0 | 0.0 | 0.0 | 0.0 | 0.0 | 0.0 | 0.0 | 0.0 | 0.0 |
| 24 | 2000 | 0.0 | 0.0 | 0.0 | 0.0 | 0.0 | 0.0 | 0.0 | 0.0 | 0.0 | 0.0 | 0.0 | 12.6 |
| 25 | 2001 | 0.0 | 0.0 | 0.0 | 0.0 | 0.0 | 0.0 | 33.9 | 0.0 | 0.0 | 0.0 | 0.0 | 0.0 |
| 26 | 2002 | 0.0 | 0.0 | 0.0 | 0.0 | 0.0 | 0.0 | 0.0 | 0.0 | 0.0 | 0.0 | 0.0 | 25.0 |
| 27 | 2003 | 0.0 | 0.0 | 0.0 | 0.0 | 0.0 | 0.0 | 28.0 | 0.0 | 0.0 | 0.0 | 0.0 | 0.0 |
| 28 | 2004 | 4.5 | 0.0 | 0.0 | 0.0 | 0.0 | 0.0 | 0.0 | 0.0 | 0.0 | 0.0 | 0.0 | 26.0 |
| 29 | 2005 | 24.0 | 62.0 | 13.0 | 0.0 | 0.0 | 3.8 | 0.0 | 0.0 | 0.0 | 0.0 | 0.0 | 0.0 |
| 30 | 2006 | 0.0 | 0.0 | 0.0 | 0.0 | 0.0 | 0.0 | 0.0 | 14.0 | 0.0 | 0.0 | 0.0 | 235.0 |
| 31 | 2007 | 0.0 | 7.0 | 133.0 | 0.0 | 0.0 | 314.0 | 2.0 | 47.0 | 0.0 | 0.0 | 0.0 | 2.0 |
| 32 | 2008 | 10.0 | 6.0 | 0.0 | 0.0 | 0.0 | 4.0 | 0.0 | 5.0 | 0.0 | 0.0 | 0.0 | 55.0 |
| 33 | 2009 | 9.0 | 0.0 | 0.0 | 0.0 | 0.0 | 0.0 | 2.0 | 2.0 | 0.0 | 0.0 | 0.0 | 12.0 |
| 34 | 2010 | 31.0 | 18.0 | 0.0 | 0.0 | 0.0 | 60.0 | 84.0 | 0.0 | 0.0 | 0.0 | 0.0 | 18.0 |
| 35 | 2011 | 0.0 | 9.0 | 16.0 | 0.0 | 0.0 | 0.0 | 56.0 | 2.0 | 11.0 | 0.0 | 14.0 | 3.0 |
| 36 | 2012 | 23.0 | 4.0 | 0.0 | 0.0 | 0.0 | 0.0 | 0.0 | 0.0 | 0.0 | 0.0 | 0.0 | 14.0 |
| 37 | 2013 | 0.0 | 2.0 | 0.0 | 57.0 | 0.0 | 7.0 | 0.0 | 0.0 | 0.0 | 0.0 | 0.0 | 0.0 |
| 38 | 2014 | 10.0 | 15.0 | 0.0 | 0.0 | 0.0 | 0.0 | 8.0 | 0.0 | 0.0 | 0.0 | 0.0 | 0.0 |
| 39 | 2015 | 36.0 | 24.0 | 8.0 | 0.0 | 0.0 | 0.0 | 0.0 | 5.0 | 0.0 | 0.0 | 0.0 | 0.0 |
| 40 | 2016 | 0 | 0 | 6 | 0 | 0 | 0.1 | 0 | 0 | 0 | 0 | 0 | 0 |
| 41 | 2017 | 18.4 | 1 | 0 | 0 | 0 | 0 | 9 | 1 | 0 | 0 | 0 | 0 |
| | | **10.7** | **10.0** | **9.9** | **1.6** | **0.2** | **9.7** | **11.3** | **3.8** | **0.3** | **2.0** | **0.5** | **11.8** |

FIGURE A.8: Data Source: Courtesy of PMD

| | | Precipitatoin Data - Panjgur (1977 to 2017) | | | | | | | | | | | |
|---|---|---|---|---|---|---|---|---|---|---|---|---|---|
| | | Jan | Feb | Mar | Apr | May | Jun | Jul | Aug | Sep | Oct | Nov | Dec |
| S.no | Years | PanjgurJan | PanjgurFeb | PanjgurMar | PanjgurApr | PanjgurMay | PanjgurJun | PanjgurJul | PanjgurAug | PanjgurSep | PanjgurOct | PanjgurNov | PanjgurDec |
| 1 | 1977 | 42.6 | 9.9 | 2.3 | 7.1 | 0.6 | 4.3 | 68.6 | 14.8 | 0.0 | 0.0 | 8.1 | 11.7 |
| 2 | 1978 | 0.0 | 10.4 | 1.0 | 5.4 | 0.0 | 0.0 | 45.9 | 43.7 | 0.0 | 0.0 | 3.8 | 0.0 |
| 3 | 1979 | 4.8 | 28.2 | 40.3 | 17.5 | 0.0 | 0.0 | 0.0 | 0.0 | 0.0 | 0.0 | 0.0 | 28.1 |
| 4 | 1980 | 1.4 | 6.3 | 16.8 | 2.0 | 0.0 | 0.0 | 0.0 | 0.0 | 0.0 | 18.0 | 0.0 | 41.6 |
| 5 | 1981 | 0.0 | 10.2 | 38.6 | 0.0 | 0.0 | 0.0 | 11.7 | 0.0 | 0.0 | 0.0 | 0.0 | 0.0 |
| 6 | 1982 | 35.1 | 53.3 | 35.7 | 46.6 | 19.9 | 0.0 | 0.0 | 1.3 | 0.0 | 3.0 | 0.0 | 43.8 |
| 7 | 1983 | 11.7 | 32.8 | 0.5 | 13.2 | 0.0 | 0.0 | 12.7 | 42.6 | 0.0 | 0.0 | 0.0 | 10.9 |
| 8 | 1984 | 6.0 | 0.0 | 19.3 | 0.0 | 0.0 | 0.0 | 31.8 | 3.3 | 24.1 | 0.0 | 0.0 | 8.7 |
| 9 | 1985 | 18.0 | 0.0 | 14.8 | 6.9 | 0.0 | 0.0 | 30.9 | 0.0 | 0.0 | 0.0 | 0.0 | 8.1 |
| 10 | 1986 | 3.0 | 40.6 | 8.8 | 0.0 | 0.0 | 6.4 | 0.1 | 53.9 | 0.0 | 0.0 | 2.8 | 0.0 |
| 11 | 1987 | 1.8 | 12.7 | 24.9 | 8.3 | 13.2 | 4.8 | 14.7 | 0.0 | 0.0 | 0.0 | 0.0 | 0.0 |
| 12 | 1988 | 25.6 | 4.1 | 0.0 | 0.0 | 0.0 | 2.3 | 114.2 | 0.0 | 0.5 | 0.0 | 0.0 | 0.0 |
| 13 | 1989 | 0.0 | 0.0 | 0.0 | 0.0 | 6.1 | 0.0 | 6.1 | 2.8 | 0.0 | 0.0 | 3.0 | 4.6 |
| 14 | 1990 | 17.0 | 47.3 | 0.0 | 2.8 | 9.3 | 0.0 | 0.0 | 0.0 | 5.0 | 0.0 | 0.7 | 9.4 |
| 15 | 1991 | 35.3 | 29.9 | 14.1 | 0.0 | 0.0 | 0.0 | 0.0 | 0.0 | 0.0 | 0.0 | 0.0 | 0.0 |
| 16 | 1992 | 48.5 | 8.6 | 13.7 | 19.2 | 0.6 | 0.0 | 0.0 | 21.0 | 0.0 | 18.6 | 0.0 | 7.0 |
| 17 | 1993 | 11.5 | 0.0 | 0.8 | 14.3 | 0.0 | 0.0 | 1.2 | 0.0 | 0.0 | 0.0 | 0.0 | 0.0 |
| 18 | 1994 | 2.5 | 13.3 | 0.0 | 16.9 | 0.0 | 0.0 | 42.5 | 14.0 | 1.4 | 3.5 | 0.0 | 7.6 |
| 19 | 1995 | 3.4 | 16.3 | 6.7 | 15.3 | 0.0 | 0.0 | 23.5 | 0.0 | 0.0 | 0.0 | 0.0 | 47.2 |
| 20 | 1996 | 36.5 | 6.8 | 26.1 | 0.0 | 0.0 | 10.1 | 3.8 | 0.0 | 0.0 | 0.0 | 0.0 | 0.0 |
| 21 | 1997 | 39.3 | 0.0 | 67.3 | 66.8 | 7.6 | 13.3 | 12.4 | 12.4 | 0.4 | 41.9 | 37.5 | 5.4 |
| 22 | 1998 | 14.7 | 1.8 | 38.2 | 0.0 | 0.0 | 0.0 | 1.8 | 0.0 | 25.0 | 0.0 | 0.0 | 0.0 |
| 23 | 1999 | 0.0 | 32.1 | 26.4 | 0.0 | 0.0 | 0.0 | 0.0 | 0.0 | 5.0 | 0.0 | 0.0 | 0.0 |
| 24 | 2000 | 3.5 | 0.0 | 0.0 | 0.0 | 14.0 | 2.1 | 0.0 | 0.0 | 0.0 | 0.0 | 0.0 | 1.9 |
| 25 | 2001 | 0.0 | 7.2 | 3.0 | 0.0 | 0.0 | 2.0 | 21.6 | 0.0 | 0.0 | 0.0 | 0.0 | 0.0 |
| 26 | 2002 | 0.0 | 1.0 | 6.1 | 0.0 | 10.0 | 6.0 | 0.0 | 13.0 | 0.0 | 0.0 | 7.0 | 0.0 |
| 27 | 2003 | 0.0 | 7.8 | 5.7 | 0.0 | 0.0 | 0.0 | 24.5 | 0.0 | 0.0 | 0.0 | 0.0 | 0.0 |
| 28 | 2004 | 7.0 | 0.0 | 0.0 | 0.0 | 3.0 | 0.0 | 1.0 | 0.0 | 0.0 | 0.0 | 0.0 | 63.0 |
| 29 | 2005 | 3.0 | 99.6 | 63.3 | 0.0 | 0.0 | 0.0 | 0.0 | 0.0 | 0.0 | 0.0 | 0.0 | 0.0 |
| 30 | 2006 | 8.0 | 0.0 | 8.0 | 0.0 | 0.0 | 0.0 | 3.0 | 16.0 | 2.0 | 0.0 | 3.0 | 83.0 |
| 31 | 2007 | 0.0 | 12.0 | 9.0 | 0.0 | 0.0 | 118.9 | 0.0 | 23.0 | 0.0 | 0.0 | 0.0 | 0.0 |
| 32 | 2008 | 17.5 | 1.0 | 0.0 | 3.0 | 0.0 | 26.0 | 0.0 | 21.0 | 0.0 | 0.0 | 0.0 | 7.0 |
| 33 | 2009 | 38.0 | 0.0 | 8.5 | 4.0 | 0.0 | 0.0 | 0.0 | 0.0 | 0.0 | 0.0 | 0.0 | 9.0 |
| 34 | 2010 | 8.0 | 43.5 | 0.0 | 0.0 | 2.0 | 0.0 | 0.0 | 0.0 | 0.0 | 0.0 | 0.0 | 0.0 |
| 35 | 2011 | 0.0 | 36.0 | 43.0 | 32.0 | 3.0 | 0.0 | 7.0 | 16.0 | 0.0 | 0.0 | 0.0 | 2.0 |
| 36 | 2012 | 17.0 | 5.0 | 0.0 | 11.0 | 17.0 | 0.0 | 5.0 | 0.0 | 0.0 | 0.0 | 0.0 | 9.0 |
| 37 | 2013 | 0.0 | 18.0 | 17.0 | 24.0 | 0.0 | 0.0 | 1.0 | 16.0 | 7.0 | 0.0 | 0.0 | 0.0 |
| 38 | 2014 | 30.0 | 5.0 | 21.0 | 16.0 | 1.0 | 0.0 | 0.0 | 0.0 | 0.0 | 0.0 | 1.0 | 0.0 |
| 39 | 2015 | 13.0 | 13.0 | 8.0 | 4.0 | 20.0 | 0.0 | 0.0 | 0.0 | 0.0 | 0.0 | 0.0 | 0.0 |
| 40 | 2016 | 0 | 0 | 30 | 6 | 1 | 7 | 12 | 0 | 0 | 0 | 0 | 0 |
| 41 | 2017 | 21 | 1 | 0 | 0 | 15 | 0 | 0 | 0 | 0 | 0 | 0 | 0 |
| | | **12.8** | **15.0** | **15.1** | **8.3** | **3.5** | **5.0** | **12.1** | **7.7** | **1.7** | **2.1** | **1.6** | **10.0** |

FIGURE A.9: Data Source: Courtesy of PMD

| | | Precipitatoin Data - Pasni (1977 to 2017) | | | | | | | | | | | |
|---|---|---|---|---|---|---|---|---|---|---|---|---|---|
| | | Jan | Feb | Mar | Apr | May | Jun | Jul | Aug | Sep | Oct | Nov | Dec |
| S.no | Years | PasniJan | PasniFeb | PasniMar | PasniApr | PasniMay | PasniJun | PasniJul | PasniAug | PasniSep | PasniOct | PasniNov | PasniDec |
| 1 | 1977 | 0.4 | 0.0 | 0.0 | 0.0 | 0.0 | 0.0 | 1.5 | 1.4 | 0.0 | 0.0 | 0.3 | 28.4 |
| 2 | 1978 | 9.9 | 3.5 | 3.0 | 0.0 | 0.0 | 3.1 | 8.5 | 63.0 | 0.0 | 0.0 | 0.0 | 0.0 |
| 3 | 1979 | 47.8 | 24.4 | 0.0 | 0.0 | 0.6 | 0.5 | 0.0 | 0.0 | 0.0 | 4.0 | 0.0 | 143.0 |
| 4 | 1980 | 33.2 | 1.4 | 17.6 | 0.0 | 0.0 | 0.5 | 0.0 | 0.0 | 0.0 | 56.5 | 0.0 | 13.2 |
| 5 | 1981 | 1.0 | 0.0 | 56.5 | 0.0 | 0.0 | 0.0 | 0.0 | 0.0 | 0.0 | 0.0 | 0.0 | 0.0 |
| 6 | 1982 | 38.4 | 174.9 | 12.0 | 25.4 | 0.0 | 0.0 | 0.0 | 1.2 | 0.0 | 0.0 | 3.4 | 100.9 |
| 7 | 1983 | 0.1 | 11.4 | 0.1 | 1.8 | 0.0 | 0.0 | 4.0 | 153.8 | 0.0 | 0.0 | 0.0 | 1.2 |
| 8 | 1984 | 3.3 | 0.0 | 197.9 | 0.0 | 0.0 | 0.0 | 0.0 | 5.0 | 0.0 | 0.0 | 0.0 | 2.0 |
| 9 | 1985 | 0.0 | 0.0 | 0.0 | 0.0 | 0.0 | 0.0 | 0.0 | 0.0 | 0.0 | 0.0 | 0.0 | 36.0 |
| 10 | 1986 | 8.0 | 60.7 | 9.5 | 0.0 | 0.0 | 0.0 | 0.0 | 19.2 | 0.0 | 0.0 | 0.0 | 0.0 |
| 11 | 1987 | 11.6 | 1.0 | 10.0 | 0.0 | 0.0 | 0.0 | 0.0 | 0.0 | 0.0 | 0.0 | 0.0 | 0.0 |
| 12 | 1988 | 29.4 | 6.1 | 0.0 | 0.0 | 0.0 | 0.0 | 0.0 | 0.0 | 0.0 | 0.0 | 0.0 | 0.0 |
| 13 | 1989 | 1.2 | 2.5 | 10.5 | 0.0 | 0.0 | 0.0 | 0.0 | 0.0 | 0.0 | 0.0 | 0.0 | 4.0 |
| 14 | 1990 | 2.8 | 5.8 | 0.0 | 0.0 | 0.0 | 0.0 | 0.0 | 0.0 | 0.0 | 0.0 | 0.0 | 12.4 |
| 15 | 1991 | 154.0 | 0.0 | 65.0 | 0.0 | 0.0 | 0.0 | 0.0 | 0.0 | 0.0 | 0.0 | 0.0 | 10.0 |
| 16 | 1992 | 50.1 | 51.0 | 21.0 | 0.0 | 0.0 | 0.0 | 0.0 | 25.0 | 0.0 | 0.0 | 0.0 | 16.0 |
| 17 | 1993 | 27.0 | 1.0 | 0.0 | 0.3 | 0.0 | 0.3 | 2.9 | 13.9 | 1.3 | 0.0 | 0.0 | 0.0 |
| 18 | 1994 | 12.5 | 4.6 | 0.0 | 5.0 | 0.0 | 0.0 | 57.0 | 0.0 | 20.0 | 0.0 | 0.0 | 60.0 |
| 19 | 1995 | 0.0 | 44.0 | 25.0 | 0.0 | 0.0 | 0.0 | 12.0 | 0.0 | 0.0 | 0.0 | 0.0 | 49.0 |
| 20 | 1996 | 108.0 | 0.0 | 8.3 | 0.0 | 5.0 | 0.0 | 0.0 | 0.0 | 0.0 | 0.0 | 0.0 | 0.0 |
| 21 | 1997 | 35.0 | 0.0 | 69.8 | 0.0 | 14.0 | 0.0 | 0.0 | 0.0 | 0.0 | 31.0 | 22.0 | 6.0 |
| 22 | 1998 | 7.0 | 46.5 | 12.0 | 0.0 | 0.0 | 0.0 | 1.2 | 0.0 | 0.0 | 0.0 | 0.0 | 0.0 |
| 23 | 1999 | 12.1 | 45.0 | 11.0 | 0.0 | 0.0 | 0.0 | 0.0 | 0.0 | 0.0 | 0.0 | 0.0 | 0.0 |
| 24 | 2000 | 0.0 | 0.0 | 0.0 | 0.0 | 0.0 | 0.0 | 0.0 | 0.0 | 0.0 | 0.0 | 0.0 | 0.0 |
| 25 | 2001 | 0.0 | 0.0 | 0.0 | 0.0 | 0.0 | 0.0 | 21.0 | 0.0 | 0.0 | 0.0 | 0.0 | 0.0 |
| 26 | 2002 | 0.0 | 5.0 | 0.0 | 0.0 | 0.0 | 0.0 | 0.0 | 0.0 | 0.0 | 0.0 | 2.0 | 33.0 |
| 27 | 2003 | 45.1 | 0.0 | 0.0 | 22.2 | 0.0 | 0.0 | 48.0 | 0.0 | 0.0 | 0.0 | 0.0 | 4.0 |
| 28 | 2004 | 22.5 | 0.0 | 0.0 | 0.0 | 0.0 | 0.0 | 0.0 | 0.0 | 0.0 | 0.0 | 0.0 | 39.0 |
| 29 | 2005 | 18.0 | 13.6 | 38.0 | 0.0 | 0.0 | 0.0 | 0.2 | 0.0 | 0.0 | 0.0 | 0.0 | 0.0 |
| 30 | 2006 | 1.0 | 1.0 | 1.0 | 0.0 | 0.0 | 0.0 | 0.0 | 4.2 | 0.0 | 0.0 | 0.0 | 109.6 |
| 31 | 2007 | 0.0 | 3.8 | 53.5 | 0.0 | 0.0 | 106.3 | 42.0 | 1.3 | 0.0 | 0.0 | 0.0 | 0.0 |
| 32 | 2008 | 87.2 | 26.9 | 0.0 | 0.0 | 0.0 | 0.0 | 1.2 | 12.0 | 0.0 | 1.8 | 0.0 | 43.2 |
| 33 | 2009 | 35.2 | 0.0 | 1.5 | 0.0 | 0.0 | 2.0 | 2.0 | 0.0 | 1.0 | 0.0 | 1.2 | 7.0 |
| 34 | 2010 | 21.0 | 62.0 | 0.0 | 0.0 | 0.0 | 139.0 | 13.0 | 0.0 | 0.0 | 0.0 | 0.0 | 12.8 |
| 35 | 2011 | 0.0 | 0.0 | 11.0 | 2.0 | 0.0 | 0.0 | 0.0 | 0.0 | 0.0 | 0.0 | 18.0 | 2.0 |
| 36 | 2012 | 46.4 | 8.0 | 0.0 | 0.0 | 0.0 | 0.0 | 0.0 | 0.0 | 0.0 | 0.0 | 0.0 | 81.0 |
| 37 | 2013 | 0.0 | 3.0 | 3.0 | 36.0 | 0.0 | 22.0 | 0.0 | 16.0 | 0.0 | 0.0 | 22.0 | 0.0 |
| 38 | 2014 | 19.0 | 4.0 | 0.0 | 0.0 | 0.0 | 0.0 | 0.0 | 0.0 | 0.0 | 0.0 | 0.0 | 0.0 |
| 39 | 2015 | 8.0 | 0.0 | 21.0 | 0.0 | 0.0 | 0.0 | 0.0 | 0.0 | 0.0 | 0.0 | 0.0 | 0.0 |
| 40 | 2016 | 0 | 0 | 15.4 | 0 | 0 | 0 | 0 | 0 | 0 | 0 | 0 | 0 |
| 41 | 2017 | 7.8 | 0.6 | 0 | 0 | 0 | 0 | 0 | 0 | 0 | 0 | 0 | 0 |
| | | **22.0** | **14.9** | **16.4** | **2.3** | **0.5** | **6.7** | **5.2** | **7.7** | **0.5** | **2.3** | **1.7** | **19.8** |

FIGURE A.10: Data Source: Courtesy of PMD

| | | Precipitatoin Data - Quetta (1977 to 2017) | | | | | | | | | | | |
|---|---|---|---|---|---|---|---|---|---|---|---|---|---|
| | | Jan | Feb | Mar | Apr | May | Jun | Jul | Aug | Sep | Oct | Nov | Dec |
| S.no | Years | QuettaJan | QuettaFeb | QuettaMar | QuettaApr | QuettaMay | QuettaJun | QuettaJul | QuettaAug | QuettaSep | QuettaOct | QuettaNov | QuettaDec |
| 1 | 1977 | 91.5 | 6.0 | 0.6 | 10.4 | 16.0 | 19.2 | 48.1 | 14.0 | 0.0 | 0.0 | 25.2 | 8.6 |
| 2 | 1978 | 68.0 | 58.3 | 18.2 | 16.5 | 0.0 | 0.0 | 121.8 | 1.1 | 0.0 | 0.0 | 23.1 | 10.5 |
| 3 | 1979 | 70.8 | 90.2 | 112.3 | 7.5 | 0.0 | 0.0 | 0.0 | 0.0 | 0.0 | 0.0 | 0.0 | 68.1 |
| 4 | 1980 | 69.9 | 30.0 | 95.5 | 2.7 | 0.0 | 5.2 | 0.0 | 0.0 | 0.0 | 24.8 | 13.1 | 3.6 |
| 5 | 1981 | 111.9 | 105.1 | 63.5 | 0.0 | 17.0 | 0.0 | 2.0 | 0.0 | 0.0 | 13.0 | 0.0 | 35.0 |
| 6 | 1982 | 178.0 | 189.2 | 232.4 | 30.4 | 23.0 | 0.0 | 0.0 | 50.0 | 0.0 | 68.8 | 16.0 | 162.0 |
| 7 | 1983 | 61.0 | 61.0 | 68.1 | 148.0 | 29.0 | 0.0 | 22.0 | 173.0 | 0.0 | 0.0 | 0.0 | 71.2 |
| 8 | 1984 | 58.2 | 19.4 | 40.5 | 5.8 | 0.0 | 0.0 | 0.0 | 1.3 | 0.0 | 0.0 | 0.0 | 18.0 |
| 9 | 1985 | 54.6 | 0.0 | 78.0 | 88.8 | 0.0 | 0.0 | 0.0 | 0.0 | 0.0 | 0.0 | 0.0 | 35.7 |
| 10 | 1986 | 4.2 | 102.8 | 45.8 | 0.0 | 0.0 | 0.0 | 1.0 | 66.0 | 0.0 | 0.0 | 19.6 | 4.5 |
| 11 | 1987 | 18.4 | 30.2 | 93.1 | 2.0 | 5.0 | 0.0 | 0.0 | 7.1 | 0.0 | 0.0 | 0.0 | 0.0 |
| 12 | 1988 | 29.6 | 14.8 | 121.1 | 0.0 | 0.0 | 0.0 | 59.5 | 0.0 | 0.0 | 0.0 | 0.0 | 34.0 |
| 13 | 1989 | 46.7 | 30.4 | 86.2 | 13.0 | 0.0 | 0.6 | 1.2 | 0.6 | 0.0 | 0.0 | 13.0 | 51.4 |
| 14 | 1990 | 137.1 | 79.5 | 40.8 | 2.8 | 0.0 | 0.0 | 0.0 | 1.6 | 0.0 | 0.0 | 1.0 | 50.4 |
| 15 | 1991 | 102.3 | 90.4 | 148.2 | 30.6 | 3.8 | 0.0 | 0.0 | 0.0 | 12.4 | 0.0 | 10.6 | 30.4 |
| 16 | 1992 | 29.4 | 57.1 | 66.8 | 158.7 | 5.8 | 0.0 | 0.2 | 4.2 | 0.0 | 21.0 | 0.0 | 66.4 |
| 17 | 1993 | 167.6 | 14.3 | 30.6 | 16.3 | 0.2 | 4.4 | 0.0 | 0.0 | 0.0 | 0.0 | 0.0 | 0.0 |
| 18 | 1994 | 48.4 | 35.2 | 26.6 | 4.6 | 29.0 | 0.0 | 64.0 | 22.0 | 62.0 | 0.0 | 0.0 | 13.0 |
| 19 | 1995 | 13.0 | 41.0 | 30.0 | 11.0 | 0.0 | 0.0 | 85.0 | 0.0 | 0.0 | 8.0 | 0.0 | 145.7 |
| 20 | 1996 | 34.0 | 34.0 | 43.0 | 1.0 | 8.0 | 2.0 | 0.0 | 0.0 | 0.0 | 3.0 | 0.0 | 9.0 |
| 21 | 1997 | 50.0 | 5.0 | 77.0 | 32.0 | 3.0 | 8.0 | 33.0 | 11.0 | 0.0 | 57.0 | 11.0 | 22.0 |
| 22 | 1998 | 61.0 | 38.0 | 58.0 | 6.0 | 17.0 | 4.0 | 3.0 | 0.0 | 0.0 | 0.0 | 0.0 | 0.0 |
| 23 | 1999 | 43.0 | 36.0 | 10.0 | 0.0 | 0.0 | 0.0 | 0.0 | 16.0 | 0.0 | 0.0 | 1.0 | 0.0 |
| 24 | 2000 | 15.5 | 14.0 | 3.0 | 0.0 | 0.0 | 0.0 | 0.0 | 1.0 | 0.0 | 0.0 | 0.0 | 131.0 |
| 25 | 2001 | 0.0 | 46.0 | 27.0 | 6.0 | 0.0 | 0.0 | 0.0 | 0.0 | 0.0 | 0.0 | 0.0 | 14.5 |
| 26 | 2002 | 5.0 | 23.8 | 40.0 | 44.0 | 0.0 | 0.0 | 0.0 | 0.0 | 0.0 | 0.0 | 15.5 | 51.0 |
| 27 | 2003 | 35.4 | 95.1 | 10.0 | 3.0 | 30.0 | 0.0 | 46.0 | 0.0 | 0.0 | 0.0 | 30.0 | 0.0 |
| 28 | 2004 | 60.8 | 14.0 | 0.0 | 0.0 | 3.0 | 0.0 | 0.0 | 0.0 | 0.0 | 0.0 | 4.0 | 40.0 |
| 29 | 2005 | 59.0 | 141.0 | 72.0 | 4.0 | 30.5 | 0.0 | 0.0 | 0.0 | 0.0 | 0.0 | 4.0 | 0.0 |
| 30 | 2006 | 17.0 | 8.0 | 26.5 | 6.0 | 2.0 | 0.0 | 2.0 | 38.0 | 0.0 | 0.0 | 72.0 | 35.0 |
| 31 | 2007 | 11.0 | 131.0 | 40.0 | 17.0 | 0.0 | 61.0 | 20.0 | 0.0 | 0.0 | 0.0 | 1.0 | 16.0 |
| 32 | 2008 | 97.0 | 15.0 | 0.0 | 6.0 | 1.0 | 2.5 | 0.0 | 2.0 | 0.0 | 0.0 | 0.0 | 11.0 |
| 33 | 2009 | 67.0 | 78.0 | 13.0 | 38.0 | 7.0 | 0.0 | 1.0 | 0.0 | 0.0 | 0.0 | 1.0 | 84.0 |
| 34 | 2010 | 45.0 | 51.0 | 6.0 | 16.0 | 7.0 | 5.0 | 0.0 | 1.0 | 0.0 | 2.0 | 0.0 | 0.0 |
| 35 | 2011 | 20.0 | 112.0 | 119.0 | 81.0 | 3.0 | 2.0 | 0.0 | 8.0 | 46.0 | 31.0 | 35.0 | 2.0 |
| 36 | 2012 | 43.0 | 65.0 | 17.0 | 137.0 | 6.0 | 0.0 | 0.0 | 0.0 | 6.0 | 0.0 | 8.0 | 31.0 |
| 37 | 2013 | 4.1 | 94.2 | 41.1 | 35.0 | 0.0 | 0.1 | 0.1 | 24.0 | 0.0 | 0.0 | 20.1 | 0.1 |
| 38 | 2014 | 2.4 | 31.0 | 73.5 | 23.4 | 36.5 | 0.1 | 0.0 | 0.1 | 0.1 | 0.2 | 0.3 | 1.0 |
| 39 | 2015 | 18.0 | 10.0 | 77.5 | 33.1 | 4.2 | 0.1 | 1.0 | 0.2 | 1.0 | 4.0 | 34.1 | 5.1 |
| 40 | 2016 | 56.3 | 0 | 67.3 | 4.3 | 11.3 | 14.1 | 3 | 0.1 | 0 | 0 | 0 | 0.4 |
| 41 | 2017 | 102 | 23.14 | 54.44 | 22.9 | 7.2 | 37 | 0.02 | 13.1 | 0 | 0 | 3.52 | 0.4 |
| | | **53.8** | **51.7** | **55.5** | **26.0** | **7.5** | **4.0** | **12.5** | **11.1** | **3.1** | **5.7** | **8.8** | **30.8** |

FIGURE A.11: Data Source: Courtesy of PMD

| | | Precipitatoin Data - Sibbi (1977 to 2017) | | | | | | | | | | | |
|---|---|---|---|---|---|---|---|---|---|---|---|---|---|
| | | Jan | Feb | Mar | Apr | May | Jun | Jul | Aug | Sep | Oct | Nov | Dec |
| S.no | Years | SibbiJan | SibbiFeb | SibbiMar | SibbiApr | SibbiMay | SibbiJun | SibbiJul | SibbiAug | SibbiSep | SibbiOct | SibbiNov | SibbiDec |
| 1 | 1977 | 8.8 | 0.0 | 0.0 | 22.1 | 0.0 | 46.1 | 42.3 | 26.0 | 1.5 | 0.0 | 8.3 | 0.7 |
| 2 | 1978 | 5.0 | 8.6 | 1.6 | 1.1 | 0.0 | 0.0 | 100.3 | 20.6 | 1.8 | 0.0 | 2.0 | 0.0 |
| 3 | 1979 | 14.3 | 54.4 | 91.1 | 55.6 | 0.0 | 0.0 | 0.0 | 75.9 | 0.0 | 0.0 | 0.6 | 1.5 |
| 4 | 1980 | 10.1 | 2.3 | 19.5 | 0.0 | 0.0 | 11.0 | 8.9 | 10.0 | 1.0 | 11.0 | 0.0 | 2.0 |
| 5 | 1981 | 6.4 | 6.3 | 32.6 | 0.0 | 4.7 | 0.0 | 38.1 | 6.0 | 0.0 | 0.0 | 0.0 | 0.0 |
| 6 | 1982 | 11.4 | 10.9 | 23.3 | 0.0 | 0.0 | 0.0 | 24.0 | 36.2 | 0.0 | 21.5 | 13.3 | 35.1 |
| 7 | 1983 | 6.7 | 21.1 | 6.0 | 3.0 | 7.0 | 0.0 | 28.7 | 71.0 | 0.0 | 0.0 | 0.0 | 2.2 |
| 8 | 1984 | 0.0 | 0.0 | 7.7 | 0.0 | 0.0 | 0.0 | 21.5 | 29.2 | 0.0 | 0.0 | 0.0 | 0.0 |
| 9 | 1985 | 0.0 | 0.0 | 0.1 | 35.3 | 0.0 | 0.0 | 42.5 | 31.4 | 0.0 | 0.0 | 0.0 | 9.1 |
| 10 | 1986 | 0.2 | 21.0 | 15.0 | 29.8 | 0.0 | 0.0 | 15.0 | 82.7 | 0.0 | 0.0 | 4.3 | 0.0 |
| 11 | 1987 | 4.0 | 21.6 | 35.2 | 3.2 | 30.1 | 0.0 | 20.0 | 2.0 | 0.0 | 0.0 | 0.0 | 0.0 |
| 12 | 1988 | 5.9 | 2.0 | 59.4 | 0.0 | 0.0 | 0.0 | 56.5 | 50.0 | 7.0 | 0.0 | 0.0 | 1.6 |
| 13 | 1989 | 4.0 | 0.0 | 111.3 | 0.0 | 0.0 | 2.0 | 69.9 | 101.0 | 9.0 | 0.0 | 5.1 | 9.0 |
| 14 | 1990 | 5.1 | 49.5 | 15.0 | 3.0 | 25.0 | 5.0 | 7.0 | 29.0 | 3.0 | 0.0 | 2.0 | 0.0 |
| 15 | 1991 | 13.0 | 25.0 | 26.0 | 24.3 | 12.0 | 0.0 | 0.0 | 20.0 | 34.0 | 0.0 | 1.0 | 19.7 |
| 16 | 1992 | 65.0 | 24.0 | 17.0 | 49.9 | 1.0 | 0.5 | 39.0 | 82.0 | 19.0 | 18.0 | 0.0 | 6.5 |
| 17 | 1993 | 37.7 | 2.0 | 14.0 | 18.0 | 0.7 | 0.7 | 87.7 | 5.0 | 12.0 | 0.0 | 0.0 | 0.0 |
| 18 | 1994 | 0.0 | 59.9 | 13.0 | 11.0 | 1.2 | 14.0 | 65.5 | 55.0 | 87.1 | 0.0 | 0.0 | 9.9 |
| 19 | 1995 | 1.1 | 2.9 | 8.2 | 28.5 | 0.0 | 0.0 | 112.8 | 21.8 | 0.0 | 8.1 | 0.0 | 8.3 |
| 20 | 1996 | 13.0 | 27.5 | 5.8 | 0.0 | 9.6 | 2.5 | 47.9 | 0.0 | 0.0 | 0.0 | 0.0 | 0.0 |
| 21 | 1997 | 20.2 | 0.0 | 30.6 | 0.0 | 41.2 | 60.1 | 45.4 | 14.6 | 0.0 | 65.2 | 13.1 | 17.0 |
| 22 | 1998 | 8.8 | 5.7 | 31.5 | 3.0 | 0.7 | 0.0 | 29.0 | 19.7 | 0.0 | 1.6 | 0.0 | 0.0 |
| 23 | 1999 | 17.0 | 27.4 | 18.7 | 0.0 | 14.2 | 0.0 | 0.0 | 40.7 | 0.0 | 0.0 | 0.0 | 0.0 |
| 24 | 2000 | 1.1 | 9.4 | 0.0 | 0.0 | 0.0 | 0.0 | 19.0 | 86.9 | 0.0 | 0.0 | 0.0 | 2.9 |
| 25 | 2001 | 0.0 | 3.0 | 0.0 | 1.1 | 0.0 | 27.3 | 93.9 | 43.6 | 47.2 | 0.0 | 0.0 | 0.0 |
| 26 | 2002 | 0.0 | 0.7 | 1.0 | 0.0 | 0.0 | 0.0 | 0.0 | 3.4 | 0.0 | 0.0 | 0.0 | 4.6 |
| 27 | 2003 | 5.6 | 17.3 | 4.0 | 0.0 | 10.5 | 2.0 | 60.5 | 51.0 | 14.0 | 0.0 | 0.7 | 0.0 |
| 28 | 2004 | 23.8 | 0.0 | 0.0 | 0.0 | 0.0 | 12.0 | 0.0 | 0.0 | 0.0 | 0.0 | 0.0 | 21.0 |
| 29 | 2005 | 8.4 | 64.9 | 110.0 | 0.0 | 4.2 | 0.0 | 10.5 | 50.4 | 26.0 | 0.0 | 0.0 | 0.0 |
| 30 | 2006 | 0.0 | 11.2 | 22.9 | 3.1 | 0.0 | 0.0 | 10.3 | 80.7 | 0.0 | 0.0 | 2.0 | 39.5 |
| 31 | 2007 | 1.0 | 71.1 | 56.2 | 0.0 | 0.0 | 188.1 | 6.6 | 32.0 | 4.5 | 0.0 | 0.0 | 12.4 |
| 32 | 2008 | 6.6 | 9.8 | 1.3 | 2.5 | 2.0 | 75.2 | 65.3 | 6.7 | 14.4 | 0.0 | 0.0 | 22.7 |
| 33 | 2009 | 53.0 | 3.9 | 3.3 | 0.0 | 0.0 | 1.0 | 28.5 | 32.4 | 0.0 | 0.0 | 0.0 | 4.0 |
| 34 | 2010 | 1.2 | 1.9 | 0.3 | 0.6 | 0.0 | 0.0 | 107.6 | 93.2 | 43.0 | 0.0 | 0.0 | 0.0 |
| 35 | 2011 | 0.0 | 54.5 | 30.2 | 54.8 | 37.0 | 0.0 | 74.0 | 21.6 | 29.0 | 0.0 | 1.5 | 0.0 |
| 36 | 2012 | 8.7 | 1.6 | 2.0 | 32.7 | 0.0 | 26.6 | 42.6 | 106.0 | 112.0 | 0.0 | 0.0 | 0.0 |
| 37 | 2013 | 0.0 | 98.0 | 53.1 | 0.2 | 5.1 | 0.2 | 37.0 | 66.1 | 0.0 | 0.0 | 0.1 | 0.0 |
| 38 | 2014 | 0.0 | 9.0 | 0.2 | 0.1 | 8.0 | 0.0 | 6.1 | 17.0 | 12.0 | 0.0 | 0.0 | 0.1 |
| 39 | 2015 | 7.0 | 2.0 | 23.2 | 9.0 | 18.0 | 0.7 | 25.0 | 22.1 | 0.0 | 0.0 | 0.2 | 0.0 |
| 40 | 2016 | 0.2 | 0 | 25.1 | 10.5 | 8.5 | 70.7 | 57 | 60.1 | 2.5 | 0 | 0 | 0 |
| 41 | 2017 | 41 | 3 | 0.01 | 0 | 5 | 97 | 38.01 | 0.01 | 28 | 0 | 11 | 0 |
| | | **10.1** | **17.9** | **22.3** | **9.8** | **6.0** | **15.7** | **38.6** | **39.1** | **12.4** | **3.1** | **1.6** | **5.6** |

FIGURE A.12: Data Source: Courtesy of PMD

| | | Precipitatoin Data - Zhob (1977 to 2017) | | | | | | | | | | | |
|---|---|---|---|---|---|---|---|---|---|---|---|---|---|
| | | Jan | Feb | Mar | Apr | May | Jun | Jul | Aug | Sep | Oct | Nov | Dec |
| S.no | Years | ZhobJan | ZhobFeb | ZhobMar | ZhobApr | ZhobMay | ZhobJun | ZhobJul | ZhobAug | ZhobSep | ZhobOct | ZhobNov | ZhobDec |
| 1 | 1977 | 40.0 | 0.0 | 15.0 | 31.0 | 1.0 | 3.0 | 53.0 | 120.0 | 42.0 | 0.0 | 10.0 | 1.2 |
| 2 | 1978 | 39.3 | 12.0 | 10.0 | 10.0 | 0.0 | 5.0 | 13.1 | 13.7 | 2.1 | 0.0 | 1.0 | 11.0 |
| 3 | 1979 | 78.0 | 20.0 | 103.9 | 15.3 | 2.0 | 0.0 | 23.3 | 85.0 | 13.0 | 14.3 | 11.0 | 7.0 |
| 4 | 1980 | 24.9 | 66.0 | 101.1 | 6.8 | 1.0 | 21.4 | 29.5 | 24.6 | 14.8 | 19.5 | 7.4 | 1.0 |
| 5 | 1981 | 19.3 | 33.9 | 53.3 | 8.2 | 79.8 | 0.0 | 84.6 | 29.0 | 0.0 | 5.3 | 0.0 | 0.0 |
| 6 | 1982 | 30.1 | 45.6 | 97.7 | 23.0 | 31.5 | 0.0 | 5.6 | 57.5 | 0.0 | 25.6 | 18.9 | 40.7 |
| 7 | 1983 | 2.9 | 58.2 | 30.6 | 115.8 | 11.5 | 0.4 | 46.2 | 87.2 | 0.0 | 0.0 | 0.0 | 11.8 |
| 8 | 1984 | 4.1 | 6.4 | 5.0 | 25.2 | 0.0 | 23.6 | 120.5 | 107.0 | 0.7 | 0.0 | 0.2 | 10.3 |
| 9 | 1985 | 14.8 | 15.8 | 9.9 | 21.3 | 2.9 | 0.0 | 75.9 | 14.6 | 0.0 | 0.0 | 0.0 | 9.6 |
| 10 | 1986 | 2.0 | 21.9 | 64.3 | 22.6 | 18.1 | 9.2 | 11.0 | 18.4 | 0.0 | 0.0 | 11.3 | 0.0 |
| 11 | 1987 | 4.9 | 42.1 | 97.2 | 4.8 | 25.9 | 19.5 | 28.0 | 42.0 | 0.0 | 0.0 | 0.0 | 0.0 |
| 12 | 1988 | 15.8 | 7.5 | 66.2 | 9.2 | 0.0 | 8.3 | 53.4 | 94.4 | 14.5 | 0.0 | 0.0 | 17.5 |
| 13 | 1989 | 12.3 | 7.5 | 137.6 | 7.6 | 0.0 | 10.6 | 77.0 | 48.8 | 0.0 | 0.0 | 0.0 | 25.8 |
| 14 | 1990 | 50.3 | 57.5 | 24.7 | 47.2 | 28.3 | 10.2 | 11.4 | 165.1 | 26.5 | 0.0 | 0.0 | 39.1 |
| 15 | 1991 | 32.9 | 47.1 | 88.2 | 127.3 | 58.1 | 44.5 | 14.8 | 20.7 | 31.9 | 2.0 | 0.0 | 5.7 |
| 16 | 1992 | 39.9 | 10.7 | 19.0 | 108.0 | 21.4 | 4.2 | 69.1 | 48.5 | 1.0 | 20.0 | 1.0 | 14.9 |
| 17 | 1993 | 17.0 | 8.0 | 12.2 | 42.9 | 22.0 | 17.0 | 77.0 | 12.0 | 9.2 | 0.0 | 0.0 | 0.0 |
| 18 | 1994 | 16.0 | 35.0 | 59.0 | 52.0 | 0.8 | 54.0 | 95.0 | 3.3 | 58.0 | 0.0 | 3.0 | 16.0 |
| 19 | 1995 | 1.0 | 24.6 | 51.3 | 68.5 | 17.5 | 0.0 | 57.5 | 31.0 | 7.6 | 8.0 | 0.0 | 12.0 |
| 20 | 1996 | 15.2 | 19.0 | 27.0 | 26.8 | 27.6 | 15.0 | 80.5 | 113.9 | 0.0 | 0.0 | 0.0 | 5.1 |
| 21 | 1997 | 13.2 | 5.8 | 40.2 | 51.9 | 12.3 | 65.9 | 138.2 | 52.5 | 0.0 | 71.6 | 30.5 | 12.9 |
| 22 | 1998 | 18.3 | 33.8 | 41.1 | 1.2 | 27.9 | 20.5 | 65.7 | 37.0 | 6.0 | 1.0 | 0.0 | 0.0 |
| 23 | 1999 | 17.5 | 44.9 | 36.1 | 0.0 | 14.1 | 0.6 | 57.9 | 17.0 | 11.7 | 0.0 | 0.0 | 0.0 |
| 24 | 2000 | 3.3 | 8.0 | 22.0 | 0.0 | 3.0 | 5.4 | 82.0 | 26.9 | 4.0 | 0.0 | 0.0 | 8.8 |
| 25 | 2001 | 0.0 | 8.0 | 30.5 | 11.0 | 9.0 | 19.0 | 21.2 | 7.0 | 4.0 | 0.0 | 0.0 | 8.0 |
| 26 | 2002 | 0.0 | 31.0 | 47.0 | 48.0 | 0.0 | 29.0 | 28.0 | 11.2 | 30.4 | 19.0 | 29.0 | 4.0 |
| 27 | 2003 | 11.3 | 45.0 | 24.0 | 12.0 | 0.0 | 1.0 | 59.0 | 87.0 | 3.0 | 0.0 | 1.0 | 0.0 |
| 28 | 2004 | 38.3 | 8.0 | 0.0 | 16.0 | 3.0 | 13.2 | 38.0 | 11.0 | 13.0 | 4.0 | 7.7 | 32.7 |
| 29 | 2005 | 7.4 | 62.6 | 74.5 | 22.0 | 40.3 | 8.6 | 118.2 | 23.2 | 3.0 | 0.0 | 0.0 | 0.0 |
| 30 | 2006 | 8.2 | 4.0 | 41.4 | 6.3 | 18.4 | 46.0 | 58.5 | 8.0 | 19.0 | 0.0 | 62.2 | 31.6 |
| 31 | 2007 | 1.3 | 81.5 | 41.0 | 2.0 | 24.6 | 77.0 | 80.0 | 23.0 | 8.0 | 0.0 | 1.0 | 18.0 |
| 32 | 2008 | 21.0 | 8.0 | 6.0 | 21.6 | 5.3 | 74.8 | 122.0 | 19.0 | 15.0 | 0.0 | 0.0 | 12.0 |
| 33 | 2009 | 23.0 | 33.4 | 34.0 | 47.6 | 0.0 | 9.9 | 99.4 | 9.1 | 5.5 | 0.0 | 0.0 | 7.6 |
| 34 | 2010 | 11.2 | 3.0 | 22.5 | 7.0 | 15.0 | 7.0 | 117.7 | 118.4 | 0.0 | 0.0 | 0.0 | 0.0 |
| 35 | 2011 | 2.0 | 35.5 | 33.7 | 12.0 | 3.0 | 3.0 | 12.1 | 0.0 | 0.0 | 2.0 | 6.3 | 0.0 |
| 36 | 2012 | 6.4 | 27.0 | 0.0 | 53.5 | 4.6 | 31.0 | 41.6 | 53.0 | 31.0 | 0.0 | 0.0 | 14.5 |
| 37 | 2013 | 0.0 | 51.0 | 56.0 | 22.0 | 5.0 | 36.0 | 4.0 | 38.0 | 0.0 | 0.0 | 9.0 | 0.0 |
| 38 | 2014 | 0.0 | 25.0 | 66.0 | 29.0 | 24.0 | 4.0 | 15.0 | 24.0 | 22.0 | 0.0 | 10.0 | 0.0 |
| 39 | 2015 | 19.0 | 27.0 | 22.0 | 12.0 | 24.0 | 18.0 | 45.5 | 63.3 | 54.0 | 5.0 | 9.0 | 0.0 |
| 40 | 2016 | 16 | 0 | 51 | 46 | 17 | 9 | 25 | 40 | 2 | 0 | 0 | 0 |
| 41 | 2017 | 23 | 21.01 | 20 | 0.01 | 6 | 2 | 47.02 | 33 | 2 | 42 | 0 | 0 |
| | | **17.1** | **26.9** | **43.5** | **29.1** | **14.8** | **17.7** | **56.2** | **44.8** | **11.1** | **5.8** | **5.6** | **9.2** |

FIGURE A.13: Data Source: Courtesy of PMD

# Annexure B

| Loss Error in MLR for the month of JANUARY for both training period (1977-2015) and validation period (2016-2020) | | | | | | |
|---|---|---|---|---|---|---|
| **Year** | **Observation** | **Observed Precp** | **Estimated Precp** | **Residuals** | **RMSE** | **MAE** |
| 1977 | 1 | 47.258 | 52.598 | -5.340 | 28.515 | 5.340 |
| 1978 | 2 | 30.860 | 20.224 | 10.636 | 113.125 | 10.636 |
| 1979 | 3 | 33.960 | 34.220 | -0.260 | 0.068 | 0.260 |
| 1980 | 4 | 26.800 | 26.097 | 0.703 | 0.495 | 0.703 |
| 1981 | 5 | 30.120 | 18.736 | 11.384 | 129.602 | 11.384 |
| 1982 | 6 | 70.002 | 38.798 | 31.204 | 973.669 | 31.204 |
| 1983 | 7 | 23.504 | 17.136 | 6.368 | 40.558 | 6.368 |
| 1984 | 8 | 23.282 | 25.983 | -2.701 | 7.295 | 2.701 |
| 1985 | 9 | 24.720 | 43.814 | -19.094 | 364.587 | 19.094 |
| 1986 | 10 | 3.720 | -0.700 | 4.420 | 19.539 | 4.420 |
| 1987 | 11 | 10.400 | -5.460 | 15.860 | 251.548 | 15.860 |
| 1988 | 12 | 18.860 | 39.156 | -20.296 | 411.913 | 20.296 |
| 1989 | 13 | 20.080 | 19.571 | 0.509 | 0.260 | 0.509 |
| 1990 | 14 | 63.000 | 51.630 | 11.370 | 129.286 | 11.370 |
| 1991 | 15 | 43.600 | 47.075 | -3.475 | 12.076 | 3.475 |
| 1992 | 16 | 69.340 | 63.910 | 5.430 | 29.484 | 5.430 |
| 1993 | 17 | 64.580 | 46.688 | 17.892 | 320.137 | 17.892 |
| 1994 | 18 | 14.440 | 13.887 | 0.553 | 0.306 | 0.553 |
| 1995 | 19 | 10.160 | 17.982 | -7.822 | 61.190 | 7.822 |
| 1996 | 20 | 30.080 | 34.254 | -4.174 | 17.419 | 4.174 |
| 1997 | 21 | 36.960 | 41.437 | -4.477 | 20.047 | 4.477 |
| 1998 | 22 | 45.420 | 45.673 | -0.253 | 0.064 | 0.253 |
| 1999 | 23 | 27.240 | 32.951 | -5.711 | 32.613 | 5.711 |
| 2000 | 24 | 11.460 | 22.373 | -10.913 | 119.101 | 10.913 |
| 2001 | 25 | 0.144 | -5.556 | 5.700 | 32.489 | 5.700 |
| 2002 | 26 | 4.520 | 23.781 | -19.261 | 370.975 | 19.261 |
| 2003 | 27 | 16.540 | 19.867 | -3.327 | 11.070 | 3.327 |
| 2004 | 28 | 48.460 | 46.138 | 2.322 | 5.390 | 2.322 |
| 2005 | 29 | 20.140 | 24.720 | -4.580 | 20.976 | 4.580 |
| 2006 | 30 | 7.780 | 13.425 | -5.645 | 31.867 | 5.645 |
| 2007 | 31 | 5.360 | 18.516 | -13.156 | 173.071 | 13.156 |
| 2008 | 32 | 55.960 | 32.716 | 23.244 | 540.267 | 23.244 |
| 2009 | 33 | 47.140 | 38.662 | 8.478 | 71.872 | 8.478 |
| 2010 | 34 | 13.000 | 12.170 | 0.830 | 0.688 | 0.830 |
| 2011 | 35 | 8.980 | 20.151 | -11.171 | 124.785 | 11.171 |
| 2012 | 36 | 22.080 | 22.801 | -0.721 | 0.520 | 0.721 |
| 2013 | 37 | 0.820 | -6.485 | 7.305 | 53.369 | 7.305 |
| 2014 | 38 | 1.880 | 14.708 | -12.828 | 164.562 | 12.828 |
| 2015 | 39 | 11.600 | 18.805 | -7.205 | 51.914 | 7.205 |
| 2016 | 1 | 16.260 | 10.754 | 5.506 | 30.321 | 5.506 |
| 2017 | 2 | 48.200 | 34.337 | 13.863 | 192.187 | 13.863 |
| 2018 | 3 | 0.100 | 1.003 | -0.903 | 0.815 | 0.903 |
| 2019 | 4 | 19.600 | 23.988 | -4.388 | 19.256 | 4.388 |
| 2020 | 5 | 24.740 | 30.743 | -6.003 | 36.032 | 6.003 |
| **Training period (1977-2015)** | | | | | **11.021** | **8.375** |
| **Validation period (2016-2020)** | | | | | **7.465** | **6.133** |

FIGURE B.1: Author's work

| Loss Error in MLR for the month of JUNE for both training period (1977-2015) and validation period (2016-2020) | | | | | | |
|---|---|---|---|---|---|---|
| **Year** | **Observation** | **Observed Precp** | **Estimated Precp** | **Residuals** | **RMSE** | **MAE** |
| 1977 | 1 | 46.560 | 43.581 | 2.979 | 8.875 | 2.979 |
| 1978 | 2 | 16.380 | 35.331 | -18.951 | 359.135 | 18.951 |
| 1979 | 3 | 3.200 | 18.384 | -15.184 | 230.545 | 15.184 |
| 1980 | 4 | 9.680 | 17.906 | -8.226 | 67.673 | 8.226 |
| 1981 | 5 | 1.420 | 1.891 | -0.471 | 0.222 | 0.471 |
| 1982 | 6 | 3.820 | 20.891 | -17.071 | 291.419 | 17.071 |
| 1983 | 7 | 5.360 | 8.208 | -2.848 | 8.109 | 2.848 |
| 1984 | 8 | 6.660 | 15.376 | -8.716 | 75.975 | 8.716 |
| 1985 | 9 | 13.780 | -0.191 | 13.971 | 195.186 | 13.971 |
| 1986 | 10 | 7.540 | 8.378 | -0.838 | 0.702 | 0.838 |
| 1987 | 11 | 8.280 | 19.381 | -11.101 | 123.231 | 11.101 |
| 1988 | 12 | 13.920 | 20.726 | -6.806 | 46.319 | 6.806 |
| 1989 | 13 | 17.480 | 22.586 | -5.106 | 26.071 | 5.106 |
| 1990 | 14 | 10.660 | 19.924 | -9.264 | 85.830 | 9.264 |
| 1991 | 15 | 11.360 | 8.302 | 3.058 | 9.353 | 3.058 |
| 1992 | 16 | 5.720 | 6.622 | -0.902 | 0.813 | 0.902 |
| 1993 | 17 | 26.800 | 28.119 | -1.319 | 1.741 | 1.319 |
| 1994 | 18 | 14.842 | 14.237 | 0.605 | 0.366 | 0.605 |
| 1995 | 19 | 8.042 | 7.495 | 0.547 | 0.299 | 0.547 |
| 1996 | 20 | 46.080 | 43.050 | 3.030 | 9.183 | 3.030 |
| 1997 | 21 | 66.940 | 47.038 | 19.902 | 396.102 | 19.902 |
| 1998 | 22 | 28.220 | 25.136 | 3.084 | 9.509 | 3.084 |
| 1999 | 23 | 7.780 | 7.128 | 0.652 | 0.425 | 0.652 |
| 2000 | 24 | 2.400 | 1.844 | 0.556 | 0.309 | 0.556 |
| 2001 | 25 | 15.722 | 24.021 | -8.299 | 68.878 | 8.299 |
| 2002 | 26 | 7.722 | -2.328 | 10.050 | 100.994 | 10.050 |
| 2003 | 27 | 18.000 | 23.117 | -5.117 | 26.187 | 5.117 |
| 2004 | 28 | 15.002 | 23.404 | -8.402 | 70.585 | 8.402 |
| 2005 | 29 | 7.182 | 11.552 | -4.370 | 19.097 | 4.370 |
| 2006 | 30 | 29.922 | 17.708 | 12.214 | 149.190 | 12.214 |
| 2007 | 31 | 84.600 | 62.872 | 21.728 | 472.100 | 21.728 |
| 2008 | 32 | 39.400 | 36.300 | 3.100 | 9.610 | 3.100 |
| 2009 | 33 | 8.180 | 23.659 | -15.479 | 239.607 | 15.479 |
| 2010 | 34 | 12.300 | 10.107 | 2.193 | 4.808 | 2.193 |
| 2011 | 35 | 10.800 | 1.924 | 8.876 | 78.783 | 8.876 |
| 2012 | 36 | 9.220 | -1.327 | 10.547 | 111.237 | 10.547 |
| 2013 | 37 | 28.180 | 8.923 | 19.257 | 370.838 | 19.257 |
| 2014 | 38 | 5.420 | -1.976 | 7.396 | 54.700 | 7.396 |
| 2015 | 39 | 21.460 | 16.735 | 4.725 | 22.326 | 4.725 |
| 2016 | 1 | 24.480 | 3.274 | 21.206 | 449.692 | 21.206 |
| 2017 | 2 | 42.800 | 18.314 | 24.486 | 599.545 | 24.486 |
| 2018 | 3 | 9.200 | 1.459 | 7.741 | 59.922 | 7.741 |
| 2019 | 4 | 11.400 | -1.421 | 12.821 | 164.376 | 12.821 |
| 2020 | 5 | 9.600 | 12.977 | -3.377 | 11.407 | 3.377 |
| **Training period (1977-2015)** | | | | | **9.801** | **7.614** |
| **Validation period (2016-2020)** | | | | | **16.031** | **13.926** |

FIGURE B.2: Author's work

| Loss Error in PCR for the month of JANUARY for both training period (1977-2015) and validation period (2016-2020) | | | | | | |
|---|---|---|---|---|---|---|
| **Year** | **Observation** | **Observed Precp** | **Estimated Precp** | **Residuals** | **RMSE** | **MAE** |
| 1977 | 1 | 47.258 | 52.080 | -4.822 | 23.256 | 4.822 |
| 1978 | 2 | 30.860 | 30.393 | 0.467 | 0.218 | 0.467 |
| 1979 | 3 | 33.960 | 33.094 | 0.866 | 0.751 | 0.866 |
| 1980 | 4 | 26.800 | 21.700 | 5.100 | 26.013 | 5.100 |
| 1981 | 5 | 30.120 | 35.813 | -5.693 | 32.413 | 5.693 |
| 1982 | 6 | 70.002 | 68.038 | 1.964 | 3.858 | 1.964 |
| 1983 | 7 | 23.504 | 28.811 | -5.307 | 28.163 | 5.307 |
| 1984 | 8 | 23.282 | 13.913 | 9.369 | 87.785 | 9.369 |
| 1985 | 9 | 24.720 | 19.791 | 4.929 | 24.295 | 4.929 |
| 1986 | 10 | 3.720 | 5.253 | -1.533 | 2.351 | 1.533 |
| 1987 | 11 | 10.400 | 5.380 | 5.020 | 25.197 | 5.020 |
| 1988 | 12 | 18.860 | 25.294 | -6.434 | 41.391 | 6.434 |
| 1989 | 13 | 20.080 | 28.403 | -8.323 | 69.273 | 8.323 |
| 1990 | 14 | 63.000 | 50.465 | 12.535 | 157.118 | 12.535 |
| 1991 | 15 | 43.600 | 47.975 | -4.375 | 19.143 | 4.375 |
| 1992 | 16 | 69.340 | 62.104 | 7.236 | 52.360 | 7.236 |
| 1993 | 17 | 64.580 | 56.648 | 7.932 | 62.923 | 7.932 |
| 1994 | 18 | 14.440 | 9.162 | 5.278 | 27.856 | 5.278 |
| 1995 | 19 | 10.160 | 1.879 | 8.281 | 68.579 | 8.281 |
| 1996 | 20 | 30.080 | 45.868 | -15.788 | 249.257 | 15.788 |
| 1997 | 21 | 36.960 | 33.931 | 3.029 | 9.178 | 3.029 |
| 1998 | 22 | 45.420 | 45.594 | -0.174 | 0.030 | 0.174 |
| 1999 | 23 | 27.240 | 30.789 | -3.549 | 12.592 | 3.549 |
| 2000 | 24 | 11.460 | 17.986 | -6.526 | 42.591 | 6.526 |
| 2001 | 25 | 0.144 | 15.165 | -15.021 | 225.615 | 15.021 |
| 2002 | 26 | 4.520 | 3.618 | 0.902 | 0.813 | 0.902 |
| 2003 | 27 | 16.540 | 20.053 | -3.513 | 12.343 | 3.513 |
| 2004 | 28 | 48.460 | 43.618 | 4.842 | 23.449 | 4.842 |
| 2005 | 29 | 20.140 | 4.470 | 15.670 | 245.545 | 15.670 |
| 2006 | 30 | 7.780 | 4.945 | 2.835 | 8.036 | 2.835 |
| 2007 | 31 | 5.360 | 19.719 | -14.359 | 206.184 | 14.359 |
| 2008 | 32 | 55.960 | 42.801 | 13.159 | 173.164 | 13.159 |
| 2009 | 33 | 47.140 | 45.515 | 1.625 | 2.641 | 1.625 |
| 2010 | 34 | 13.000 | 1.329 | 11.671 | 136.212 | 11.671 |
| 2011 | 35 | 8.980 | 6.706 | 2.274 | 5.172 | 2.274 |
| 2012 | 36 | 22.080 | 20.700 | 1.380 | 1.904 | 1.380 |
| 2013 | 37 | 0.820 | 16.702 | -15.882 | 252.226 | 15.882 |
| 2014 | 38 | 1.880 | 12.716 | -10.836 | 117.416 | 10.836 |
| 2015 | 39 | 11.600 | 15.831 | -4.231 | 17.904 | 4.231 |
| 2016 | 1 | 16.260 | 20.282 | -4.022 | 16.180 | 4.022 |
| 2017 | 2 | 48.200 | -11.057 | 59.257 | 3511.335 | 59.257 |
| 2018 | 3 | 0.100 | 0.219 | -0.119 | 0.014 | 0.119 |
| 2019 | 4 | 19.600 | 9.611 | 9.989 | 99.773 | 9.989 |
| 2020 | 5 | 24.740 | 26.800 | -2.060 | 4.244 | 2.060 |
| **Training period (1977-2015)** | | | | | **7.999** | **6.480** |
| **Validation period (2016-2020)** | | | | | **26.950** | **15.089** |

FIGURE B.3: Author's work

| Loss Error in PCR for the month of JUNE for both training period (1977-2015) and validation period (2016-2020) | | | | | | |
|---|---|---|---|---|---|---|
| **Year** | **Observation** | **Observed Precp** | **Estimated Precp** | **Residuals** | **RMSE** | **MAE** |
| 1977 | 1 | 46.560 | 43.825 | 2.735 | 7.480 | 2.735 |
| 1978 | 2 | 16.380 | 16.125 | 0.255 | 0.065 | 0.255 |
| 1979 | 3 | 3.200 | 10.036 | -6.836 | 46.731 | 6.836 |
| 1980 | 4 | 9.680 | 8.754 | 0.926 | 0.857 | 0.926 |
| 1981 | 5 | 1.420 | 4.749 | -3.329 | 11.083 | 3.329 |
| 1982 | 6 | 3.820 | 6.463 | -2.643 | 6.986 | 2.643 |
| 1983 | 7 | 5.360 | 4.831 | 0.529 | 0.280 | 0.529 |
| 1984 | 8 | 6.660 | 12.713 | -6.053 | 36.638 | 6.053 |
| 1985 | 9 | 13.780 | 15.411 | -1.631 | 2.659 | 1.631 |
| 1986 | 10 | 7.540 | 6.581 | 0.959 | 0.919 | 0.959 |
| 1987 | 11 | 8.280 | 5.026 | 3.254 | 10.592 | 3.254 |
| 1988 | 12 | 13.920 | 6.163 | 7.757 | 60.168 | 7.757 |
| 1989 | 13 | 17.480 | 17.874 | -0.394 | 0.156 | 0.394 |
| 1990 | 14 | 10.660 | 10.249 | 0.411 | 0.169 | 0.411 |
| 1991 | 15 | 11.360 | 9.780 | 1.580 | 2.495 | 1.580 |
| 1992 | 16 | 5.720 | 6.501 | -0.781 | 0.610 | 0.781 |
| 1993 | 17 | 26.800 | 29.584 | -2.784 | 7.751 | 2.784 |
| 1994 | 18 | 14.842 | 10.519 | 4.323 | 18.684 | 4.323 |
| 1995 | 19 | 8.042 | 9.058 | -1.016 | 1.031 | 1.016 |
| 1996 | 20 | 46.080 | 41.454 | 4.626 | 21.399 | 4.626 |
| 1997 | 21 | 66.940 | 65.484 | 1.456 | 2.120 | 1.456 |
| 1998 | 22 | 28.220 | 26.259 | 1.961 | 3.846 | 1.961 |
| 1999 | 23 | 7.780 | 4.292 | 3.488 | 12.168 | 3.488 |
| 2000 | 24 | 2.400 | 8.218 | -5.818 | 33.853 | 5.818 |
| 2001 | 25 | 15.722 | 10.106 | 5.616 | 31.539 | 5.616 |
| 2002 | 26 | 7.722 | 8.063 | -0.341 | 0.116 | 0.341 |
| 2003 | 27 | 18.000 | 21.848 | -3.848 | 14.807 | 3.848 |
| 2004 | 28 | 15.002 | 23.204 | -8.202 | 67.266 | 8.202 |
| 2005 | 29 | 7.182 | 9.749 | -2.567 | 6.592 | 2.567 |
| 2006 | 30 | 29.922 | 31.748 | -1.826 | 3.335 | 1.826 |
| 2007 | 31 | 84.600 | 82.428 | 2.172 | 4.717 | 2.172 |
| 2008 | 32 | 39.400 | 39.770 | -0.370 | 0.137 | 0.370 |
| 2009 | 33 | 8.180 | 14.416 | -6.236 | 38.889 | 6.236 |
| 2010 | 34 | 12.300 | 14.308 | -2.008 | 4.031 | 2.008 |
| 2011 | 35 | 10.800 | 5.483 | 5.317 | 28.273 | 5.317 |
| 2012 | 36 | 9.220 | 3.374 | 5.846 | 34.174 | 5.846 |
| 2013 | 37 | 28.180 | 28.286 | -0.106 | 0.011 | 0.106 |
| 2014 | 38 | 5.420 | -0.446 | 5.866 | 34.406 | 5.866 |
| 2015 | 39 | 21.460 | 23.747 | -2.287 | 5.231 | 2.287 |
| 2016 | 1 | 24.480 | 6.967 | 17.513 | 306.690 | 17.513 |
| 2017 | 2 | 42.800 | 55.696 | -12.896 | 166.300 | 12.896 |
| 2018 | 3 | 9.200 | 27.599 | -18.399 | 338.517 | 18.399 |
| 2019 | 4 | 11.400 | 26.594 | -15.194 | 230.844 | 15.194 |
| 2020 | 5 | 9.600 | 10.719 | -1.119 | 1.253 | 1.119 |
| **Training period (1977-2015)** | | | | | **3.797** | **3.030** |
| **Validation period (2016-2020)** | | | | | **14.447** | **13.024** |

FIGURE B.4: Author's work

**Loss Error in MLR (NSE,PBIAS & RSR) for the month of JANUARY (1977-2020)**

| Year | Observation | Observed Precp | Predicted Precp | Residuals | RMSE | NSE-(Numerator) | NSE-(Denomenator) | PBIAS |
|---|---|---|---|---|---|---|---|---|
| 1977 | 1 | 47 | 53 | -5 | 29 | 29 | 764 | -5 |
| 1978 | 2 | 31 | 20 | 11 | 113 | 113 | 126 | 11 |
| 1979 | 3 | 34 | 34 | 0 | 0 | 0 | 206 | 0 |
| 1980 | 4 | 27 | 26 | 1 | 0 | 0 | 52 | 1 |
| 1981 | 5 | 30 | 19 | 11 | 130 | 130 | 110 | 11 |
| 1982 | 6 | 70 | 39 | 31 | 974 | 974 | 2539 | 31 |
| 1983 | 7 | 24 | 17 | 6 | 41 | 41 | 15 | 6 |
| 1984 | 8 | 23 | 26 | -3 | 7 | 7 | 13 | -3 |
| 1985 | 9 | 25 | 44 | -19 | 365 | 365 | 26 | -19 |
| 1986 | 10 | 4 | -1 | 4 | 20 | 20 | 253 | 4 |
| 1987 | 11 | 10 | -5 | 16 | 252 | 252 | 85 | 16 |
| 1988 | 12 | 19 | 39 | -20 | 412 | 412 | 1 | -20 |
| 1989 | 13 | 20 | 20 | 1 | 0 | 0 | 0 | 1 |
| 1990 | 14 | 63 | 52 | 11 | 129 | 129 | 1882 | 11 |
| 1991 | 15 | 44 | 47 | -3 | 12 | 12 | 575 | -3 |
| 1992 | 16 | 69 | 64 | 5 | 29 | 29 | 2472 | 5 |
| 1993 | 17 | 65 | 47 | 18 | 320 | 320 | 2022 | 18 |
| 1994 | 18 | 14 | 14 | 1 | 0 | 0 | 27 | 1 |
| 1995 | 19 | 10 | 18 | -8 | 61 | 61 | 89 | -8 |
| 1996 | 20 | 30 | 34 | -4 | 17 | 17 | 109 | -4 |
| 1997 | 21 | 37 | 41 | -4 | 20 | 20 | 301 | -4 |
| 1998 | 22 | 45 | 46 | 0 | 0 | 0 | 666 | 0 |
| 1999 | 23 | 27 | 33 | -6 | 33 | 33 | 58 | -6 |
| 2000 | 24 | 11 | 22 | -11 | 119 | 119 | 67 | -11 |
| 2001 | 25 | 0 | -6 | 6 | 32 | 32 | 379 | 6 |
| 2002 | 26 | 5 | 24 | -19 | 371 | 371 | 228 | -19 |
| 2003 | 27 | 17 | 20 | -3 | 11 | 11 | 9 | -3 |
| 2004 | 28 | 48 | 46 | 2 | 5 | 5 | 832 | 2 |
| 2005 | 29 | 20 | 25 | -5 | 21 | 21 | 0 | -5 |
| 2006 | 30 | 8 | 13 | -6 | 32 | 32 | 140 | -6 |
| 2007 | 31 | 5 | 19 | -13 | 173 | 173 | 203 | -13 |
| 2008 | 32 | 56 | 33 | 23 | 540 | 540 | 1321 | 23 |
| 2009 | 33 | 47 | 39 | 8 | 72 | 72 | 758 | 8 |
| 2010 | 34 | 13 | 12 | 1 | 1 | 1 | 44 | 1 |
| 2011 | 35 | 9 | 20 | -11 | 125 | 125 | 113 | -11 |
| 2012 | 36 | 22 | 23 | -1 | 1 | 1 | 6 | -1 |
| 2013 | 37 | 1 | -6 | 7 | 53 | 53 | 353 | 7 |
| 2014 | 38 | 2 | 15 | -13 | 165 | 165 | 315 | -13 |
| 2015 | 39 | 12 | 19 | -7 | 52 | 52 | 64 | -7 |
| 2016 | 40 | 16 | 11 | 6 | 30 | 30 | 11 | 6 |
| 2017 | 41 | 48 | 34 | 14 | 192 | 192 | 817 | 14 |
| 2018 | 42 | 0 | 1 | -1 | 1 | 1 | 381 | -1 |
| 2019 | 43 | 20 | 24 | -4 | 19 | 19 | 0 | -4 |
| 2020 | 44 | 25 | 31 | -6 | 36 | 36 | 26 | -6 |
| | **STDEV** | **20** | **26** | | **11** | **5015** | **18459** | **10** |
| | **Aveg** | **25.98** | | | **7.465** | | | |
| | **Sum** | **1153.15** | | | | | | |

| | |
|---|---|
| **NSE** | **0.7283** |
| **PBIAS** | **0.86%** |
| **RSR** | **0.5618** |

FIGURE B.5: Author's work

**Loss Error in MLR (NSE,PBIAS &RSR) for the month of JUNE (1977-2020)**

| Year | Observation | Observed Precp | Predicted Precp | Residuals | RMSE | NSE-(Numerator) | NSE-(Denomenator) | PBIAS |
|---|---|---|---|---|---|---|---|---|
| 1977 | 1.0 | 46.6 | 43.6 | 3.0 | 8.9 | 8.9 | 857.6 | 3.0 |
| 1978 | 2.0 | 16.4 | 35.3 | -19.0 | 359.1 | 359.1 | 0.8 | -19.0 |
| 1979 | 3.0 | 3.2 | 18.4 | -15.2 | 230.5 | 230.5 | 198.1 | -15.2 |
| 1980 | 4.0 | 9.7 | 17.9 | -8.2 | 67.7 | 67.7 | 57.7 | -8.2 |
| 1981 | 5.0 | 1.4 | 1.9 | -0.5 | 0.2 | 0.2 | 251.4 | -0.5 |
| 1982 | 6.0 | 3.8 | 20.9 | -17.1 | 291.4 | 291.4 | 181.1 | -17.1 |
| 1983 | 7.0 | 5.4 | 8.2 | -2.8 | 8.1 | 8.1 | 142.0 | -2.8 |
| 1984 | 8.0 | 6.7 | 15.4 | -8.7 | 76.0 | 76.0 | 112.7 | -8.7 |
| 1985 | 9.0 | 13.8 | -0.2 | 14.0 | 195.2 | 195.2 | 12.2 | 14.0 |
| 1986 | 10.0 | 7.5 | 8.4 | -0.8 | 0.7 | 0.7 | 94.8 | -0.8 |
| 1987 | 11.0 | 8.3 | 19.4 | -11.1 | 123.2 | 123.2 | 80.9 | -11.1 |
| 1988 | 12.0 | 13.9 | 20.7 | -6.8 | 46.3 | 46.3 | 11.3 | -6.8 |
| 1989 | 13.0 | 17.5 | 22.6 | -5.1 | 26.1 | 26.1 | 0.0 | -5.1 |
| 1990 | 14.0 | 10.7 | 19.9 | -9.3 | 85.8 | 85.8 | 43.8 | -9.3 |
| 1991 | 15.0 | 11.4 | 8.3 | 3.1 | 9.4 | 9.4 | 35.0 | 3.1 |
| 1992 | 16.0 | 5.7 | 6.6 | -0.9 | 0.8 | 0.8 | 133.5 | -0.9 |
| 1993 | 17.0 | 26.8 | 28.1 | -1.3 | 1.7 | 1.7 | 90.7 | -1.3 |
| 1994 | 18.0 | 14.8 | 14.2 | 0.6 | 0.4 | 0.4 | 5.9 | 0.6 |
| 1995 | 19.0 | 8.0 | 7.5 | 0.5 | 0.3 | 0.3 | 85.3 | 0.5 |
| 1996 | 20.0 | 46.1 | 43.0 | 3.0 | 9.2 | 9.2 | 829.7 | 3.0 |
| 1997 | 21.0 | 66.9 | 47.0 | 19.9 | 396.1 | 396.1 | 2466.5 | 19.9 |
| 1998 | 22.0 | 28.2 | 25.1 | 3.1 | 9.5 | 9.5 | 119.8 | 3.1 |
| 1999 | 23.0 | 7.8 | 7.1 | 0.7 | 0.4 | 0.4 | 90.2 | 0.7 |
| 2000 | 24.0 | 2.4 | 1.8 | 0.6 | 0.3 | 0.3 | 221.3 | 0.6 |
| 2001 | 25.0 | 15.7 | 24.0 | -8.3 | 68.9 | 68.9 | 2.4 | -8.3 |
| 2002 | 26.0 | 7.7 | -2.3 | 10.0 | 101.0 | 101.0 | 91.3 | 10.0 |
| 2003 | 27.0 | 18.0 | 23.1 | -5.1 | 26.2 | 26.2 | 0.5 | -5.1 |
| 2004 | 28.0 | 15.0 | 23.4 | -8.4 | 70.6 | 70.6 | 5.2 | -8.4 |
| 2005 | 29.0 | 7.2 | 11.6 | -4.4 | 19.1 | 19.1 | 101.9 | -4.4 |
| 2006 | 30.0 | 29.9 | 17.7 | 12.2 | 149.2 | 149.2 | 159.9 | 12.2 |
| 2007 | 31.0 | 84.6 | 62.9 | 21.7 | 472.1 | 472.1 | 4532.6 | 21.7 |
| 2008 | 32.0 | 39.4 | 36.3 | 3.1 | 9.6 | 9.6 | 489.5 | 3.1 |
| 2009 | 33.0 | 8.2 | 23.7 | -15.5 | 239.6 | 239.6 | 82.7 | -15.5 |
| 2010 | 34.0 | 12.3 | 10.1 | 2.2 | 4.8 | 4.8 | 24.8 | 2.2 |
| 2011 | 35.0 | 10.8 | 1.9 | 8.9 | 78.8 | 78.8 | 41.9 | 8.9 |
| 2012 | 36.0 | 9.2 | -1.3 | 10.5 | 111.2 | 111.2 | 64.9 | 10.5 |
| 2013 | 37.0 | 28.2 | 8.9 | 19.3 | 370.8 | 370.8 | 118.9 | 19.3 |
| 2014 | 38.0 | 5.4 | -2.0 | 7.4 | 54.7 | 54.7 | 140.6 | 7.4 |
| 2015 | 39.0 | 21.5 | 16.7 | 4.7 | 22.3 | 22.3 | 17.5 | 4.7 |
| 2016 | 40.0 | 24.5 | 3.3 | 21.2 | 449.7 | 449.7 | 51.9 | 21.2 |
| 2017 | 41.0 | 42.8 | 18.3 | 24.5 | 599.5 | 599.5 | 651.5 | 24.5 |
| 2018 | 42.0 | 9.2 | 1.5 | 7.7 | 59.9 | 59.9 | 65.2 | 7.7 |
| 2019 | 43.0 | 11.4 | -1.4 | 12.8 | 164.4 | 164.4 | 34.5 | 12.8 |
| 2020 | 44.0 | 9.6 | 13.0 | -3.4 | 11.4 | 11.4 | 58.9 | -3.4 |
| | **STDEV** | **17.28** | **16.61** | | **9.80** | **5031.27** | **12858.8** | **62.9** |
| | **Aveg** | **16.61** | | | | | | |
| | **Sum** | **793.51** | | | | | | |

| | |
|---|---|
| **NSE** | **0.6087** |
| **PBIAS** | **7.92%** |
| **RSR** | **0.5673** |

FIGURE B.6: Author's work

**Loss Error in PCR (NSE,PBIAS &RSR) for the month of JANAURY (1977-2020)**

| Year | Observation | Observed Precp | Predicted Precp | Residuals | RMSE | NSE-(Numerator) | NSE-(Denomenator) | PBIAS |
|---|---|---|---|---|---|---|---|---|
| 1977 | 1.0 | 47.3 | 52.1 | -4.8 | 23.3 | 23.3 | 764.0 | -4.8 |
| 1978 | 2.0 | 30.9 | 30.4 | 0.5 | 0.2 | 0.2 | 126.4 | 0.5 |
| 1979 | 3.0 | 34.0 | 33.1 | 0.9 | 0.8 | 0.8 | 205.7 | 0.9 |
| 1980 | 4.0 | 26.8 | 21.7 | 5.1 | 26.0 | 26.0 | 51.6 | 5.1 |
| 1981 | 5.0 | 30.1 | 35.8 | -5.7 | 32.4 | 32.4 | 110.3 | -5.7 |
| 1982 | 6.0 | 70.0 | 68.0 | 2.0 | 3.9 | 3.9 | 2538.6 | 2.0 |
| 1983 | 7.0 | 23.5 | 28.8 | -5.3 | 28.2 | 28.2 | 15.1 | -5.3 |
| 1984 | 8.0 | 23.3 | 13.9 | 9.4 | 87.8 | 87.8 | 13.4 | 9.4 |
| 1985 | 9.0 | 24.7 | 19.8 | 4.9 | 24.3 | 24.3 | 26.0 | 4.9 |
| 1986 | 10.0 | 3.7 | 5.3 | -1.5 | 2.4 | 2.4 | 252.7 | -1.5 |
| 1987 | 11.0 | 10.4 | 5.4 | 5.0 | 25.2 | 25.2 | 85.0 | 5.0 |
| 1988 | 12.0 | 18.9 | 25.3 | -6.4 | 41.4 | 41.4 | 0.6 | -6.4 |
| 1989 | 13.0 | 20.1 | 28.4 | -8.3 | 69.3 | 69.3 | 0.2 | -8.3 |
| 1990 | 14.0 | 63.0 | 50.5 | 12.5 | 157.1 | 157.1 | 1882.1 | 12.5 |
| 1991 | 15.0 | 43.6 | 48.0 | -4.4 | 19.1 | 19.1 | 575.2 | -4.4 |
| 1992 | 16.0 | 69.3 | 62.1 | 7.2 | 52.4 | 52.4 | 2472.4 | 7.2 |
| 1993 | 17.0 | 64.6 | 56.6 | 7.9 | 62.9 | 62.9 | 2021.7 | 7.9 |
| 1994 | 18.0 | 14.4 | 9.2 | 5.3 | 27.9 | 27.9 | 26.8 | 5.3 |
| 1995 | 19.0 | 10.2 | 1.9 | 8.3 | 68.6 | 68.6 | 89.4 | 8.3 |
| 1996 | 20.0 | 30.1 | 45.9 | -15.8 | 249.3 | 249.3 | 109.5 | -15.8 |
| 1997 | 21.0 | 37.0 | 33.9 | 3.0 | 9.2 | 9.2 | 300.8 | 3.0 |
| 1998 | 22.0 | 45.4 | 45.6 | -0.2 | 0.0 | 0.0 | 665.8 | -0.2 |
| 1999 | 23.0 | 27.2 | 30.8 | -3.5 | 12.6 | 12.6 | 58.1 | -3.5 |
| 2000 | 24.0 | 11.5 | 18.0 | -6.5 | 42.6 | 42.6 | 66.5 | -6.5 |
| 2001 | 25.0 | 0.1 | 15.2 | -15.0 | 225.6 | 225.6 | 379.2 | -15.0 |
| 2002 | 26.0 | 4.5 | 3.6 | 0.9 | 0.8 | 0.8 | 227.9 | 0.9 |
| 2003 | 27.0 | 16.5 | 20.1 | -3.5 | 12.3 | 12.3 | 9.5 | -3.5 |
| 2004 | 28.0 | 48.5 | 43.6 | 4.8 | 23.4 | 23.4 | 831.9 | 4.8 |
| 2005 | 29.0 | 20.1 | 4.5 | 15.7 | 245.5 | 245.5 | 0.3 | 15.7 |
| 2006 | 30.0 | 7.8 | 4.9 | 2.8 | 8.0 | 8.0 | 140.1 | 2.8 |
| 2007 | 31.0 | 5.4 | 19.7 | -14.4 | 206.2 | 206.2 | 203.3 | -14.4 |
| 2008 | 32.0 | 56.0 | 42.8 | 13.2 | 173.2 | 173.2 | 1320.8 | 13.2 |
| 2009 | 33.0 | 47.1 | 45.5 | 1.6 | 2.6 | 2.6 | 757.5 | 1.6 |
| 2010 | 34.0 | 13.0 | 1.3 | 11.7 | 136.2 | 136.2 | 43.8 | 11.7 |
| 2011 | 35.0 | 9.0 | 6.7 | 2.3 | 5.2 | 5.2 | 113.1 | 2.3 |
| 2012 | 36.0 | 22.1 | 20.7 | 1.4 | 1.9 | 1.9 | 6.1 | 1.4 |
| 2013 | 37.0 | 0.8 | 16.7 | -15.9 | 252.2 | 252.2 | 353.3 | -15.9 |
| 2014 | 38.0 | 1.9 | 12.7 | -10.8 | 117.4 | 117.4 | 314.6 | -10.8 |
| 2015 | 39.0 | 11.6 | 15.8 | -4.2 | 17.9 | 17.9 | 64.3 | -4.2 |
| 2016 | 40.0 | 16.3 | 20.3 | -4.0 | 16.2 | 16.2 | 11.3 | -4.0 |
| 2017 | 41.0 | 48.2 | -11.1 | 59.3 | 3511.3 | 3511.3 | 817.0 | 59.3 |
| 2018 | 42.0 | 0.1 | 0.2 | -0.1 | 0.0 | 0.0 | 380.9 | -0.1 |
| 2019 | 43.0 | 19.6 | 9.6 | 10.0 | 99.8 | 99.8 | 0.0 | 10.0 |
| 2020 | 44.0 | 24.7 | 26.8 | -2.1 | 4.2 | 4.2 | 26.2 | -2.1 |
| | **STDEV** | **19.6** | 24.8 | | **8.0** | **6126.8** | **18459.0** | **63.0** |
| | **Aveg** | **24.78** | | | | | | |
| | **Sum** | **1153.15** | | | | | | |

| | |
|---|---|
| **NSE** | **0.6681** |
| **PBIAS** | **5.47%** |
| **RSR** | **0.4077** |

FIGURE B.7: Author's work

**Loss Error in PCR (NSE,PBIAS &RSR) for the month of JUNE (1977-2020)**

| Year | Observation | Observed Precp | Predicted Precp | Residuals | RMSE | NSE-(Numerator) | NSE-(Denomenator) | PBIAS |
|---|---|---|---|---|---|---|---|---|
| 1977 | 1 | 46.6 | 43.8 | 2.7 | 7.5 | 7.5 | 857.6 | 2.7 |
| 1978 | 2 | 16.4 | 16.1 | 0.3 | 0.1 | 0.1 | 0.8 | 0.3 |
| 1979 | 3 | 3.2 | 10.0 | -6.8 | 46.7 | 46.7 | 198.1 | -6.8 |
| 1980 | 4 | 9.7 | 8.8 | 0.9 | 0.9 | 0.9 | 57.7 | 0.9 |
| 1981 | 5 | 1.4 | 4.7 | -3.3 | 11.1 | 11.1 | 251.4 | -3.3 |
| 1982 | 6 | 3.8 | 6.5 | -2.6 | 7.0 | 7.0 | 181.1 | -2.6 |
| 1983 | 7 | 5.4 | 4.8 | 0.5 | 0.3 | 0.3 | 142.0 | 0.5 |
| 1984 | 8 | 6.7 | 12.7 | -6.1 | 36.6 | 36.6 | 112.7 | -6.1 |
| 1985 | 9 | 13.8 | 15.4 | -1.6 | 2.7 | 2.7 | 12.2 | -1.6 |
| 1986 | 10 | 7.5 | 6.6 | 1.0 | 0.9 | 0.9 | 94.8 | 1.0 |
| 1987 | 11 | 8.3 | 5.0 | 3.3 | 10.6 | 10.6 | 80.9 | 3.3 |
| 1988 | 12 | 13.9 | 6.2 | 7.8 | 60.2 | 60.2 | 11.3 | 7.8 |
| 1989 | 13 | 17.5 | 17.9 | -0.4 | 0.2 | 0.2 | 0.0 | -0.4 |
| 1990 | 14 | 10.7 | 10.2 | 0.4 | 0.2 | 0.2 | 43.8 | 0.4 |
| 1991 | 15 | 11.4 | 9.8 | 1.6 | 2.5 | 2.5 | 35.0 | 1.6 |
| 1992 | 16 | 5.7 | 6.5 | -0.8 | 0.6 | 0.6 | 133.5 | -0.8 |
| 1993 | 17 | 26.8 | 29.6 | -2.8 | 7.8 | 7.8 | 90.7 | -2.8 |
| 1994 | 18 | 14.8 | 10.5 | 4.3 | 18.7 | 18.7 | 5.9 | 4.3 |
| 1995 | 19 | 8.0 | 9.1 | -1.0 | 1.0 | 1.0 | 85.3 | -1.0 |
| 1996 | 20 | 46.1 | 41.5 | 4.6 | 21.4 | 21.4 | 829.7 | 4.6 |
| 1997 | 21 | 66.9 | 65.5 | 1.5 | 2.1 | 2.1 | 2466.5 | 1.5 |
| 1998 | 22 | 28.2 | 26.3 | 2.0 | 3.8 | 3.8 | 119.8 | 2.0 |
| 1999 | 23 | 7.8 | 4.3 | 3.5 | 12.2 | 12.2 | 90.2 | 3.5 |
| 2000 | 24 | 2.4 | 8.2 | -5.8 | 33.9 | 33.9 | 221.3 | -5.8 |
| 2001 | 25 | 15.7 | 10.1 | 5.6 | 31.5 | 31.5 | 2.4 | 5.6 |
| 2002 | 26 | 7.7 | 8.1 | -0.3 | 0.1 | 0.1 | 91.3 | -0.3 |
| 2003 | 27 | 18.0 | 21.8 | -3.8 | 14.8 | 14.8 | 0.5 | -3.8 |
| 2004 | 28 | 15.0 | 23.2 | -8.2 | 67.3 | 67.3 | 5.2 | -8.2 |
| 2005 | 29 | 7.2 | 9.7 | -2.6 | 6.6 | 6.6 | 101.9 | -2.6 |
| 2006 | 30 | 29.9 | 31.7 | -1.8 | 3.3 | 3.3 | 159.9 | -1.8 |
| 2007 | 31 | 84.6 | 82.4 | 2.2 | 4.7 | 4.7 | 4532.6 | 2.2 |
| 2008 | 32 | 39.4 | 39.8 | -0.4 | 0.1 | 0.1 | 489.5 | -0.4 |
| 2009 | 33 | 8.2 | 14.4 | -6.2 | 38.9 | 38.9 | 82.7 | -6.2 |
| 2010 | 34 | 12.3 | 14.3 | -2.0 | 4.0 | 4.0 | 24.8 | -2.0 |
| 2011 | 35 | 10.8 | 5.5 | 5.3 | 28.3 | 28.3 | 41.9 | 5.3 |
| 2012 | 36 | 9.2 | 3.4 | 5.8 | 34.2 | 34.2 | 64.9 | 5.8 |
| 2013 | 37 | 28.2 | 28.3 | -0.1 | 0.0 | 0.0 | 118.9 | -0.1 |
| 2014 | 38 | 5.4 | -0.4 | 5.9 | 34.4 | 34.4 | 140.6 | 5.9 |
| 2015 | 39 | 21.5 | 23.7 | -2.3 | 5.2 | 5.2 | 17.5 | -2.3 |
| 2016 | 40 | 24.5 | 7.0 | 17.5 | 306.7 | 306.7 | 51.9 | 17.5 |
| 2017 | 41 | 42.8 | 55.7 | -12.9 | 166.3 | 166.3 | 651.5 | -12.9 |
| 2018 | 42 | 9.2 | 27.6 | -18.4 | 338.5 | 338.5 | 65.2 | -18.4 |
| 2019 | 43 | 11.4 | 26.6 | -15.2 | 230.8 | 230.8 | 34.5 | -15.2 |
| 2020 | 44 | 9.6 | 10.7 | -1.1 | 1.3 | 1.3 | 58.9 | -1.1 |
| | **STDEV** | **17.3** | 18.7 | | **3.8** | **1605.9** | **12858.8** | **-30.1** |
| | **Aveg** | **18.72** | | | | | | |
| | **Sum** | **793.51** | | | | | | |

| | |
|---|---|
| **NSE** | **0.8751** |
| **PBIAS** | **-3.79%** |
| **RSR** | **0.2198** |

FIGURE B.8: Author's work